TECHNISCHE UNIVERSITÄT DARMSTADT

Development of photo-responsive synthetic RNA devices

Dissertation von
Thea Sabrina Lotz

zur Erlangung des angestrebten akademischen Grades
des Doktor rerum naturalium (Dr. rer. nat.)

Technischen Universität Darmstadt
Fachbereich Biologie

Erstgutachterin: Prof. Dr. Beatrix Süß
Zweitgutachterin: Prof. Dr. Felicitas Pfeifer

Darmstadt im Jahr 2018

Lotz, Thea Sabrina: Development of photo-responsive synthetic RNA devices
Darmstadt, Technische Universität Darmstadt
Veröffentlichungsjahr der Dissertation auf TUprints: 2019
Tag der mündlichen Prüfung: 29. 10. 2018

Science is magic that works

Kurt Vonnegut

Teile dieser Arbeit wurden bereits veröffentlicht in:

Parts of this work have already been published in:

T. S. Lotz, and B. Suess, “Small-Molecule-Binding Riboswitches” *Microbiology Spectrum*, vol. 6, no. 4, 2018.

M. Schmidt, K. Hamacher, F. Reinhardt, T. S. Lotz, F. Groher, S. Jager, and B. Suess, “SICOR: Subgraph Isomorphism Comparison of RNA Secondary Structures” In revision.

T. S. Lotz, T. Halbritter, C. Kaiser, M. M. Rudolph, L. Kraus, F. Groher, S. Wahl, J. Wachtveitl, A. Heckel, and B. Suess, “A light-responsive RNA aptamer for an azobenzene derivative” Submitted.

Table of Contents

1 Summary

The different functions of RNA have led to great and increasing interest in the field of synthetic biology. One such example of versatile RNA molecules used in synthetic biology is aptamers. Aptamers are able to bind to a wide range of target molecules with a high affinity and specificity, which is why they are often compared to antibodies. Using the SELEX method, they can be generated *in vitro* against target molecules for a broad range of possible applications. In nature, they work as the sensing domain of riboswitches and regulate gene expression by binding their cognate target molecule. Riboswitches can also be generated synthetically from *in vitro* generated aptamers.

In the course of this work, a novel RNA aptamer which selectively binds to one of two light-induced isoforms of a specific small molecule ligand (azoCm) was developed. The potential function of such an aptamer as a riboswitch was evaluated.

A previously carried out SELEX experiment against azoCm yielded a specifically binding aptamer (aptamer 42). At the beginning of this work, its secondary structure was analyzed using in-line probing. As it was previously shown aptamer 42 could not work as a riboswitch regulating GFP expression in the model organisms *Saccharomyces cerevisiae*, other aptamers from the same SELEX were tested under the same conditions using *in vivo* screening. As no functional riboswitch could be identified, a new SELEX experiment using a new aptamer library was started.

The new affinity SELEX yielded aptamers specifically binding to azoCm. However, *in vivo* screening of aptamers from this SELEX did not result in an azoCm dependent riboswitch. Therefore, a novel light SELEX method was developed and established. This light SELEX protocol enriched isoform selective aptamers by a light-induced conformational change of azoCm during the SELEX process. As *in vivo* screening of light SELEX aptamers did not yield a riboswitch again, *in vitro* binding studies of aptamers from the light SELEX were performed. Comparing three aptamers which showed the highest discrimination between the two isoforms of azoCm to each other led to the discovery of a 13 nt sequence motif that only these aptamers shared. A next-generation sequencing experiment performed with the SELEX and light SELEX rounds revealed that this sequence motif (“light motif”) was specifically enriched during light SELEX rounds, but was gradually depleted during the later, more stringent affinity SELEX. Based on this discovery, a new library for SELEX was designed, containing the partially randomized light motif, as well as entirely randomized flanking

regions. SELEX performed with this light motif doped library led to a fast enrichment within five rounds, and aptamers from this SELEX were tested regarding their *in vivo* functionality. From the aptamers tested *in vivo*, four showed gene regulatory function, however with a low regulatory factor of 1.25- to 1.35-fold. Based on the best functional aptamer B2, partially randomized aptamer libraries were generated for further *in vivo* screenings. While the regulatory factor of B2 could not be improved using this approach, a modified version of it called B2-1 could be shown to regulate gene expression in yeast cells in an azoCm dose-dependent manner. To learn more about the aptamer B2-1, its binding affinity was analyzed using isothermal calorimetry. The kD of B2-1 was determined to be 23 nM, depending on the calculation model used. A truncated version of B2-1 showed a low micromolar binding to azoCm, indicating that structurally relevant parts of B2-1 had been deleted during the truncation. However, both B2-1 and its truncated version did selectively bind to only one isoform of azoCm, while binding to the other isoform could not be detected.

The aptamer developed in this work shows a much stronger discrimination between the two isoforms of its light-switchable ligand than previously reported isoform-selective aptamers. It also shows the highest binding affinity to its ligand compared to the isoform-selective aptamers in literature to date. While a riboswitch based on this aptamer shows only slight regulatory function, dose dependent regulation of gene expression could be shown. This work therefore constitutes the first steps towards the generation of a light dependent riboswitch.

1.1 Deutsche Zusammenfassung

Die verschiedenen Funktionen von RNA haben zu einem großen und zunehmenden Interesse für das Feld der synthetischen Biologie geführt. Ein Beispiel für vielseitige RNA-Moleküle in der synthetischen Biologie sind Aptamere. Aptamere sind in der Lage, an ein breites Spektrum von Zielmolekülen mit hoher Affinität und Spezifität zu binden, weshalb sie oft mit Antikörpern verglichen werden. Mit der SELEX-Methode können Aptamere für bestimmte Zielmoleküle *in vitro* für ein breites Anwendungsspektrum generiert werden. In der Natur fungieren sie als Sensordomäne von Riboswitchen und regulieren die Genexpression, indem sie an ihr Zielmolekül binden. Riboswitche können mittels synthetischer Biologie auch aus *in vitro* selektierten Aptameren erzeugt werden.

Im Rahmen dieser Arbeit wurde ein neuartiges RNA-Aptamer entwickelt, welches selektiv an eine von zwei lichtinduzierten Isoformen eines bestimmten niedermolekularen Liganden (azoCm) bindet. Die potenzielle Funktion eines solchen Aptamers als Riboswitch wurde untersucht.

Ein zuvor durchgeführtes SELEX-Experiment gegen azoCm ergab ein spezifisch bindendes Aptamer (Aptamer 42). Zu Beginn dieser Arbeit wurde dessen Sekundärstruktur mit Hilfe von In-Line Probing analysiert. Wie vorhergehende Untersuchungen zeigten, besaß Aptamer 42 keine Riboswitch-Funktion zur Regulation der GFP-Expression im Modellorganismus *Saccharomyces cerevisiae*. Daher wurden andere Aptamere aus der gleichen SELEX unter gleichen Bedingungen mittels *in vivo* Screening getestet. Da kein funktionsfähiger Riboswitch identifiziert werden konnte, wurde ein neues SELEX-Experiment mit einer neuen Aptamer Bibliothek durchgeführt.

Die neue SELEX ergab Aptamere, die spezifisch an azoCm binden. Das *in vivo* Screening von Aptameren aus dieser SELEX führte jedoch nicht zu einem funktionsfähigen azoCm abhängigen Riboswitch. Darum wurde eine neuartige Licht-SELEX Methode entwickelt und durchgeführt. Aptamere aus dieser Licht-SELEX wurden durch eine lichtinduzierte Konformationsänderung von azoCm während des SELEX-Prozesses erzeugt. Dies führte zu einer Anreicherung von Isoform-selektiven Aptameren. Da *in vivo* Screening der Aptamere aus der Licht-SELEX wiederum keine Riboswitch-Funktion zeigte, wurden *in vitro* Bindungsstudien durchgeführt. Der Vergleich von drei Aptameren, die die unterschiedlichste Bindungsspezifität zwischen den beiden Isoformen von azoCm zeigten, führte zur Entdeckung eines 13 nt Sequenzmotivs, das nur diesen Aptameren gemeinsam war. Next

Generation Sequencing der SELEX und Licht-SELEX Runden ergab, dass dieses Sequenzmotiv ("Lichtmotiv") während der Licht-SELEX Runden spezifisch angereichert wurde, während es sich in den Runden der klassischen SELEX mit hoher Stringenz stufenweise verringerte. Basierend auf dieser Entdeckung wurde eine neue Aptamer Bibliothek für SELEX entworfen, die sowohl das teilweise randomisierte Lichtmotiv als auch vollständig randomisierte Randbereiche enthielt. Eine SELEX mit dieser das Lichtmotiv enthaltenden Bibliothek führte zu einer schnellen Anreicherung innerhalb von fünf Runden. Aptamere aus dieser SELEX wurden auf ihre *in vivo* Funktionalität getestet. Von den getesteten Aptameren zeigten vier eine genregulatorische Funktion in *S. cerevisiae*, allerdings mit einem niedrigen Regulationsfaktor von 1,25- bis 1,35-fach. Basierend auf dem am stärksten regulierenden Aptamer B2 wurden teilweise randomisierte Aptamer-Bibliotheken für weitere *in vivo* Screenings generiert. Während der regulatorische Faktor von B2 mit diesem Ansatz nicht verbessert werden konnte, konnte eine modifizierte Version namens B2-1 entwickelt werden, die die Genexpression in *S. cerevisiae* dosisabhängig reguliert. Um mehr über das Aptamer B2-1 zu erfahren, wurde seine Bindungsaffinität mittels Isothermer Titrationskalorimetrie analysiert. Die Dissoziationskonstante von B2-1 lag im niedrigen nanomolaren Bereich (23 nM). Eine verkürzte Version von B2-1 zeigte eine niedrige mikromolare Bindung an azoCm, was darauf hindeutete, dass strukturell relevante Teile von B2-1 während der Verkürzung wegfielen. Sowohl B2-1 als auch seine verkürzte Version banden jedoch selektiv nur an eine Isoform von azoCm, während eine Bindung an die andere Isoform nicht festgestellt werden konnte.

Das in dieser Arbeit entwickelte Aptamer zeigt eine viel stärkere Diskriminierung zwischen den beiden Isoformen seines lichtschaltbaren Liganden als andere bisher publizierte Isoform-selektive Aptamere. Es zeigt auch die höchste Bindungsaffinität zu seinem Liganden als Isoform-selektive Aptameren in der bisherigen Literatur. Während ein auf diesem Aptamer basierender Riboswitch nur eine geringe regulatorische Funktion aufweist, konnte eine dosisabhängige Regulation der Genexpression nachgewiesen werden. Diese Arbeit beinhaltet daher die ersten Schritte zur Erzeugung eines lichtabhängigen Riboswitches.

2 Introduction

2.1 Theoretical background

2.1.1 Synthetic biology

Cells are the smallest functional units that make up organisms [1]. In the case of microorganisms as most bacteria and yeasts, they actually represent the entire organism (unicellular organisms). In multicellular organisms they can be highly specialized and can provide one crucial function in organisms (e.g. different cells within the islets of Langerhans are producing insulin or hormones depending on blood sugar levels [2]). Some can also be able to move, proliferate and communicate on their own [3]. Cells are composed out of cytoplasm which contains many biomolecules such as proteins and nucleic acids, as well as more complex structures like organelles [3]. Today, researchers in cell biology and related fields often use tools generated by synthetic biology to analyze gene regulation and cellular functions. Synthetic biology is an emerging field of interdisciplinary research, rooted in biology. While the term "synthetic biology" was coined as early as 1910 by Stéphane Leduc [4-6], the field of synthetic biology has been taking up speed with the advent of fast and cost-efficient molecular cloning techniques, such as PCR (3.2.6), easily accessible restriction enzymes (3.2.4), as well as sequencing methods (3.2.10). Today, the interdisciplinary research together with fields like electrical and chemical engineering push the boundaries of understanding and designing new artificial biological pathways, entire synthetic organisms or abstract devices isolating cellular functions, such as cell-free protein expression systems [7-9]. A bottom-up approach to synthetic biology is the construction of novel genetic circuits. DNA sequences not naturally occurring together are combined into an engineered and optimized network, in which the DNA sequences, their RNA transcripts or their protein products can influence and modulate each other. For example, elements like DNA-binding proteins able to recruit or block RNA polymerases [10], and RNA translational repressors can modulate gene expression in these circuits [11, 12]. Riboswitches play an increasingly important role in this "genetic toolbox" [13], as they allow an RNA-based regulation, independent of protein factors. In a hypothetical "plug-and-play" toolbox, all of these elements could be combined at will and would function like the parts of a mechanically engineered machine [14].

2.1.2 Genetic engineering

Today, function and regulation of genes are studied using molecular biology techniques. Genes are found on chromosomes, which consist of a tightly coiled DNA (deoxyribonucleic acid) strand, wrapped around packaging proteins called histones [15]. A gene is a section of DNA coding for a protein. In order to generate these proteins from DNA, first DNA is transcribed to RNA (ribonucleic acid), using a cell's internal RNA polymerase enzymes. This transcript is called messenger RNA (mRNA) and serves as the blueprint for protein synthesis. The mRNA is processed by a set of ribosomes, which decode the information stored in nucleotide triplets in order to generate a specific amino acid chain, the protein. The process of transcription and translation, called protein biosynthesis, is very similar in prokaryotes and eukaryotes, however differences exist [15, 16].

While DNA (Deoxyribonucleic acid), the carrier of all genetic information, is typically composed of two complementary nucleotide strands, RNA is a single stranded polynucleotide tasked with various functions within the cell (see Figure 1).

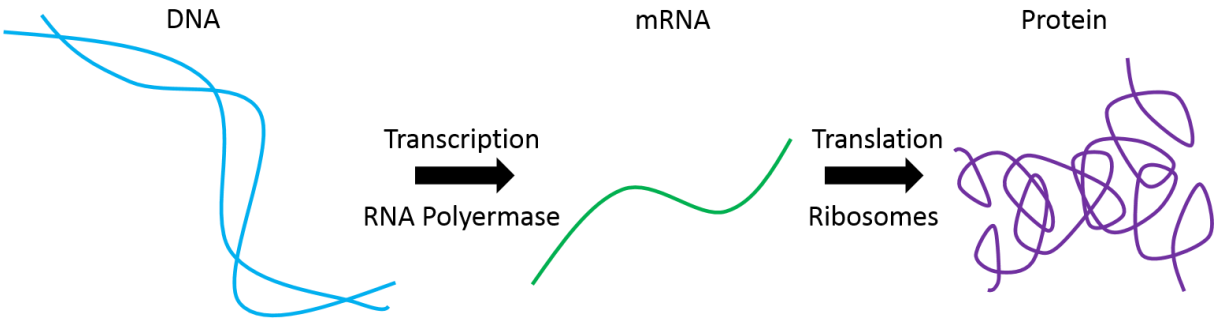

Figure 1: **Typical process of protein biosynthesis in cells** DNA (blue, left) is a double stranded molecule in the cell, which is transcribed to the single stranded mRNA (green, middle) by the enzyme RNA polymerase. mRNA is then translated into a protein (purple, right) by the ribosomes. The two steps, transcription and translation, are called protein biosynthesis.

In order to analyze the function or regulation of genes of interest (GOI), new recombinant DNA is artificially constructed. The process of generating recombinant DNA is often referred to as cloning [17]. In general, its goal is the construction of new genetic element combinations, which would not exist like that in nature [18]. The desired genetic elements are assembled in a plasmid (also called backbone-plasmid or vector), a circular double-stranded DNA molecule. Plasmids typically contain replication origins (ORIs) and selection markers for a certain organism, so that the plasmid DNA can be transferred into it and then be processed and replicated like any other DNA of the host organism. This enables, for example,

the study of gene regulation, cell differentiation or even human disease targets in a living organism. To enable transfection or transformation of cells in an efficient manner, cells need to be made artificially "competent", to increase their natural ability to take up foreign DNA. Cells are put under stress conditions (e.g. drastic temperature changes or high salt concentrations of surrounding media) to make their cell membrane and/or cell walls permeable for DNA more easily. The resulting so-called competent cells can be prepared in the laboratory using different methods [19].

2.1.3 Regulation of gene expression

Gene regulation is a process in which a gene's expression is modulated by DNA sequences located mostly up- or downstream of its DNA locus (before or after the gene), but also by other substances (RNA, proteins, hormones etc.). One of the most immediate interactions of a gene is with its promoter [20]. The promoter is typically situated immediately in front of the 5' end of the gene's coding sequence and contains the transcription start site (TSS), a binding site for RNA polymerase, as well as transcription factor binding sites. Without it, transcription cannot be initiated properly. Other sequences of the DNA influencing the regulation of genes are enhancers, which can be as far away as ten million base pairs (bp) from the gene itself [21], and silencers, which act as binding sites for transcription factors such as repressors to silence gene expression [22]. Promoters, silencers and enhancers all work to regulate gene expression on the transcriptional level. Promoter regions in front of the mRNA can also contain binding regions for RNA binding proteins, which can regulate RNA stability and processing and thereby gene expression, as well. Translational control of gene expression is often executed by the modulation of translation initiation. Inhibitory protein binding to parts of the translation initiation machinery can for example prohibit its binding to mRNA [23]. A prominent mechanism of translational gene regulation is riboswitches, which is described in detail in chapter 2.1.5.

2.1.4 RNA and regulatory RNA

Similar to DNA, RNA is composed of a chain of nucleotides. Differences between RNA and DNA are the sugar components that make up their nucleobases, with RNA containing ribose

whereas DNA contains 2-deoxyribose. Another difference is the substitution of the nucleobase thymidine in DNA by uracil in RNA. RNA is typically a single-stranded molecule, while DNA is mostly in double-stranded form. This leads to different structural properties of DNA and RNA; with DNA being typically more stable and rigid, while RNA is more flexible, and prone to self-degradation, as well as enzymatic attacks. The structural flexibility of RNA provides more freedom for spatial configuration, making it a versatile tool for the cell to carry out different functions [24, 25].

Transcription and translation are the two steps of protein biosynthesis, which is the process of turning genetic information into a protein. Transcription describes the copying of a DNA nucleotide sequence into a complementary and antiparallel RNA. The synthesis of this RNA is performed by the enzyme RNA polymerase II. The RNA transcript should consist of a perfect copy of the DNA sequence. If the copied DNA contains information for the building of a protein, the resulting RNA (mRNA) has to be processed before being translated into a protein by ribosomes. A mRNA transcript includes not only a gene's protein coding sequence, but regulatory sequences as well [26].

During the processing of the freshly copied mRNA (pre-mRNA, Figure 2), so-called "nonsense" regions of the RNA are removed, and structures adding stability (e.g. 5' cap and 3' poly(A)tail, Figure 2) are added. However, certain untranslated regions of the mRNA are not removed during mRNA processing, namely the 5' and 3' untranslated regions (UTRs). They are positioned before the start codon (5', "upstream") and after the stop codon (3', "downstream"). They play a role in the stability, localization and translational regulation of the mRNA.

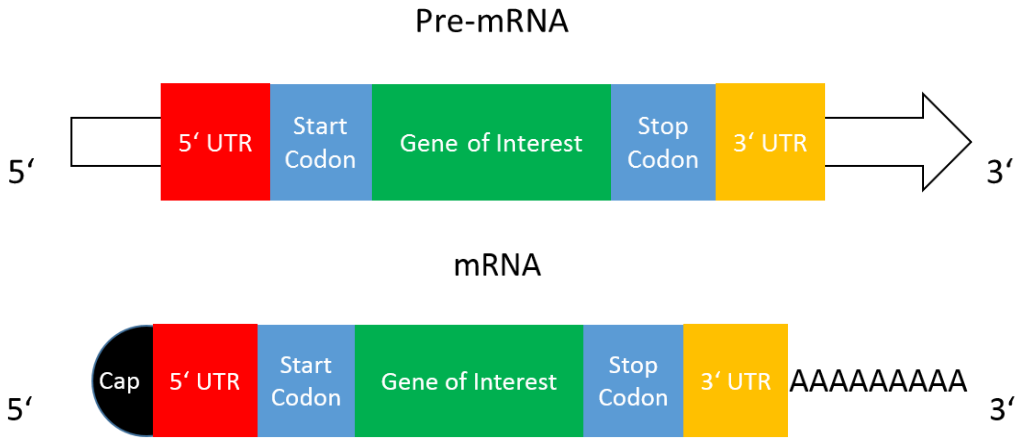

Figure 2: **Pre-mRNA and processed mRNA** Shown are the unprocessed mRNA transcript of DNA (pre-mRNA, upper section) and the processed, translatable mRNA (lower section). Both forms of RNA contain the 5' UTR on their 5' end, followed by the start codon and the gene of interest. After the stop codon, the 3' UTR follows. The processed mRNA also contains a 5' cap and a 3' poly(A)tail, to increase its stability.

There are different types of RNA in an organism, with the most important being messenger (mRNA), ribosomal (rRNA) and transfer RNA (tRNA). While mRNA provides the ribosome with information about protein construction ("coding RNA"), tRNA and rRNA are non-coding RNAs (ncRNAs) and part of the translation process in protein synthesis [26]. Other types of RNA play important roles in the regulation of gene expression, influencing transcription, translation, RNA maturation (splicing) as well as many other important functions in the cell. This includes, for example, micro RNAs (miRNA) and small interfering RNAs (siRNA), which can lead to mRNA degradation by RNA interference (RNAi) [27-31]. Antisense RNA (asRNA) is used by both pro- and eukarya to regulate gene expression using longer RNA molecules of typically more than 200 nt in length (long non-coding RNA, lncRNA) [32]. asRNAs can also impact transcription and RNA processing by binding complementary to a stretch of DNA or RNA [33]. In prokaryotes, small regulatory RNAs (sRNAs) control the translation initiation of genes or influence the activity of proteins by specifically binding to them [34]. They can also work on a post-transcriptional level by base pairing with the mRNA.

ncRNAs can work in *cis* (encoded at the same genetic location, but on the opposite strand to the RNAs they act upon), but also in *trans* (encoded at a distance from the gene locus of the RNA they act upon). An example of *cis*-acting gene regulation is riboswitches, a stretch of RNA typically located in the 5' UTR of a mRNA.

There are several advantages when gene expression is regulated via RNA alone as opposed to regulation in combination with proteins. It allows (i) faster regulatory responses, (ii) easier transfer of a single-step genetic control element to other organisms, and (iii) flexible combination with different downstream readout platforms for a maximum of regulatory outputs [14].

2.1.5 Natural riboswitches

Riboswitches are highly structured RNA sequence elements which are typically located in the 5' UTR of mRNAs (Figure 2). Discovered in 2002 [35-37], their study and their potential rapidly lead to the development of a new branch of RNA and genetic regulation research [38, 39]. Riboswitches often regulate processes related to metabolism by interacting with a metabolite (or other small molecules) of the cell. Conformational changes in their three-

dimensional structure are triggered by this interaction ("ligand binding"), and the expression of a gene downstream of the riboswitch is altered. Riboswitches consist of two domains, the so-called aptamer domain (2.1.6) and the expression platform [40]. The aptamer domain selectively recognizes its corresponding ligand and binds to it.

Common regulating mechanisms are transcription termination or translation initiation, less frequently ribozyme-mediated mRNA degradation or the control of splicing. Figure 3 shows a schematic on how re-structuring of the RNA can inhibit gene expression upon ligand binding.

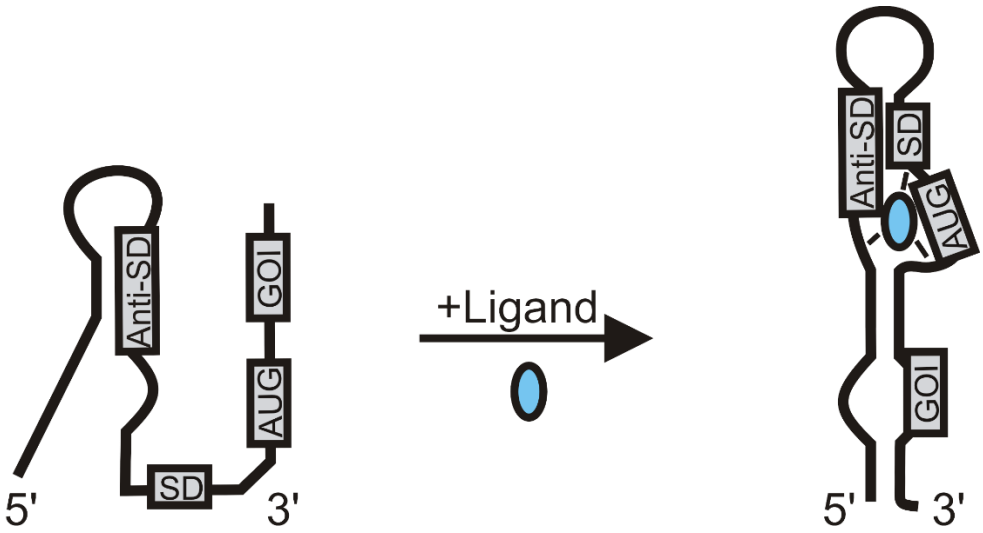

Figure 3: **Example of bacterial riboswitch function** Shown is the structural change a riboswitch sequence can undergo upon ligand binding (blue circle). Without ligand present (left), the RNA structure sequesters the anti-Shine-Dalgarno (Anti-SD) sequence, thereby leaving the Shine-Dalgarno (SD) sequence free to access by ribosomes, gene expression can take place. Addition of the ligand leads to a re-structuring of the RNA, bringing the Anti-SD and SD in close contact, so they can bind to each other. Ribosomes cannot access the SD anymore and gene expression is inhibited. Adapted from Lotz *et al*. [41].

Riboswitches are widely distributed in bacteria but are increasingly discovered in eukaryotes. A prominent example is the thiamine pyrophosphate (TPP) riboswitch, which is the only riboswitch known to date to occur in all three domains of life (Bacteria [35, 42], Archaea [43], and Eukarya (fungi [44, 45], plants [44, 46-49], and algae [50]). Interestingly, these examples of the TPP riboswitch, while composed of a highly conserved consensus core structure, can regulate gene expression using different mechanisms, as detailed below.

In bacteria, transcription termination can be regulated by the presence of a terminator structure consisting of the aptamer domain and a sequence complementary to the 3′ part of the aptamer. This structure can be formed or dissolved in a ligand-dependent manner, leading to an activation or inhibition of transcription (e.g. the different functionalities of the purine riboswitch [51, 52]).

The process of translation initiation can be regulated as well. In the absence or presence of a ligand, a stem-loop structure is formed between the aptamer domain and a sequence complementary to the Shine-Dalgarno (SD) sequence. This sequestering or release of the SD sequence blocks or activates translation initiation (e.g. the SAM-III riboswitch and the Adenine riboswitch, resp. [53, 54]). Other, less common methods for riboswitches to regulate gene expression are through the formation of ribozymes (self-cleavage of RNA upon ligand interaction by the *glmS* riboswitch [55] or splicing in eukaryotes (by the TPP riboswitch [48]). While most riboswitches are located in the 5' UTR of a DNA, typically between promoter and the gene itself ("*cis*"-acting riboswitches), they can regulate also gene expression from a faraway DNA region (regulation in "*trans*",), operating e.g. like a small RNA [56].

Most natural riboswitches bind selectively to second-messenger signal molecules like cyclic di-guanosine monophosphate (cyclic di-GMP**)** [57] or to coenzymes like TPP or *S*-adenosylmethionine (SAM) [58]. These molecules can both be generated from RNA nucleotide building blocks, which is one of the reasons that the so-called "RNA world" theory is widely accepted today [59]. In the so-called time of the "RNA world", no proteins or DNA had evolved yet, and their current roles had to be carried out by RNA, relying on other RNA-derived substances [36, 59, 60]. The natural riboswitches of today are considered descendants of these old regulatory systems, with some on the edge of extinction [61].

It seems feasible to make use of these natural riboswitches in a synthetic biology context. The study of natural riboswitches also can teach synthetic biologists how to make new, synthetic riboswitches (2.1.9) [62].

2.1.6 Aptamers

Aptamers are small single-stranded oligonucleotides, typically consisting of ribonucleic acid (RNA). There are also examples of single strand DNA (ssDNA) aptamers [63], as well as peptide aptamers [64]. The common feature of aptamers is their ability to bind a target molecule (ligand) with very high affinity and specificity [65, 66]. Because of that they are often compared to antibodies, being described as 'chemical antibodies' [67]. Their selective discrimination can be so specific that they are able to differentiate even between enantiomers [68, 69].

Aptamers typically consist of 30 to 70 nucleotides and take on unique three-dimensional structures upon ligand recognition [70].

The aptamer binds specifically by partially or entirely enveloping its target-molecule, coupled with non-covalent molecular interactions between the aptamer and its target. These interactions include most prominently hydrogen bonds, base-stacking and electrostatic interactions [71].

Aptamers are typically synthetically produced, mostly by using the *in vitro* method "SELEX" (systematic evolution of ligands by exponential enrichment (2.1.7) [72, 73]), which was first described in 1990 by two research groups in parallel (Tuerk & Gold, Ellington & Szostak [72, 73]). In nature, they occur as the sensing domains of riboswitches, responsible for binding a target molecule and thereby effecting a change in gene expression (2.1.5, 2.1.9).

Aptamers are also increasingly in the focus of researchers looking for new therapeutic approaches. Next to their relatively small physical size and molecular weight (Typical IgG antibody: 150 kDA [74]; typical aptamer size 6–30 kDa [75, 76]) they unite a flexible structure, with a quick, easy and reproducible production (low batch-to-batch variability), as well as adding the possibility of chemical modifications [77-81]. On top of that, they can be highly stable and show a very low immunogenicity and toxicity [60, 82, 83].

There is evidence that many aptamers are easily internalized into cells upon binding to cellular receptors [67]. Next to their potential use as direct therapeutics this could make them useful carriers for the in-organism delivery of therapeutic small interfering RNAs (siRNAs), microRNAs and conventional drugs as well [67].

The advantage of administering aptamers as medication opposed to having the organism produce them, lies in the possible chemical modification of specific nucleotides [81], which can dramatically increase the half-life of aptamers within the organism (less than 10 min when unmodified [80]).

Until the conclusion of this thesis, there has been only one FDA approved aptamer drug available (pegaptanib/Macugen® in the therapy of exudative macular degeneration, [84, 85]). However, several further aptamer drugs are presently undergoing clinical trials, some having reached late-stage phases [86, 87]. Especially cancer treatment emerges as a new field of application, with aptamers being considered not only as cancer therapeutics, but also as cancer biomarkers, *in vitro* diagnostics and *in vivo* imaging systems [88].

The generation of novel aptamers and their potential application in synthetic biology are at the core of the presented thesis. In the course of this thesis, novel aptamers selectively binding to one isoform of a photo-switchable molecule should be developed.

2.1.7 SELEX

SELEX (systematic evolution of ligands by exponential enrichment) is a method for the development of aptamers, in which an iterative selection procedure is carried out [72, 73]. The starting point of each SELEX is a random combinatorial library (or "pool") of 10^{14}-10^{16} sequences, with the amount of potential sequences typically limited by the synthesis capability of the library supplier [89]. Even though larger libraries of up to 10^{20} oligonucleotides are technically feasible [90], they are very rarely used in practice [91].

While DNA and peptide libraries exist, this thesis only discusses RNA libraries. RNA libraries are prepared by *in vitro* transcription of a chemically synthesized DNA pool (2.1.8). Specific aptamer sequences can be enriched during SELEX and dominate the library population, hence the term "evolution" in the method's name [67].

At the start of each SELEX, an RNA library is incubated with its target molecule (typically immobilized on a non-reactive carrier material) in a suitable buffer system. RNA aptamers with a binding affinity for the target molecule (ligand) are separated from the rest of the library in a partitioning or selection step. Commonly, after incubating the RNA with the target molecule, several washing steps occur, to remove any unbound aptamers that do not show affinity to the target molecule from the library. The ligand-binding aptamers are recovered in an elution step, which can be carried out using unspecific means or specific elution. Unspecific elution employs thermal or chemical denaturation of the RNA-ligand binding, complexation of divalent cations with EDTA [68], or the application of a salt gradient [92]. Specific elution ("affinity elution") is carried out by the incubation of the bound RNA-ligand complex with a highly concentrated free target molecule solution. Competition between the free and immobilized target molecule leads to the elution of aptamers, however binding aptamer sequences can be lost in this step if they remain bound to the immobilized target molecule. Amplification of the aptamers is performed through reverse transcription into cDNA (complementary DNA) and subsequent amplification by polymerase chain reaction (PCR). During the PCR, oligonucleotides introducing a T7 polymerase promoter are used,

leading to a pool of aptamer PCR products which can be immediately used as a template for *in vitro* RNA transcription. The resulting RNA constitutes the potentially enriched aptamer pool for the next round of SELEX.

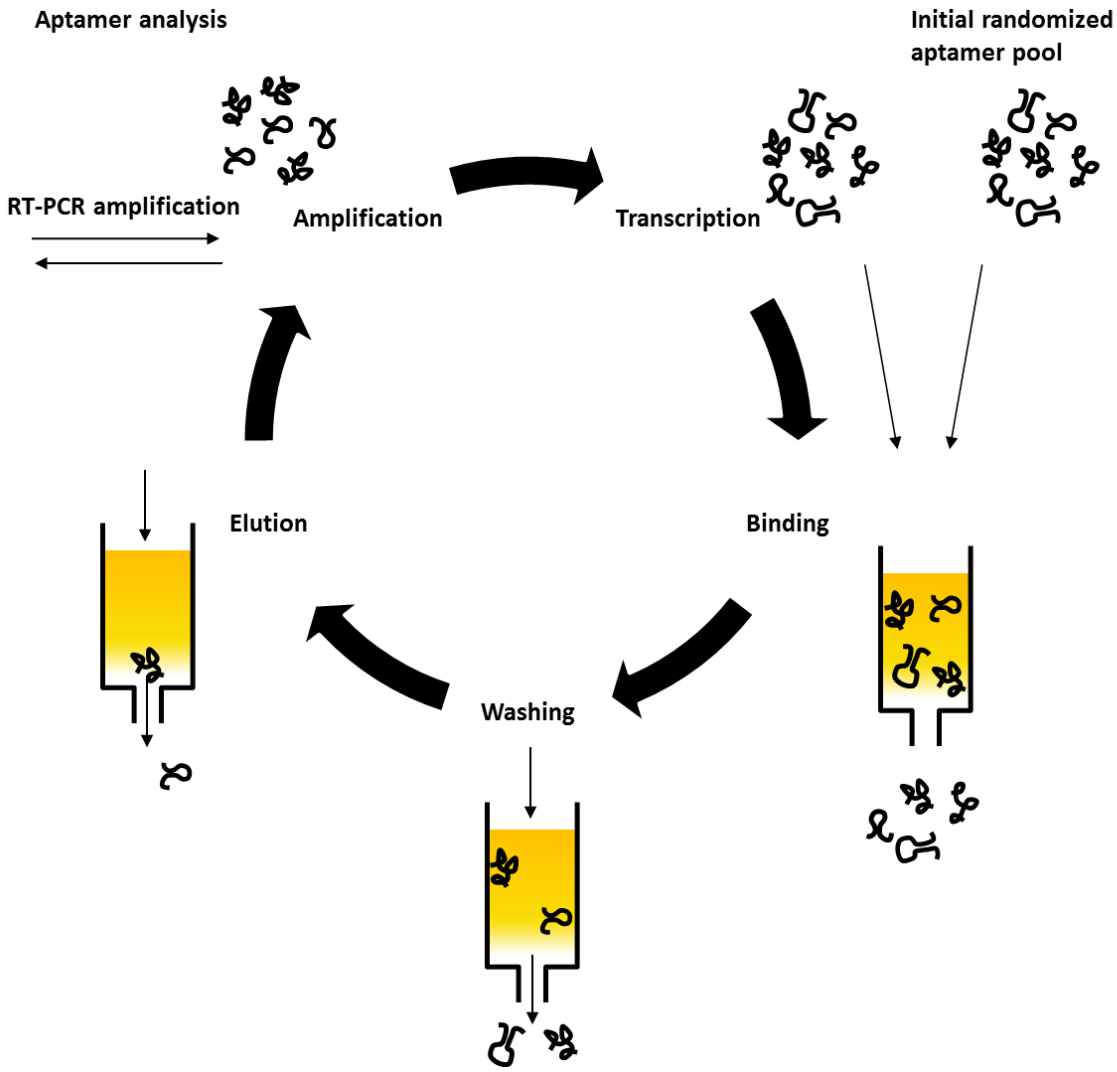

Figure 4: **Schematic representation of the SELEX process**. Shown are the five main SELEX steps of every round, binding, washing, elution, amplification and transcription of the RNA aptamers. Prior to the first SELEX round, an initial randomized RNA aptamer pool is applied to a ligand-derived column and binding of the aptamers occurs. If the progress of a SELEX is monitored, samples of amplified aptamers can be taken for analysis following the RT-PCR amplification step.

Particularly in the first rounds of a SELEX, a negative SELEX step is carried out additionally. In this step, the RNA library is incubated with the non-derivatized carrier material prior to the selection step, to avoid enriching RNA aptamers that show primarily an affinity to the carrier. Another common technique in SELEX is counter selection. To enable the generated aptamers to differentiate between closely related molecules, the RNA library is incubated with the

undesired target molecule prior to incubation with the target molecule, as demonstrated for the theophylline aptamer [65].

Typically, the progression of a SELEX is monitored as it advances. This can be done via radioactive labelling of nucleotides incorporated into the RNA during transcription. This way, all incubation fractions the RNA undergoes (with the carrier material, with the target material, washing steps as well as elution) can be quantified using "radioactive counts" (measured in counts per minute, cpm). Over the course of the different SELEX rounds, an increase in cpm in the elution fractions can indicate an enrichment of RNA aptamers which have been eluted from the immobilized target. Most SELEX experiments require eight to fifteen rounds to show enrichment of one or more aptamer families [93]. Aptamers from rounds that show enrichment by measurement of cpm can be integrated into backbone-vectors and amplified in single-clone bacterial cultures (typically *Escherichia coli*) to obtain enough genetic material for sequencing. That way, aptamer sequences can be identified and compared to each other. Families (groups of aptamers with minor sequences differences) and conserved motifs (sequence stretched within a larger sequence) can be identified and secondary and tertiary structure predictions can be carried out using bioinformatic tools, such as mfold (Table 12), LocARNA (Table 12, [94, 95]) or SICOR [96].

Once the sequence of aptamers is known, further experiments like affinity assays (3.2.15), structural probing (2.1.14, 3.2.14) and tests regarding their ability to act a riboswitch can take place (2.1.11, 3.3.8).

Often, the most abundant aptamers from a SELEX round show good binding abilities. But in some cases, rarely occurring aptamer sequences ("orphans"), without any structural or sequence familiarity to the other aptamers discovered, show the best binding properties [97]. One of the reasons for this can lie in the bias introduced into the RNA libraries in every round by steps such as reverse transcription, PCR or *in vitro* transcription [98-100]. Aptamers with e.g. a strong secondary structure might be artificially decreased in these steps, because the enzymes involved have difficulties processing them, even though they might be some of the best aptamers fitting to the target molecule.

There are many different protocols for SELEX, sometimes based on very different and complex techniques, such as surface plasmon resonance spectroscopy (SPR) [101-103] or capillary electrophoresis (CE) [104]. When a new aptamer is to be generated by SELEX, the choice of the method is often based on the later application of the aptamer (e.g. if the aptamer is to be used as a therapeutic biomarker, whole cell SELEX might be an appropriate tool [105,

106]). Otherwise, the decision on a SELEX method often depends on the equipment and know-how already present in the research group [107, 108]. The most common method for SELEX remains the immobilization of the ligand on a matrix, so that column based SELEX can be carried out. However, all SELEX protocols, even those using DNA or peptide libraries, share the core steps described above: target binding, partitioning of binding aptamers, aptamer recovery and re-amplification of aptamers.

The SELEX protocol used during this thesis is based on ligand immobilization on a non-reactive resin (see Figure 10). The resin is placed inside a column, allowing solution used for RNA binding, washing and elution to flow through it and the collection of these liquid fractions for process monitoring. The SELEX method is referred to as "affinity SELEX" in the course of this work.

2.1.8 Aptamer libraries

The starting library used for any SELEX determines the basic elements the final aptamers show, namely their size and overall structure. An aptamer in an RNA library typically consists of three different sequence stretches: 5' and 3' binding regions ("constant regions") for oligonucleotides used in re-amplification of the recovered aptamers, as well as the core region in which a set number of nucleotides in a randomized composition later mostly makes up the reactive center of the aptamer. However, it is possible that the constant regions are involved in the structural folding of the aptamer, more rarely also in the binding of the target molecule [109]. The number of randomized nucleotides of the core region is usually chosen to be between 30 to 70 nucleotides [70], but more complex libraries of 120 nt [110] or 134 nt [111] exist and have led to the selection of functional aptamers. The number of molecules usable in the first round of SELEX is typically limited to 10^{14} to 10^{16} sequences, due to synthesis limitations by the library supplier [89, 90]. Hence, any aptamer library with more than 25 randomized nucleotides cannot be covered in its entire sequence space. The theoretically possible number of sequences in the library is calculated as 4^n, with 4 representing the four possible nucleotides (A, C, G, T/U), and *n* the amount of randomized nucleotide positions. A typical library of 30 nt therefore contains 1.15×10^{18} sequences, a 70 nt even 1.39×10^{42} sequences. Therefore, if a SELEX against a target molecule is not successful, it could be

possible that the application of a different library, even of the same size, could contain binding aptamers not found in the particular library used.

A strategy that has been used in the generation of SELEX libraries, is pre-structuring parts of the aptamers. Incorporating sequence stretches that reliably fold into certain structures (e.g. stem-loops) are supposed to increase the overall stability of all aptamers generated. In turn, this is supposed to lead to more complex and more ligand-affine aptamers [112, 113].

In order to generate aptamers with a high target molecule affinity, one aim of SELEX has often been to generate aptamers with a low dissociation constant (kD), a measure indicating how strongly a molecule binds to another one (equilibrium dissociation constant between an aptamer and its ligand) [114-116]. To achieve this, the stringency of SELEX conditions can be increased during different rounds. Ways to increase stringency can be the introduction of more washing steps, elution of the RNA with a lower target molecule concentration or reducing the incubation time of the RNA with the immobilized target before the first wash steps.

So far, SELEX has been performed against a multitude of different targets. From ions like Zn^{2+} [117], small molecules like amino acids [118], up to cells [119] and even entire organisms [120], the range of SELEX using a variation of libraries can be enormous.

Particularly small molecules are of interest for biotechnological and pharmaceutical application (2.1.6). They do pose a challenge in SELEX, however, as they do not have as many functional groups in which interactions with the aptamer can take place, as for example proteins. Small molecule targets with a lower number of rotatable bonds and thus fewer degrees of freedom are said to have better interaction with macromolecules like RNA aptamers [121].

During this thesis, different libraries for SELEX were used and are discussed. The process of optimizing the production of the initial library DNA template is described, different SELEX procedures were tested and compared, and the reasoning for the finalized SELEX protocols are discussed. New findings regarding the development of small molecule binding aptamers may improve current knowledge in the field. The insights gained from this thesis could therefore help to improve further RNA based research and may possibly enhance the effectiveness of other SELEX studies.

2.1.9 Synthetic eukaryotic riboswitches

RNA is a molecule of great interest to synthetic biologists, as it unites several useful functions in one molecule: it can act as both a sensor and effector, it can take on highly specific three-dimensional structures and it can sense ambient conditions like temperature, acidity, or a specific molecule's concentration [55, 56, 122-125]. Therefore, the development of synthetic aptamers able to fulfil such specific functions as part of a riboswitch is of major interest to the field of synthetic biology. Coupling such synthetic aptamers to an expression platform could deliver synthetic riboswitches tailored to specific applications. For example, transcriptional riboswitches have been constructed in a modular approach combining expression platforms from natural riboswitches with aptamer domains both derived from riboswitches and selected *in vitro* [126, 127]. The best-known synthetic riboswitches in bacteria are using the theophylline aptamer as their sensing domain [128, 129].

While there are many natural riboswitches in bacteria, in eukaryotes only one has been discovered so far [130]. The need to develop synthetic riboswitches for eukaryotic systems is therefore even greater than for bacteria. A few well-working examples of eukaryotic synthetic riboswitches exist, regulating gene expression depending on the presence of the ligands tetracycline, neomycin, and ciprofloxacin [131-133]. They were generated by inserting selectively ligand binding aptamers identified through SELEX (2.1.7) into the 5′ UTR of a gene of interest on a plasmid vector. Binding of the aptamer domain to the ligand is expected to lead to a restructuring of the riboswitch, generating a "roadblock" which the translational machinery cannot pass, thereby inhibiting gene expression. In order to screen aptamers for this restructuring capability, the next step towards a riboswitch typically involves an *in vivo* screening approach in the organism of choice to identify functional genetic constructs. These constructs could then be further analyzed and optimized for other potential applications. This way, synthetic riboswitches have already been used to control pre-mRNA splicing [134-136], microRNA processing [137, 138], or internal ribosome entry site-mediated translation initiation [139]. Next to *in vitro* generation of new aptamers and improvement of *in vivo* screening systems to identify functional riboswitches, other steps towards the generation of new riboswitches are *in silico* design and structure prediction methods [140-142]. Particularly structure prediction methods are helpful for the design of new experiments, and are frequently referenced and used in this thesis.

The development of an aptamer able to bind to a novel small molecule would be an important result of the presented thesis, whereas novel synthetic riboswitch working in eukaryotic organisms would significantly enrich the toolbox of synthetic biologists.

2.1.10 Yeast as a model organism for the development of synthetic riboswitches

Saccharomyces cerevisiae is a prominent model organism in molecular biology, partly because humans have thousands of years of experience working with this yeast in the production of beer, bread etc., and partly because it is an example of unicellular eukaryotes, which can be grown fast and easily [143-145]. In biotechnology yeast cultures are widely used as cell factories to produce various proteins [146], as well as a model organism to study gene regulation.

As eukaryotes, *S. cerevisiae* cells are able to glycosylate proteins, meaning they are able to attach sugar chains to proteins, a necessity for the function of many biotechnologically relevant proteins [147]. Furthermore, they are able to secrete these (glyco-) proteins into the surrounding nutrient medium – a big advantage for biotechnologists. The proteins produced in yeasts are identical or very similar to the proteins of animals or of humans, making yeast a focus of many research groups and a tool in genetic engineering as well as synthetic biology [148].

Gene regulation in yeast cells is very similar to other eukaryotes. Therefore, riboswitches developed in yeast would be expected to work in a comparable manner in other eukaryotic cells, e.g. human cell lines. Corresponding examples of synthetic riboswitches have been published, e.g. the recently developed ciprofloxacin-riboswitch [133]. This shows that riboswitches developed in yeast cells are not necessarily limited to their genetic context, but applications in fields like novel therapeutic approaches are conceivable.

For this reason, research in this thesis carried out in *S. cerevisiae* could be a valuable addition to the analysis of synthetic biology applications in other eukaryotic systems, such as humans.

2.1.11 *In vivo* screening

The development of novel synthetic riboswitches from aptamers is not trivial and has, particularly for application in eukaryotes, been only successful a handful of times [132, 133,

149]. While a SELEX can enrich highly specific aptamers, these aptamers do not necessarily function as riboswitches *in vivo*.

The typical process of generating a synthetic eukaryotic riboswitch consists of the integration of an aptamer into the 5' UTR of a gene of interest (often a reporter gene) [132]. If the aptamer can recognize and bind its ligand in the biological context, the scanning process of the ribosomes and thus translation in the presence of the target molecule would be inhibited. Depletion of the target molecule would lead to the resumption of protein expression [150, 151].

For the first verification of a functional riboswitch, a screening method developed by Weigand *et al*. can be applied, as in this stage it is not important, whether the target molecule is photo-responsive or not [132]. Weigand *et al*. could show that for a SELEX-enriched pool of neomycin-binding aptamers only a few sequences could be used as switching elements in *S. cerevisiae*. Only aptamers, which were poorly structured in the unbound state but underwent a distinct conformational change upon ligand binding, were also able to regulate translation in a ligand-dependent fashion. As many aptamers derived from SELEX already exhibit a preformed, stable tertiary structure in the absence of the ligand, this seems to limit their application as riboswitches, and thus makes *in vivo* screening of *in vitro* enriched pools almost inevitable [129, 152].

The *in vivo* screening method is based upon the integration of an aptamer library in the 5' UTR of the reporter gene GFP (green fluorescence protein) on a plasmid backbone. A large range of plasmids containing the different aptamers is generated, and yeast cells are transformed with the DNA. After growth on selective solid media, cell colonies (clones) can be individually transferred into multi-well plates and grown in liquid culture. The resulting cell culture can then be split in two identical, parallel samples. To only one of the samples, a defined amount of the ligand molecule is added, and the culture is grown in its presence.

2.1.12 Fluorescence analysis

Fluorescence measurement of cell cultures has become a standard analysis method when fluorescent proteins or compounds are used in biological settings [153]. Particularly proteins from the GFP family are used in molecular biology to accurately quantify, localize or even track cellular processes [154-158]. The measurement of GFPs' fluorescence involves using a

beam of light (with a wavelength of 395 nm) that excites the electrons in GFP and causes them to emit light; typically of a wavelength of 509 nm [159]. This emitted light is then detected and quantified as "counts" of detected signals on the detector. A biological sample producing a lot of GFP would emit many more counts of fluorescence than a sample not or barely producing GFP.

Often, sophisticated machines are used to measure fluorescence levels. Here, the approaches can differ vastly as well. Two such methods used to measure a lot of samples in parallel are described in the following.

Similar to measuring absorbance of a cell culture in single cuvettes in a spectrophotometer (Table 3), a microplate reader can be used to measure multi-well plates (typically 96 wells). A beam of light of a certain wavelength is used to either excite electrons of molecules in the cell culture wells and thereby enable fluorescence measurements or used to measure a culture's density using its refractory index to measure absorbance. Microplate readers typically allow the beam of light to pass through the sample from above or below, giving a measurement of the mean fluorescence or absorbance of all cells in the culture.

A second method to measure many samples in parallel is flow cytometry. Opposed to a microplate reader, fluorescence is not measured as a mean of the culture, but individual cells are moved through a "flow cell" (measurement chamber). Inside the flow cell, the cytometer measures the fluorescence level of each individual cell with a sensor. The output of the measurement is the mean and median fluorescence values of a set number of single cells. The cytometer can measure several fluorescence levels per cell as well. This is useful e.g. to measure GFP and the fluorescence protein mCherry at the same time in the same cell. Some cytometers contain a sorting system next to the fluorescence sensor (fluorescence-activated cell sorting, FACS). Using previously defined parameters, the cell sorter is able to divert single cells fitting these parameters (e.g. emitting a certain wavelength of light) into separate tube for collection. Cell sorting is a powerful tool to divide large diverse cell populations into subgroups or even single cells for later use.

In this thesis fluorescence measurements were used to investigate the influence of riboswitches on the production of fluorescent reporter genes. FACS was used to sort cells according to their individual fluorescence levels.

2.1.13 Next generation sequencing (NGS)

DNA sequencing has been a standard method for molecular biologists since the 1970s [160-162]. Sequencing methods have continued to improve since then, leading to a selection of commercial sequencing facilities available. The development of automated DNA sequencing has enabled the Human Genome Project in the early 2000s to analyze the first human genome in its entirety [163-165]. Since then, large-scale sequencing techniques have evolved dramatically, making the analysis of large amounts of DNA affordable and therefore useful for a broad range of experiments. The application of next-generation sequencing (NGS) or deep-sequencing methods for SELEX experiments allows detailed analysis of individual selection rounds. Applying NGS to SELEX can make decisions for downstream experiment like *in vivo* screening or *in vitro* binding studies of aptamers easier and sheds light into the "black box" SELEX has been described as [166].

2.1.14 Structural characteristics and analysis of RNA aptamers and riboswitches

As single-stranded nucleotides RNA aptamers can take on complex structures. Typical secondary structure elements are hairpins, internal loops, nucleotide bulges and junctions [167]. Tertiary structure elements are possible as well, such as pseudo-knots, kissing-complexes and tetraloop-tetraloop interactions [61, 168]. Tertiary structures can additionally be stabilized by kations [169].

In the formation of aptamer-ligand complexes, electrostatic interactions, stacking interactions as well as hydrogen bonds between the functional groups of the ligands and the RNA bases play an important role.

Aptamers are very flexible molecules and can adopt more than one conformation and several complex tertiary structures without ligand [170, 171]. Therefore, their structural analysis is at the same time highly important and laborious. The binding process to a target induces a conformational change in the aptamer. This is why most aptamer structures to date are only solved in combination with their respective target molecule, as only the binding of the ligand leads to the adoption of a rigid and relatively inflexible structure [172]. This allows structural analysis which comprises time-consuming methods, necessary to capture accurate information. There is a number of these complex methods, all allowing for their own advantages and weaknesses. Smallangle X-ray scattering (SAXS) analysis can deliver

information on different conformations of a riboswitch in solution, but it does not yield high-resolution insights [173, 174]. As a contrast, X-ray crystallography [175-177] leads to very highly resolved results, but can only show the details of one "time-frozen" conformation, which is why X-ray crystallography is typically carried out with the aptamer's ligand present. Nuclear magnetic resonance (NMR) spectroscopy [178, 179] is able to deliver atomic-resolution information on several conformational states in solution, but its limits regarding molecule size are dramatic, with aptamers and riboswitches often above the upper threshold [180, 181]. Despite of these various limitations, plenty of aptamer and riboswitch structures have been solved (in the case of NMR, often their reaction core motifs). A lot has been and is being learned by the application of these methods. To get a comprehensive overview over a molecule's structure, however, it can be necessary to combine several of these methods, which takes a lot of expertise and often years to complete. A new method emerging to reduce a few of these obstacles is single-molecule fluorescence resonance energy transfer (smFRET) [172, 182, 183]. It has recently been used to study the dynamics of ligand-free riboswitch structures in particular, as the observation of one isolated molecule makes signal-to-noise compensation of such flexible structures much easier and even allows the following of kinetic events inside the sample. Folding of RNA can be observed in "Live Mode" using this technique [184].

Altogether, RNA structure determination remains a complex issue. As researchers in the aptamer and riboswitch field often lack the expertise or equipment to employ these high-tech methods, faster, low-tech methods are often employed as a first look into RNA structure [51]. One such method is in-line probing [185, 186]. This probing method exploits the inherent instability of RNA single-stranded regions. Single-stranded RNA is more flexible and can perform nucleophilic attacks on itself, taking on the so-called "in-line position", leading to a self-degradation over time [186, 187]. Double stranded RNA regions, on the contrary, are more stable and less prone to self-degrade, a behavior which is mimicked by single-stranded nucleotides that are part of ligand molecule interactions. Incubating an RNA of interest over a longer time period (up to several days) with the target molecule and the subsequent visualization of the degradation bands on a gel leads to a distinct pattern giving information on stable und unstable regions in the RNA. Incubation of the RNA together with a ligand molecule leads to a modified degradation pattern, highlighting ligand binding nucleotides or regions within the RNA (Figure 5) [188].

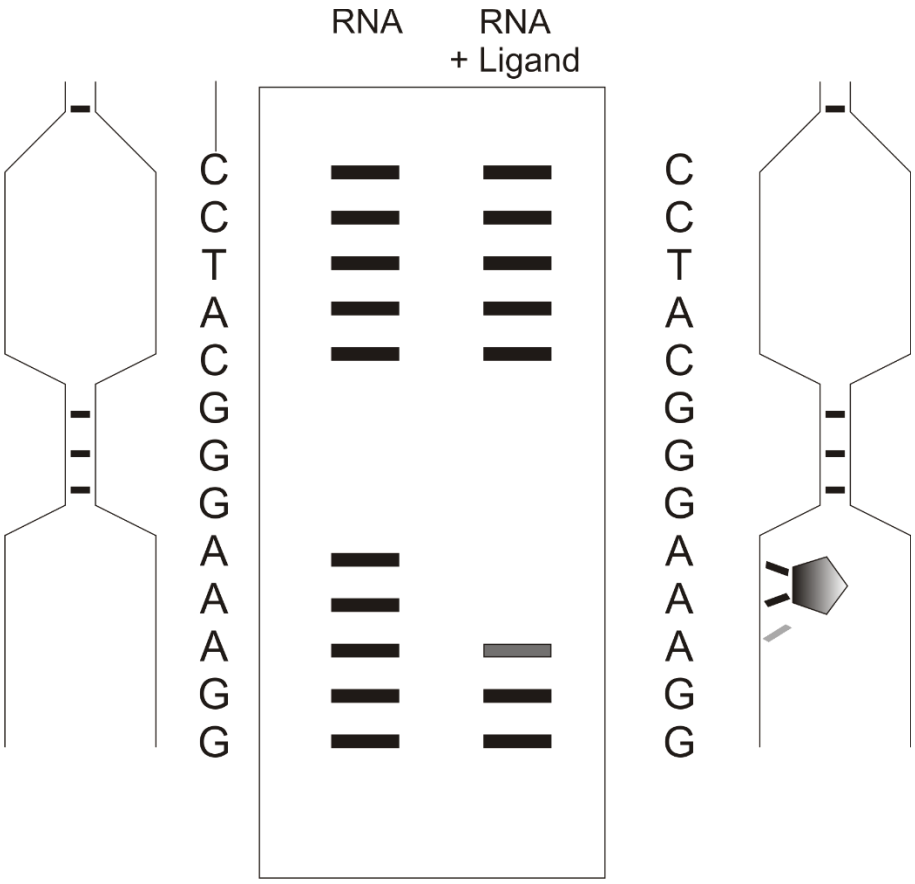

Figure 5: **Schematic depiction of an in-line probing gel.** Shown is an exemplary cleavage pattern of RNA incubated with and without ligand. Changes occur in the secondary structure configuration of the RNA upon binding of the metabolite (RNA structures left and right of the gel). Nucleotides locked into position by ligand binding are less flexible and less likely to self-cleave by taking on the in-line conformation, thus cleavage bands are reduced. The figure was adapted from Regulski *et al*. [186].

Adding variations of ligand concentration to the RNA even allows for the approximation of the dissociation constant (kD). As the in-line reaction can be carried out in aqueous solution, it yields structural information which can be more likely to reflect the natural state of the RNA inside their organisms. Because in-line probing and other structural probing methods yield results in a fast and easy manner, without the need for sophisticated and specialized material, many researchers in the aptamer and riboswitch field first apply in-line probing to obtain information on the secondary structure of putative riboswitches [51]. For the mentioned reasons, in-line probing was used in the course of this thesis as well.

After growth, the two parallel cultures (with and without ligand) are analyzed and compared to each other. As an aptamer acting as a riboswitch should reduce gene expression (and therefore GFP fluorescence levels) when its ligand is present, the GFP value of the culture with ligand should be lower than in the culture grown without ligand.

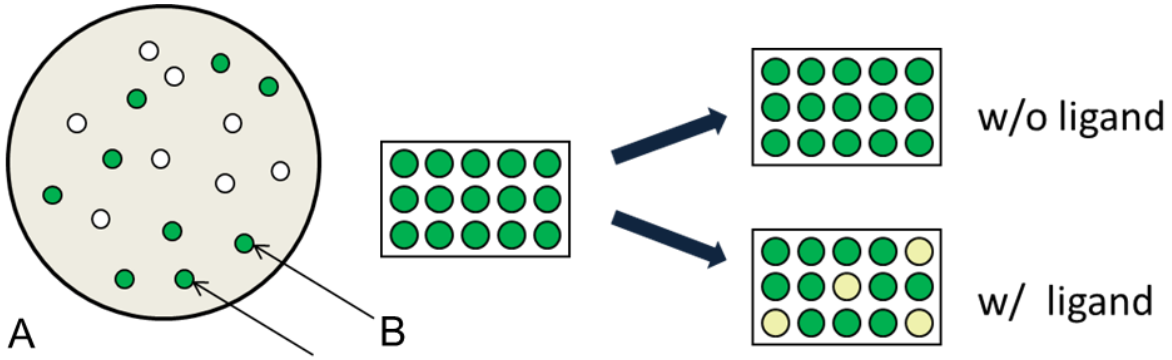

Figure 6: Schematic *in vivo* screening process A Shown is a solid media plate with yeast colonies displaying different levels of GFP fluorescence, low or none (white) and medium and high fluorescence (green, arrows). **B** Inoculated and grown yeast colonies in a multi-well plate showing medium or high fluorescence (green) are split into two new multi-well plates. Of the two plates, one contains ligand in the medium, which leads to a decrease in GFP expression when a riboswitch can interact with it (white wells in plate). Comparison of the fluorescence levels of corresponding wells between the two wells can therefore lead to the identification of a ligand responsive riboswitch. The figure was adapted from Weigand *et al*. [132].

The regulatory activity for an aptamer/riboswitch is calculated as the quotient of the GFP values of the two cultures (Equation 1).

Equation 1: **General calculation of the regulation factor of a riboswitch using a fluorescence gene**

$$\frac{\text{GFP fluorescence without ligand}}{\text{GFP fluorescence with ligand}} = \text{regulation factor (x} - \text{fold)}$$

As controls, plasmids without GFP expression and with constitutive GFP expression (GFP ON and GFP OFF) are grown and measured in parallel to any experiment. Aptamers developed in the course of this thesis were to be tested in such an *in vivo* setting, to examine any potential riboswitch abilities they might possess.

2.2 Motivation and relevant previous results from the Suess and Heckel group

2.2.1 Development of a light-switchable riboswitch

Synthetically produced aptamers have the potential to act as a riboswitch (2.1.9). Light-switchable aptamers could bring advantages if used as part of a riboswitch in a biological application, as light is an ideal trigger for reactions in the cell. It can be controlled spatially, temporally and in terms of its intensity without major technical effort. Most cells do not respond to light as a stimulus, so other cellular processes are not disrupted [189-191]. Light of an adequate wavelength does not damage cells or their content, but as most cells are at least partially translucent, it can reach the inner regions and stimulate a response from a light-sensing aptamer or riboswitch [192-194]. Thus, light-switchable riboswitches could be promising tools for genetic circuits, as they would add another synthetic class of orthogonal triggers to the "toolbox" of genetic engineers, particularly when they show a reversible turning "on" and "off" of gene expression (Figure 7). In nature, no mechanism is known in which nucleic acids act as photoreceptors and regulate gene expression [195].

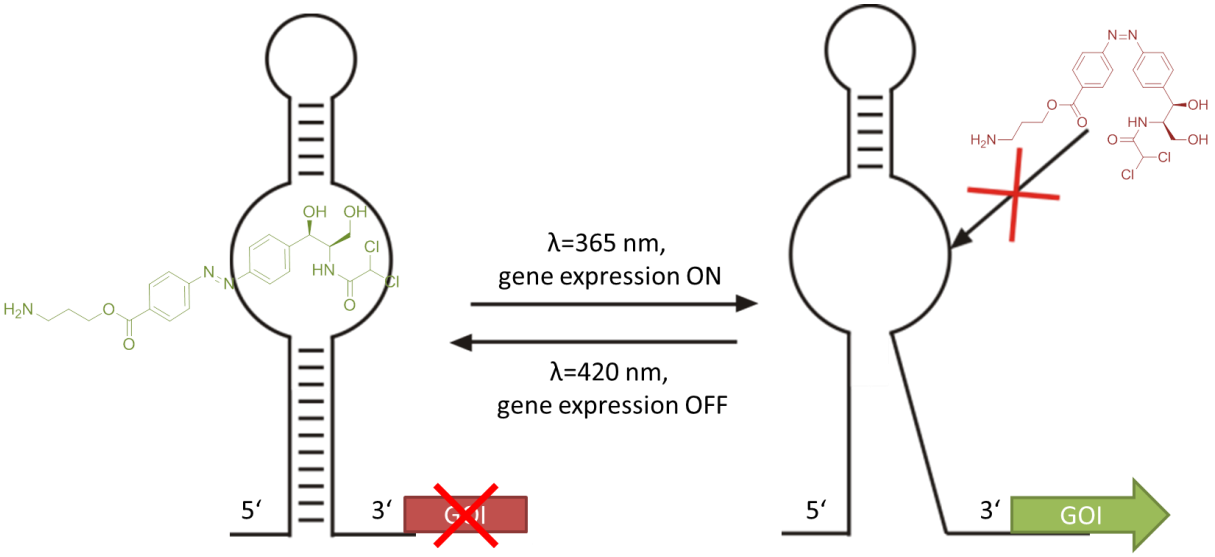

Figure 7: **Schematic representation of the function of a synthetic light-regulated riboswitch** Shown is a riboswitch on the left, able to bind the *trans* isoform of azoCm, and thereby repressing gene expression. azoCms *trans* state is induced by irradiation with light of λ=365 nm. On the right, the conformation of azoCm has been switched to *cis*, using light of λ=420 nm. The *cis* isoform cannot be bound by the riboswitch anymore, and gene expression is turned on. The system is reversible upon changing of the irradiation wavelength. The figure was adapted from Rudolph [196].

Light-switchable aptamers developed in this thesis should therefore also be tested regarding their regulative functions in an *in vivo* setting within living cells. Because not all aptamers

working well *in vitro* show a functionality of a riboswitch *in vivo*, as many aptamers as possible from an enriched SELEX round were tested regarding their regulation ability (see 2.1.11). As this photo-responsive riboswitch would have two responsive states, dependent on the wavelength of light surrounding the system, *in vivo* analysis of the regulative ability of the riboswitch could be carried out in two stages as well. Firstly, binding and the subsequent structural change of the riboswitch to its target would need to be verified. Secondly, the reversibility of this binding upon irradiation with a fitting wavelength would need to be verified.

2.2.2 azoCm - a light-switching molecule

During the last decade, light controlled tools have come into the focus of the biological and biochemical research area as they offer spatial and temporal control of processes [189]. The development of new light sources, mainly light-emitting diodes (LEDs) and light amplification by stimulated emission of radiation (lasers), have benefited this research area. Light from these sources can be controlled to only emit a certain wavelength, without emitting additional, potentially harmful, wavelengths. Regulation of biological processes by light has already been carried out in transparent organisms such as the nematode *Caenorhabditis elegans* or the zebra fish *Danio rerio* [193]. In large, non-transparent organisms, light control of reactions close to the skin surface has been carried out. Recently, research groups have demonstrated that ultraviolet (UV-) light can penetrate the tissue of mice [194]. Even experiments with glass fibers inserted into the brain of mice to control behavior have been executed [197].

Previously to this thesis, Dr. Thomas Halbritter from the Heckel Lab in Frankfurt has developed a light-switchable small molecule; called azoCm (Figure 8, Table 2 [198, 199]). azoCm is a molecule of the azobenzene group. It can undergo a photochromic isomerization process, meaning it can reversibly switch from its *trans* to its *cis* conformation. Both isomerization states have different absorption spectra [198]. The basic structure of azobenzenes consists of two phenyl rings, which are connected by nitrogen double bonds (*N=N*). These two nitrogen atoms are called “azo group” and give the family of molecules its name. In the thermally preferred state, the molecule takes on a planar conformation, the *trans*

state. Irradiation with ultra violet (UV) light with a wavelength of about 350 nm induces the isomerization to the *cis* state (Figure 9).

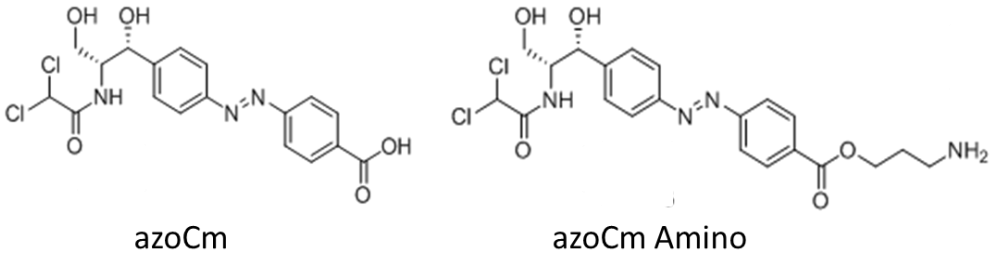

Figure 8: **azoCm and azoCm Amino** Shown is the light-switchable compound azoCm, left with a carbon terminal group (COOH), right with a NH_2 terminal group (Amino).

In the *cis* state, the phenyl rings are inclined at about 55° to each other, however, due to an overlay of the UV/VIS spectra, a photostationary state with a maximum of 80% *cis* can be achieved [189, 200]. The isomerization back to the *trans* state is induced by irradiation with visible light (VIS) of about 450 nm, or thermally by heating (Figure 9). The isomerization to *trans* takes place within picoseconds, the thermal backreaction takes up to several days at room temperature.

The azobenzene can be chemically modified on both phenyl rings, the substituents having a decisive influence on the isomerization wavelengths and the stability of the two states. Due to high quantum yields during isomerization and low photobleaching, azobenzenes have been widely used to date [198, 200-202].

The developed azobenzene azoCm was designed to be a favorable target molecule to be used in biological systems. The substituent groups of the phenyl rings were modified in a way that lead to a *trans-cis* isomerization at 365 nm, a wavelength on the longer spectrum of UV light and less likely to cause any damage in biological systems [201, 202]. They were also chosen to grant azoCm a long stability in aqueous solution, a necessity when working in biological systems and not typical for azobenzenes [199]. Next to a stable azobenzene compound compatible with aqueous conditions (azoCm-COOH, usually referred to as azoCm), a derivative was designed (azoCm Amino or azoCm-NH_2). To allow immobilization of azoCm on the surface of Affi-gel 10 (Table 1), the matrix used in SELEX experiments, a primary amino group on the molecule was necessary to allow the formation of a stable amide bond. If not specifically mentioned otherwise, azoCm Amino was only used to generate the azoCm

derived matrix for SELEX. All elution steps during SELEX and all *in vivo* screening experiments were carried out using the original compound azoCm.

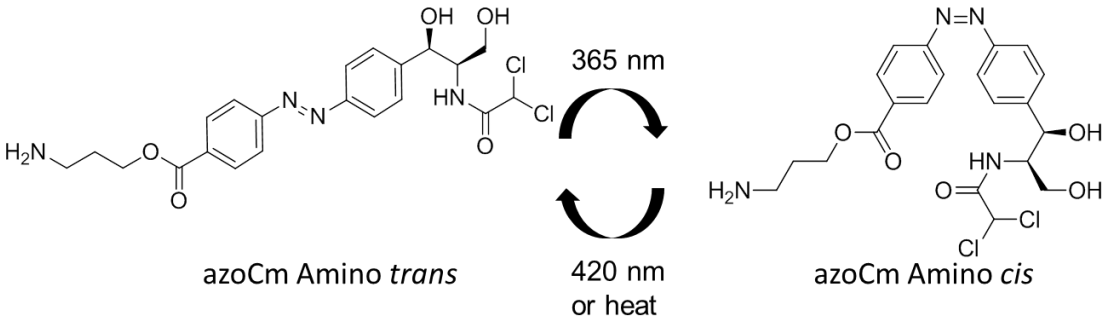

Figure 9: ***Trans-cis* isomerization of azoCm Amino** Shown are the two isoforms azoCm Amino can take on upon irradiation with different wavelengths of light. Light with λ=365 nm leads to the *cis*, light with λ=420 nm leads to the *trans* conformation. The reaction from *cis* to *trans* can also occur thermally (not shown), but at a much slower rate.

Due to the properties of azoCm, toxicity studies using several biological model systems were carried out previously to this thesis. As demonstrated in Lotz *et al*., azoCm shows toxicity at high concentrations of 1 mM in human cells, and no detectable toxicity for *Bacillus subtilis*, *E. coli* and *S. cerevisiae* for up to a 5 mM ligand solution [198]. Therefore, the use of lower concentrations would make azoCm a feasible molecule to use in biological application. Tests carried out during this thesis were typically carried out using 100 µM ligand solutions.

2.2.3 SELEX against azoCm

A main goal of this thesis was the development of an aptamer (using the SELEX method), which selectively binds to only one isoform of azoCm. So far, three other research groups have carried out SELEX against photochromic molecules [203-205]. Of the three small molecules used as targets, only one contained an azobenzene photosensitive group [205]. The used azobenzene was flanked by three amino acids, making it a small peptide target molecule. Using SPR, Hayashi *et al*. could detect RNA aptamers binding the *trans* isoform of their peptide target with a high nanomolar to a low micromolar kD. Binding to its *cis* isoform was reported as ten times worse, making it an example of a successful light-selective RNA against an azobenzene target [205, 206].

In order to be able to use azoCm as a target molecule in SELEX, a modified version of it had to be developed to allow covalent binding to a carrier material. As immobilization of the

target molecule is crucial during the applied affinity SELEX method, Dr. Thomas Halbritter designed an azoCm derivative with a NH_2-group attached to a C2-linker to allow coupling of azoCm to a carrier matrix (0) while keeping it accessible for aptamers to interact with.

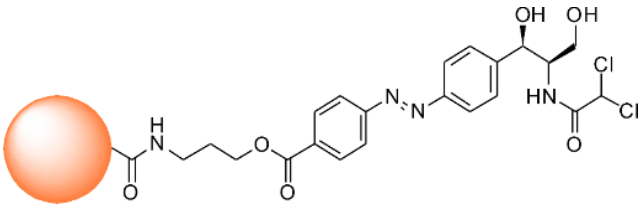

Figure 10: **AzoCm-NH_2** AzoCm-NH_2 is shown covalently coupled to activated resin (red sphere).

A SELEX carried out against azoCm previously to this thesis yielded aptamers binding in an isoform selective manner (4.1, see [196, 198]). Its development over the nine SELEX rounds carried out is shown in chapter 4.2. A gradual enrichment of RNA until round 5 can be observed, after which unspecific elution with 20 mM EDTA was switched to specific elution using a 5 mM azoCm solution.

2.2.4 An existing light-selective aptamer against azoCm

A truncated aptamer from the SELEX described in 2.2.3 called “aptamer 42” was analyzed using isothermal titration calorimetry (ITC, 3.2.13), allowing the determination of its binding constant (kD). The 42 nt long RNA aptamer was able to bind to azoCm in its *trans* form with a kD of 3.55 ± 0.04 µM, while showing no binding to its *cis* form (two independent measurements, example see Figure 11).

While the aptamers generated by Rudolph did show isoform specific binding to azoCm *trans*, testing the two aptamer versions in an *in vivo* context showed that they could not work as riboswitches [196]. Introducing them into the 5’ UTR in front of the reporter gene GFP (compare to 3.3.8) reduced all GFP expression to background levels, comparable to a negative control which did not contain a start codon in front of the GFP gene. Therefore, a closer analysis of the generated aptamers was planned, to find out more about their structural properties. Additionally, it was planned to generate a new aptamer binding isoform selectively to azoCm.

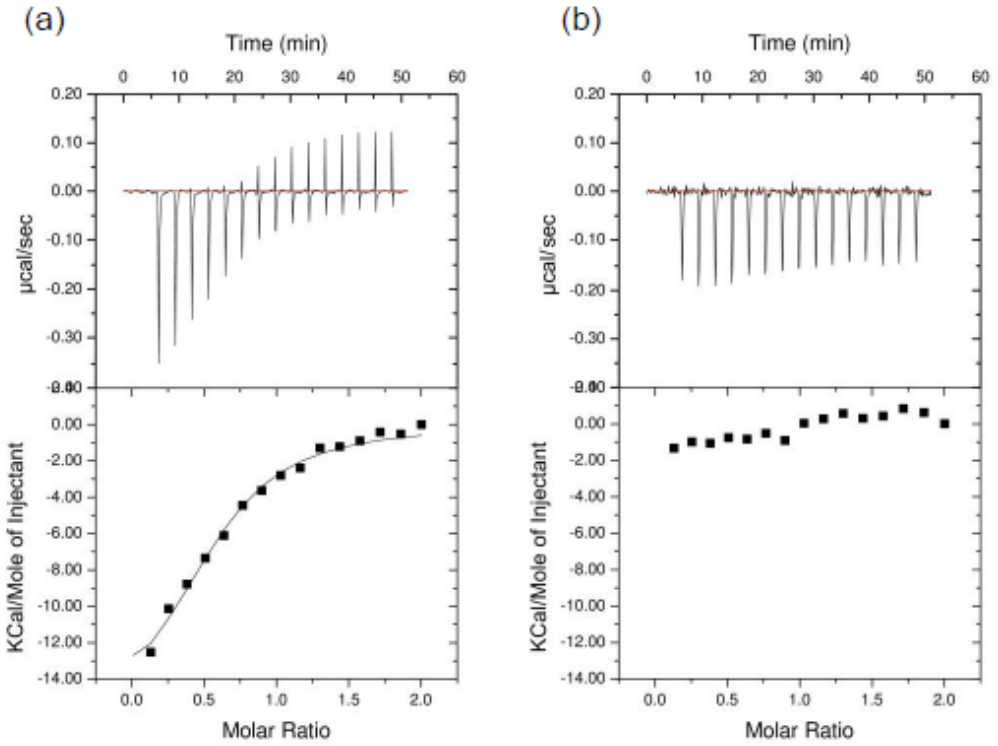

Figure 11: **ITC measurement of aptamer 42 with 200 µM azoCm**. **A** A kD of 3.55 ± 0.04 µM was determined upon binding of aptamer 42 with 200 µM azoCm *trans*. **B** ITC measurement of aptamer 42 with 200 µM azoCm *cis*. No binding could be determined. ITC measurements were carried out by Rudolph [196].

In a 2D structure prediction using mfold (Table 12), aptamer 42 showed the structures shown in Figure 12. The verification of the structural prediction of the truncated version by in-line probing constituted the first objective of this doctoral thesis (3.2.14).

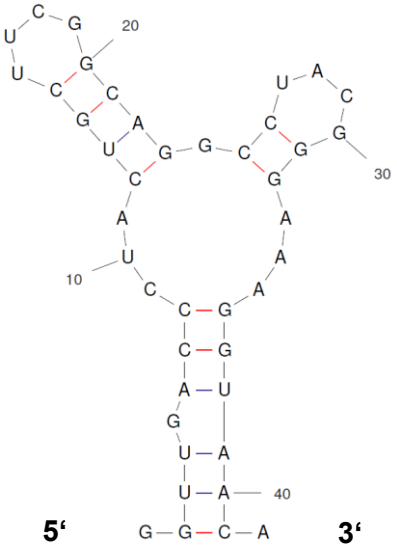

Figure 12: **Predicted secondary structure of aptamer 42** For structure prediction of the shown aptamer 42 the software mfold was used (Table 12**).**

2.3 Objectives

The aim of the presented work was to generate RNA aptamers specifically binding to one of two photo-inducible isoforms of a small azobenzene-derived molecule, called azoCm. From such aptamers, a light-selective riboswitch should be engineered. In order to achieve this, four steps were taken in the course of this work (see Figure 13):

- Performing a SELEX against azoCm and generating specifically binding aptamers.
- Developing a light SELEX protocol to generate isoform specific aptamers.
- Testing selected aptamers *in vitro* regarding their binding ability and affinity.
- Analysis of selected aptamers *in vivo* whether they show regulatory function and can work as riboswitches.

To generate aptamers binding specifically to azoCm, the compound was used as a target during SELEX. Throughout the SELEX rounds, the majority of RNA aptamers from a large randomized library are eliminated and at the end an enriched aptamer pool with mainly ligand-specific aptamers is generated. Aptamers from this SELEX should be tested regarding their binding affinity and specificity to azoCm.

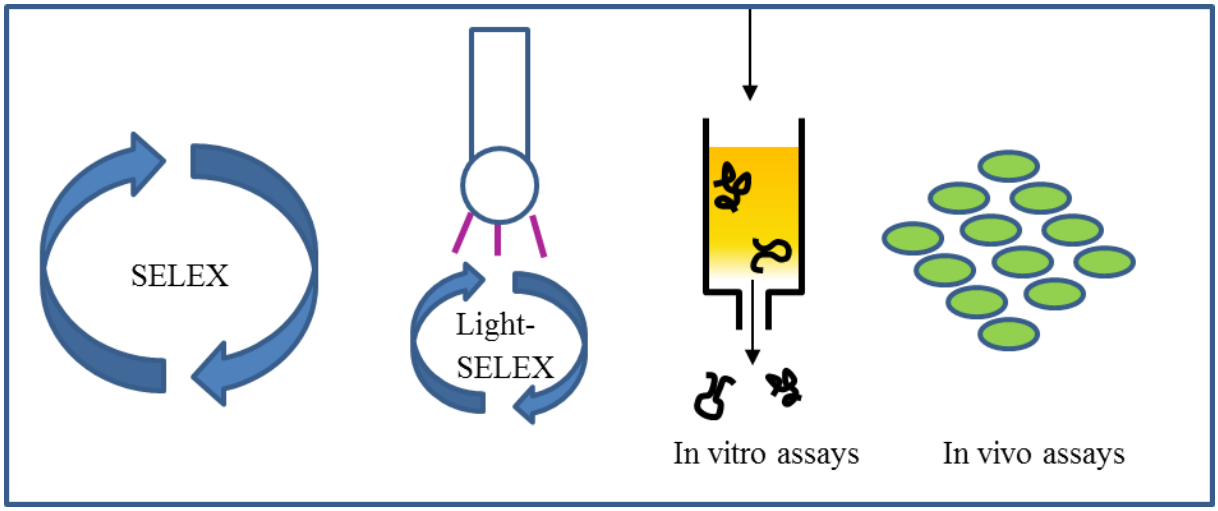

Figure 13: **Planned steps performed to generate a light-sensitive riboswitch** As a first step, SELEX against a light-selective molecule is performed. A light SELEX protocol is developed and applied to the SELEX pools derived from the previous SELEX. Aptamers from the light SELEX are tested in *in vitro* and in *in vivo* assays, to discover a new light-sensitive riboswitch for *S. cerevisiae*.

As the molecule azoCm undergoes a reversible conformation change induced by white light and UV light, respectively, these properties should be used to develop a light SELEX protocol. The protocol should be designed to ensure that the generated aptamers bind selectively to only one of the two isoforms of azoCm.

The possibility of using these aptamers in an *in vivo* context should be investigated. The aptamers should be introduced into the 5' UTR of a reporter gene (GFP) to measure GFP expression in dependence of added ligand in *Saccharomyces cerevisiae*. The successful gene regulation in dependence of azoCm would be the first indication of a functional riboswitch. To generate a functional light-dependent riboswitch, it needs to be proven that addition of the photo-switchable molecule azoCm and irradiation with light of an adequate wavelength is able to regulate gene expression in a reversible manner. Using such a light-dependent riboswitch, gene expression in cells could be turned on and off in reversibly and with exact spatial and temporal control using only light as a trigger. A successful experiment would prove the establishment of a novel, light-dependent synthetic riboswitch.

3 Material and Methods

If not otherwise mentioned, water or MQ always refers to purified water from a PURELAB flex 2 purification machine (Table 3).

If not stated otherwise, alcohol or pure alcohol always refers to 99.6% ethanol (ethanol absolute), or 99.6% ethanol diluted with MQ, e.g. used for washing nucleic acids. Methylated ethanol was used to clean surfaces only.

3.1 Listing of the used resources and chemicals

In the following, the resources used in this thesis are listed.

Table 1: **Chemicals**

Chemical	Manufacturer
[γ-^{32}P] ATP	Hartmann Analytics
[α-^{32}P] UTP	Hartmann Analytics
2-Propanol (Isopropanol)	Sigma-Aldrich
6x DNA loading dye	New England Biolabs
Acetic acid	Carl Roth GmbH
Acetone	Sigma-Aldrich
azoCm	Detailed in Table 2
azoCm Amino	Detailed in Table 2
Adenine	Carl Roth GmbH
Affi-Gel 10 Gel	Bio-Rad Laboratories GmbH
Agar	Carl Roth GmbH
Agarose peqGold Universal	PeqLab
Ammonium sulphate	Carl Roth GmbH
Ampicillin	Carl Roth GmbH
Bromophenol blue	Carl Roth GmbH
Butanol	Carl Roth GmbH
Calcium chloride dehydrate ($CaCl_2$)	Carl Roth GmbH
Chloroform	Carl Roth GmbH
Compound 3	Detailed in Table 2
CytoFLEX Sheath Fluid	Beckman Coulter GmbH
D(+)-Glucose	Carl Roth GmbH
D-Sorbitol	Carl Roth GmbH
Difco Yeast	BD
Disodium phosphate dihydrate ($Na_2HPO4 \cdot$	Carl Roth GmbH

2 H_2O)	
Dimethyl sulfoxide (DMSO)	Carl Roth GmbH
dNTPs	PeqLab
Dithiothreitol (DTT)	Roche
Ethanolamine	Carl Roth GmbH
Ethidium bromide	Carl Roth GmbH
Ethanol absolute (99,6%)	VWR
Ethylenediaminetetraacetic acid (EDTA)	Carl Roth GmbH
FlowClean Cleaning Agent	Beckman Coulter
Formamide	Carl Roth GmbH
Glycerin/glycerol	Carl Roth GmbH
GlycoBlue™ Coprecipitant	Ambion
Glycogen	Thermo Fisher Scientific
Kohrsolin	Bode Chemie GmbH
Lithium acetate (LiAc)	Carl Roth GmbH
MEM amino acid mix	Sigma-Aldrich
Methanol	Carl Roth GmbH
Methylated ethanol	Richter Chemie GmbH
Molox RNase inhibitor	moloX GmbH
MQ	Produced with PURELAB flex 2, see Table 2
Neomycin trisulphate	Carl Roth GmbH
NTPs	Peqlab
PEG 4000	Carl Roth GmbH
Peptone	Carl Roth GmbH
Potassium chloride (KCl)	Carl Roth GmbH
Potassium dihydrogen phosphate (KH_2PO4)	Carl Roth GmbH
RNase ZAP	Sigma-Aldrich
Roti Szint Eco Plus (Scintillation Cocktail)	Carl Roth GmbH
Sodium acetate	Carl Roth GmbH
Sodium azide	Carl Roth GmbH
Sodium carbonate (Na_2CO_3)	Carl Roth GmbH
Sodium citrate	Carl Roth GmbH
Sodium chloride (NaCl)	Carl Roth GmbH
Sodium phosphate, monobasic, anhydrous (NaH_2PO4)	Carl Roth GmbH
Sorbitol	Carl Roth GmbH
Spermidine	Sigma-Aldrich
Sulfuric Acid (H_2SO_4), 96%	Carl Roth GmbH
Tetracycline hydrochloride	Sigma-Aldrich
Tris-HCl	Carl Roth GmbH
Triton X-100	Carl Roth GmbH
Tryptone	Carl Roth GmbH

Yeast extract	Oxoid
Yeast nitrogen base	Becton, Dickinson and Company
Yeast tRNA	Life Technologies

Table 2: **Small molecule compounds used in this thesis**

Compounds	Published in	Structural formula
azoCm	Lotz *et al*. [198]	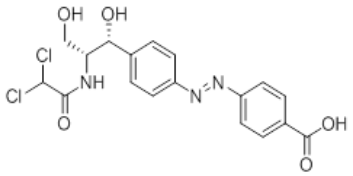
azoCm-NH_2 or azoCm Amino	Lotz *et al*. [198]	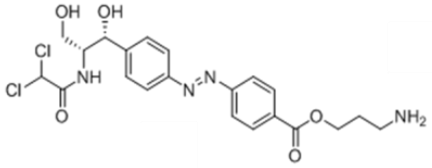
Compound 3	Halbritter & Kaiser *et al*. [207]	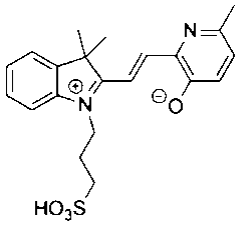

Table 3: **Appliances and disposables**

Equipment	Manufacturer
-20°C Freezer	Liebherr
24 Well plate (u-bottom)	Greiner bio-one Inc
-80°C Freezer	New Brunswick
96 Deep well plate (u-bottom)	Greiner bio-one Inc
96 Well plate (flat bottom)	Greiner bio-one Inc
ATL224I Analytical Balance	Acculab Sartorius group
ATL8201-I digital gram scale	Acculab Sartorius group
Autoclave Tuttnauer 3870 ELV-3	Tuttnauer Biomedis
Benchtop Centrifuge Micro Star 17	VWR international GmbH
Bio-Spin® Chromatographic columns	Bio-Rad
BREATHseal™	Greiner Bio-One
Bunsen burner	Carl Roth GmbH

Chicane flask (50 mL, 250 mL, 500 mL, 1000 mL)	Schott Duran
Consort EV243 power supply	Wolflabs
CytoFLEX S Flow Cytometer	Beckman Coulter GmbH
Electrophoresis Power Supply Consort	PeqLab
Electroporation cuvette (0,1 and 0,2 cm)	Bio-Rad
Eppendorf multichannel pipette	Eppendorf
Eppendorf™ ThermoStat Plus	Fisher scientific
Falcon™ Cell Strainers, 40µm	Thermo Fisher Scientific
FastPrep®-24	MP Biomedicals
Fluorescent Image Analyzer FLA-500	Fujifilm
Fluorolog FL3-22 Spektrofluorometer	Horiba
Flüssigkeitsszintillationszähler 1409 (scintillation counter)	Wallac Monza
Gel electrophoresis chamber	Carl Roth GmbH
Gel documentation chamber	INTAS
Glassbeads (0.25–0.5 mm)	Carl Roth GmbH
Glassbeads (425-600 µm)	Sigma-Aldrich
Glasfrit	Duran
Heating block	VWR
Heraeus Pico 17 centrifuge	Thermo Fisher Scientific
Ika vortex genius 3	Sigma-Aldrich
Image Eraser SF	Molecular Dynamics
Incubation Shaker Multitron	Infors AG
Incubator	Thermo Fisher Scientific
Incubator Titramax 1000	Heidolph Instruments
LED LENSER® - T7	LED LENSER
Leica M50 with GFP plus filter 10446143	Leica Microsystems GmbH
Magnetic stirrer Ikamag Reo	IKA
Magnetic stirrer IKA RET basic	IKA
Membrane filter SUPOR 450, 0,2 µM	Pall Corporation
Membrane filter SUPOR 450, 0,45 µM	Pall Corporation
MicroCal PEAQ iTC200	Malvern Instruments
Microcentrifuge tube 1.5 mL, 2 mL	Greiner bio-one Inc
Micropipette (2 µL, 20 µL, 200 µL, 1000 µL)	Gilson Inc
MicroPulser Electroporator	Bio-Rad
Microplate Reader Infinite 200 PRO	Tecan
Multifuge 1L-R	Heraeus Christ
NanoDrop ND 1000 Spectrophotometer	PeqLab
Nitrile gloves	Starlab International GmbH
PeqSTAR 96 Universal Gradient	PeqLab
Peqstar XS PCR Cycler	PeqLab

Petri dish, plastic	Sarstedt
pH-meter 766 calimatic	Knick
Storage Phosphor Screen, 20 x 23 cm	Fujifilm
Pipette controllers Pipetboy	VWR International GmbH
Pipette tip Gilson® - Style (10, 20, 200, 1000 µL)	Greiner bio-one Inc
Power station 300	Labnet
Purelab® flex	Elga
Refrigerator	Liebherr
Refrigerator	Comfort Refrigeration Inc
Rotating mixer CAT-RM5	CAT M. Zipperer GmbH
Sigma 4 – 16KS	Sigma Laborzentrifugen GmbH
Single use pipette (5 mL, 10 mL, 25 mL)	Greiner bio-one Inc
Spektrophotometer Ultrospec 2100 pro	Biochrom Ltd
Sterile Bench	BioFlow Technik
Sterilfilter Filtropur S 0,2 µm	Sarstedt
Terasaki plate	Greiner Bio-one Inc
Test tube	Schott Duran
Thermocycler peqSTAR 96 Universal	PeqLab
Thermometer “Platinum Ultra-Accurate Digital Traceable Thermometer”	Traceable® Products
Thermomixer Comfort	Eppendorf AG
ThermoStat plus	Eppendorf AG
TipOne® Filter Tips (10/20, 20, 200, 1000 µL)	StarLab
Tissue-Box	Carl Roth GmbH
Towels	Hegro Eichler GmbH
Tube Cellstar®, 15 mL, 50 mL	Greiner bio-one Inc
UV/VIS spectrophotometer	Amersham Biosciences
UV handlamp Nu-6 KL	Benda
UVLED 365	Fabrikat Bonn
Waterbath WNB14	Memmert

Table 4: **Kits and systems**

Name	Manufacturer
TOPO-XL PCR Cloning Kit	Invitrogen (Thermo Fisher Scientific)
Wizard® SV Gel and PCR Clean-Up System	Promega, USA
Zymoclean™ Gel DNA Recovery Kit	Zymo Research
Frozen EZ Yeast Transformation II Kit™	Zymo Research

QIAprep® Spin Miniprep Kit	QIAGene
QIAprep® Spin Midiprep Kit	QIAGene
QIAquick® PCR purification Kit	QIAGene

Table 5: **Enzyme systems and DNA standards**

Enzymes & buffers	Manufacturer
40 U Ribonuclease Inhibitor (Molox)	moloX GmbH
AgeI HF®	New England Biolabs
Antarctic Phosphatase	New England Biolabs
Antarctic Phosphatase Buffer (AP Buffer)	New England Biolabs
First Strand Buffer	Invitrogen (Thermo Fisher Scientific)
NheI HF®	New England Biolabs
peqGold 1kb DNA Ladder	PeqLab
peqGold Ultra Low Range DNA Ladder	PeqLab
Q5® High GC Enhancer	New England Biolabs
Q5® Reaction Buffer (5x)	New England Biolabs
Q5 polymerase	
RNA-free DNase	Ambion Life Technologies
RNase T1	Thermo Fisher Scientific
SuperScript IV Reverse Transcriptase	Invitrogen (Thermo Fisher Scientific)
T4 Ligase buffer	New England Biolabs
T4 Polynucleotide Kinase	New England Biolabs
T4 Polynucleotide Kinase Reaction Buffer (PNK Buffer)	New England Biolabs
T7 RNA Polymerase	New England Biolabs
Taq DNA Polymerase	New England Biolabs
Thermopol Buffer	New England Biolabs

Table 6: **Oligonucleotides used in this work, in 5’ to 3’ direction**

Name	Specifications	Sequence
Library 1A	For partially structured SELEX pool	GGGAGACGCAACTGAATGAANNNNNNNNNNNNNN NNNNNNNNNNNCTGCTTCGGCAGNNNNNNNNNNNN NNNNNNNNNNNNNNTCCGTAACTAGTCGCGTCAC
Library 1B	For N64 randomized SELEX pool	GGGAGACGCAACTGAATGAANNNNNNNNNNNNNN NNNNNNNNNNNNNNNNNNNNNNNNNNNNNNNNNN NNNNNNNNNNNNNNNTCCGTAACTAGTCGCGTCAC
Library 1		GTATAATACGACTCACTATAGGGAGACGCAACTGAA

fwd		TGAA
Library 1 rev		GTGACGCGACTAGTTACGGA
Library 2	For N74 randomized SELEX pool	GTGGATCCGACCGTGGTGCCNNNNNNNNNNNNNNN NNNNNNNNNNNNNNNNNNNNNNNNNNNNNNNNNN NNNNNNNNNNNNNNNNNNNNNNNNGCAGTGAAGG CTGAGCTCC
Library 2 fwd		TCTAATACGACTCACTATAGGAGCTCAGCCTTCACTG C
Library 2 rev		GTGGATCCGACCGTGGTGCC
Library doped	For Doped SELEX pool	CCAAGTAATACGACTCACTATAGGGCCAAGCTAGAT CTACCGGTNNNNNNNNNNNNNNNNNNNNNNNNNNN NNN[GG](CCTACGGGAAAGG)NNNNNAAAATGGCTA GCAAAGGAGAAGAACTTTTCACT [ ] 50% randomized, ( ) 6% randomized
Library doped fwd		CCAAGTAATACGACTCACTATAGGGCCAAGCTAGAT CTACCGGT
Library doped rev		AGTGAAAAGTTCTTCTCCTTTGCTAGCCATTTT
GFP rev	Sequencing of aptamers in pWHE601	CCACTGACAGAAAATTTGTGC
Library B2-10	B2-derived pool for *in vivo* screening	ATCTACCGGT(GCTCCCTTTAGATGTTAGTCGAAGAC ATCTAACCTACGGGAAAGGAGACC)AAAATGGCTAG CAAAGGAGAAGAACTTTTCACTGGAG ( ) 10% randomized
Library B2-6N6	B2-derived pool for *in vivo* screening, truncated	ATCTACCGGT(GCTCCCTTTAGA)NNNNNN(TCTAACC TACGGGAAAGGAGACC)AAAATGGCTAGCAAAGGAG AAGAACTTTTCACTGGAG ( ) 6% randomized
Library B2-N6	B2-derived pool for *in vivo* screening, truncated	ATCTACCGGTGCTCCCTTTAGANNNNNNTCTAACCTA CGGGAAAGGAGACCAAAATGGCTAGCAAAGGAGAA GAACTTTTCACTGGAG
Libraries B2 rev		GTCCAGTGAAAAGTTCTTCTCCTTTGC
Library B2-5	B2-derived pool for *in vivo* screening	GCATACAATCAACTCCAAGCTAGATCTACCGGT(GCT CCCTTTAGATGTTAGTCGAAGACATCTAACCTACGGG AAAGGAGACC)AAAATGGCTAGCAAAGGAGAAGAAC TTTTCACT

		( ) 5% randomized
Library B2-1 7	Riboswitch B2-1 derived pool for *in vivo* screening	GTTTCTTTTTCTGCACAATATTTCAAGCTATACCAA(G CATACAATCAACTCCAAGCTAGATCTACCGGT)GCTC CCTTTAGAGGTTTGTCGAAGACCTCTAACCTACGGGA AAGGAGACCAAAATGGCTAGCAAAGGAGAAGAACT TTTCACT
		( ) 2.5% randomized
Library B2-1 8	Riboswitch B2-1 derived pool for *in vivo* screening	GTTTCTTTTTCTGCACAATATTTCAAGCTATACCAA(G CATACAATCAACTCCAAGCTAGATCTACCGGTGCTCC CTTTAGAGGTTTGTCGAAGACCTCTAACCTACGGGAA AGGAGACC)AAAATGGCTAGCAAAGGAGAAGAACTT TTCACT
		( ) 6% randomized
Library 7/8 fwd		GTTCTCGTTCCCTTTCTTCCTTGTTTCTTTTTCTGCACA ATATTTCAAGCTATACCAA
Library 7/8 rev		AGAATTGGGACAACTCCAGTGAAAAGTTCTTCTCCTT TGCTAGCCATTTT
HR_fwd	HR in pWHE601 fwd	CAAGCTATACCAAGCATACAATCAACTCCAAGCTAG ATCTACCGGTGGAGCTCAGCCTTCACTGC
HR_rev1	HR in pWHE601 rev	CAAGAATTGGGACAACTCCAGTGAAAAGTTCTTCTC CTTTGCTAGCCATTTT GTGGATCCGACCGTGGTGCC
HR_rev2	HR in pWHE601 rev plus G (frameshift)	CAAGAATTGGGACAACTCCAGTGAAAAGTTCTTCTC CTTTGCTAGCCATTTTG GTGGATCCGACCGTGGTGCC
HR_rev3	HR in pWHE601 rev plus TG (frameshift)	CAAGAATTGGGACAACTCCAGTGAAAAGTTCTTCTC CTTTGCTAGCCATTTTTGTGGATCCGACCGTGGTGCC
B2-1 fwd		CCAAGCTAGATCTACCGGTGCTCCCTTTAGAGGTTTG TCGAAGACCTCTAACCTACG
B2-1 rev		AGTGAAAAGTTCTTCTCCTTTGCTAGCCATTTTGGTCT CCTTTCCCGTAGGTTAGAGGTCTTCGACAAACCTC
B2-1 short fwd		CCAAGTAATACGACTCACTATAGGTCTACCGGTGCTC CCTTTAGAGGTTTGTCGAAGACC
B2-1 short rev		GGTCTCCTTTCCCGTAGGTTAGAGGTCTTCGACAAAC CTCTAAAGGGAGCACCGG
42 fwd		CCAAGTAATACGACTCACTATAGGTTGACCCTACTGC TTCGGCAGGCCTACG
42 rev		TGTTACCTTTCCCGTAGGCCTGCCGAAGCAGTAGGGT CAACCTATAGTGAG
pWHE60		CCACTGACAGAAAATTTGTGCCC

1-seq pSP64 fwd	ATGAGCCCGAAGTGGCGAGCC

Table 7: **Aptamer sequences**

Name	Sequence
42	GGUUGACCCUACUGCUUCGGCAGGCCUACGGGAAAGGUAACA
1	GUGUUCCGACACGUGAACUCCAGCCCCCUUAAUAACGCUGUCGACCC UUGCGCUGUUACCUACGGGAAAGGGGU
3	UAGGGACCCUAAAGCAGGGCUUCAACGGAUACGGCCAUGAGGCGUUC UAGGAACCAAAGAGCGUAAUAAGCAAUC
5	AGUUAAUGCACGACGCAGUGAUCGACGUAGGUAGAAAAGCGAUAAG UAUGGGCCUAAUCCGAUACCGCGAUCAC
10	GAAUGCUAACAUCCGAUUGUCCAGUACUGCCUUGGUAUAAGUCUGA AUACGUGGAUCCGACCGUGGUGCC
11	UUCCAUCCAUUCUCACCCGUGGAUGAAAAGGGACCCGUAUAAGCACA GAGGCCGCCGAGGAGCCAAGGAACCAAU
12	CCCCUCCCUACUGUGACUGAACGAACCCACAGUAGGGCCUACGGGAA AGGGGAGUGACCUGGCCCAAAGCCACC
13	AGUUAAUACACGACGCAGUGAUCGACGUAGGUAGAAAAGCGAUAAG UAUGGGCCUAAUCCGAUACCGCGAUCGC
14	AAAACCGAUUUAAAGGCUACCCAGUGAUCCAUGGAGUAGGAAAAGC UGCUAACGAGCCGCUCCAUCCAGCCGA
15	CCCGCAACCGCGACCCCUUGCCGCCUGAGGCUAAAUGCCCCUCUACG GAAAAGCGGAAGACUCGUGAGUGGGA
16	AGUUAAUACACGACGCAGUGAUCGACGUAGGUAGAAAAGCGAUAAG UAUGGGCCUAAUCC
A	AGUUAAUACACGACGCAGUGAUCGACGUAGGUAGAAAAGCGAUAAG UAUGGGCCUAAUCCGAUACCGCGAUCAC
E	GACGGGCUCCCGCACCUGAGGUGUCUGCCAGAAACGACAAACGUCGC CUCGGCCACCACUCUGGUUACAAGAGG
B2-1	CCAAGCUAGAUCUACCGGUGCUCCCUUUAGAGGUUUGUCGAAGACCU CUAACCUACGGGAAAGGAGACCAAAAUGGCUAGCAAAGGAGAAGAA CUUUUCACU
B2-1 short	UCUACCGGUGCUCCCUUUAGAGGUUUGUCGAAGACCUCUAACCUACG GGAAAGGAGACC

Table 8: **Plasmids**

Plasmid	Characteristics	Reference/Provided by
pWHE601	*Gfp*	Adapted from Dr. Julia Weigand,
pWHE601*	*ΔATG-gfp*	Adapted from Dr. Julia Weigand
pWHE601_neo	*Neo_gfp*	Adapted from Dr. Julia Weigand
pCBB05	*gfp* *mCherry*	Adapted from Dr. Cristina Bofill-Bosch
pCBB06	*ΔATG-gfp* *mCherry*	Adapted from Dr. Cristina Bofill-Bosch
pCBB07	*Neo_gfp* *mCherry*	Adapted from Dr. Cristina Bofill-Bosch
pSP64	T7 promoter with aptamer insertion site	Promega

Table 9: **Organisms**

Organism	Genotype
Escherichia coli 10-beta (New England Biolabs)	Δ*(ara-ley) 7697 araD139 fhuA* Δ*lacX74 galK16 galE15 e14-* ϕ*80*d*lacZ*Δ*M1*5 *rec1A rel1A end1A nupG rpsL* (Str^R) *rph spoT1*Δ*(mrr-hsdRMS-mcrBC)*
Saccharomyces cerevisiae RS453α	*MATα ade2 trp1-1 can1-100 leu2-3 leu2-112 his3-1 ura3-52*
Escherichia coli (*E. coli*)	F$^-$ *mcr*A Δ(*mrr-hsd*RMS-*mcr*BC) φ80*lacZ*ΔM15 Δ*lac*X74 *rec*A1 *ara*D139 Δ(*ara-leu*)7697 *gal*U *gal*K *rps*L (Str^R) *end*A1 *nup*G

Table 10: **Solutions and buffers**

General solutions	Composition (in distilled water)
1x PCR buffer	10 mM Tris-Cl (pH 9.0), 50 mM KCl, 0.1% Triton X-100
1x SELEX buffer [208]	10 mM Tris-HCl (pH 7.6), 250 mM NaCl, 5 mM $MgCl_2$

2x RT-PCR mix	1x PCR buffer (see above), 1x first strand buffer, 2 mM DTT, 1 µM Library_fwd oligo, 1 µM Library_rev oligo, 1.5 mM $MgCl_2$ and 0.3 mM dNTPs (each)
Agarose solution for gels	1% (w/v) or 3% (w/v) of agarose in 1x TAE buffer, autoclaved
Ampicillin stock solution (1000x)	100 mg/mL ampicillin, sterile-filtered
dNTP solution	12.5 mM of dATP, dCTP, dGTP and dTTP, each
Electroporation buffer	1 M Sorbitol, 1 mM $CaCl_2$
Ethidium bromide stock solution (10x)	10 mg/mL ethidium bromide
In-line reaction buffer	10 mM Tris-Cl (pH 8.3), 10 mM $MgCl_2$, 100 mM KCl)
Phosphate buffered saline	140 mM NaCl; 10 mM KCl; 6.4 mM Na_2HPO_4, 2 mM K_2PO_4
Sodium azide solution	0.002% solution of NaN_3
SSC (20x, for 1 L)	3 mM NaCl, 340 mM Sorbitol
ssDNA	DNA from salmon testes (salmon sperm DNA), autoclaved, 10 mg/mL
TAE buffer (50x)	2 M Tris-HCl; 1 M acetic acid (conc.); 50 mM EDTA (pH 8.0)
TE (10x)	1 mM EDTA, 2 M Tris-HCl
TE/LiOAc-buffer (1x)	100 mM 1x TE buffer, 100 mM LiOAc
TK mix (SELEX)	40 mM Tris-Cl (pH 8.0), 5 mM DTT, 2.5 mM NTPs (each), 15 mM $MgCl_2$, 100 U T7 RNA Polymerase, 40 U ribonuclease inhibitor
Urea solution	5 M urea
Yeast tRNA stock solution	25 mg/mL yeast tRNA in MQ, heated to 95°C for 5 min and cooled rapidly, then frozen

Table 11: **Culture media**

Medium	Composition	Concentration
dYT medium	Yeast extract	1.0% (w/v)
	Tryptone	1.6% (w/v)
	Sodium chloride	0.5% (w/v)
	Fill to 1 L with distilled water	

LB medium	Tryptone	1% (w/v)
	Yeast extract	0.5% (w/v)
	NaCl	1% (w/v)
	Agar	1.5% (w/v)
	Fill to 1 L with distilled water	
SCD-URA medium	Glucose	2% (w/v)
	Ammonium sulphate	0.55% (w/v)
	Yeast nitrogen base	0.2% (w/v)
	Adenine	0.0012% (w/v)
	MEM amino acid mix	2% (v/v)
	Agar	1% (w/v)
	Fill to 1 L with distilled water	
YPD medium	Yeast extract	1% (w/v)
	Peptone	2% (w/v)
	Glucose	4% (w/v)
	Agar	2% (w/v)
	Fill to 1 L with distilled water	

For liquid media, no agar was used in the preparation process.

Table 12: **List of software and databases**

Software	Use	Copyright
Clustal omega [209-211]	Multiple sequence alignment	EMBL-EBI
CorelDrawX4	Design of graphics	Corel Corporation
Cytometer software CytExpert	Fluorescence measurements of single cells from 96 well plates	Beckman Coulter GmbH
Endnote X7 and X8	Literature management	Clarivate Analytics
FluorEssence™	Fluorescence spectroscopy	Horiba
i-control for Microplate Reader Infinite 200 PRO	Reading of 96 well plates	Tecan
ImageJ 1.49b [212, 213]	Image processing	Wayne Rasband, National Institute of Health (NIH), USA
Mfold [214-216]	Secondary structure prediction of RNA	Rensselaer Polytechnic Institute
MicroCal PEAQ-ITC Analysis Software 1.1.0.1262	Analysis and image generation of ITC experiments	Malvern Instruments

Microsoft Office 2010	Excel, Word and Powerpoint used for text processing, calculations and image design	Microsoft corporation, USA
Nanodrop software ND-1000 V 3.8.1	Analysis of nucleic acid quantities	Thermo Fisher Scientific
New England Biolabs web server (https://www.neb.com/)	Specifications for enzymes	New England Biolabs
Vector NTI 11.0	Sequence analysis, plasmid design	Life Technologies

3.2 Molecular biology methods

If not stated differently, the following biological standard methods were carried out according to Sambrook *et al*. [217]:

- DNA ligation
- DNA restriction
- Nucleic acid detection on agarose gels using UV light and ethidium bromide
- PAA gel electrophoresis
- Purification of radioactive nucleic acids using PAA gels

If not stated differently, PCR was carried out according to Landt *et al.* [218].
If not stated differently, *E. coli* cells were transformed with plasmid DNA according to the protocol from Hanahan *et al* [219].
Libraries for SELEX or *in vivo* screenings were ordered at Microsynth Seqlab, Germany.

3.2.1 Autoclaving and sterilizing

Chicane flasks and bottles, as well as growth media were autoclaved at 121°C for 20 min at 2 bar pressure. Glass pipettes were stored in Kohrsolin solution (Table 1) before washing and dry heat sterilizing at 200°C for at least 30 min. Heat sensitive substances were sterile-filtered using a filter pore size of 0.22 µM.

3.2.2 Plasmid DNA extraction

To amplify plasmids, one singe colony of *E. coli* cells containing the plasmid of choice was grown in liquid culture medium with the appropriate antibiotic for selection. To extract plasmids, a Miniprep or Midiprep Kit by QIAgen (Table 4) was used on 4 or 100 mL of bacteria culture, respectively.

3.2.3 Nucleotide quantification and analysis

An analysis of aqueous nucleic acid solutions regarding their purity and concentration was carried out using a NanoDrop ND 1000 Spectrophotometer (Table 3). An absorption spectrum of wave lengths between 220 nm and 350 nm was generated and values were converted by the appropriate software to receive nucleotide concentrations (Table 12, using Lambert-Beer's Law [220-222]).

3.2.4 Restriction of DNA

To digest DNA, an appropriate amount of the chosen restriction enzymes (type II restriction enzymes) was added to the DNA, using the respective buffer (all specifications regarding the enzymes were taken from the NEB biolabs database (Table 12); enzymes see Table 5). The total volume of the reaction was adjusted to 50 µL with MQ. The digestion reaction was incubated at 37°C for 1 h in a 1.5 mL reaction tube, and subsequently purified or analyzed on an agarose gel (see 3.2.11).

3.2.5 Ligation of DNA

Ligation of DNA fragments was performed using T4 DNA ligase either at room temperature for 1 h or at 16°C for 16 h. The reaction was carried out in ligase buffer (enzyme and buffer see Table 5). The molar ratio of insert to vector was typically 5:1, if not mentioned otherwise. After ligation, the generated DNA was either purified for further use, or directly used for transformation of organisms.

3.2.6 Polymerase chain reaction

The polymerase chain reaction (PCR) was used for *in vitro* amplification of DNA. In the course of this work it was employed for construction purposes (to generate large DNA libraries from a small amount of template), analytical purposes (RT-PCR analysis), cloning projects, and in the course of the SELEX procedure. If not stated differently, PCR was carried

out according to Landt *et al*. [218]. PCR variations are described and listed in the corresponding context (e.g. RT-PCR see 3.2.7).

3.2.7 RT-PCR (reverse transcription polymerase chain reaction)

Reverse Transcription-PCR (RT-PCR) was used to reversely transcribe RNA into DNA and then exponentially enrich this DNA using a one-pot reaction.

The library of different RNAs generated during one SELEX round (3.4.3) was used as starting material of the RT-PCR. 50 µL of eluted RNA in water were added to 48 µL of 2x RT-PCR mix (Table 10) and 1 µL each of the enzymes Taq polymerase and SuperScript II reverse transcriptase (Table 5).

The reverse transcription was carried out at in a thermocycler, following the program below (Table 13). PCR-products were analyzed on a 3% agarose gel (3.2.11) and could be directly used as a template for new RNA transcriptions (3.2.8).

Table 13: **PCR program for reverse transcription**

Temperature	time		PCR steps
54°C	10 min		Initial melting
96°C	1 min	6 – 14 cycles	Melting
58°C	1 min		Primer annealing
72°C	1 min		Elongation

RT-PCR was also used to transcribe RNA aptamer libraries into cDNA templates to amplify DNA for homologous recombination into yeast cells. For this, RT-PCR products were generated according to Table 13, and then amplified with oligonucleotides containing a 30 - 50 nt overhang for recombination into the chosen plasmid.

3.2.8 *In vitro* transcription of RNA

In vitro transcription is a method to generate RNA from a DNA template outside of an organism, using purified RNA polymerase in an adequate buffer [223]. *In vitro* transcription was used in smaller and larger scales during this thesis.

As part of the SELEX process, 10 µL of RT-PCR product (3.2.7, 3.4.3) were added to 87 µL TK mix (Table 10); subsequently 2 µL of T7 polymerase, as well as 1 µL of Molox RNAse inhibitor (Table 1) were added. If the RNA is to be used for radionuclide detection, 1 µL of [α-^{32}P] UTP were added to the reaction during the transcription process. The transcription mixture was incubated for 2 h at 37°C.

In order to produce RNA in large quantities, a run-off transcription was carried out, using either linearized plasmid or a PCR product as template. 1-2 mg of template were mixed with 200 mM Tris-HCl (pH 8.0), 20 mM magnesium acetate, 50 mM DTT, 2 mM spermidine, 15 µL T7 polymerase and 4 mM of ATP, CTP, GTP and UTP each. The reaction was incubated for 12 - 16 h at 37°C.

To purify the produced RNA, it was ethanol-precipitated, dissolved in formamide containing 25 mM EDTA and loaded on a 6% denaturing polyacrylamide gel (containing 8 M urea, [217]).

The product band visualized by UV shadowing was excised, eluted overnight in 300 mM sodium acetate (pH 6.5) and then ethanol-precipitated. The resulting purified RNA pellet was dissolved in a suitable amount of water and molarity was determined.

3.2.9 Phosphorylation and dephosphorylation of the RNA 5' end

In order to generate radioactively labelled RNA, 5' ^{32}[P] end-labelling of previously generated RNA can be performed. For that purpose, RNA has to be dephosphorylated firstly. Dephosphorylation was carried out using Antarctic Phosphatase (Table 5) according to the manufacturer's instructions. Typically, 10 pmol of RNA were incubated in AP buffer at 37°C for 1 h (Table 5).

Phosphorylation of the previously dephosphorylated RNA was performed in a radioisotope laboratory. In a total volume of 50 µL, 3 mM dephosphorylated RNA in water were mixed with 2 µL (10 U) of T4 Polynucleotide kinase (Table 5), the appropriate amount of PNK buffer and 3 µL (10 mM) of [γ-^{32}P] ATP. The reaction was incubated for 1-3 h at 37°C.

Purification of 5' radiolabelled RNA was carried out according to Sambrook *et al*. [217].

3.2.10 Sequencing

For Sanger sequencing [160, 224], 0.7-1 µg of DNA were diluted in 12 µL of MQ, 3 µL of the appropriate sequencing oligonucleotide were added, and the sample was submitted to Microsynth Seqlab, Germany.

3.2.11 Gel electrophoresis

Agarose gel electrophoresis was used to separate differently sized DNA fragments. Depending on the size of the nucleotide fragments, agarose concentrations of 1% (w/v) for fragments >1000 bp, and 3% (w/v) for fragments of 1000 to 50 bp were used to cast gels (Table 1).

To apply the nucleic acid mixture to the gel, app. 250 - 500 ng of DNA were mixed with 6x DNA loading dye and transferred into the gel pockets. As a standard of size, different ladders are used, depending on the nucleotide size to be analyzed (Table 5).

Electrophoresis was carried out using 150 V of electric tension in a gel chamber filled with 1x TAE buffer. Afterwards, the gel was incubated for 5-10 min in a staining bath containing ethidium bromide to enable analysis by UV light.

PAA Gel electrophoresis of RNA (denaturing or native) was carried out according to Sambrook *et al*. [217].

3.2.12 DNA and RNA purification methods

In order to purify DNA or RNA from a mixture, there are several methods. The applied method was chosen according to the downstream application of the DNA or RNA.

Ammonium acetate purification

Precipitation by ammonium acetate was performed by adding half the solution's volume of 7.5 M ammonium acetate and 2.5 time the solution's volume of ethanol absolute (Table 1) to the nucleic acid solution, and then mixing all ingredients using a vortexer. The mix was incubated on ice for 10 minutes and then centrifuged at 17000 x G at RT in a tabletop

centrifuge. The supernatant is removed, and 4 times the original solution's volume of 70% ethanol is added. After centrifuging at 17000 x G at RT, the supernatant was removed. This washing step is repeated once. The remaining nucleic acid pellet was air dried at RT for 5 - 10 min. The pellet was taken up in an appropriate amount of water to proceed with further experiments, or stored in water at -20°C.

Sodium acetate precipitation

Sodium acetate based precipitation was performed by adding the 0.1x solution volume of sodium acetate and the 2.5x volume of ethanol absolute to the nucleic acid solution to be precipitated. If only a small amount of nucleic acids is precipitated using this method, 15 µg GlycoBlue (Table 1) can be added to increase visibility of the nucleic acids. The mixture was incubated for at least 1 h at -20°C and then centrifuged at 17000 x G at 4°C. After removing the supernatant, 2x volumes of 70% ethanol were added to the pellet to wash it. After 10 min of centrifugation at 17000 x G at 4°C, the supernatant is removed. This step was carried out 2 times. After removal of the last supernatant, the pelleted nucleic acids were air dried at RT for at least 5 min. The dry pellet was resolved in an appropriate amount of water and stored at -20°C.

Butanol precipitation

For butanol precipitation, the nucleic acid solution was mixed with 10 times the volume of butanol and vortexed for 1 min. Afterwards, the reaction was centrifuged at RT for 30 min at 17000 x G. The supernatant was discarded, washed with 70% ethanol and centrifuged at RT for 10 min at 17000 x G. After repeating the washing step, the precipitate was air dried at 37°C, then solved in the appropriate amount of MQ at 45°C.

3.2.13 ITC measurements (isothermal titration calorimetry)

10 µM RNA was folded using an adequate folding program (important for correct secondary and tertiary structure) and diluted in 350 µL 1x SELEX buffer (Table 10). Depending on the ligand concentration, the same percentage of DMSO was added to the RNA solution to achieve the same buffer background for both solutions (e.g. 100 µM final ligand concentration contains 0.1% DMSO, so the final DMSO concentration of the RNA solution

was adjusted to 0.1% as well). azoCm was dissolved from its stock solution in 100% DMSO to a 100 or 200 µM solution in 1x SELEX buffer (Table 10).

ITC experiments were carried out with a MicroCal PEAQ iTC200 (Table 3) with the sample cell (app. 300 µL) containing 10 µM RNA and 100 - 200 µM ligand solution in the injector syringe (app. 60 µL). After thermal equilibration at 25°C, an initial 150 s delay and one initial 0.4 µL injection, 18 serial injections of 2.0 µL at intervals of 150 s and at a stirring speed of 750 rpm were performed. Raw data was recorded as power (µc s^{-1}) over time (min). The temperature associated with each titration peak was integrated and plotted against the corresponding molar ratio of ligand and RNA. The dissociation constant (kD) was extracted from a curve fit of the corrected data calculated using the MicroCal PEAQ-ITC Analysis Software 1.1.0.1262 (Table 12). Measurements were repeated at least twice. The protocol was adapted from Groher *et al.* [133].

3.2.14 In-line probing

For in-line probing, RNA was dephosphorylated and 5' ^{32}[P] end-labelled as previously described (3.2.9). After PAA gel purification (3.2, 3.2.11), 35 kCPM of multiple 5′ ^{32}[P] -labelled RNA samples were incubated for 2.8 - 3 d at 22°C in in-line reaction buffer, with and without different concentrations of ligand. To generate size markers, a separate 5′ ^{32}[P] -labelled RNA sample was incubated under alkaline conditions for 3 min at 96°C in 50 mM sodium carbonate (pH 9.0). Incubation for 3 min at 55°C with 20 U RNase T1 at denaturing conditions of a second sample generated a marker enabling the identification of guanine nucleotides [186]. After the in-line reaction, alkaline hydroxylation or RNase T1 treatment, RNA samples were ethanol precipitated and the pellet was dissolved in 5 M urea solution. All reactions were applied on one gel (e.g. 12% PAA urea) and separated by denaturing polyacrylamide gel electrophoresis. Afterwards, gels were dried and analyzed using phosphoimaging. The procedure was adapted according from Regulski *et al*. [186] and Groher *et al*. [133].

3.2.15 Single clone binding studies

For single clone binding studies, 100 kCPM of a ^{32}[P]-labelled RNA were pipetted in an azoCm derivatized column. The flow-through was collected. Afterwards, the column was washed 4 times with 1 mL of 1x SELEX buffer, and then 2 times with 500 µL of 1x SELEX buffer. The last two steps were split up to check in the scintillation measurement whether background levels of radioactivity were reached. The RNA was eluted using an appropriately concentrated azoCm solution, either in *cis* or in *trans* form, or using 1x SELEX buffer for background radiation data. All fractions were collected and measured in a scintillation counter to assess their radioactive nucleic acid content. The ratio of radioactivity measured in the elution fractions compared to all fractions was calculated in percent. In order to compare binding studies between different RNAs, elution values with azoCm *trans* were normalized to 100% (sum CPM of trans ligand elution). azoCm *cis* and 1x SELEX buffer elution results were compared to that normalized value (sum CPM of one elution relative to *trans* ligand elution in percent, see Equation 2).

Equation 2: **Calculation of eluted RNA relative to eluted RNA by azoCm in percent**

$$\frac{sum\ CPM of\ any\ one\ elution}{sum\ CPM\ of\ trans\ ligand\ elution} \times 100$$

$$= sum\ CPM\ of\ one\ elution\ relative\ to\ trans\ ligand\ elution\ in\ percent\ (\%)$$

3.3 *In vivo* methods

The following methods were carried out using the microorganisms *E. coli* and *S. cerevisiae*.

3.3.1 Stock keeping and cultivation of microorganisms

Strains of *E. coli* were kept in glycerol stocks at -80°C. To this end, 1 mL of the chosen *E. coli* strain in LB medium was mixed with 15% (v/v) glycerol and shock-frozen in liquid nitrogen, then stored in a freezer at - 80°C.

To grow *E. coli* cells in liquid medium, LB medium with or without a fitting antibiotic for selection was used, if not otherwise mentioned. They were incubated in chicane flasks or glass vials at 37°C during constant shaking (120 - 150 rpm) in a temperature adjustable shaker (Table 3), or in 96 deep well plates and grown at 37°C in a plate shaker. On solid medium, 100 - 150 µL of cell culture medium was streaked out on LB plates (with or without antibiotics for selection) and incubated at 37°C. Cultures on medium plates were stored at 4°C for up to two weeks.

S. cerevisiae strains were also kept stored as glycerol stocks at -80°C. To this end, 1 mL of yeast liquid culture were mixed with 15% (v/v) glycerol and stored at – 80°C.

To grow *S. cerevisiae* in liquid medium, YPD or SCD-URA medium was used. They were incubated in chicane flasks or glass vials at 30°C during constant shaking (120 - 150 rpm) in a temperature adjustable shaker (Table 3), or in 96 deep well plates and grown at 30°C in a plate shaker. On solid medium, 50 - 100 µL of cell culture medium was streaked out on medium plates and incubated at 30°C for 2 - 3 d. Cultures on medium plates were stored at 4°C for up to four weeks.

3.3.2 Generation and transformation of competent *E. coli* cells

If not stated differently, competent *E. coli* cells were prepared and transformed with plasmid DNA according to the protocol from Hanahan *et al*. [219].

In order to receive high yields for experiments where a maximum of plasmids should be transferred to cells, highly competent commercial cells (NEB 10-beta, Table 9) were used.

They were transformed with plasmid DNA using electroporation, and treated according to manufacturer's instructions.

3.3.3 Generation and transformation of EZII chemically competent yeast cells

To generate chemical competent *S. cerevisiae* cells for daily use, the Frozen EZ Yeast Transformation II Kit™ was used, according to manufacturer's instructions. The method is based on the lithium acetate method (3.3.4) [225].

To transform the yeast cells with DNA, 50 - 100 µL of cells were mixed with 200 - 1000 ng of plasmid DNA and suspended in 5 times the volume of EZ3 buffer (part of the Kit in Table 4). The cells were incubated for 45 - 180 min at 30°C, under frequent mixing. 100 - 150 µL of the mix were plated on SCD-URA agar plates and incubated for 2 d at 30°C.

3.3.4 Transformation of yeast with the lithium acetate method

To transform aptamer libraries from different SELEX rounds into *S. cerevisiae*, a high efficiency standard transformation method was used in order to cover as many different aptamers as possible (3.3.4, 3.3.5) [226]). The protocol was adapted from Gietz and Schiestl [227], the modified transformation mix components are shown in Table 14.

Table 14: **Transformation mix for the lithium acetate transformation of yeast**

Transformation mix components	Volume (µL) or mass (µg)
Yeast cells (in TE/LiOAc buffer (1x) buffer, Table 10)	50 µL
Denatured salmon sperm DNA	50 µg
Linearized vector DNA	110 ng
Insert DNA	10x molar excess to linearized plasmid
40% PEG4000-solution (with TE/Lithium acetate, Table 10)	300 µL

After transformation, cells were plated on SCD-URA plates (Table 11) and grown as described in 3.3.1.

3.3.5 Electroporation of yeast cells

To transform aptamer libraries from different SELEX rounds into *S. cerevisiae*, a second high efficiency transformation method was used in order to cover as many different aptamers as possible (compare to 3.3.4). The protocol was adapted from Benatuil *et al*. [228].

Cells of the yeast strain RS453α were grown in 100 mL YPD medium to an OD600 of 1.2. Cells were kept on ice afterwards until the second incubation step. The cells were harvested by centrifugation at 4°C for 3 min at 1600 x G. The supernatant was discarded; the pellet was washed twice with 25 mL MQ and centrifuged again. The washed pellet was suspended in 25 mL electroporation buffer (Table 10). The cell suspension was centrifuged again at 4°C for 3 min at 1600 x G, the supernatant was discarded and the pellet was resuspended in 10 mL 0.1 M LiAc / 0.01 M DTT solution. The suspension was incubated in a 50 mL Erlenmeyer flask at 30°C for 30 min at a shaker with 150 rpm to condition the cells.

Cells were transferred into a 50 mL reaction tube and centrifuged at 4°C for 3 min at 1600 x G. The supernatant was discarded and the pellet resuspended in 50 mL ice-cold electroporation buffer (1 M Sorbitol / 1 mM $CaCl_2$). Again, the cells were centrifuged at 4°C for 3 min at 1600 x G and the supernatant was discarded. Finally, the cell pellet was resuspended in a small amount of electroporation buffer, creating a final cell suspension volume of 1 mL.

For transformation, 400 µL cell suspension were mixed with 1 – 1.3 µg of vector DNA and twice the amount of insert DNA. For positive and negative controls, 100 µL cell suspension and 0.25 – 0.325 µg of plasmid DNA were used (linearized plasmid for re-ligation control, circular plasmid for transformation efficiency control). After incubation for 5 min on ice, the cells were electroporated at 2.5 kV and 25 µΩ. After electroporation, the cells were transferred into a 50 mL Erlenmeyer flask containing 8 mL YPD Sorbitol buffer (0.5 M Sorbitol / YPD) and incubated at 30°C for 1 h at 150 rpm shaking. The controls were transferred into test tubes containing 2 mL YPD Sorbitol Buffer.

After incubation, the suspension was transferred into a 50 mL reaction tube and centrifuged at RT for 3 min at 1600 x G. The supernatant was discarded and the pellet resuspended in a small volume of SCD-URA resulting in a final volume of 1 mL. A serial dilution from 10^{-3} to 10^{-5} in SCD-URA was carried out, 150 µL of each dilution step were plated and incubated at 30°C for 2 d. The remaining cell suspension was split into four 250 mL chicane flasks, each containing 62.5 mL SCD-URA. The cell cultures were incubated at 30°C for 2 d at 150 rpm.

The controls were transferred into a 2 mL reaction tube, centrifuged at RT for 3min at 1600 x G and resuspended in 250 µL SCD-URA after discarding the supernatant. 150 µL were plated on SCD-URA agar plates and incubated at 30°C for 2 d. Comparison of the transformation efficiency and re-ligation controls resulted in information on the efficiency of the homologous recombination of vector and insert DNA.

3.3.6 Fluorimeter measurements

Fluorescence measurements were performed on a Fluorolog FL3-22 (Table 3) with an excitation wavelength set to 474 nm (slit 2 nm) and an emission wavelength of 509 nm (slit 2 nm). The integration time was set to 0.5 s and temperature was adjusted to 28°C. Afterwards, OD_{600} for each culture was determined and fluorescence intensity was normalized to it. As negative control, pWHE601* (Table 8) was analyzed in parallel as a blank and its value was subtracted from all data, as cells containing pWHE601* did not express any GFP. Cells expressing GFP constitutively were transformed with pWHE601 (Table 8) and were used as a positive control. Both controls were treated equally as the riboswitch-controlled constructs. Each experiment was performed in duplicates and reproduced at least three times
The protocol was adapted from Groher *et al*. [133].

3.3.7 Flow cytometry

Flow cytometry was performed on a CytoFLEX S Flow Cytometer (Table 3). A data set was comprised over the mean and median values from a set number of single cell fluorescence reads. Typically, 5000, 10000 or 25000 cells were measured.
To measure single cells from a cell population, liquid cultures of bacteria, yeast or human cells were grown under appropriate conditions and diluted 1:10 in 1xPBS (Table 10) in 96 well plates (flat bottom, Table 3).

The measuring template shown in Table 15 was used for riboswitch *in vivo* screening (3.3.8). For second screening rounds, the number of cells measured was doubled to 10000 cells.

Table 15: **Cytometer measurement settings for *in vivo* screening**

Cytometer variable	Variable settings
Gain forward scatter	15
Gain side scatter	15
Gain 510 nm	50
Gain 610 nm	50
Flow rate	30 µL/min
Cells measured	5000 or 10000 in 120 s

3.3.8 Yeast *in vivo* screening

In vivo screening of yeast was carried out to find potential new riboswitches. The cells were transformed with a plasmid containing an aptamer, typically from a library of aptamers generated through a SELEX round. Cells from liquid culture were spread on several SCD-URA plates in a way that assured a moderate colony density to simplify single clone picking.

In vivo screening consisted of several rounds: first, second and third round of screening.

During the first round of screening, candidates that deviated from the plate regulation average (calculated without the controls) more than 0.2 points were considered as hits and were taken into the second round of screening. They were streaked out to single colony on SCD-URA plates and incubated at 30°C for 3 d. Four single clones per plate were measured using the same conditions as in round one. Could the regulation factor from round one be verified in at least two of the four clones from round 2, the positive culture was cultivated in 4 mL SCD-URA at 30°C for 1 d and the plasmid DNA was extracted. *E. coli* cells were transformed with the plasmid and grown on plate. Four single *E. coli* colony were picked, their plasmids were isolated, and EZII competent yeast cells (Table 9) were transformed with one single plasmid per sample. They were grown and measured again using conditions from round 1. If the regulation factor could be verified again, a riboswitch was considered discovered, and replications of this measurement could begin. The passaging through *E. coli* cells was necessary as *S. cerevisiae* can take up more than one plasmid in a transformation, which can lead to falsely positive results in fluorescence measurements. A yeast culture streaked out to single colony, which is then cultured in liquid media typically only contains one plasmid sequence [229].

Two different variants of screening were carried out; one using the Tecan Microplate Reader Infinite 200 PRO (Table 3). The protocol was based on Weigand *et al*. [132].

A second variation of the screening was based on single cell measurement in a flow cytometer (Table 3). The protocol for this screening variant was adopted from Groher *et al*. [133].

Next to the measurement method, the biggest difference between the two screening protocols was the growth conditions of the yeast cultures. In the flow cytometry approach, cultures were grown in 96 well plates while shaking, where in the Tecan reader approach, cultures were grown in 96 well plates without shaking.

In both methods, regulation factors were assessed. They were calculated by dividing the GFP fluorescence value of a colony grown without ligand by the fluorescence value of the same colony grown with ligand (Equation 3).

Equation 3: **Basic regulation factor calculation**

$$\frac{GFP\ fluorescence\ (colony\ grown\ without\ ligand)}{GFP\ fluorescence\ (colony\ grown\ with\ ligand)} = switching\ factor$$

Corrections to these values were calculated according to the different methods used for measurement of fluorescence. In the case of Tecan reader measurement, each fluorescence value was divided by the cultures' corresponding OD_{600} value prior to calculation of the regulation factor, to remove errors due to a different cell number in each culture. In the case of flow cytometric measurement, this kind of correction is irrelevant because the flow cytometer measures a set number of single cells. As an improvement to the flow cytometry based *in vivo* screening, a plasmid with a constitutively expressed mCherry gene was introduced as a plasmid backbone for screening by Dr. Cristina Bofill-Bosch (pCBB, Table 8). To calculate regulation factors, the GFP fluorescence value of each colony (with and without ligand) was first divided by the culture's mCherry fluorescence value, to avoid errors due to a different individual level of gene expression. The two different error correction calculations are shown in Equation 4 and Equation 5).

Equation 4: **Corrected regulation factor using OD_{600}**

$$\frac{\frac{GFP\ fluorescence\ (colony\ grown\ without\ ligand)}{OD600\ (colony\ grown\ without\ ligand)}}{\frac{GFP\ fluorescence\ (colony\ grown\ with\ ligand)}{OD600\ (colony\ grown\ with\ ligand)}} = corrected\ switching\ factor$$

Equation 5: **Corrected regulation factor using mCherry**

$$\frac{\frac{GFP\ fluorescence\ (colony\ grown\ without\ ligand)}{mCherry\ fluorescence\ (colony\ grown\ without\ ligand)}}{\frac{GFP\ fluorescence\ (colony\ grown\ with\ ligand)}{mCherry\ fluorescence\ (colony\ grown\ with\ ligand)}} = corrected\ switching\ factor$$

During screening, candidates that showed a decrease in relative GFP expression by a factor of 1.3 were considered positive hits and were taken into the next round of screening.

Both *in vivo* screening methods have in common that a set of controls is included in each 96 well plate of clones that is measured. To minimize false positive hits during screening, three controls were included in each plate, using different plasmid backbones for the different measurement methods. These controls included a control of functional, constitutive gene expression (GFP on, pWHE601 or pCBB006), a control showing no gene expression because the construct is lacking an ATG start codon upstream of the *gfp* reporter gene (GFP off, pWHE601* or pCBB005) and a riboswitch control, containing the neomycin upstream of the *gfp* reporter gene (GFP regulated by neomycin, pWHE601-neo or pCBB007 (Table 8).
In vivo screening results from yeast cells containing one type of aptamers (e.g. aptamers from the same SELEX round) are displayed as boxplots. The median of regulatory factors is given.

3.4 SELEX procedure

For SELEX, a large diverse nucleic acid library is necessary. Conception and development of the libraries used in this thesis are described in chapters 4.3 and 4.13. In general, the library for SELEX needs to be as diverse as possible to cover as many potential sequences as possible (2.1.8). Libraries for SELEX were ordered at Microsynth Seqlab, Germany.

SELEX consists of several steps, as well as pre-requisites that must be fulfilled before starting. The SELEX carried out in this thesis is column-based affinity SELEX. Before starting the SELEX itself, the following pre-requisites must be provided:

- A large diverse RNA library and aliquots of this library labelled radioactively
- Columns containing resin with immobilized ligand
- SELEX buffer stock

The subsequent column-based affinity SELEX consisted of 5 main steps:

- Loading a radioactively labelled RNA library onto the ligand-derivatized columns,
- Washing the columns with buffer to elute unbound RNA molecules,
- Elution of the bound RNAs using high salt concentrations or free ligand solution,
- Reverse transcription and amplification of eluted RNA using RT-PCR
- Re-transcription of the enriched library by *in vitro* transcription using a nucleotide mix containing radioactive [α-^{32}P] UTP.

In the following, the relevant steps are described.

3.4.1 Ligand immobilization

The commercially available activated resin Affi-Gel 10 (Table 1, 20 mL column material, capacity 15 µmol/mL gel) was filtered through a glass frit previously cleaned with H_2SO_4 and MQ and washed with ice-cold isopropanol.
7.5 mL of resin were filled up to 10 mL with DMSO. To this, 5 mL of a 3 mM ligand solution (dissolved in 100% DMSO) were added.

To make mock or pre-columns for depletion of RNAs in the SELEX library able to bind the affinity matrix, 5 mL of DMSO without ligand can be added to 10 mL of washed, activated resin, instead.

The reaction was incubated for 4 h on a rotating mixer (Table 3) and afterwards filtered through a glass frit and washed twice with DMSO. To deactivate remaining NHS esters, 5 mL of a 0.1 M ethanolamine solution (pH 8.0) were added to the derivatized column material and incubated for 1 h at RT on a rotating mixer. Afterwards, the derivatized and deactivated column material was washed several times with DMSO and finally mixed 1: 1 with a 0.002% sodium azide solution. For each individual column, 1 mL of the mixture was aliquoted into chromatography columns (Table 3, 1.2 mL bed volume) and stored at 4°C.

3.4.2 SELEX buffer

For SELEX, a buffer based on Berens *et al*. [208] (see Table 10) and supposed to mimic the environment within a yeast cell, was prepared. The buffer consisted of 10 mM Tris-HCl, 250 mM NaCl and 5 mM $MgCl_2$. As yeast growing in a glucose rich-medium is reported to have an internal pH value of 7 to 8, the buffer was adjusted to pH 7.6 [230].

As it is important for SELEX to provide stable conditions during the SELEX process, 2 L of a 5x stock solution were prepared to be sufficient for all experiments (buffer composition see Table 10).

3.4.3 SELEX process

The SELEX process consists of 5 main steps making up one round of SELEX. The steps were repeated sequentially, so that a round continued with the material generated in the previous round. Data points were collected for each round to analyze the progress of the SELEX process. To explain the process, it is shown here in an overview of the complete procedure, while details to the protocols can be found in the respective Material and Methods sections (3.2.7, 3.2.8, 3.2.9, 3.2.11, 3.2.12, 3.2.12).

1.2x 10^{15} RNA molecules from the initial library were spiked with approximately 250 kCPM (kilo counts per minute) of 5’ 32P-labelled RNA library in MQ (3.2.9) to use in the first

round. RNA folding was performed by heating the mixture to 95°C for 5 min, then cooled on ice for 5 min. Afterwards, 100 µL of 5x SELEX buffer, 6 µL of yeast tRNA (final concentration 0.3 µg/µL) and 144 µL of MQ were added. The mixture was incubated for 15 min at RT. In the meantime, the column (and pre-column if applicable) was washed with 10 volumes of 1x SELEX buffer (10x 500 µL). The RNA mixture was then applied to the column (or pre-column) and incubated at RT for 30 min (flow-through fraction).

Afterwards, the column was washed in steps of column volumes (CV=500 µL), using 1x SELEX buffer (wash fractions). The number of washing-steps ranged from 10 to 20, depending on the applied stringency.

RNA was then eluted by either 4 CV of 20 mM EDTA or 1 or 5 mM azoCm (elution fractions). During the process, stringency could also be increased by a decreased binding time of the RNA library to the column from 30 to 15 min, or pre-elution steps (pre-elution fractions). All fractions of liquids (all of a volume of 1 CV) were collected individually. 10 µL of each fraction were measured in a scintillation counter to follow the progress of SELEX (3.4.4).

Eluted RNA fractions were pooled and precipitated with sodium acetate (3.2.12) in the presence of 15 µg GlycoBlue™ Coprecipitant (Table 1). The air-dried pellets were dissolved in a total volume of 50 µL MQ and reverse-transcribed and amplified (RT-PCR, 3.2.7). Product formation was monitored on a 3% agarose gel (3.2.11).

For the following rounds (all except round 1), RNA was transcribed according to 3.2.8. In short, 10 µL of RT-PCR product were mixed with TK SELEX mix (Table 10) and 33 nM [α-^{32}P] UTP (Table 1) in a total volume of 100 µL. Purification was performed using the sodium acetate precipitation protocol, according to 3.2.12.

In all SELEX rounds but the first, 500 kCPM RNA were folded, diluted in 1x binding buffer with yeast tRNA and subsequently loaded onto the column for the next round of SELEX.

3.4.4 SELEX process analysis

To get comparable results enabling the assessment of aptamer enrichment within the SELEX process, all flow-through, wash, pre-elution and elution fractions during SELEX were collected and measured regarding their radioactivity. For this, 10 µL of each fraction were measured in 2 mL scintillation cocktail in a scintillation counter.

Higher radioactive counts measured corresponded to a greater number of radioactively labelled aptamers in the corresponding fraction. For each round, the ratio of the sum of ligand eluted radioactivity in CPM to the sum of CPM of all fractions (flow-through, wash, elution) of a sample was calculated in percent. Over the course of SELEX, an increase in percentage should be a sign of enrichment of specifically binding aptamers in the elution. The percentages over the rounds are displayed as bar diagrams or as curves.

4 Results

4.1 In-line probing of aptamer 42

A SELEX previously to this work against azoCm yielded aptamer 42 (2.2.3, 2.2.4), able to bind the molecule azoCm in an isoform selective manner. In order to understand more about this aptamer, a structural analysis by in-line probing was carried out (3.2.14).

Radioactively labelled RNA of aptamer 42 was incubated for 3 d with different ligand concentrations (10, 100 nM, 1, 10 and 100 µM, and without ligand) in in-line buffer.

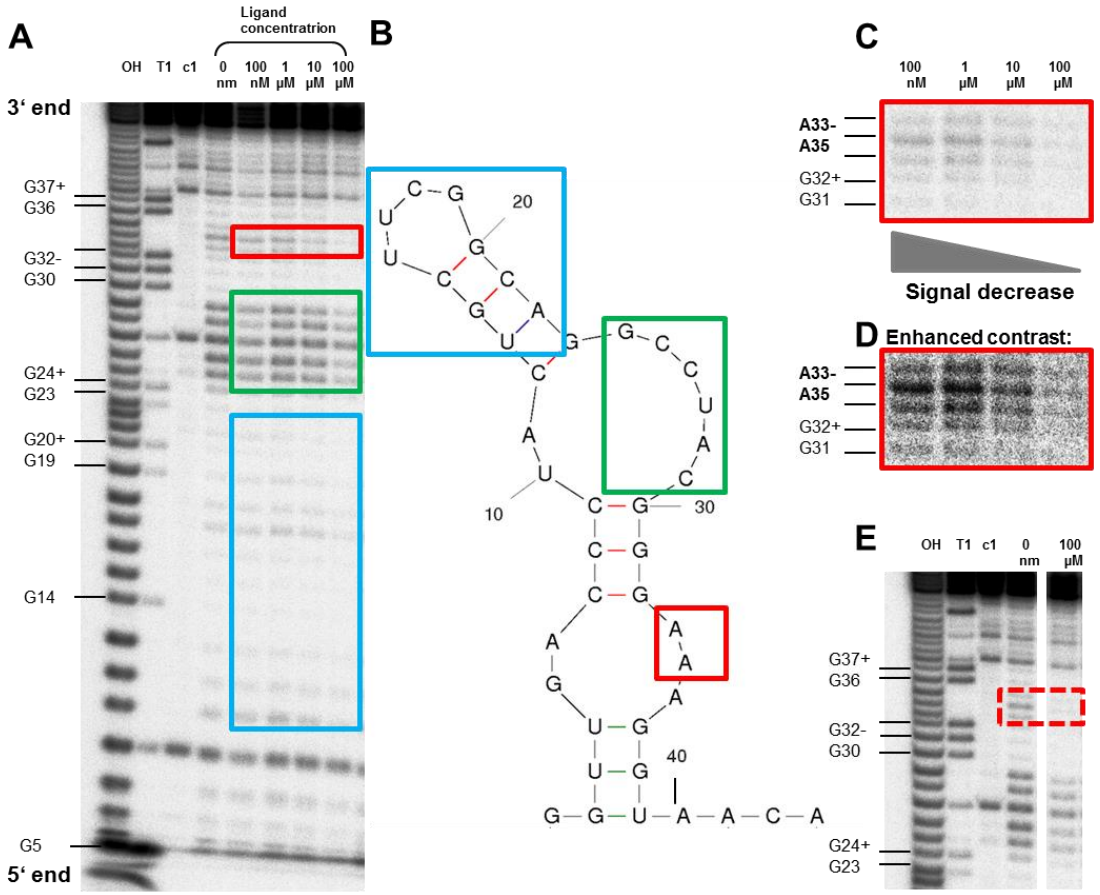

Figure 14: **In-line probing of aptamer 42 A** In-line probing gel of aptamer 42 on a 15% PAA urea gel. Lanes show from left to right: alkaline hydrolysis ladder (one band for every nucleotide in the aptamer sequence) RNase T1d-ladder (digest of aptamer sequence after every G in the sequence), aptamer incubated with 0 nM, 100 nM, 1 µM, 10 µM, 100 µM ligand. Marked in red are the two nucleotides showing a decrease in band intensity with increased ligand concentration, marked in green are nucleotides showing digestion products due to structure flexibility, marked in blue are nucleotides not showing digestion products due to structure stability. **B** Refined secondary structure after results from in-line probing gel in A were taken into account. The red, green and blue marked areas show a structure that would fit with experimental results. **C** Shown is a close-up on the two nucleotides affected by increasing ligand concentration from 100 nM to 100 µM (left to right). **D** Shown is the close-up on the gel from C with an increased contrast to visually emphasize the difference in band intensities with increased ligand concentration. **E** Direct comparison of the nucleotide bands without any ligand present (0 nM) and with 100 µM ligand present (red dashed rectangle).

Separation of the samples on a 15% PAA gel showed a fragmentation pattern (Figure 14A). Cleavage controls were carried out in parallel to receive ladders enabling an exact assignment of each band to a nucleotide in the sequence. An alkaline hydrolysis ladder (first lane on the left, Figure 14A) showed a band for each nucleotide in the sequence, a RNase T1 enzyme treated ladder showed a band for every G residue in the sequence, as well as a few unspecific breakdown bands (between G5 and G14, lower quarter of the gel, Figure 14A).

In-line probing analysis of aptamer 42 showed a distinct cleavage pattern, as depicted in Figure 14A. There were three regions noticeable, marked in blue (U13-A22), green (G24-C29) and red (A33+A34). Nucleotides inside the blue rectangle showed barely any bands on the gel, indicating a very stable and most probably base-paired region. The nucleotides within the green rectangle show a strong band at each position, indicating a flexible, most probably single stranded region in the aptamer. Nucleotides within the red rectangle show a ligand concentration dependent decrease in band intensity, a behavior not seen in the green and blue region.

From this cleavage pattern, information about the secondary structure of RNA aptamer 42 could be derived. Comparison to a previously assumed 2D structure gathered by mfold prediction (Table 12, compare Figure 12) revealed regions that did not fit with the cleavage pattern presented on the gel. Nucleotides inside the blue rectangle, which are indicating a stable base-paired region, correspond with nucleotides U13-A22, which are single-stranded in the previously predicted structure (Figure 12). Opposed to that, the nucleotides within the green rectangle of the gel (Figure 14A+B), indicate a flexible, single-stranded region of the aptamer, however the predicted structure in Figure 12 shows them to be base-paired.

Using mfold, the stable tetraloop UUCG [231, 232] is formed (U13-A22), which can be found in the previously predicted structure shown chapter 2.2.4. However, the experimental data gathered from in-line probing could not support this predicted secondary structure of aptamer 42. While the UUCG tetraloop is still formed in the data-based structure prediction (blue region), refolding of the nucleotides in the green region led to the predicted structure shown in Figure 14B. For future studies, this secondary structure was assumed to represent the correct folding, because like that the areas marked in red, green and blue show a structure fitting the experimental results (Figure 14B).

Data regarding aptamer-ligand interaction could be gathered by in-line probing as well. As described before, the nucleotides within the red rectangle show a ligand concentration dependent decrease in band intensity, a behavior not observable in the green and blue region.

This indicated that at these two Adenine positions (A33+A34), ligand interaction may take place. A close-up on the gel in this region makes the effect clearer (Figure 14C), particularly when the contrast of the close-up image is enhanced using ImageJ (Table 12, Figure 14D) [212, 213]. Comparing the aptamer column without any ligand to the one where 100 µM ligand were present (Figure 14E, red dashed rectangle) shows that the stability of this aptamer position (particularly A34) is strongly increased upon ligand addition, as less spontaneous cleavage occurs.

In-line probing of aptamer 42 did not only lead to a new 2D structure proposal, it also yielded first indications of aptamer positions which could be involved in interactions with its ligand azoCm.

4.2 *In vivo* screening of affinity SELEX Rudolph

Rudolph could show that aptamer 42 could not function as a riboswitch in yeast cells [196]. As it is known that many well-characterized aptamers cannot be used as riboswitches *in vivo*, a method developed by Weigand *et al*. was used, allowing the isolation of *in vivo* active riboswitches from an *in vitro* enriched SELEX pool (2.1.11) [132]. Other aptamers of the SELEX by Rudolph were tested regarding their function as a riboswitch in the course of this work.

DNA from round 6 from the SELEX by Rudolph (marked in red, see Figure 15) was amplified using PCR (primer pair “Library 1 fwd” and “rev”, Table 6). The resulting aptamer templates were cloned into the 5’ UTR of a GFP gene on the plasmid pWHE601 (Table 8). Figure 15 shows the result of yeast *in vivo* screening of round 6 of SELEX Martin (2.2.3). Shown in brackets at the top is the amount of 1907 colonies tested in the first round of screening. Clones that seemed to indicate riboswitching (upper whisker of boxplot) were tested in a second round of screening in quadruplets, and, from cultures seeming to show switching, plasmids were extracted. They were passaged through *E. coli* cells, and then re-transformed into yeast cells for a third and last round of screening (2.1.11, 3.3.8).

From the graph shown in Figure 15B, none of the 1907 colonies analyzed showed any azoCm dependent regulation of gene expression after a third round of analysis. From this it was concluded that all experimental results from the first round of *in vivo* screening showing

regulatory factors in the upper quartile (upper whisker) or lower quartile (lower whisker) of results were outliers due to measurement or method inconsistencies.

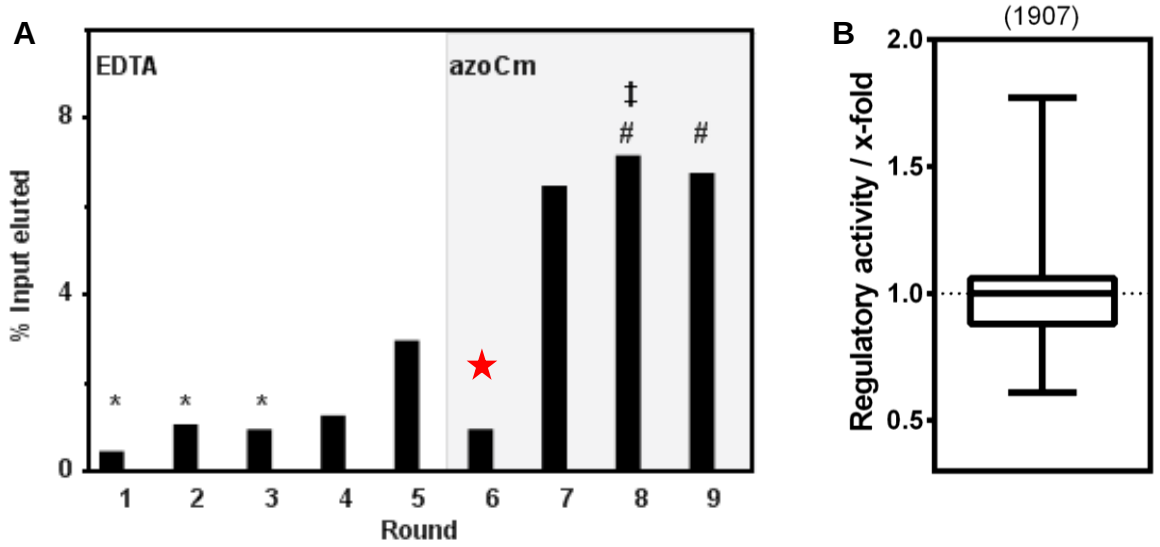

Figure 15: ***In vivo* screening of SELEX Rudolph A** Shown is the fraction of loaded RNA that could be eluted from azoCm-derivatized columns after each round of SELEX performed by Rudolph [196]. RNA was eluted by either 20 mM EDTA (round 1–5) or 5 mM azoCm (round 6–9). In the first three rounds, a negative selection step was performed (*). In round 8, stringency was increased by raising the number of column washes from 10 to 25 and an increased timeframe for the elution of the RNA from the column (‡). Pre-elution steps were performed in round 8 and 9, adding an additional pre-elution step per round (#)The red star marks the SELEX round used for *in vivo* screening. **B** This boxplot shows the summarized *in vivo* screening in *S. cerevisiae* for round 6 (R6). For each investigated clone, the regulatory activity was calculated as ratio of GFP fluorescence with and without 100 µM azoCm (x-fold). The number written above the boxplot indicates the number of clones analyzed. The median of all analyzed clones in R6 was 1.0.

As the aptamer discovered in the first SELEX did not work as a riboswitch, nor did any of the aptamers tested in *in vivo* screening, the SELEX carried out by Rudolph (Figure 15B) was considered useful to generate specific aptamers, but unfitting to generate specific riboswitches.

4.3 Development of a new pool for SELEX against azoCm

The first SELEX yielded specifically binding aptamers with a low micromolar kD, but no aptamers showed any regulation *in vivo* [196]. Aptamers already seemed to be so tightly structured that any GFP expression was completely repressed without adding the ligand to the cells. As these aptamers were too pre-structured to be useful in a riboswitch context, and engineering had not improved them [196], a new SELEX strategy was planned.

The RNA pool used in the first SELEX consisted of a 1:1 mix of two different pools ("pool 1", see Figure 16) [112, 233]. One of the pools contained a fully randomized region, while the other contained a pre-structured element supposed to increase aptamer stability (Figure 16). The randomized pool has a randomized region of 64 nucleotides. The pre-structured pool has a 4 bp stem topped by a stable UUCG tetraloop, flanked by 26 randomized nucleotides on each side. Both pools are flanked on the 5' and 3' ends of their randomized regions by constant regions (necessary for cDNA synthesis and PCR amplification during SELEX). The 5' and 3' constant regions of the RNA pools were chosen so that they could enter into Watson-Crick base-pairings with each other, thus releasing the (partially) randomized core region for interaction with the ligand.

As most aptamers identified from the first SELEX did contain the stable stem loop structure, it was concluded that they were too stable to be used as riboswitches in an *in vivo* application. Therefore, the pool designed for the first SELEX of this thesis was adapted from Famulok *et al*. [112] and consisted of a 74 randomized nucleotide region (N74) flanked by two constant regions ("pool2", Figure 16, Table 6). This design should allow a long flexible randomized aptamer region without any pre-set bias towards aptamer stability.

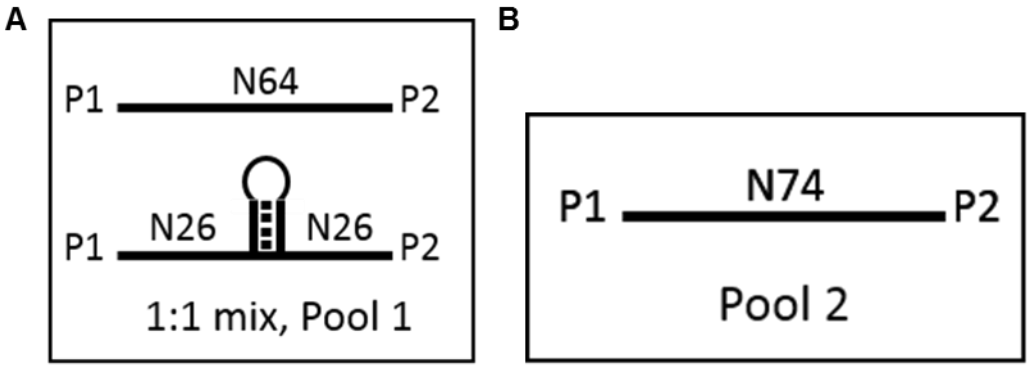

Figure 16: **Pool Rudolph (Pool 1) and new SELEX pool (pool 2) A** The pool used for a previous SELEX consisted of a 1:1 mix of two different pools. One pool contained a fully randomized region of 64 nucleotides (N64), while the other contained a pre-structured 4 bp stem topped by a stable UUCG tetraloop, flanked by 26 randomized nucleotides on each side (N26). Both pools are flanked on the 5' and 3' ends of their randomized regions by constant primer binding regions (P1, P2). **B** The newly designed pool for SELEX consists of a 74 randomized nucleotide region (N74) flanked by two constant primer binding regions (P1, P2).

Primers were designed which could bind to the constant regions, with the forward primer containing a T7 promoter on the 5' end to generate cDNA for PCR amplification of the aptamers during SELEX. From the PCR products, aptamers could directly be transcribed to RNA again (pool and primer sequences in Table 6).

To use the newly designed pool in SELEX, a highly diverse starting pool is necessary to provide a broad sequence space where as many nucleotide combinations as possible can be found to make up a specifically binding aptamer. In order to generate this pool, the initial pool-oligonucleotide was ordered from the DNA synthesis company Seqlab (Table 6). This oligo is taken and amplified in a large scale using PCR (primer pair "Library 2 fwd" and "rev", Table 6). In order to receive the maximum amount of DNA possible from this PCR, different protocols were tested and optimized.

4.3.1 Pool PCR optimization

Since a high variability of the source library is important, the PCR protocol for the amplification of the DNA provided by the synthesis company Seqlab had to be optimized. This is necessary to generate the maximum amount of aptamers from the starting library without getting overamplification of PCR products, which could introduce bias into the aptamers' diversity and distribution. After the optimization of the PCR protocol, the large-scale production of the DNA library follows, since large amounts of DNA are required to produce an RNA library.

First, a so-called scout PCR is carried out, which shows whether the chosen PCR protocol works and which number of amplification cycles might be optimal. To this end, a PCR mix made, and PCR was carried out for 16 cycles using the PCR program described in Table 16.

Table 16: **PCR test program for pool scout PCRs**

T	t		PCR steps
98°C	30 s		Initial melting
98°C	10 s		Melting
58°C	10 s	repeat in cycles	Primer annealing
72°C	10 s		Elongation

Shown are the temperature (T) applied in each PCR step, as well as the time (t) during which the temperature is applied. The final three steps are repeated for a number of cycles.

After rounds 5, 7, 9, 11, 13 and 15, 5 µL of the reaction were taken from each PCR sample and mixed with 6x DNA loading dye. Comparison of the results after different numbers of cycles allowed determination of the optimal number of cycles for this reaction. A negative

control was carried out as well, using the same PCR mix but containing no template DNA. Figure 17 shows a distinct band at the expected size of 129 bp on a 3% agarose gel.

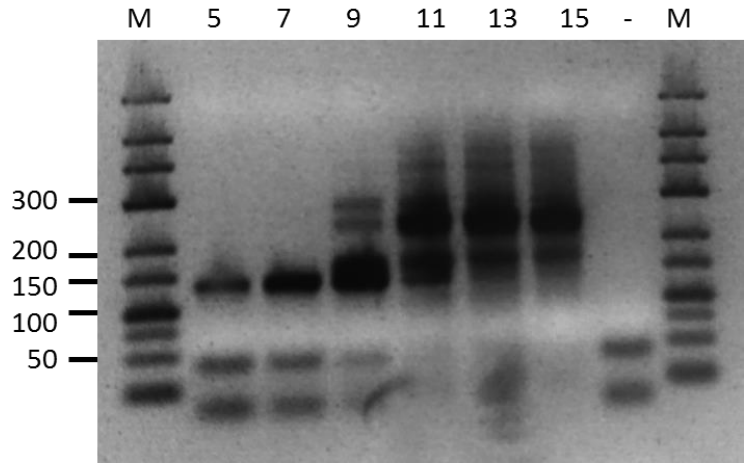

Figure 17: **Agarose gel of pool 2 scout PCR** Shown is a 3% agarose gel with lanes representing bands of different amounts of cycles tested to amplify pool 2 via the PCR program described in (Table 16). Shown from left to right in the lanes are PCR-results with: Marker (M), 5, 7, 9, 11, 13, 15 cycles resp. and the negative control sample containing no template (-). Annealing temperature was 58°C.

As Figure 17 shows, starting from 9 cycles of PCR amplification, overamplification bands begin to appear in the samples. As the amplified band representing 129 bp was weaker after 5 cycles than after 7 cycles, 6 to 8 cycles were considered to be the optimal number of PCR cycles for the amplification.

In order to further optimize PCR conditions, different annealing temperatures were tested, parallel to a range of amplification cycles determined before. Temperatures tested were 54, 58 and 62°C, the different amount of cycles tested were 6, 7, 8, as wells as 9 cycles, as a control. Samples were taken as described before and applied on a 3% agarose gel (Figure 17).

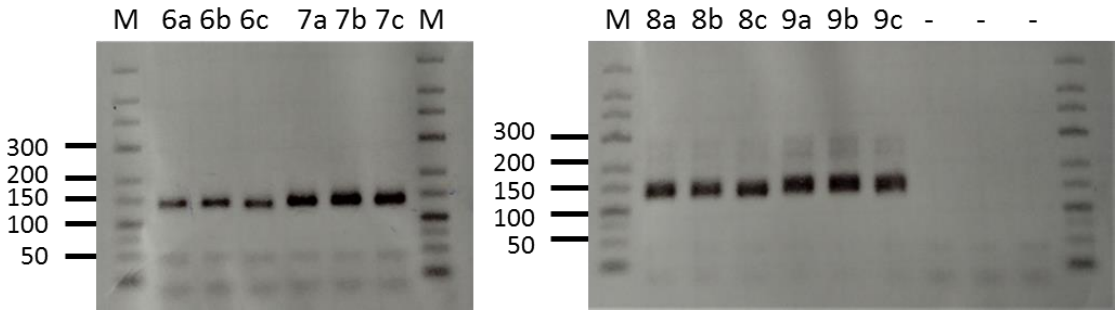

Figure 18: **Agarose gel of pool 2 scout PCR, details** Shown is a 3% agarose gel of the different amount of cycles tested to amplify pool 2 via the PCR program described in (Table 17). Shown from left to right in the lanes are: Marker (M), 6 cycles: 6a (54°C), 6b (58°C) 6c (62°C); 7 cycles: 7a (54°C), 7b (58°C) 7c (62°C); 8 cycles: 8a (54°C), 8b (58°C) 8c (62°C); 9 cycles: 9a (54°C), 9b (58°C) 9c (62°C) ; negative control sample containing no template (-, 54°C).

Figure 18 shows the strongest and cleanest results at 54°C and 7 cycles of amplification. PCR efficiency was calculated according to Hall *et al*. [234]. The final optimized PCR program can be found in Table 17.

Table 17: **Finalized pool amplification PCR protocol**

T	t		PCR steps
98°C	30 s		Initial melting
98°C	10 s		Melting
54°C	10 s	repeat in cycles	Primer annealing
72°C	10 s		Elongation

Shown are the temperature (T) applied in each PCR step, as well as the time (t) during which the temperature is applied. The final three steps are repeated for 7 cycles.

4.3.2 SELEX pool generation

The optimized PCR protocol was applied in a 45 mL PCR reaction carried out in 96 well plates, using the entire remaining synthesized pool sample as template. The resulting DNA pool was precipitated using sodium acetate precipitation (3.2.12) and resuspended in a total volume of 2 mL of water. From this pool DNA solution with a concentration of 4.25 µg/µL (or 1.2x 10^{-10} mol/µL), 68.3 µL (or 8.3x10^{-9} mol) were used in a 10 mL transcription sample (3.2.8). This amount of DNA should contain the tenfold number of molecules than in the initial sample of the pool oligo received from the synthesis company. As matrices are transcribed multiple times during *in vitro* transcription reactions, this should result in several RNA copies of all possible sequences contained in the synthesized pool sample. The RNA pool was transcribed as described in chapter 3.2.8. The transcribed pool was precipitated using sodium acetate precipitation and purified using PAA gels (chapters 3.2.11, 3.2.12). Resuspended in 2 mL of RNase free water, the RNA pool had a concentration of 194 pmol/µL. This pool RNA stock solution was used for SELEX experiments carried out in this thesis.

To calculate the potential sequence space covered by the generated pool, the amount of synthesized pool oligo used in the PCR was calculated based on the concentration (200 nmol/L) and volume of the oligo (4 mL) according to Equation 6:

Equation 6: **Calculation of DNA amount of substance in mol used for SELEX pool generation**

$$200\ \frac{nmol}{L} *\ 0.004\ L = 0.8\ nmol =\ 8x\ 10^{-10}\ mol$$

Multiplication with the Avogadro constant resulted in the total amount of molecules used in the PCR (Equation 7):

Equation 7: **Calculation of total DNA molecules used for SELEX pool generation**

$$8x\ 10^{-10}\ mol * 6.022x\ 10^{23}\ mol^{-1} = 4.8x\ 10^{14}\ molecules$$

The generated aptamer pool does not cover the sequence space possible in the used N74 library (4^{74}=3.57x 10^{44} potential sequences, see 2.1.8). Having used the complete amount of synthesized pool oligo for the large-scale PCR, a bigger sequences space could not be achieved. It is possible to find a specifically binding aptamer in the generated sequence space, but it should be kept in mind that not all possible nucleotide combinations in the randomized region are represented in the generated pool.

In an RNA pool, equal nucleotide distribution across the sequences is important to not incur bias before the start of a SELEX. Therefore, from the original pool DNA, 20 random candidates were sequenced as representatives. Sequencing of the 20 candidates showed a distribution among the nucleotides as shown in Figure 19 in the randomized region of the aptamer (N_{mean}=74.25 nucleotides).

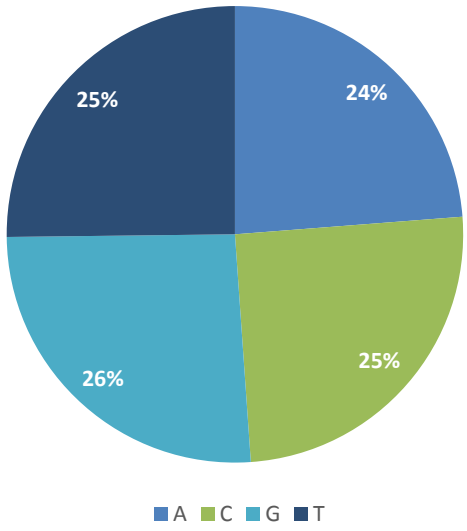

Figure 19: **DNA nucleotide distribution in a random sample of aptamers from pool 2** Shown is the distribution of the different nucleotides in the randomized region of the aptamer of 20 randomly selected aptamers (mean of nucleotides per aptamer was 74.25 nucleotides).

As all nucleotides were represented more than 23% but less than 26%, equal distribution of all nucleotides in the randomized region was assumed.

4.4 SELEX against azoCm

The generated N74 RNA library with the variability of 10^{14} was used for SELEX against azoCm (Table 2). azoCm Amino derivatized Affi-gel was used as column material (Table 1, Table 2).

In a typical SELEX round, first, radioactively labelled RNA is folded using temperature differences to make it take on its natural three-dimensional structure. SELEX buffer and yeast tRNA are added and the RNA is applied on an azoCm derived column. The flow-through of the liquid passing the column is collected. After an incubation period which allows the RNA time to bind to the immobilized ligand, washing steps are carried out, each in fractions of "column volumes" (CV, the same volume the column material takes up, in this SELEX, 500 µL). After washing, the bound RNA is eluted either unspecifically with 20 mM EDTA or free ligand solution (in this case, 5 mM azoCm). Typically, 4 elution steps of 1 CV each are carried out per SELEX round. All liquid fractions (flow-through, washing, elution) are collected individually and aliquots are measured in a scintillation counter, to judge the relative amount of radioactive RNA in each fraction. After the SELEX, all elution fractions are pooled and used for RT-PCR (3.2.7) for amplification. The DNA resulting from this is used as the template for an *in vitro* transcription of RNA (spiked with radioactive nucleic acids), which in turn makes up the RNA starting pool for the next SELEX round. This process is repeated for several consecutive rounds to generate an RNA pool enriched with ligand binding aptamers. The detailed SELEX protocol can be found in chapter 0.

In contrast to the first SELEX, where unspecific elution was continued until round 5 (2.2.3, Table 18 [196]), in this SELEX already in the second round unspecific elution was switched to specific elution. In the first round of SELEX all bound RNAs were eluted with 20 mM EDTA, whereas starting from round 2, a 5 mM ligand solution was used. To remove RNAs with an affinity towards the column matrix itself, in rounds 1-4, non-derivatized pre-columns were used. All RNAs which were able to pass these columns were transferred to the azoCm Amino derivatized columns for specific binding. Table 18 gives an overview over the conditions applied.

The first enrichment was visible in round 5 (0.9%), round 6 verified this enrichment with 4.8% RNA elution (Figure 20 and Figure 21). Different variations in the SELEX strategy were applied starting from round 7, where the stringency of elution was increased to generate binders with a high binding affinity [235]. The amounts of eluted RNA using the different strategies are shown in Figure 20.

One way to increase stringency in this SELEX was the increase of washing steps, which would remove aptamers binding not as strongly to the immobilized ligand as others. Another method used were so-called pre-elution steps, carried out with ligand solution after the last washing step but before the elution samples were collected for re-amplification of the aptamers. These pre-elution steps are supposed to remove aptamers from the SELEX, which quickly lose their binding to the immobilized ligand as soon as free ligand solution is present (fast k_{off} rate [236]). As aptamers eluted by pre-elution steps were discarded, they were removed from the RNA pools used for the next SELEX round. The last stringency increasing method in course of this SELEX was the reduction of binding time for the RNA aptamers of a round. After application of the aptamers on the column, the waiting time before the first washing step, in which the aptamers have time to initiate binding to the immobilized ligand, was reduced, to wash away aptamers showing a slow ligand binding (slow k_{on} rate [236]). As aptamers from washing steps were discarded, those aptamers with a slow binding were removed from the SELEX as well. Table 18 lists in which round which stringency method was used.

In the first SELEX variation (S1), stringency was increased by raising the amount of washes in round 7 from 10 to 15 washes, as well as pre-eluting the RNA with 1x CV of 1 mM azoCm (Figure 20). In round 8, 20 washing steps were used. The incubation time of RNA on the column was shortened from 30 min to 15 min, two 1 mM pre-elution steps were carried out (Table 18). As can be seen in Figure 20, elution percentages of round 7 and 8 were 4.8 and 11%, respectively (S1). As this meant no reduction of percentage in eluted RNA compared to round 6, it was concluded that the degree of stringency was too low.

Table 18: **SELEX conditions tested**

Round / Variation	1	2	3	4	5	6	7	8	9
Rudolph/old	PC, U	PC, U	PC, U	PC, U	PC, U			W25, 2x #	W25, 3x #
First	PC, U	PC, Elu 5 mM	PC, Elu 5 mM	PC, Elu 5 mM	Elu 5 mM	Elu 5 mM	W15, 1x # 1 mM, Elu 5 mM	Incu15, W20, 2x # 1 mM, Elu 5 mM	
Second							W20, 2x # 1 mM, Elu 5 mM	Incu15, W20, 2x # 5 mM, Elu 5 mM	
Third							W20, 2x # 5 mM, Elu 5 mM	W20, 2x # 5 mM, Elu 5 mM	Incu15, W20, 2x # 5 mM, 25 min wait, Elu 5 mM

Shown is a comparison of the different ways SELEX rounds against azoCm were carried out. Conditions per round are listed. It is shown whether a pre-column (PC) was used and if unspecific elution (U) or specific elution with a certain azoCm concentration was applied (Elu mM). No markings indicated washing of the column with 10 CV of 1x SELEX buffer, all differing volumes of washes are indicated (W). Pre-elution steps are marked by (#), shortened incubation times from 30 min of the RNA on the column before the first are marked by (Incu). If, instead of proceeding directly to the next elution step a waiting period was applied, (min wait) is shown. For comparison, the previous SELEX against azoCm by Rudolph was included.

In a second SELEX variation (S2), washings steps in round 7 were increased directly to 20 and two pre-elution steps with 1 mM azoCm were carried out (Figure 20). In round 8, the same conditions as in the first variation were used. As can be seen in Figure 20, in this second approach the amount of eluted RNA was much higher (16 und 11%, S2) than in the first variation S1. This indicated that the increased stringency was not successful immediately in round 7, therefore another variation was started.

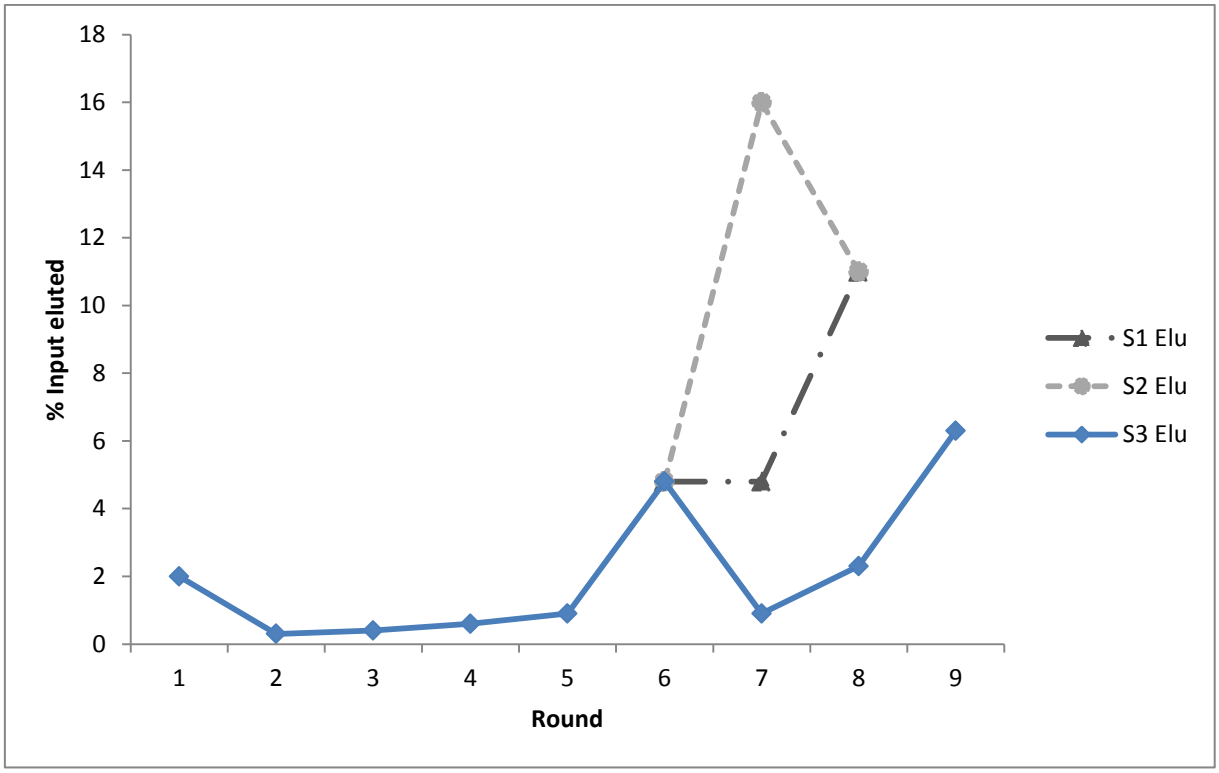

Figure 20: **Summary of all SELEX variations against azoCm using pool 2**. Shown is the summary of eluted RNA per RNA input in percent for every SELEX round of pool 2. Starting after the first distinct enrichment can be observed in round 6, variations in the SELEX procedure eluted differing amounts of RNA (see Table 18).

In the third variation of SELEX (S3), stringency was increased in round 7 by doubling the number of column washes from 10 to 20 for all consecutive rounds (Figure 20). Additionally, two pre-elution steps using 5 mM azoCm were performed starting from round 7. In round 9, binding time of the RNA to the column was reduced from 30 min to 15 min. Also, after every elution step, the RNA was left to incubate on the column for 25 min. These stringency steps lead to Elution percentages were gradually increasing from 0.9%, to 2.3% until 6.3% were reached in round 9. As the elution percentages in round 7 (0.9%) were lower than in round 6 (4.8%) for the first time, but still showed a gradual increase (enrichment) over the rounds, these SELEX stringency steps and the resulting SELEX rounds were taken for the final SELEX summary and used in future experiments. The final SELEX process with the amounts of eluted RNA per round is shown in Figure 21.

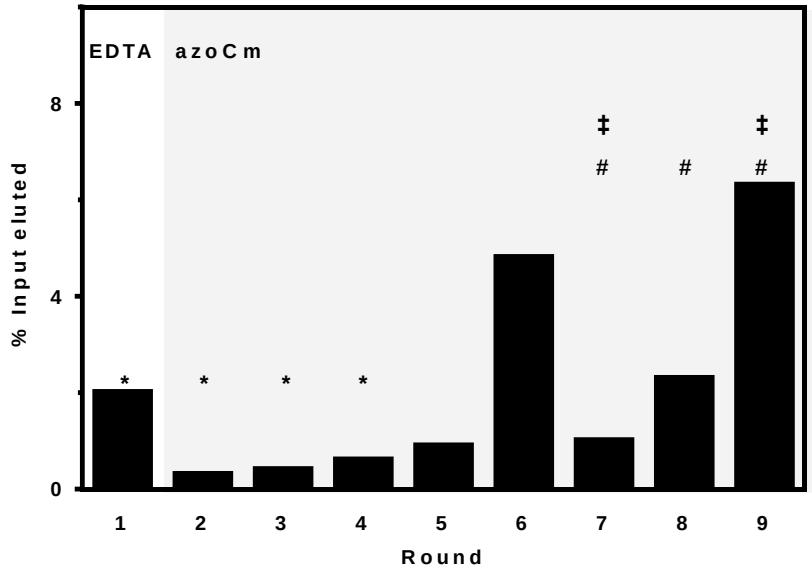

Figure 21: **Summary SELEX against azoCm** Shown is the fraction of loaded RNA that could be eluted from azoCm-derivatized columns after each selection round. RNA was eluted by either 20 mM EDTA (round 1) or 5 mM azoCm (round 2-9). In the first four rounds, a negative selection was performed (*). In round 7 and 9 stringency was increased by doubling the number of column washes or a decreased binding time of the RNA pool to the column, respectively (‡). Two pre-elution steps with 5 mM azoCm were performed starting from round 7 (#).

4.5 Binding studies of affinity SELEX aptamers

To find out whether the SELEX did actually enrich azoCm binding aptamers, binding studies of individual aptamers were carried out. 20 individual candidates of the PCR pools resulting from round 6 and round 9 of SELEX were cloned by TOPO TA cloning (Table 4) and sequenced. Interestingly, only 6 different sequences could be found, with A (Table 19) being the most abundant (12 copies in 20 tested aptamers). Aptamer RNA was prepared from candidates A, D, E and F (Table 19) by *in vitro* transcription (3.2.8), as those were the two most abundant aptamers from round 6 and 9, each.

The elution capacity of the RNA aptamers was tested using column binding assays. This experiment was carried out by B. Sc. Georg Pietruschka, as part of his internship in our laboratory. The aptamers were radioactively body-labeled and after folding (3.4.3), 100000 counts of radioactive RNA were filled to a volume of 500 µL using a mixture of 1x SELEX buffer with 2.3 µg/µL yeast tRNA.

Table 19: **Aptamer sequences from affinity SELEX rounds 6 and 9**

Sequence name	Number of copies	SELEX round	Sequence
A	12	6	AGTTAATACACGACGCAGTGATCGACGTAGGTA GAAAAGCGATAAGTATGGGCCTAATCCGATACC GCGATCAC
B	1	6	AAGGACCCTAGGCAGGGGGCTTCGTTACGAGAG CAAGACCAGGAACCACGGGCTTGCTCTTCTGCA CAAAACGA
C	1	6	GGTCGGTCGAGGACCTTAGACCGTCAGCTTCTTC TCCGGTGTAAAGGCTGTGAGACCAGGAGGCCAA GAACCAA
D	2	6	GCGACTAGAACCCATGTTGCGAAGTCGACCTGT GACCCGAGTGAAGCGGGAAAGCAAGGACGAGC CTTCAATCC
E	3	9	GACGGGCTCCCGCACCTGAGGTGTCTGCCAGAA ACGACAAACGTCGCCTCGGCCACCACTCTGGTT ACAAGAGG
F	1	9	TTTCTGTCTTACGACAACGATAATAAAATGTGGC GAGGCTAACCGGTACGGATACAGTACGGGCGAC AATGGTCC

Listed are the sequence names, abundance and the sequences within a group of 20 randomly selected aptamers from round 6 and 9 of the SELEX against azoCm. While some sequences occur only once in 20 sequences (B, C,F) others occur multiple times (D, E), with one occurring 12 times out of 20 aptamers (A).

The attempt to elute binding RNA molecules was carried out with different solutions (5 mM *trans* azoCm, 5 mM *cis* azoCm or buffer). In Figure 22, the results of two measurements are shown in percent of RNA recovered from input RNA (Equation 2).

All aptamers tested showed a specific elution of RNA from the columns with both azoCm *trans* and *cis* as compared to background elution (buffer elution, light grey bars). While A and D show higher RNA elution values with azoCm *trans* than with azoCm *cis*, F shows higher values with azoCm *cis* than with azoCm *trans*. Aptamer E does not show a clear difference between the eluted amounts of RNA. Evaluation of this first SELEX results led to the conclusion, that the pool seems to be already sufficiently enriched regarding single aptamers as Sequence A (Table 19) alone was found 12 times out of 20 sequenced aptamers.

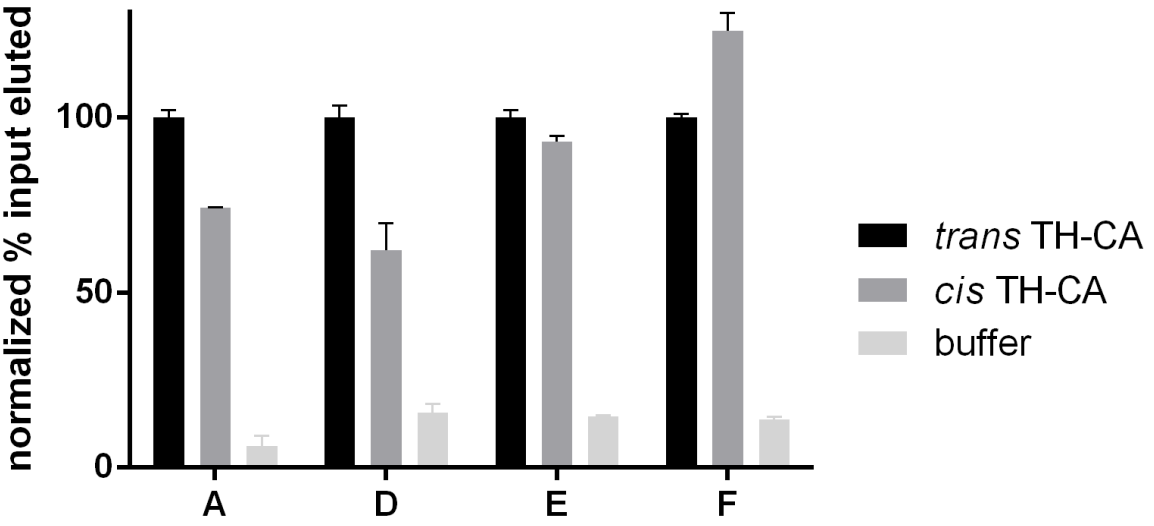

Figure 22: **Isoform specificity elution analysis** Radioactively labelled aptamers (100000 counts of RNA, A, D, E, F: see Table 19) were folded and immobilized on azoCm-NH_2-columns (folding program described in 3.4.3). The resin volume in the column (CV) was 500 µL, as was the volume of all other washing and elution steps. Four elution steps with 5 mM azoCm *trans*, 5 mM azoCm *cis* or buffer were carried out. The percentage of eluted RNA versus total RNA was calculated and each aptamer's azoCm *trans* value was normalized to 100%.

Also, all four tested aptamers (A, D, E, F) could be eluted from azoCm columns using free azoCm *trans* or azoCm *cis*, while showing almost no elution with buffer alone. These first results encouraged us to go ahead with *in vivo* screening of the aptamers aiming at the discovery of potential riboswitches.

4.6 Optimization of PCR protocol for aptamer amplification

As the goal of SELEX against azoCm was not only to generate specific aptamers, but also to test their ability to function as light-dependent riboswitches in yeast cells, aptamers were to be tested in an *in vivo* screening system. For this, aptamer pool sequences were introduced into the 5' UTR of the reporter gene GFP using homologous recombination (2.1.2).

In order to generate a plasmid pool containing as many aptamer sequences as possible, first amplification of the aptamers with primers suitable for homologous recombination needed to be optimized. A particular feature of PCR design for aptamers resulting from SELEX is that only one forward primer, but three different reverse primers are required. The aptamer pool is amplified in three samples: each using the forward, and one of the three reverse primers, which contain (a) no additional nucleotide (b) an additional G and (c) an additional TG (Table 20). This diversity is introduced to cover all potential reading frames of the aptamers in an *in vivo* context, as during SELEX random start codons (ATG) could be formed. These additional

ATGs should be in frame with the correct start codon to not provide an additional mRNA product with a different length. A mix of the three reverse primers should provide functional variations of every aptamer.

Table 20: **Sequence pool 2 and primers used to amplify aptamers from pool 2 for Homologous recombination (HR)**

Pool/ Primer	Sequence
Pool	**5'** GGAGCTCAGCCTTCACTGC-[N74]-GGCACCACGGTCGGATCCAC **3'**
Fwd	**5'** CAAGCTATACCAAGCATACAATCAACTCCAAGCTAGATCTACCGGT GGAGCTCAGCCTTCACTGC **3'**
Rev1	**5'** GGCACCACGGTCGGATCCACAAAATGGCTAGCAAAGGAGAAGAAC TTTTCACTGGAGTTGTCCCAATTCTTG **3'**
Rev2	**5'** GGCACCACGGTCGGATCCAC**C**AAAATGGCTAGCAAAGGAGAAGAA CTTTTCACTGGAGTTGTCCCAATTCTTG **3'**
Rev3	**5'** GGCACCACGGTCGGATCCAC**CA**AAAATGGCTAGCAAAGGAGAAGA ACTTTTCACTGGAGTTGTCCCAATTCTTG **3'**

Shown are the sequences of the aptamer pool 2, the forward primer and the three different reverse primers used in PCR when aptamers from a SELEX round should be amplified for subsequent homologous recombination in yeast cells with the plasmid pWHE601 (Table 8). Marked in blue and green are the binding sequences of the forward and reverse primers on the pool DNA. The Kozak sequence (AAA) and the start codon (ATG) are underlined. Unmarked regions in the primers are homologous recombination regions, corresponding to the plasmid pWHE601. As for easier comparison of the pool DNA to the reverse primers, they are noted in 3' to 5' direction, the additional G or TG in the sequences of reverse primers 2 and 3 (marked in pink) are shown here as the corresponding C and CA.

Before combining the plasmid backbone and the aptamers with the cells to carry out homologous recombination, all three PCR amplified aptamer variants are mixed. Only aptamers not containing a frameshift regarding the ATG and the reporter gene GFP on the plasmid should show a green fluorescence in the cells, so a selection of the appropriate aptamer length should automatically occur during *in vivo* screening.

Optimization of the PCR conditions was necessary to generate the maximum amount of aptamers from a SELEX without getting overamplification of PCR products which could introduce bias into the enriched aptamer pool. The optimization protocol was carried out using aptamers from SELEX round 9 as a test round. All further PCR amplification of this pool were carried out using the resulting protocol.

To this end, a PCR mix of each primer variant (Table 20) was made, and PCR was carried out for 16 cycles using the PCR program described in Table 17.

After 6, 8, 10, 12, 14 and 16 rounds, 5 µL of the reaction was taken from each PCR sample and analyzed on an agarose gel. As shown in Figure 23, 8 cycles produced the maximum amount of PCR product without showing bands of overamplification. This optimized PCR protocol (conditions Figure 14, 8 cycles of amplification) was performed for all other SELEX round amplifications used for *in vivo* screenings.

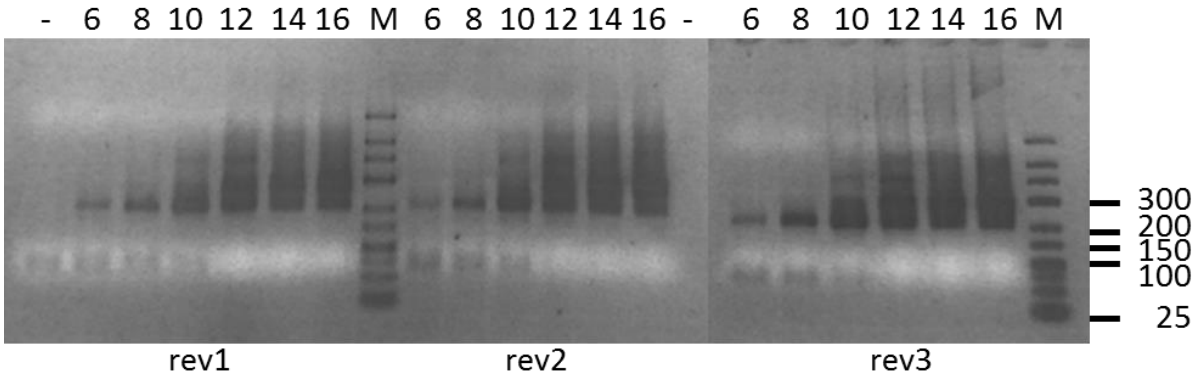

Figure 23: **Agarose gel of aptamer scout PCR** Shown is a 3% agarose gel with PCR-reactions performed with different amounts of cycles to test the amplification of aptamers from SELEX round 9 via the PCR program described in Figure 14. Shown from left to right are the PCR samples using each the forward primer and either the reverse primer 1 (rev1), 2 (rev2) or 3 (rev 3). Shown in the lanes are Marker (M), 6, 8, 10, 12, 14 and 16 cycles and the negative control sample containing no template (-).

Table 21: **PCR program for aptamer amplification for *in vivo* screening**

T	T		PCR steps
98°C	30 s		Initial melting
98°C	10 s		Melting
58°C	10 s	repeat in cycles	Primer annealing
72°C	10 s		Elongation

Shown are the temperature (T) applied in each PCR step, as well as the time (t) during which the temperature is applied. The final three steps are repeated for 8 cycles.

4.7 *In vivo* screening of affinity SELEX aptamers

To see whether the aptamers of SELEX round 6 or 9 contained riboswitches, *in vivo* screening in yeast was carried out. To this end, the aptamers from round 6 and 9 were amplified as described in Table 21 and purified using sodium acetate precipitation (3.2.12). *S. cerevisiae* cells were made competent using the lithium acetate protocol (3.3.4). The cells were then transformed with the linearized plasmid pWHE601 (Table 8) and the amplified aptamers from SELEX. As the aptamers were amplified with primers fitting for homologous recombination

(Table 6), the yeast cells could incorporate them into the linearized plasmids carrying the same homologous regions as the aptamers, thus creating at least one functional plasmid per cell, containing an aptamer and conveying also an auxotrophy marker to the transformed yeast cells which enabled them to grow on drop-out medium.

After plating and incubating the cells, colonies could be observed on the agar. Analyzing them by eye using the binocular (Table 3), all semi-fluorescent and fully fluorescent cells were marked and then transferred into individual wells on a 96 well U-bottom plate (3.3.8). Only semi- and fully fluorescent cells were analyzed, as it was assumed that a reduction of gene expression by a riboswitch would only be measurable if the initial fluorescence level of the cell was sufficient.

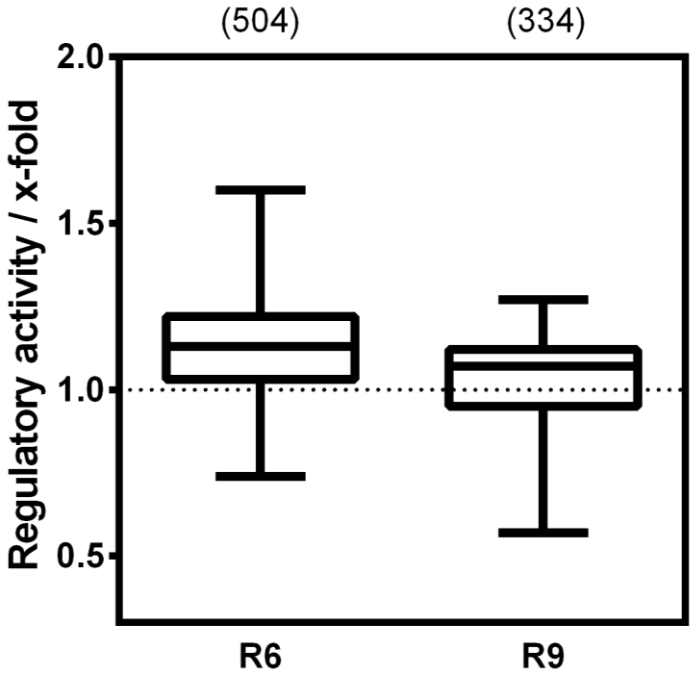

Figure 24: ***In vivo* screening of SELEX rounds R6 and R9** These boxplots show the summarized *in vivo* screening in *S. cerevisiae* for round 6 (R6) and round 9 (R9). For each investigated clone, the regulatory activity was calculated as the ratio of GFP fluorescence with and without 100 µM azoCm (x-fold). The numbers written above the boxplot indicate the number of clones analyzed. The median of all analyzed clones in R6 was 1.13 and at 1.07 in R9.

While *in vivo* screening of round 6 (R6) showed some regulatory activity above 1.0 and the median was 1.13, all outliers making up the upper antenna of the boxplot could not be validated in a second or third round of screening (3.3.8). Round 9 (R9) had a median of 1.07 and an altogether lower amount of outliers indicating a regulatory activity lower than in R6. It

shows that no riboswitches could be identified in these rounds. Therefore, this experiment was stopped at this point and a new approach to SELEX was considered and planned.

4.8 Development of a light SELEX protocol

The main goal of the SELEX against azoCm was to find aptamers that specifically bind only to its *trans* isoform. This requires a method that would enable isoform-specific selection of aptamers, which subsequently is called "light SELEX". The advantage would be, that during the SELEX only aptamers which bind to *trans* azoCm and discriminate against *cis* azoCm would be amplified, whereas those aptamers binding to the *cis* isoform of azoCm would be removed. To establish a light SELEX protocol, some control experiments had to be carried out first. The set-up of the light elution experiment is shown in Figure 25**.** The UV lamp was placed 10 cm from the column middle and the column was irradiated with light (λ=365 nm) under exclusion of other light sources. In a light SELEX experiment, RNA would be eluted from the column upon switching of the immobilized ligand from *trans* to *cis*.

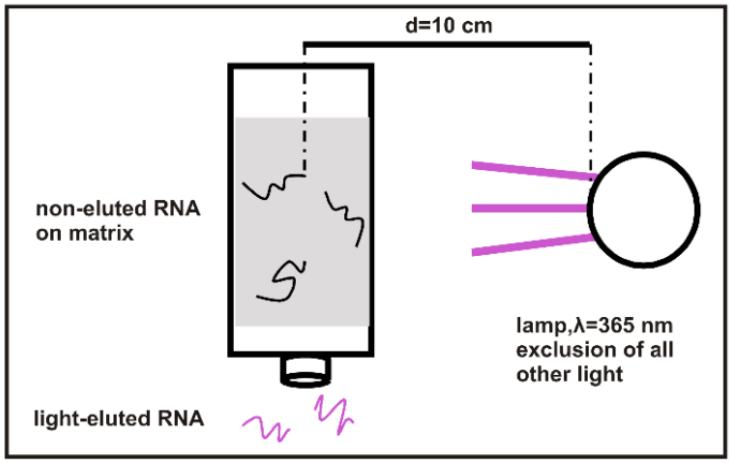

Figure 25: **Set-up of light elution method** A column with immobilized ligand was irradiated with light (λ=365 nm) while all other light sources were excluded. During irradiation, the column was washed with SELEX buffer. The UV lamp was placed 10 cm from the column middle. Aptamers losing binding ability to the ligand when it is switched from *trans* to *cis* would be washed out of the column and could be collected.

As a first step we tested whether UV light was able to penetrate the plastic columns used during the SELEX. No penetration would require a different set-up for the light SELEX.
To enable judgement about UV column penetration and the intensity and duration of UV irradiation required to switch azoCm from *trans* to *cis*, a marker molecule was used. This

molecule (“compound 3“, Table 2) was also light-switchable, and underwent a visible colour shift from white to red upon irradiation with the same wavelength of UV light needed to switch azoCm to its *cis* isoform (λ=365 nm) [207].

A small amount of marker was mixed with non-derivatized column material and a test column was filled. As the marker was not linked to the resin, quality analysis, for example whether the resin hinders any UV light penetration, could be made (example see Figure 26).

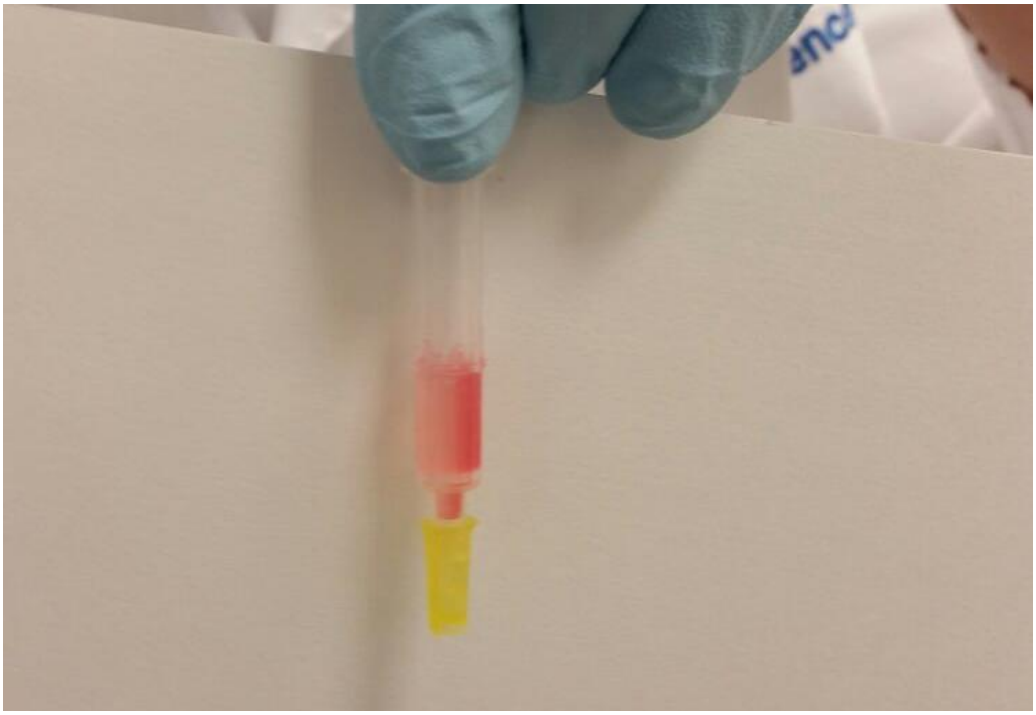

Figure 26: **Irradiated Affi-gel 10 resin with mixed in marker molecule “compound 3”** The column was irradiated for 60 s with UV light (λ=365 nm, 0.6 A, 15 V; condition 1, Table 22) from the right side, leading to a colour gradient within the column. The “compound 3” molecules on the right side of the column have been switched in a higher percentage than the ones on the left side of the column.

Irradiation time needed to switch the marker towards strong colour saturation was measured, in the assumption of a similar behavior of azoCm. Using an insertion thermometer (Table 3), temperature changes inside the column material were measured as well, to see whether a temperature increase occurred that could lead to heat-induced RNA elution, independent from light elution effects.

Parameters changed during the irradiation experiments were the amounts of amperage and voltage used to generate UV light, the volumes of 1x SELEX buffer pipetted on the column during the irradiation, and the exposure time to UV light. Additional experimental set-ups,

like shielding the column from heat inducing IR irradiation using an IR filter, or wrapping the column in aluminum foil during irradiation were tested as well.

The efficiency of the irradiation was judged by eye by gauging the saturation of red inside the column, as the marker turned red upon switching to its *cis* isoform. Preferred results would show an even distribution of red resin throughout the column while showing little to no temperature increase measured in the resin. The results of the experiment are shown in Table 22.

Table 22: **Light SELEX test conditions**

Test	Irradiation conditions	time [s]	ΔT [°C]	Results of colour saturation
1	0.6 A, 15 V	60	2	strong red colour, gradient through the column (see Figure 26)
2	0.6 A, 15 V, 20 µL 1x SELEX buffer inside the column	60	1.5	strong red colour, gradient through the column
3	0.6 A, 15 V, 300 µL 1x SELEX buffer inside the column	60	1.1	strong red colour, gradient through the column
4	0.6 A, 15 V, 300 µL 1x SELEX buffer inside the column, IR filter	60	1.1	strong red colour, gradient through the column
5	wrapped column in aluminium foil, 0.6 A, 15 V, 300 µL 1x SELEX buffer inside the column	60	0.2	no colour
6	0.2 A, 13 V	60	0.8	lesser colour saturation than in test 4
7	0.02 A, 12.9 V	60	0	low saturation of red
8	0.1 A, 13.3 V	60	0.15	higher degree of red than in test 7
9	0.15 A, 13.5 V	60	0.2	higher degree of red than in test 8
10	0.15 A, 13.5 V, turn column 180°C after 60 s	120	0.2	even degree of red throughout the column, comparable to test 6
11	wrapped column in aluminium foil, 0.15 A, 13.5 V, turn column 180°C after 60 s	120	0.05	no colour

Shown are the different UV light irradiation conditions used to test which are optimal to switch the marker molecule towards strong colour saturation within the Affi-gel (Table 1) in the column. Tested were different amperages and voltages, as well as irradiation times and directions from which the column was irradiated. Temperature changes within the column before and after irradiation were measured and the saturation of red colour within the column as a result of UV irradiation was analyzed and compared visually.

Table 22 shows, that irradiation conditions as in test 10 seem to be the most favorable ones for further experiments. An evenly distributed amount of marker molecule switched to red could be achieved with only a minimal temperature increase ($\Delta T=0.2°C$). An even distribution of red colour could be observed within the column, achieved by irradiating the column from both sides for 60 s with UV light ($\lambda=365$ nm) generated by 0.15 A and 13.5 V (2 W). Compared to condition 1, where 2°C temperature increase were measured by continuous irradiation from one side using 0.6 A and 15 V, but no even distribution of red could be detected throughout the column indicated the benefits of irradiating the column from both sides (condition 1, Table 22, Figure 26).

As a control experiment, using the same conditions as in condition 10, but wrapping the column in aluminium foil prior to irradiation led to an 0.05°C increase in temperature, making the pure heat input from irradiation negligible. However, irradiation itself accounts for a 0.15°C temperature increase within the resin, so heat induced elution of RNA is not entirely impossible.

For this reason, the developed light SELEX condition 10 was tested on RNA, to find out whether condition 10 lead to unspecific RNA elution. Four different variations of condition 10 were drafted, named α-δ. As shown in Table 23, all share the same voltage and amperage as in condition 10 from Table 22, but differ in irradiation time and methods (full-time irradiation or flashes of light). In this experiment, RNA from an enriched SELEX round selected against Kanamycin, provided by M.Sc. Adrien Boussebayle was used. The RNA aptamers were loaded onto an azoCm derived column, on which they should not be able to bind.

Table 23: **Light elution test conditions**

Test	Irradiation conditions	Elution 1	Elution 2	Elution 3	Elution 4
10α	0.15 A, 13.5 V,	60 s per side	buffer	buffer	buffer
10β	0.15 A, 13.5 V, 1 s flashes, 32 flashes total	10 flashes/side within 60 s	6 flashes/side within 60 s	buffer	buffer
10γ	0.15 A, 13.5 V	20 min/side, elute with buffer	buffer	buffer	buffer
10δ	0.15 A, 13.5 V, 1 s flashes, 16 flashes total	5 flashes/side within 60 s	3 flashes/side within 60 s	buffer	buffer

Shown are the different UV light irradiation conditions tested in each elution experiment (1-4). Unspecific RNA was pipetted onto the column and different irradiation times and methods were tested. Amperage was 0.15 A, voltage 13.5 V (resulting in a power of 2 W).

For the experiment, RNA was pipetted onto the washed column and incubated there for 15 min. After 20 washing-steps with 1x SELEX buffer, the RNA was eluted using different conditions in four elution steps. As can be seen in Table 23, either the column was irradiated continuously for a time from both sides (α, 60s/side; γ, 20 min/side), and afterwards eluted four times with 1x SELEX buffer. Or the column was irradiated in sets of light flashes of 1 s each, before the first and second elution round (β, 10 and 6 flashes per side; δ, 5 and 3 flashes/side). Afterwards, two rounds of elution with 1x SELEX buffer followed, independent from the previous irradiation conditions.

As the RNA was not supposed to bind to the column, regular amounts of eluted RNA were expected to occur. Increased RNA amounts were interpreted as heat effects leading to a higher molecule movement, thus leading to increased RNA outflow with the addition of 1x SELEX buffer.

Figure 27 shows the eluted RNA in percentage to the wash fractions for all four conditions. As can be seen, conditions 10β and γ show distinct rises in their amounts of eluted RNA with the first elution step, compared to the previous wash steps. Condition 10α shows a gradual increase of eluted RNA, 10δ shows a smaller gradual increase at a later time. Regarding this data, the decision to start a real azoCm light SELEX round using conditions 10α and δ was made.

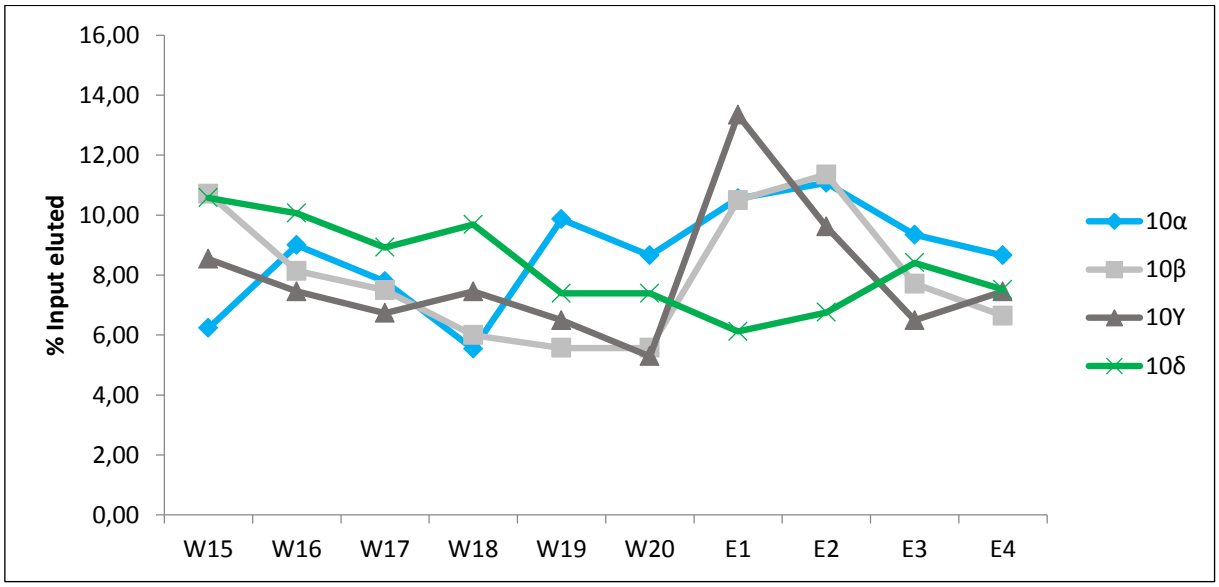

Figure 27: **Light elution experiments of unspecific RNA** Shown are the percentages of eluted RNA from the last five wash fractions as well as the elution fractions of the four different elution conditions described in Table 23. Unspecific RNA had been loaded on the column. Elution conditions 10α and 10δ showed a more or less stable amount of RNA eluted over the course of wash fraction 19 (W19) until elution fraction 4 (E4). Conditions 10β and 10γ show a 5 or 8% increase in RNA elution between W20 and E1, while 10α shows a 2% increase. Condition 10δ shows a 1.3% decrease in eluted RNA between W20 and E1.

As a starting point for the light SELEX, the last round of the conventional azoCm SELEX was chosen. The eluted and PCR amplified DNA obtained after round 9 was transcribed into RNA and radioactively marked using [α-^{32}P] UTP (3.2.8, 3.4.3). The folded RNA was pipetted onto the washed column and incubated on the column for 30 min. After 20 washes with 1x SELEX buffer, the RNA was eluted using conditions 10α or δ. At the same time, a control experiment without light elution was carried out, by simply "eluting" the RNA 4 times with 1x SELEX buffer. This served as a reference of background RNA, counting the amount of RNA that is flushed out of the columns unspecifically. The ratio between light eluted RNA and background RNA is shown in Figure 28, comparing values between the SELEX wash and elution fractions for conditions 10α and 10δ.

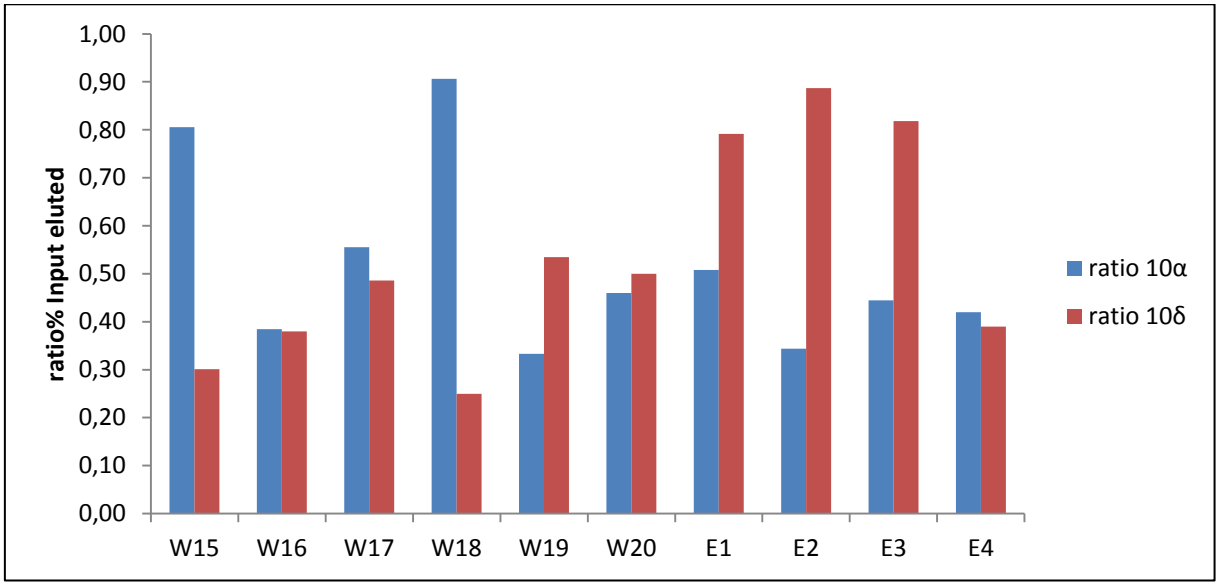

Figure 28: T**est of RNA elution using two different light elution protocols in a light SELEX round 10** Depicted are the ratios between elution percentages of light elution protocols under condition 10α (blue columns) and 10δ (red columns) resp. and a control elution without irradiation of the column starting with the SELEX pool after affinity SELEX round 9 (4.4). The last five wash fractions as well as the elution fractions are shown. Elution condition 10α shows a more or less stable amount of RNA eluted over the course of wash fraction 19 (W19) until the elution fraction 4 (E4), from an irradiation to background ratio between 0.33 and 0.51. Condition 10δ shows an RNA elution increase from a ratio of 0.5 in W20 to a ratio of 0.79 and 0.82 in E1 and E3, and 0.89 in E2.

As can be seen in Figure 28, elution condition 10α (blue bars) shows a more or less stable amount of RNA eluted over the course of wash fraction 19 (W19) until the elution fraction 4 (E4). The irradiation to background ratio fluctuates between 0.33 and 0.51. Condition 10δ however (red bars), shows an RNA elution increase from a ratio of 0.5 in W20 to a ratio of 0.79 in E1 once the column was eluted with irradiation and buffer. Elution fraction E2 even

shows an increase of irradiation to background elution ratio of 0.89. Even though in E3 no irradiation is used to elute RNA anymore and the column is only treated with 1 CV of buffer (Table 23), the eluted RNA ratio drops to 0.82 in the round, indicating plenty of light-eluted RNA molecules still in the column from the irradiation rounds E1 and E2. In E4, the eluted RNA ratio drops down to 0.39, showing little to no difference to the amount of eluted RNA with conditions 10α (E4 10 α=0.42). The increase of eluted RNA to background ratio in condition 10δ lead to the use of this protocol for further light SELEX rounds and experiments.

4.9 Light SELEX

As light SELEX was considered too stringent to use from round 1 of a SELEX, it was used as a protocol for SELEX rounds following those of the affinity SELEX against azoCm. After this SELEX had already enriched an RNA aptamer pool against azoCm *trans*, light SELEX rounds using the RNA from these pools should yield aptamers able to bind azoCm *trans*, but unable to bind azoCm *cis*. Different rounds from the azoCm affinity SELEX (4.4) were used as starting aptamer pools for light SELEX

As a start, the protocol developed for light SELEX (Table 23) was applied several rounds after round 9 of the affinity SELEX (4.4). The RNA was transcribed from the cDNA after round 9, pipetted on the column and washed using the same conditions as in affinity SELEX. While the RNA-loaded column was irradiated, it was washed with SELEX buffer to flush out RNA aptamers that were detached from the ligand due to its conformation change. Amplification of the eluted RNAs via cDNA synthesis, PCR and re-transcription into RNA lead to a light-selected RNA pool for the next light SELEX round.

The percentage of eluted RNA is shown in Figure 29. After a steady decrease in eluted RNA, there was a visible increase in round 12.

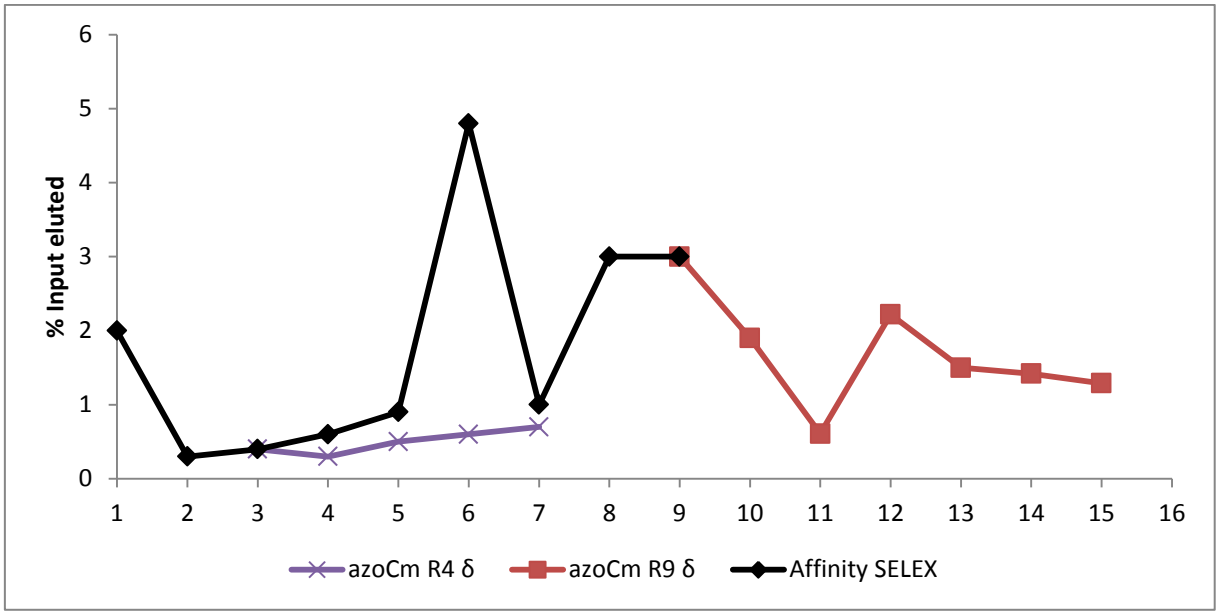

Figure 29: **Summary SELEX against azoCm with light SELEX after R3 and R9**. Shown is the fraction of input RNA that could be eluted from azoCm-derivatized columns after each selection round. RNA was eluted by either 20 mM EDTA (round 1) or 5 mM azoCm (round 2-9) in the affinity SELEX, shown in black. After Round 3 or round 9, light-elution of RNA was carried out, shown in purple and red, respectively. While light SELEX after round 3 shows a slow increase in input RNA eluted, light SELEX after round 9 shows a sharp decrease until light SELEX round 11 (LS-11). Round 12 shows an increase in eluted RNA, this trend could not be observed in rounds LS13 to 15, however.

This increase could not be sustained, however, which lead to the discontinuation of the SELEX procedure after round 15. It was theorized that light SELEX had been started too late in the SELEX process and that potentially light-elutable RNA aptamers constituted a minority in the pool, if they were not completely discriminated against by the increase in stringency in rounds 7 to 9 in the affinity SELEX.

For this reason, a second light SELEX was started after round 3 of the affinity SELEX. As a strong increase of eluted RNA was observed in the affinity SELEX from round 5 to round 6, we expected to see a fast enrichment in the light SELEX approach as well. However, over the course of 4 light-elution rounds, there seemed to be a steady increase in eluted RNA, but it was considered too gradual in comparison to the affinity SELEX to signal real aptamer enrichment (Figure 29).

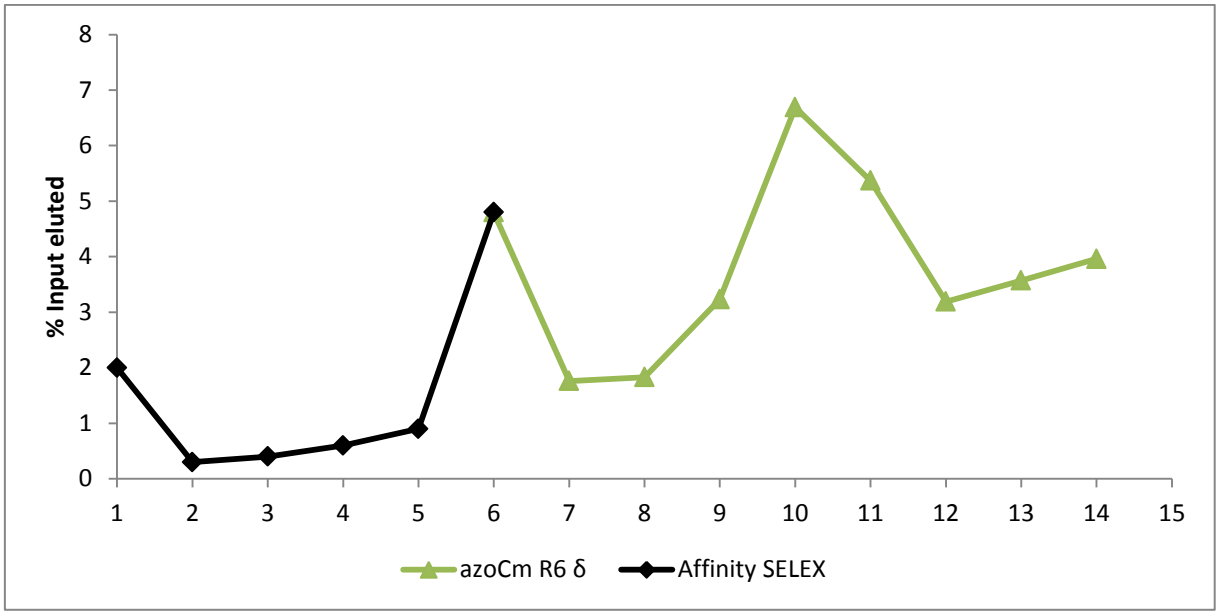

Figure 30: **Summary SELEX against azoCm with light SELEX after** R6. Shown is the fraction of input RNA that could be eluted from azoCm-derivatized columns after each selection round. RNA was eluted by either 20 mM EDTA (round 1) or 5 mM azoCm (round 2-9) in the affinity SELEX, shown in black. After Round 6, light-elution of RNA was carried out, shown in green. With the first light SELEX round (LS-7) a sharp decrease in eluted RNA could be observed. Starting with LS-8, the amount of input RNA eluted increases until LS-10. In LS-11 stringency was increased by increasing number of wash steps to 25, a drop in the percentage of eluted RNA can be observed. Starting with LS-12, the amount of input RNA eluted increases until LS14.

That is why, as a third experiment, we started a light SELEX approach starting after the enriched affinity SELEX round 6 (4.8% of input RNA eluted). As can be seen in Figure 30, enrichment of the light-selected pool could be achieved after only four rounds in round 10 to 6.7%. After round 10, the stringency of the light-elution was increased by raising the number of wash steps to 25. After a decreased RNA elution, an increase could again be achieved starting in round 13. Altogether, 8 rounds of light SELEX were carried out following six affinity SELEX rounds.

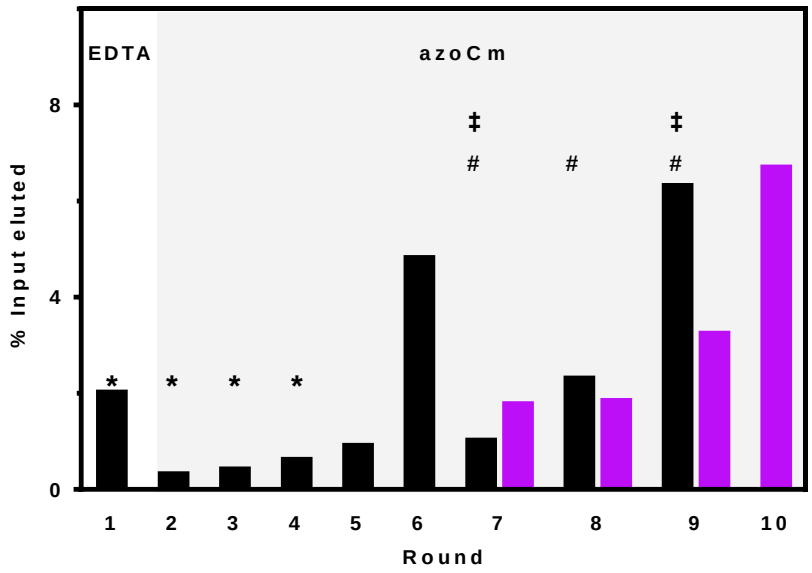

Figure 31: **Comparison of second affinity SELEX and light SELEX** Shown is the fraction of loaded RNA that could be eluted from azoCm-derivatized columns after each selection round. RNA was eluted by either 20 mM EDTA (round 1) or 5 mM azoCm (round 2-9) in the affinity SELEX (black bars). In the first four rounds, a negative selection was performed (*). In round 7 and 9 stringency was increased by doubling the number of column washes or a decreased binding time of the RNA pool to the column, respectively (‡). Two pre-elution steps were performed starting from round 7 (#). Starting with round 7, light-elution was carried out in parallel to the affinity SELEX (violet bars). To achieve RNA elution, the column was irradiated with light (λ=365 nm) under exclusion of other light sources, while washing the column with SELEX buffer. Conformational changes in the immobilized ligands should lead to the elution of isoform specific RNA aptamers, thereby enriching only aptamer families that specifically bind the ligands' *trans* isoform.

Comparison of the light SELEX rounds with the affinity SELEX rounds starting after the affinity SELEX round 6 (LS-6) shows an increase in RNA elution in both protocols. Enrichment with light SELEX needs ten rounds to reach RNA elution amounts comparable to RNA elution amounts in round 9 of affinity SELEX.

4.10 *In vivo* screening light SELEX

To assess whether some of the generated aptamers in light SELEX round 7, 8 and 9 or round 10 would function as riboswitches, *in vivo* screening in yeast was carried out. To this end, aptamers were amplified from light SELEX rounds 7 to 10 and transformation of yeast cells with this DNA and linearized plasmid pWHE601 was carried out as described in chapters 3.3.4 and 4.2 . Aptamers from light SELEX rounds 7, 8 and 9 were amplified and transformed

separately, but results were pooled in one boxplot in Figure 32, due to the low amount of samples tested.

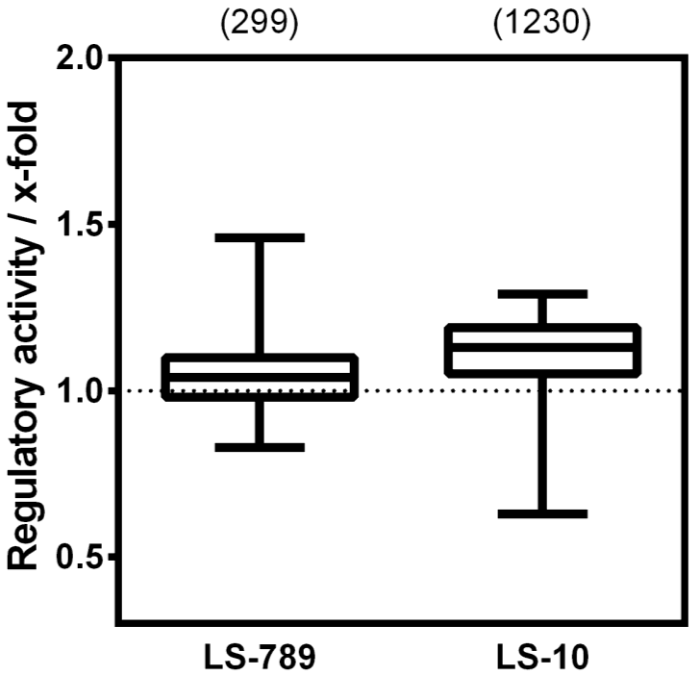

Figure 32: ***In vivo* screening of Light SELEX rounds LS-789 and LS-10** These boxplots show the summarized *in vivo* screening in *S. cerevisiae* for light SELEX rounds 7 to 9 (LS-789) and round 10 (LS-10). For each investigated clone, the regulatory activity was calculated as the ratio of GFP fluorescence with and without 100 µM azoCm (x-fold). The numbers written above the boxplot indicate the number of clones analyzed. The median of all analyzed clones in LS-789 was 1.04 and at 1.13 in LS-10.

While *in vivo* screening of light SELEX rounds 7, 8 and 9 (LS-789, Figure 32) showed some regulatory activity above 1.0 and the median was 1.04, all outliers making up the upper antenna of the boxplot could not be validated in a second or third round of screening (3.3.8). Round 10 (LS-10, Figure 32) had a median of 1.13 and an altogether lower amount of outliers indicating more regulatory activity than in rounds 7, 8 and 9. However, no riboswitches could be validated in light SELEX round 10 through a second and third round of screening as well.

4.11 Binding studies of light SELEX aptamers

As *in vivo* screening did not yield functioning riboswitches, the aptamers generated from SELEX were to be tested *in vitro* regarding their binding abilities of azoCm *trans* and *cis*.

Aptamers from light SELEX round 10 were cloned by TOPO TA cloning (Table 4). Ten representative individual aptamers were chosen and tested in an *in vitro* binding assay,

following the protocol described in chapter 3.2.15. For comparison, aptamers A and E originating from affinity SELEX rounds 6 and 9 (4.5), respectively, were tested in this experiment as well.

Firstly, aptamers were tested regarding their azoCm *trans* binding ability. To this end, elution of aptamers was carried out using 50 µM azoCm *trans* solution in 4x 500 µL elution steps, a 100 times lower concentration than in affinity SELEX rounds and previous binding studies (4.4, 4.5). Only samples showing RNA elution of more than 10% of the originally loaded RNA (10% input eluted, Figure 33) were considered good binders and taken into the next round of testing. As this experiment was considered as first look into the aptamers, and good binders were measured again in the next experiment, this experiment was carried out only once. Pre-tests for this experiment and its elution conditions were carried out by Leon Kraus, as part of his Bachelors thesis in our laboratory [237].

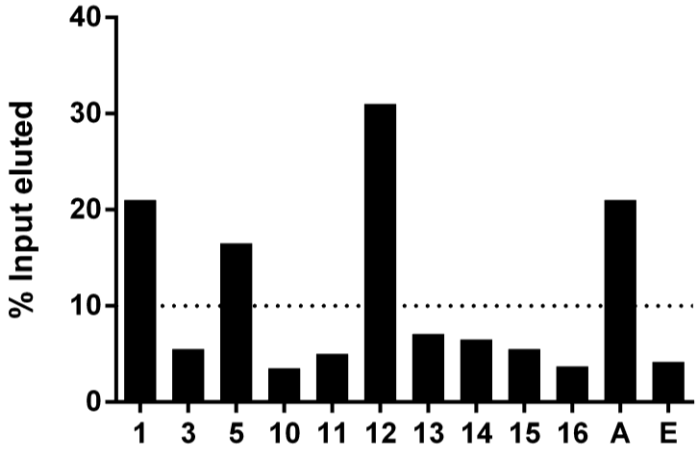

Figure 33: **Elution studies of light SELEX aptamers** Radioactively labelled aptamers from LS-10 (shown on the y-axis) were folded and pipetted on azoCm-NH_2-columns using the same conditions as during SELEX (100000 counts, folding program described in chapter 3.4.3). Four elution steps with 50 µM azoCm *trans* were carried out and the percentage of eluted RNA versus total RNA was calculated. Only four aptamers (1, 5, 12, A) showed more than 10% RNA elution (dotted line).

Figure 33 shows that four out of the twelve tested aptamer samples show more than 10% RNA elution compared to the originally loaded RNA. These four aptamers, 1, 5, 12 and A, were tested regarding their discrimination between the *trans* and the *cis* isoform of azoCm, in the next step. Elution with 1x SELEX buffer was carried out as well, as a measure of background RNA elution. As control, aptamer E from affinity SELEX round 9 was tested as well, as it did not display a selectivity towards azoCm *trans* in previous binding studies (4.5). The binding assays were carried out as described for Figure 33.

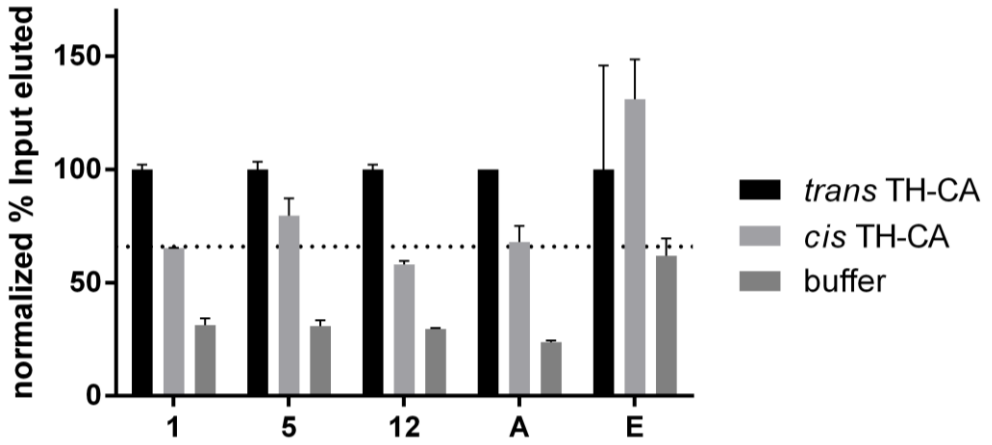

Figure 34: **Isoform specificity elution analysis** Radioactively labelled aptamers showing more than 10% elution as well as a non-binding aptamer (1,5,12,A,E; see Figure 33) were folded and immobilized on azoCm-NH_2-colums using the same conditions as during SELEX (100000 counts, folding program see chaptaer 3.4.3). 4 elution steps with 50 µM azoCm *trans*, 50 µM azoCm *cis* or buffer were carried out. The percentage of eluted RNA versus total RNA was calculated and each aptamer's azoCm *trans* value was normalized to 100%. Aptamers 12 and 1 show azoCm *cis* values below 66% (dotted line, more than 1/3 reduction compared to azoCm *trans*). Shown are the averages and standard deviations from two independent measurements.

As can be seen in Figure 34, aptamers 1 and 12 out of the five tested aptamers show more than a 33% RNA elution reduction, when comparing azoCm *cis* to azoCm *trans* elution. Elution with 1x SELEX buffer always showed lower RNA elution than elution with azoCm cis, however, indicating that a percentage of aptamers could still be eluted with azoCm *cis*.

4.12 Next generation sequencing (NGS) of SELEX

In order to get a deeper understanding of the development of the affinity and light SELEX, and to see which aptamers families would get enriched or lost during the SELEX process, Illumina next generation sequencing was performed on samples from every affinity SELEX round (round 1 to round 9) and comparable light SELEX round (LS-7 to LS-9), as shown in Figure 31.

Deep sequencing analysis of the selections was performed [198]. A total of 820000 sequences was obtained, from which identical sequences were summed up and the total read count was normalized for each round to reads per million (RPM).

First, an analysis was carried out, whether specific sequence motifs or families were enriched in the course of the different selections rounds. For this, the sum of RPM of the 100 most enriched sequences (Top100, Figure 35) was calculated for each SELEX round.

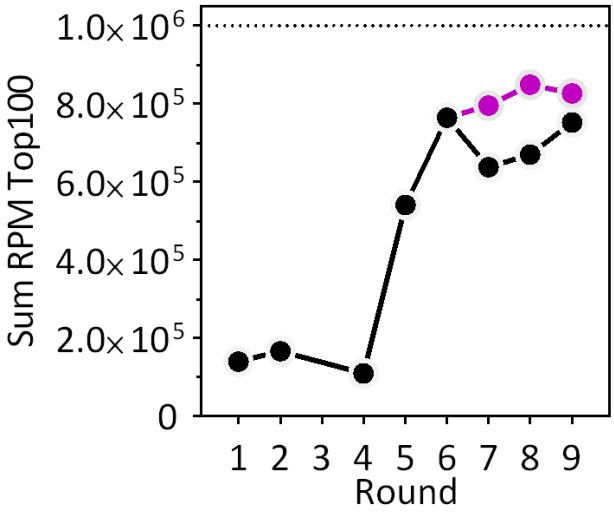

Figure 35: **Deep sequencing analysis of the most 100 most enriched sequences in affinity and light SELEX rounds** Enrichment of the 100 most enriched sequences (Top100) in each round is shown. Marked in black are the sums of the RPM for affinity SELEX and marked in violet are the ones for light SELEX.

As can be seen in Figure 35, the sum of the Top100 was enriched until round 6 (particularly between round 4 and round 6). Starting from round 7, both SELEX approaches, more stringent affinity SELEX and light SELEX, did not lead to a drastic enrichment of the Top100 anymore. In the light SELEX rounds, the enrichment continues to climb slightly, while in the affinity SELEX R7, first a drop in the enrichment of the Top100 occurs, after which enrichment starts to increase again. This was interpreted as an indication that enrichment of azoCm specific aptamers during SELEX did indeed take place as derived from the increasing amounts of eluted RNA measured during the different SELEX rounds (Figure 31). Also, the results seemed to stress that the stringency process introduced in the affinity SELEX rounds (more washes etc., Table 18) was comparably stronger than the introduction of the light SELEX protocol in the light SELEX rounds. Both ways of increasing selective pressure seem to be able to enrich a certain group of sequences in the Top100 group.

In order to identify the sequence families that were enriched using one or the other form of SELEX starting in round 7, sequences from affinity SELEX round 9 and light SELEX round LS-9 were compared using the software MEME suite (Table 12). In the light SELEX rounds, a 13 nt motif was found that showed enrichment in the light-selection rounds compared to the affinity SELEX rounds, in which the occurrence of the motif was decreased (Figure 36).

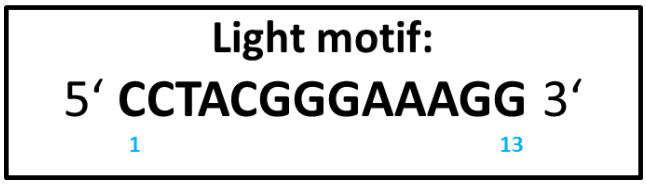

Figure 36: **Light motif** The depicted 13 nt DNA motif was discovered to be particularly enriched using the light SELEX protocol. Numbered in blue are the nucleotide positions.

Plotting the sum of sequences containing the discovered motif against the SELEX rounds showed a distinct distribution of the motif starting after round 6.

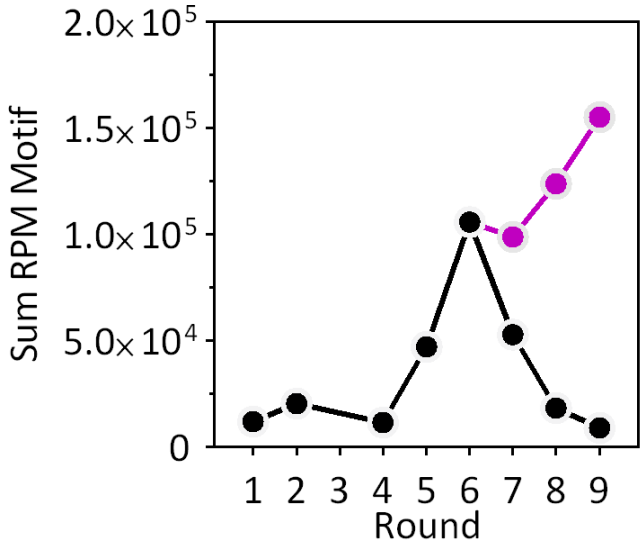

Figure 37: **Deep sequencing analysis of the sequences containing the identified motif in affinity and light SELEX rounds** Occurrence of the identified light motif (shown as the sum of sequences in RPM) within each selection round displays enrichment in the light SELEX compared to the affinity SELEX.

As can be seen in Figure 37, the sum of all sequences containing the motif (allowing one nt mismatch for sequencing errors) in the affinity SELEX round 6 was 1.05x 10^5 RPM. In the final light SELEX round LS-9, the sum of motif-containing sequences reaches 1.55x 10^5 RPM, while in the affinity round 9, it is decreased to 8.95x 10^4 RPM. This distribution of the motif indicated that it might be part of a light-selectivity conveying feature of aptamers.

After clustering the sequences into families for each round by comparing their sequence identities by Levenshtein distance. Levensthein distance (Lv dist) measures the difference between two strings of characters, e.g. sequences, by so-called single character edits, numbering the insertions, deletions or substitutions needed to change one sequence into

another [238]. In bioinformatics it is a measure on how closely related one sequence is to another. The smaller the Lv dist between two sequences is, the more closely related they are. Grouping the sequences from SELEX by comparing their Lv dist, it could be shown, that a Lv dist of five (5-fold, Figure 38) is ideal to split the sequence distribution into distinct families (clustering process adapted from Groher *et al*. [133]). This distribution is shown in Figure 38.

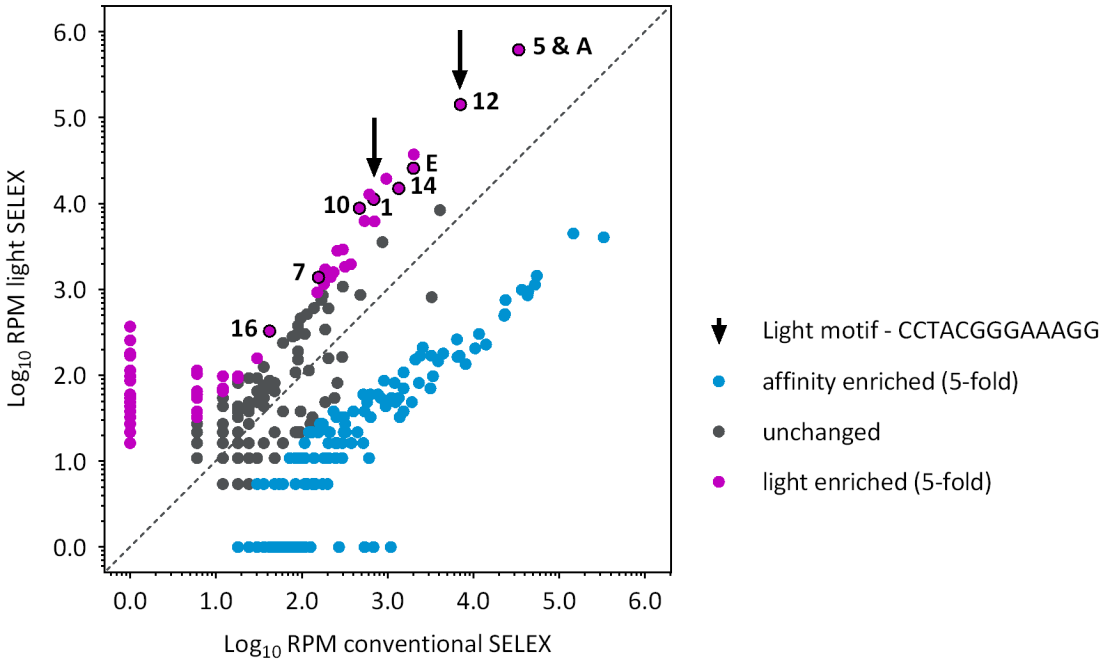

Figure 38: **Scatter plot of the families found by deep sequencing in affinity and light SELEX**. Shown in violet are aptamer families which are enriched during light SELEX rounds. Shown in blue are aptamer families enriched during affinity SELEX rounds. Aptamer families showing no changed behavior are shown in black. Aptamer families corresponding to previously tested aptamers *in vitro* binding assays are marked. Aptamer families which were previously tested in binding assays and contained the light motif are marked with an arrow.

The detailed analysis of the families enriched by light SELEX revealed 132 unique sequence families, for affinity SELEX, 243 families were identified, and 123 families could not be attributed to one or the other group (unchanged, Figure 38). Marked in Figure 38 are also aptamers, which were tested in previous binding studies (4.5), and which could be found again as enriched families in light SELEX (1, 7, 10, 12, 14, 16). Interestingly, also aptamers A and E could be found as enriched light SELEX families, even though sequence A was identified from round 6 aptamers, and sequence E was found in aptamers stemming from affinity SELEX round 9 (4.5). Notably, sequence A was identified as the same sequence family as sequence 5 (Lv dist of 5 or less, Figure 38).

Aptamer sequence 1 as well as 12 (families marked with arrows in Figure 38), which were the only aptamers tested in previous binding studies showing more than 33% reduced elution with azoCm *cis* than with azoCm *trans*, were found to contain the light motif (Figure 37). Comparing their sequences with the previously described aptamer 42 discovered in the SELEX by Rudolph [196], revealed that aptamer 42 contained the light motif as well (Table 24).

Table 24: **Comparison of aptamers containing the light motif**

Aptamer	Sequence
Light motif	5' CCUACGGGAAAGG 3'
Aptamer 1	5' GUGUUCCGACACGUGAACUCCAGCCCCCUUAAUAACGCUGUC GACCCUUGCGCUGUUACCUACGGGAAAGGGGU 3'
Aptamer 12	5' CCCCUCCCUACUGUGACUGAACGAACCCACAGUAG**GG**CCUAC GGGAAAGGGGAGUGACCUGGCCCAAAGCCACC 3'
Aptamer 42	5' GGUUGACCCUACUGCUUCGGCA**GG**CCUACGGGAAAGGUAA CA 3'

Shown is the sequence of the light motif in violet and its position in sequences of the tested aptamers (aptamers 1, 12, 42).

Two aptamers containing the light motif (12, 42) contained two additional G's in front of the 13 nt light motif, making it unclear whether they were important or not (marked bold and underlined in Table 24).

The discovered light motif might play a role in binding the ligand, as it turned up in two entirely independent SELEX processes from two very different pools. In order to test if the motif could yield more azoCm binding aptamers, a new pool for a new SELEX approach was designed.

4.13 Development of a motif doped pool

To see whether the light motif discovered (Figure 36) was indeed relevant in binding the ligand azoCm, a new pool for a new SELEX was generated, called the motif-doped pool, or "pool 3" (Figure 39). This pool should help to generate small, highly specific aptamers able to selectively and reversibly bind to only the *trans* isoform of azoCm. As the light motif always

occurred towards the 3' end of the three discovered aptamers 1, 12 and 42 (Table 24) a pool was designed consisting of 30 randomized nucleotides followed by two G's, then the 13 nt light motif and finally, 5 more randomized nucleotides. The total size of the generated aptamers should accordingly be 50 nt. In order to find potentially better variations of the motif, a 6% mutation rate was allowed for the 13 core nucleotides of the light motif. As it was not clear whether the two G's in front of the motif were a necessary or helpful addition to the motif (see Table 24), they were added on the 5' side of the motif but were allowed to mutate with a possibility of 50% (Figure 39). As described before, the 30 and 5 nt flanking the motif were randomized entirely (probability for every nucleotide per position should be 25%).

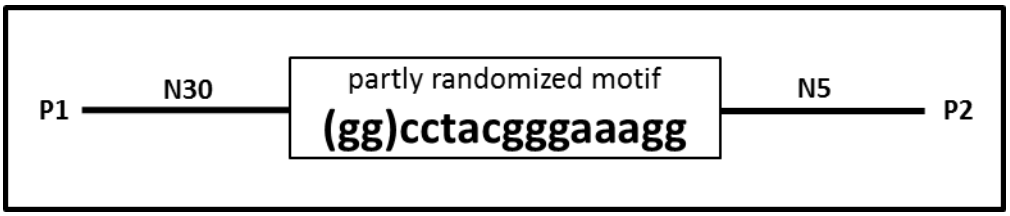

Figure 39: **Motif-doped SELEX pool** (**pool 3)** The newly designed pool for SELEX consists of a partially structured library containing a 15 nt sequence motif ((gg)cctacgggaaagg) derived from aptamers of the first and second affinity SELEX. The motif is flanked by 30 randomized nt on the motifs 5' end, and 5 randomized nt on its 3' end. The motif was partially randomized, with a 50% chance of a nucleotide exchange for the first two nt (GG), and a 6% chance for the remaining 13 nt. This partially structured library is flanked by the constant primer binding regions P1 and P2.

This oligonucleotide for this new, "motif-doped" pool was synthesized by the company Seqlab. For large scale maximum efficiency amplification by PCR (using primer pair "Library doped fwd" and "Library doped rev", Table 6), protocols were tested and optimized.

4.13.1 Motif-doped pool PCR optimization

Optimization of the PCR conditions was carried out according to (4.3.1). PCR was carried out according to the PCR protocol described in table (Table 16). Figure 40 shows a distinct band at the expected size of 127 bp on a 3% agarose gel.

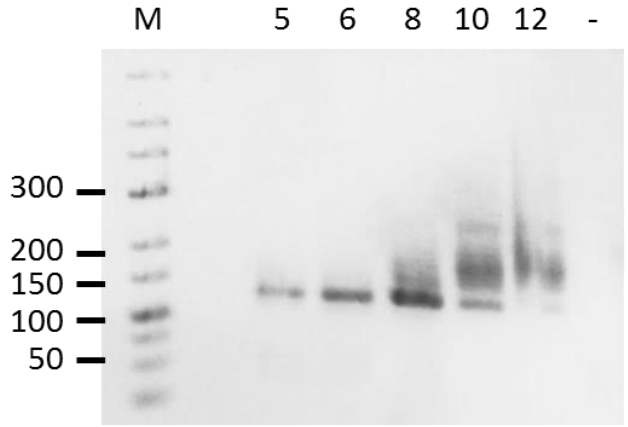

Figure 40: **Agarose gel of pool 3 scout PCR** Shown is a 3% agarose gel with PCR-reactions performed with different amounts of cycles to test amplification of pool 3 via the PCR program described in (Table 16). Shown from left to right in the lanes are: Marker (M), 5, 6, 8, 10 and 12 cycles and the negative control sample containing no template (-).

After PCR cycles 5, 6, 8, 10 and 12, 5 µL of the reaction were taken from each PCR sample and applied on a 3% agarose gel, together with a negative control reaction containing no template DNA (- , Figure 40). As can be seen in Figure 40, after 10 cycles, overamplification bands start to appear.

In order to further optimize PCR conditions, different annealing temperatures were tested, parallel to a range of amplification cycles determined before. Temperatures tested were 54, 58 and 62°C, the different amount of cycles tested were 6, 7, 8, and 9, as a control. Samples were checked on a 3% agarose gel (Figure 41).

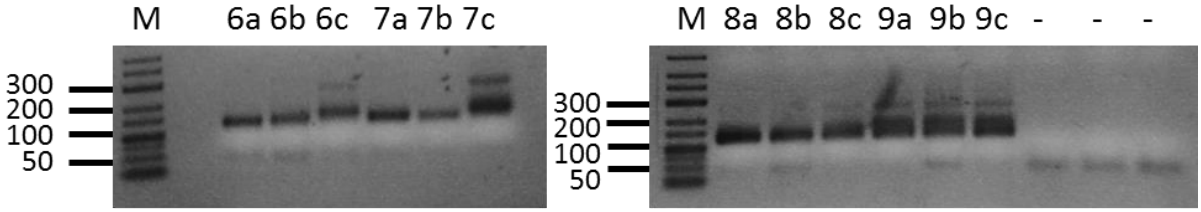

Figure 41**: Agarose gel of pool 3 scout PCR** Shown are details of a 3% agarose gel with PCR-reactions performed with different amounts of cycles to test amplification of pool 3 via the PCR program described in (Table 16). Shown from left to right in the lanes are: Marker (M), 6 cycles: 6a (54°C), 6b (58°C) 6c (62°C); 7 cycles: 7a (54°C), 7b (58°C) 7c (62°C); 8 cycles: 8a (54°C), 8b (58°C) 8c (62°C); 9 cycles: 9a (54°C), 9b (58°C) 9c (62°C) ; negative control sample containing no template (-, 54, 58, 62°C).

Figure 41 shows the strongest and cleanest results at 54°C and after 7 cycles of amplification. PCR efficiency was calculated according to Hall *et al*. [234]. The final optimized PCR program can be found in Table 17, as it is identical to the one previously used (4.3.1).

4.13.2 Motif-doped pool generation

The optimized PCR protocol was applied in a 40 mL PCR reaction carried out in 96 well plates, using the entire remaining synthesized pool sample as template. The resulting DNA pool was precipitated using sodium acetate precipitation (3.2.12) and resuspended in a total volume of 2 mL water. From this pool DNA solution with a concentration of 1.51 µg/µL (or $3.6x\ 10^{-11}$ mol/µL), 215 µL were used in a 10 mL transcription sample used to transcribe the pool (3.2.8). The transcribed pool was precipitated using sodium acetate precipitation and purified using PAA gels (3.2.11). Resuspended in 2 mL of RNase free water, the RNA pool had a concentration of 189 pmol/µL. This pool RNA stock solution was used for motif-doped SELEX experiments.

Applying the same calculations as in 4.3.2, $4.8x\ 10^{14}$ molecules were used in the motif-doped SELEX (Equation 6, Equation 7). Assuming a totally randomized nucleotide pool of 50 nt, the possible sequence space would still contain 1.27×10^{30} sequences and could not be covered with the pool applied in the SELEX. As before, all of the synthesized pool oligo had been used in the large-scale PCR and a bigger sequence space could not be achieved. The motif-doped SELEX was carried out using the developed pool.

4.14 Doped SELEX

The generated motif-doped pool was used for SELEX against azoCm. azoCm Amino derivatized sepharose gel was used as column material, like in the previous affinity and light SELEX. The SELEX protocol was carried out using the protocol for affinity SELEX as described chapter 3.4.3. After loading the RNA and incubating it for 30 min on the columns at RT, 10 washing steps of CV=500 µL with 1x SELEX buffer were carried out. For elution, a 1 mM azoCm *trans* solution was used in 4 elution steps (1 CV each) starting in SELEX round 1. This process was repeated for several consecutive rounds to generate an RNA pool enriched with ligand binding aptamers.

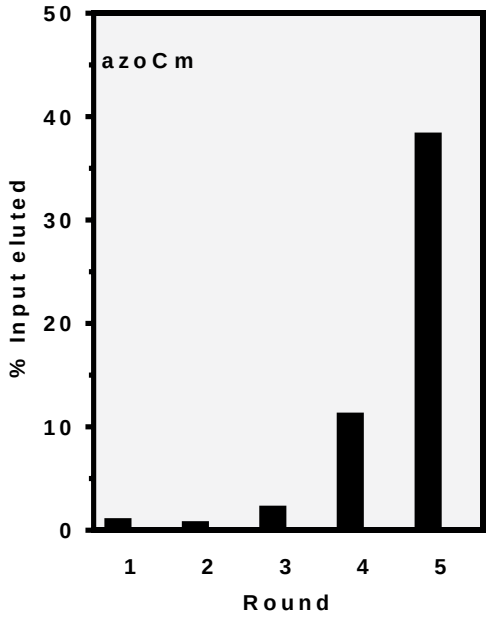

Figure 42: **Summary of motif-doped SELEX against azoCm (pool 3)** Shown is the fraction of loaded RNA that could be eluted from azoCm-derivatized columns after each selection round. RNA was eluted with 1 mM azoCm (Doped SELEX (DS) round 1-5).

As shown in Figure 42, the SELEX was quickly enriched, reaching 38% RNA elution within five rounds of SELEX. This rapid enrichment coupled with the fact that elution was achieved with 1 mM of ligand solution ($1/5^{th}$ of the concentration used in affinity SELEX) indicated that the motif was indeed relevant for ligand binding.

To analyze the development of the motif doped pool, 96 aptamers generated by TOPO TA cloning (Table 4) each for doped SELEX (DS) rounds DS2 to DS5 were sequenced. Within these sequences, no sequence was found more than twice, and even those doublets were found only 11 times in all sequenced aptamers together (Table 25). Particularly in round 5 with 38% ligand-eluted RNA from the total applied RNA at least one dominant aptamer sequence would have been expected. The failure to find one or several dominant sequences in the SELEX, while at the same time the SELEX displayed strong enrichment over the progression of rounds seemed to indicate one single factor as the determinant on how well the RNA could bind azoCm.

Table 25: **Summary of double sequences in motif-doped SELEX rounds 2-5**

Round	RNA elution	Number of doubled sequences in round	Number of doubled sequences between rounds
DS2	0.5%	6	1
DS3	2%	1	-
DS4	11.1%	2	-
DS5	38.1%	1	1

Shown are the SELEX rounds DS2 to DS5 and their respective RNA elution in percent. The amounts of sequences found twice within one round are listed, as well as the amounts of sequences found identical between one round and another.

Reducing the analysis of the aptamer sequences to the light motif alone, while disregarding the randomized regions flanking it, showed a re-enrichment of the original motif sequence (see Figure 43).

	G	G	C	C	T	A	C	G	G	G	A	A	A	G	G
A	29%	40%	0%	0%	0%	97%	0%	0%	0%	0%	100%	100%	98%	0%	40%
C	18%	2%	98%	100%	0%	0%	98%	0%	0%	0%	0%	0%	0%	2%	2%
G	23%	56%	0%	0%	0%	3%	2%	100%	100%	100%	0%	0%	0%	98%	56%
T	31%	2%	2%	0%	100%	0%	0%	0%	0%	0%	0%	0%	0%	0%	2%
	x	A/G	C	C	T	A	C	G	G	G	A	A	A	G	A/G

Figure 43: **Enrichment analysis of the sequence motif of the doped selection in DS5**. Shown is the nucleotide distribution over the different motif positions. In the first line, the original light motif is displayed. Below, the chance of one nucleotide occupying this position is listed in percent (A, C, G, T). Some positions show a 97 to 100% probability of recovering their original nucleotide after round 5 of the doped SELEX (blue markings). Other nucleotides, like the very first position (originally a G) do not show a preference for one particular nucleotide in this position (green markings). Nucleotide positions showing a 0 to 3% probability lead to the conclusion that this position does not play a role in ligand binding (yellow and white markings). In the last line, the consensus sequence of the motif region after doped SELEX round 5 (DS5) is displayed, with larger letters describing higher nucleotide conservations. Marked in red are nucleotides which occur in 100% of the tested sequences

Over the course of the doped SELEX, the initially partly randomized motif re-evolved mostly back to its original sequence (Figure 43), thus indicating the nucleotides relevant to ligand binding. Sequence positions marked in blue show a 97 to 100% probability of recovering their original nucleotide after round 5 of doped SELEX. Sequence positions marked in green, like the very first position (originally a G), do not show a preference for one particular nucleotide in this position, leading to the conclusion that this position does not play an important role in

ligand binding. Sequence positions marked in yellow and white markings show a 0 to 3% probability of being a certain nucleotide. Typically, this marks a position where another nucleotide is highly probable to occupy this position. Thus, these markings display a "negative control" on which nucleotides would be detrimental for ligand binding on this position.

For the light motif, it can be observed that a specific nucleotide is not relevant at the first position and should therefore not be involved in ligand binding (X, Figure 43). Position two of the motif is highly probable a purine base (A or G, probability sum of 96%). As it was unclear if these two positions were necessary in ligand binding (found in 2 out of 3 tested aptamers, Table 24), these results indicated that the first position plays a negligible role. The second position seems more important, however, allowing this position to be randomized with a 50% chance to either A, C or T leading to a clear preference for the nucleobase A, next to G. This indicated that position 2 of the motif plays a role in ligand binding, or potentially in stabilizing the binding pocket surrounding the ligand binding nucleotides of the aptamer. Motif positions 3 to 14 are highly conserved, with 7 out of 12 positions displaying a 100% chance of one specific nucleotide in this position. Of the 12 positions, the lowest probability observed for the original nucleotide of the motif was 97%. Therefore, the entire sequence can be considered as crucial for ligand binding or ligand binding pocket formation, as DS5 displayed 38% RNA elution in the SELEX and can be considered highly enriched as well. Position 15 of the motif shows the same behaviour as position two, with a clear preference for purine bases in this position (probability sum of 96%).

The observation of a re-enrichment of twelve nucleotides of the motif, with two purine nucleotides flanking this conserved region indicated that the light motif itself is the core binding region on which the ligand binding solely depends. It seems that the 30 (or 31) nt upstream and 5 nt downstream of the motif only serve the purpose to stabilize the aptamer in itself, whereas the motif is responsible for the binding on its own.

As no single aptamers seeming to indicate enrichment could be extracted from this SELEX, an *in vivo* screening approach able to screen higher number of aptamer sequences was planned.

4.15 Preparation of libraries and controls for FACS screening

To discover whether the motif-doped SELEX (Figure 42) did contain aptamers functioning as riboswitches in *S. cerevisiae*, *in vivo* screening was carried out. As previous *in vivo* screenings did not yield any functional riboswitches, which could be due to the method employed, a new screening approach was designed. As screening is a laborious, time- and material-consuming method, but still only a small part of the potential sequence space of the SELEX rounds can be tested, a FACS based *in vivo* screening method seemed appropriate. Adding FACS sorting steps before the manual *in vivo* screening would significantly reduce the amount of cells to test. Cell sorting was carried out at AG Kolmar by Dr. Andreas Christmann and Dr. Doreen Könning.

To set up the cell sorter and adjust the fluorescence photomultiplier for GFP accordingly, *S. cerevisiae* cells containing the control plasmid pCBB006 (Table 8) grown with and without azoCm were measured. As the plasmid contains no start codon (ATG) in front of the GFP encoding gene *gfp*, no GFP protein should be generated, thus the cells should not show any fluorescence. For the next measurement, *S. cerevisiae* cells containing the control plasmid pCBB005 (Table 8) grown with and without azoCm were used. As this construct contained a start codon in front of the *gfp* gene, the cells should show continuous expression of GFP, leading to the maximum fluorescence intensity output the genetic construct pCBB005 should be able to produce.

These two measurements were set as the high and low threshold of the experiment, respectively, representing the minimum and maximum fluorescence intensity of *S. cerevisiae* cultures containing the control plasmid pCBB with any variation of GFP expression controls (no GFP expression, continuous GFP expression, aptamer/ riboswitch regulated GFP expression).

The baseline measurements regarding cell fluorescence intensity are shown in Figure 44, with minimal differences between minimum and maximum fluorescence intensity values grown with or without azoCm in the area above 10^1 units. These differences can be regarded as background noise, according to Christmann (pers. comm.). Any differences below the value of 10^1 fluorescence units can, therefore, be neglected.

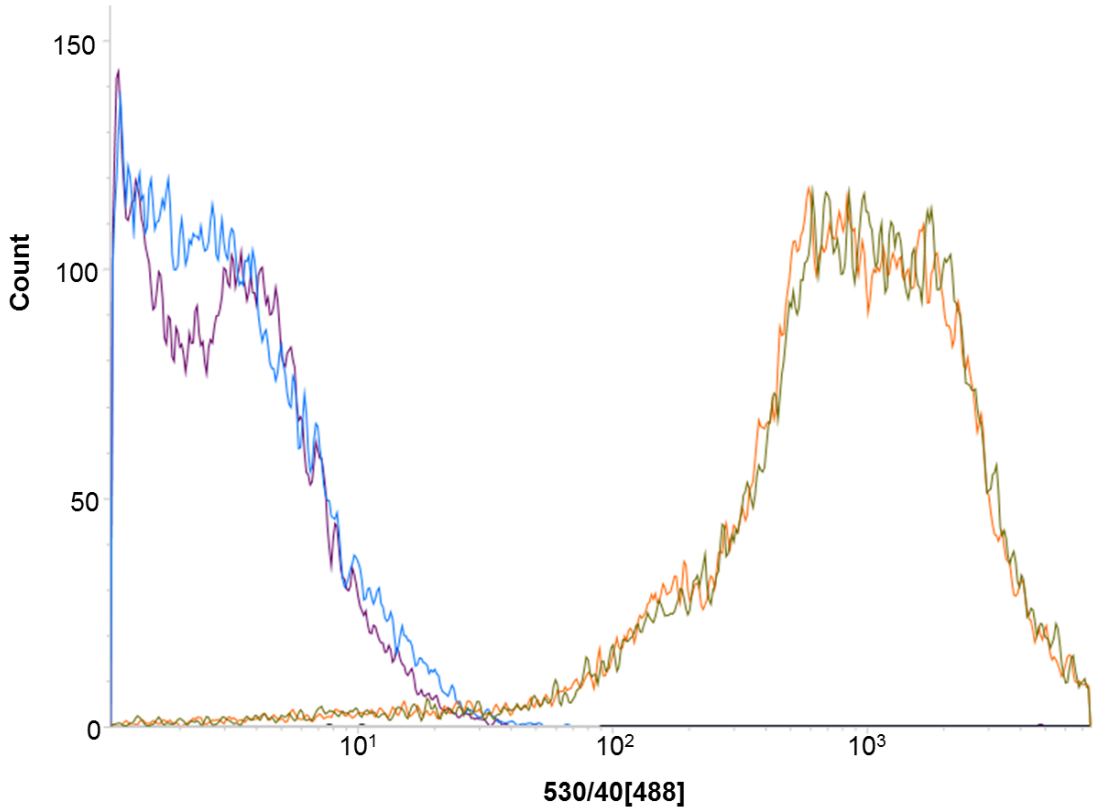

Figure 44: **First measurement of FACS controls** Shown are the fluorescence intensities of yeast cells of grown with and without azoCm in the media. The cells contained the following plasmids. Orange line: pCBB005, green line: pCBB005+azoCm, violet line: pCBB006, blue line pCBB006+azoCm. On the X-axis, the fluorescence intensity is given in units after 488 nm excitation with a fluorescence emission detection between 530 ± 20 nm which is annotated as 530/40(488). The Y-axis gives the cells counted for a specific fluorescence intensity.

To generate large *S. cerevisiae* aptamer libraries, large PCR amplifications of the aptamers from the doped SELEX pools DS3 and DS4 were ligated with digested pCBB005 plasmid backbone (3.2.4, 3.2.5). The ligations were butanol-purified (3.2.12) und transformed into commercially available *E. coli* 10-beta cells (3.3.2, Table 4). To avoid losing any transformed aptamer sequences, the entire transformation reaction was grown in a volume of 8 mL LB-medium, except for a few microliters of the reaction, which were used for dilution plating, so transformation efficiency could be quantified according to Equation 8 (an example for library DS3 is given in Equation 9).

Equation 8: **Calculation of transformation efficiency** To calculate transformation efficiency (TE), cells are transformed with circularized plasmid DNA using optimal conditions and plated on solid media. After growth, colonies per plate are counted (colony forming units, cfu). Divided by the amount of plasmid used for transformation and the final dilution of the plated cells, TE in cfu/amount plasmid can be calculated.

$$\frac{\frac{cfu\ (control\ plate)}{ng\ of\ plasmid}}{final\ dilution\ of\ plasmid\ in\ media} = TE\ [\frac{cfu}{ng\ plasmid}]$$

Equation 9: **Calculation of transformation efficiency of library DS3** Transformation efficiency (TE) of cells transformed with circularized plasmid DNA of pool DS3 is calculated. Number of colonies counted on the plate was 2040 (cfu) and divided by the amount of plasmid used for transformation and the final dilution of the plated cells (1:115). TE was calculated as 234600 cfu per ng plasmid.

$$\frac{2040\ cfu}{\frac{1\ ng\ of\ plasmid}{(1:115)}} = TE\ 234600 \frac{cfu}{ng\ plasmid}$$

Calculation of the transformation efficiency yielded a library size of 2.35x 10^5 for library DS3 (generated from aptamers of the doped SELEX round DS3) and 3.96x 10^4 for library DS4 (from aptamers from doped SELEX round 4). After growing the cells overnight, the plasmids were extracted and butanol-purified (3.2.12). The entire pool of aptamer-containing plasmids was then transformed into electrocompetent yeast cells (3.3.5). Thus, *S. cerevisiae* libraries were generated, containing the aptamers from DS3 or DS4 in a riboswitch set-up. They were kept in culture for immediate use or frozen in glycerol stocks at -80°C for later experiments.

4.15.1 Yeast library segregation and first FACS sort

To prepare the libraries for fluorescence-activated cell sorting, the *S. cerevisiae* libraries had to be grown in a segregation set-up, a method that is employed to reduce the number of plasmids that one *S. cerevisiae* cell carries (3.3.5 [228]). After segregation, the cells were strained through cell strainers (Table 3) to remove budding cells, or cells stuck to each other, and kept on ice until sorting. In parallel to the libraries, *S. cerevisiae* cells transformed with pCBB005/006/007 were inoculated in 4 mL samples. They were strained through filters as well, chilled on ice, and used as daily control measurements for the FACS sorting.

Figure 45 shows the distribution of fluorescense in the DS4 *S. cerevisiae* library as a green line. In comparison, the parallel control values of pCBB005 (blue line) and pCBB006 (brown line) show that the established FACS protocol and its thresholds are suitable for the experiment, as there are almost no cells of DS4 that lie outside of the established minimum and maximum fluorescence values. The fluorescence intensity of DS4 is almost equally distributed over the range of 10^1 to10^3 fluorescence units, with a decreasing number of cells that shift towards the minimum and maximum fluorescence values. Overall, 75% of the cells were above the values of the negative control. Figure 45 shows the two gates which were set to sort the cells, a high gate (“DS 4 high”, green gate, 25% of the cells) and a low gate (“DS 4

low", blue gate, 42% of the cells). Cell sorting was carried out until 2 millions cells per gate were isolated.

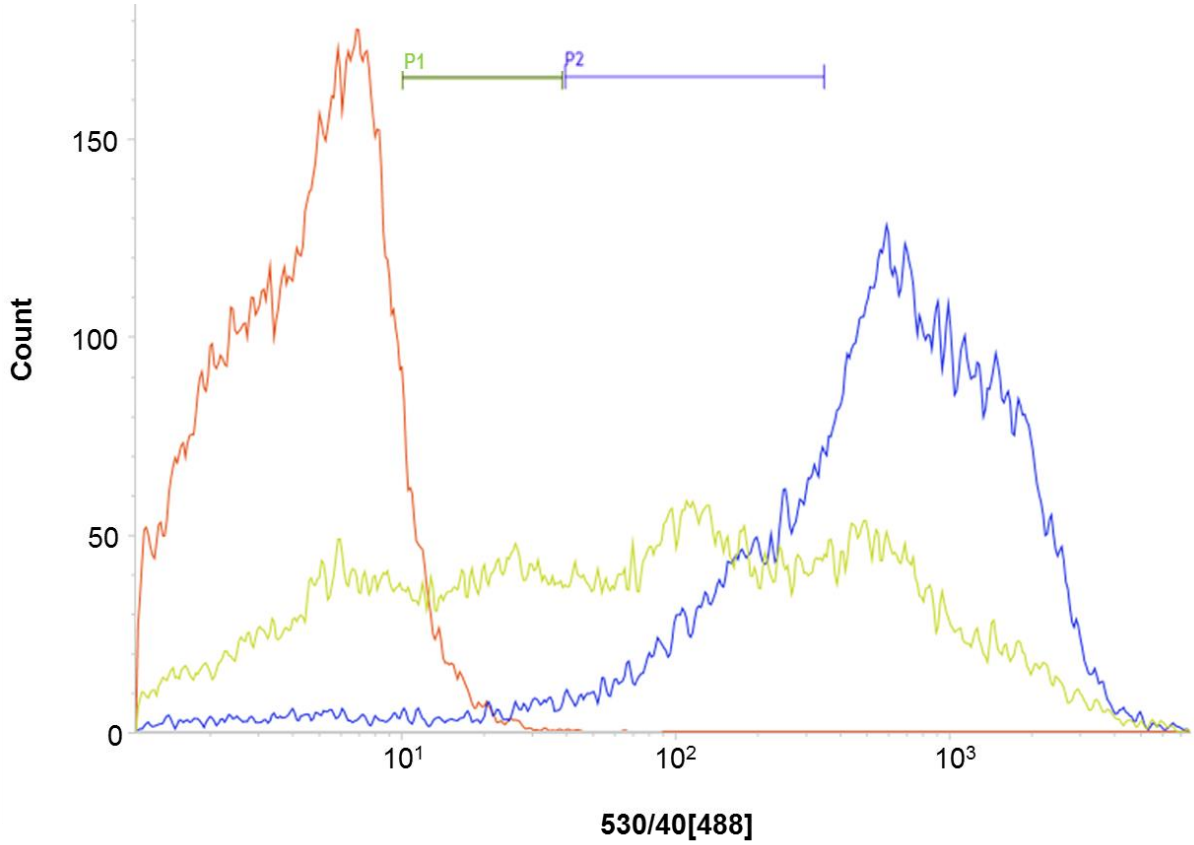

Figure 45: **First measurement of yeast cells containing DS4 aptamers** Shown are the fluorescence intensities of yeast cells containing the following plasmids: Orange line: pCBB006, green line: DS4 aptamer library, blue line: pCBB005. 2 million cells were sorted into each of the two gates, one showing low fluorescence intensity (green gate, "P1") and one showing high fluorescence intensity (blue gate, "P2"). On the X-axis, the fluorescence intensity is given in units after 488 nm excitation with a fluorescence emission detection between 530 ± 20 nm which is annotated as 530/40(488). The Y-axis gives the cells counted for a specific fluorescence intensity.

The same procedure was carried out for cells of the library DS3 (data not shown). The distribution of the cells was similar to DS4 prior to sorting, with 84% of the cells above the negative control. For DS3, the same gates as for DS4 were used, sorting 2 million cells into the high gate (32% of the total cells) and 2 million into the lower gate (40% of the total cells). All sorted cells were grown in 50 mL SCD-URA medium for 48h at 30°C. The cultivated cells were then diluted 1:100 in fresh 50 mL SCD-URA medium, grown for 24h, and then diluted 1:100 in 10 mL of medium with and without 100 µM azoCm, and grown for 24h. Parallel controls of *S. cerevisiae* cells containing pCBB005 and pCBB006 were inoculated in

4 mL again. All libraries and controls were strained through cell strainers (Table 3) and kept on ice until sorting.

4.15.2 Second FACS sort

The second FACS sorting consisted of the two libraries with their previously sorted two fluorecence groups, DS3 low, DS3 high, DS4 low and DS4 high, all cultivated with and without azoCm resp.

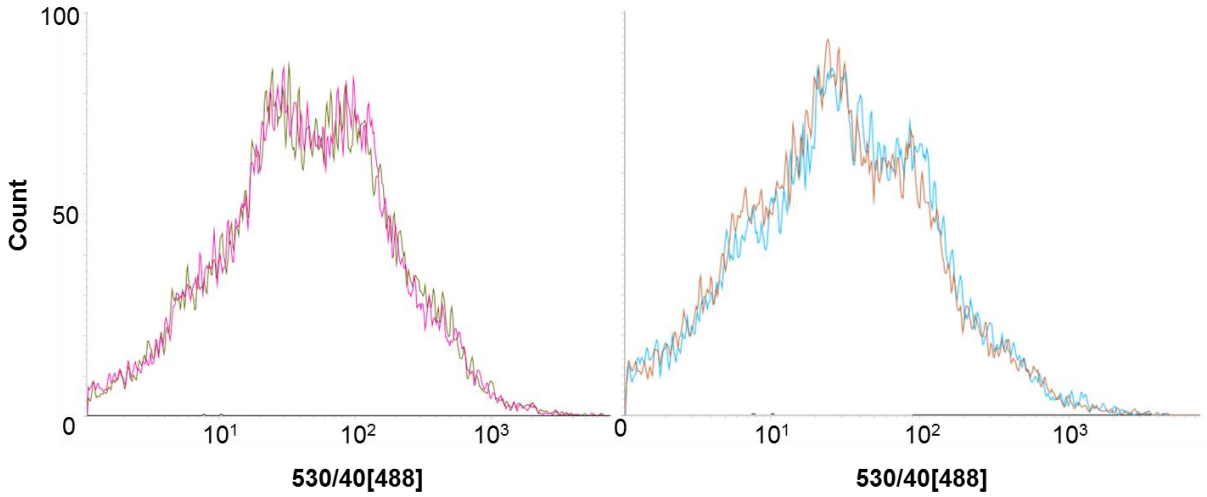

Figure 46: **Measurement of yeast cells containing sorted DS3 and DS4 cells from the "low" gate (see** Figure 45**) A** Shown are the fluorescence intensities of yeast cells from the previous DS3 low sort: green line: grown with azoCm, pink line: grown without azoCm. **B** Shown are the fluorescence intensities of yeast cells from the previous DS4 low sort: blue line: grown with azoCm, brown line: grown without azoCm. On the X-axis, the fluorescence intensity is given in units after 488 nm excitation with a fluorescence emission detection between 530 ± 20 nm which is annotated as 530/40(488). The Y-axis gives the cells counted for a specific fluorescence intensity.

Figure 46A shows the distribution of fluorescent cells of DS3 low grown without azoCm (green line) and with 100 µM azoCm (pink line). Figure 46B shows the cells of DS4 low without azoCm (brown line) and with 100 µM azoCm (blue line). As there was barely a difference between the cells grown with or without azoCm, the cells of DS3 low and DS4 low were not sorted and were discarded. Figure 47B shows the distribution of fluorescent cells of DS4 high grown without azoCm (pink line) and with 100 µM azoCm (blue line). At a fluorescence intensity of around 10^2 units there are fewer fluorescent cells in the sample grown with azoCm present as in the one without. This indicated that in this region, an azoCm

dependent regulation of GFP production could have taken place. A gate (P2) was set, and 50000 cells of the gated population (making up 11% of all cells) were sorted.

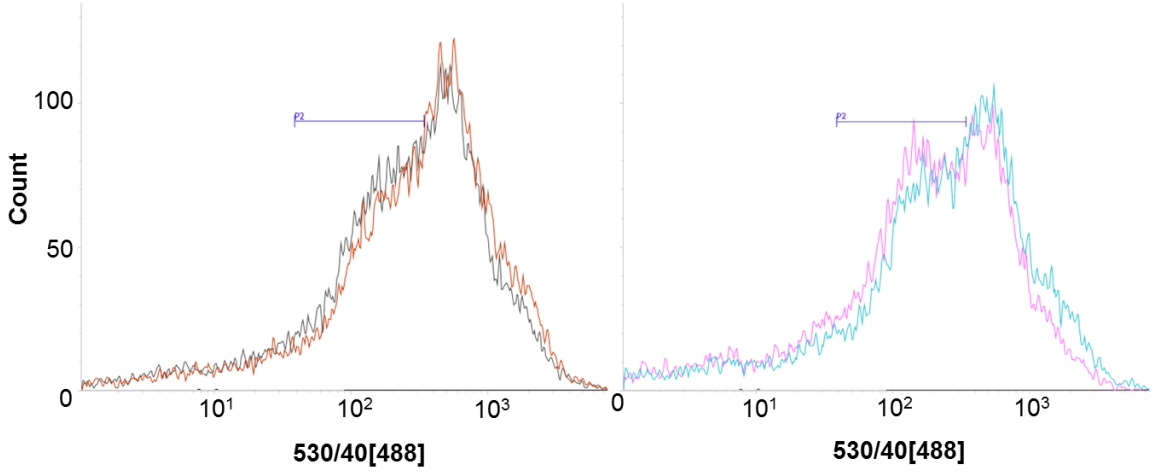

Figure 47: **Measurement of yeast cells containing sorted DS3 and DS4 cells from the "high" gate (**Figure 45**). A** Shown are the fluorescence intensities of yeast cells from the previous DS3 high sort: brown line: grown with azoCm, black line: grown without azoCm. **B** Shown are the fluorescence intensities of yeast cells from the previous DS4 high sort: blue line: grown with azoCm, pink line: grown without azoCm. Cells were sorted into one gate (blue gate, "P2"). On the X-axis, the fluorescence intensity is given in units after 488 nm excitation with a fluorescence emission detection between 530 ± 20 nm which is annotated as 530/40(488). The Y-axis gives the cells counted for a specific fluorescence intensity.

Figure 47A shows the cells of DS3 high without azoCm (black line) and with 100 µM azoCm (brown line). The same shift in fluorescence around an intensity of 10^2 as in DS4 high could be observed, even though it was less pronounced. Overall, 50000 cells of gate P2 were sorted (making up 2% of all cells).

The sorted cells were diluted to a density of 200 cells/µL and plated on 20 SCD-URA plates, for DS3 high and DS4 high, each. The remaining cells were grown in 8 mL of SCD-URA for 48 h at 30°C, then harvested and frozen in glycerol at -80°C for later use.

4.16 *In vivo* screening of doped SELEX aptamers from FACS sorted pools

To find out whether the generated aptamers in the doped SELEX (DS) rounds DS3 and DS4 contained some functioning as riboswitches, *in vivo* screening with the previously FACS sorted yeast cells was carried out. The cells were grown on SCD-URA plates and single colonies were inoculated into 96 well plates. Screening was carried out according to (3.3.8).

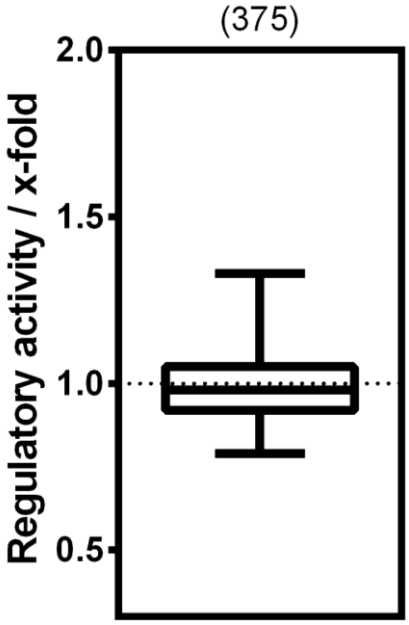

Figure 48: ***In vivo* screening of doped SELEX rounds DS3 and DS4 after FACS sorting** This boxplot shows the summarized *in vivo* screening of *S. cerevisiae* cultures for the doped SELEX rounds DS3 and DS4. For each investigated clone, the regulatory activity was calculated as the ratio of GFP fluorescence with and without 100 µM azoCm (x-fold). The numbers written above the boxplot indicate the number of clones analyzed. The median of all analyzed clones was 0.98.

The median regulatory activity of analyzed clones at *in vivo* screening of rounds DS3 and DS4 was 0.98. There were clones showing regulatory activity above 1.0 on the upper antenna of Figure 48. In a second and third screening, four aptamers with regulatory function could be validated, called B1, B2, C3 and D1 (Table 26).

Table 26: **Aptamer sequences with regulatory function discovered in DS3 and DS4 *in vivo* screening**

Ribos witch	Sequence
B1	CCCTTAGCACGACGAACTAGATGCCGTTGCTACCTACGGGAAAGGACGGT
B2	GCTCCCTTTAGATGTTAGTCGAAGACATCTAACCTACGGGAAAGGAGACC
C3	CTCAGCCCCTCAGTCGAGTGGATTCACGGCTGCCTACGGGAAAGGGTGAG
D1	CCCTTTGGTTAGAATACAGTGCTCTAGCCAACCTACGGGAAAGGACGGT

Shown are the sequences of the four aptamers from doped SELEX rounds DS3 and DS4 (B1, B2, C3, D1) showing regulatory function regarding gene expression. Marked in green is the original light motif sequence.

These regulatory aptamers were analyzed in triplicates using cytometry (3.3.7), as well as fluorimetry (3.3.6), to exclude methodical bias (Figure 49). Controls were measured as well.

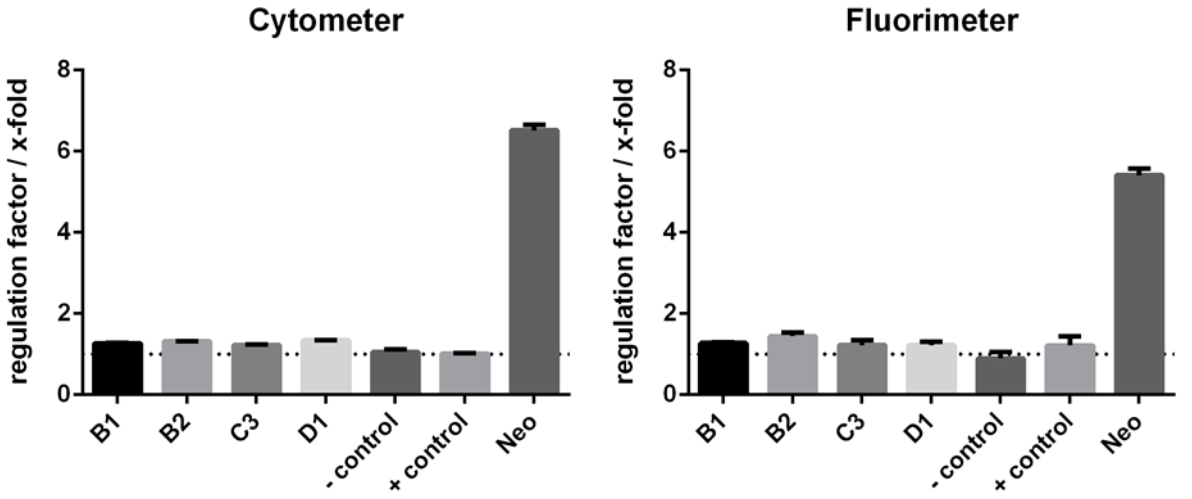

Figure 49: **Cytometric and fluorimetric measurements of regulatory aptamers from doped SELEX rounds DS3 and DS4.** Shown are the measurement of the median regulatory factors of azoCm dependent aptamers B1, B2, C3 and D1 using a cytometer (left, 3.3.7) or a fluorimeter (right, 3.3.6). As controls, cells with plasmids showing constant (+ control, pCBB005) or no GFP production (- control, pCBB006) were measured, as well as a sample containing the Neomycin riboswitch (Neo, pCBB007). A dotted line marks a regulatory factor of 1.0. All samples were measured in triplicates and with azoCm or Neomycin as ligand.

Aptamers B1, B2, C3 and D1 all show a regulatory factor of GFP expression of 1.25 to 1.35. The controls showed no influence on their fluorescence by addition of azoCm (+ and – control, Figure 49). Growing and measuring yeast cells containing plasmid pCBB007 insured that growth conditions were fitting for riboswitch activity.

As neither of the aptamers in Figure 49 showed a regulating activity of more than 1.35-fold, new pools for doped *in vivo* screening were designed. In order to be able to generate a riboswitch out of one of the aptamers showing a slight regulatory function, the aptamer B2, showing the highest and most consisted regulatory factor, was chosen as a basis for a new pool design. Randomized mutagenesis of the aptamer sequence of B2 were designed and screened *in vivo* to find a functional riboswitch.

4.17 Development of doped *in vivo* screening pools

To find azoCm dependent riboswitches with a higher regulatory factor (x-fold), four new pools for *in vivo* screening based on the B2 riboswitch were designed. The variants were based on the supposed 2D structure of the B2 riboswitch (Figure 50A), which was derived from the way the aptamer 42 was folded (Figure 14B), as the riboswitch and the aptamer contain the same core motif of 13 nucleotides (Table 26).

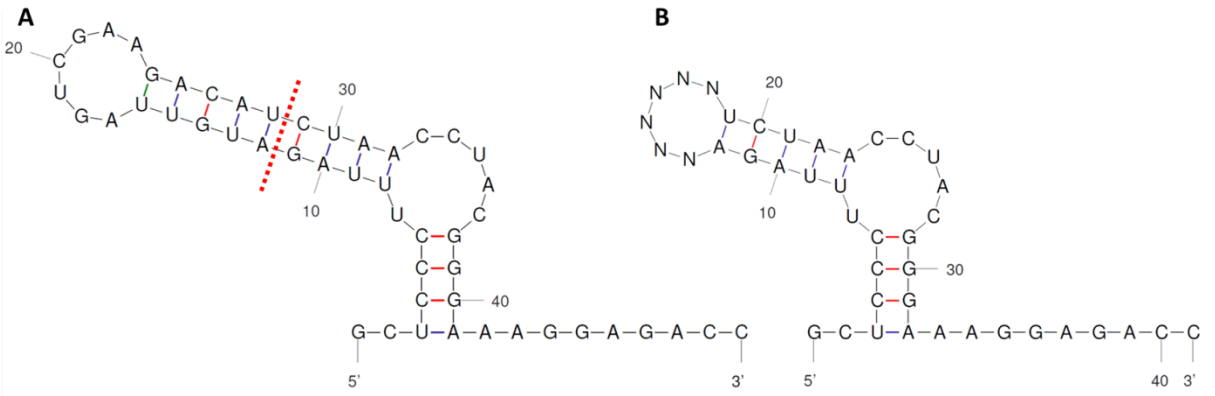

Figure 50: **Structure of B2-derived pools A** Shown is the via mfold predicted structure of riboswitch B2 (Table 12, Table 26). For B2-derived pools B2-10 and B2-5, the entire sequence was allowed a 10 or 5% nucleotide permutation rate. Marked in a dotted red line is where the sequence was truncated to generate the structural bases shown in B (pools B2-N6 and B2-6N6) **B** Shown is the mfold predicted structure of riboswitch B2-derived pools B2-N6 and B2-6N6. For pool B2-N6, the upper left loop allows for total randomization of 6 nucleotides. B2-6N6 allows for total randomization of 6 nucleotides in the left upper loop, while allowing a 6% nucleotide permutation rate in the remaining sequence.

Two variants allowed for a 5% and 10% nucleotide permutation rate of the sequence of riboswitch B2, respectively (Figure 50A). To reduce the size of the riboswitch, the two other pool variants were composed of a truncated version of B2 by removing parts of the upper arm of the structure, where no ligand binding should take place. In one pool variant, 15 nt of the upper arm of B2 (Figure 50A) were replaced with a short loop containing 6 randomized nucleotides (B2-N6, Figure 50B). In the other variant, B2-6N6, the upper arm was replaced with a N6 loop as well, with the remaining nucleotides of the sequence being allowed a nucleotide permutation rate of 6% (Figure 50B).

4.17.1 Doped *in vivo* screening pool generation

The DNA templates for the designed pools were ordered from Seqlab, as described previously. As pools for this *in vivo* screening did not undergo a SELEX experiment prior to *in vivo* screening, a smaller sequence space was acceptable. Therefore, PCR condition optimization was only carried out regarding the amount of amplification cycles used. As PCR primers, for every *in vivo* pool its forward template oligo (e.g. “Library B2-10 fwd”, Table 6) was used in combination with their common reverse oligo “Libraries B2 rev” (Table 6). The PCR products were gel purified using the Qiagen kit (Table 4). Figure 51 shows a representative 3% agarose gel of the amplification of pool B2-10, using 35, 37, and 40 cycles

of amplification (protocol see Table 16). Figure 51 shows a distinct band at the expected size of 97 bp on a 3% agarose gel.

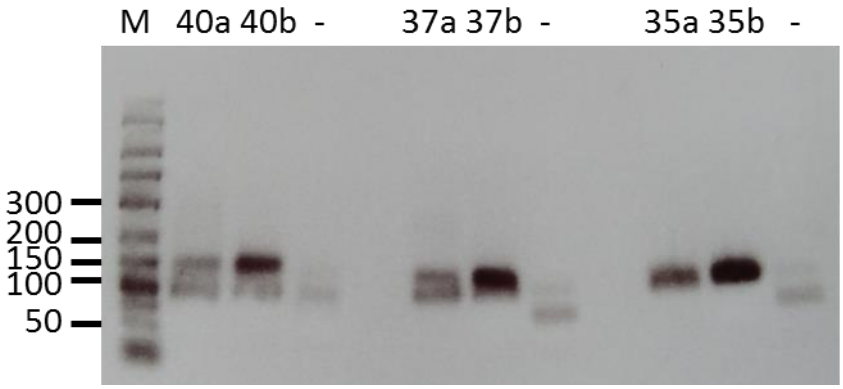

Figure 51: **Agarose gel of the PCR amplification-results of pool B2-10** Shown are Marker (M), and results of 40, 37 and 35 cycles of amplification on a 3% agarose gel. For each PCR, 5 µL of the PCR reaction (a) and the gel purified PCR product (b) were applied on the gel, as well as a negative control containing no template (-).

As can be seen in Figure 51, only the protocol with 35 cycles of PCR amplification does not show overamplification bands. Therefore, 35 cycles were used in the finalized PCR reaction using the protocols shown in Table 27 and Table 28.

All four amplified DNA pools were used as aptamer templates. The DNA was cleaved using restriction enzymes AgeI and NheI (Table 5) and ligated into the plasmid pCBB006 (Table 8), which was linearized using the same enzymes, previously (3.2.4, 3.2.5). The ligation reaction was butanol-purified (3.2.12) after 16 h of incubation. The commercial cells *E. coli* 10-beta (Table 4) were transformed with the generated plasmid library, to ensure high transformation yields. The transformed cells were grown in 8 mL LB-Amp medium per library and the plasmids were extracted after 16 h of growth using the plasmid extraction kit from QIAgen (Table 4). These generated plasmid-libraries were butanol-purified again and could be used for subsequent yeast transformation.

Table 27: **Finalized doped *in vivo* screening pool PCR amplification protocol**

T	t		PCR steps
98°C	2 min		Initial melting
98°C	10 s	repeat for 35 cycles	Melting
58°C	30 s		Primer annealing
72°C	30 s		Elongation
72°C	5 min		Elongation
98°C	2 min		Melting
58°C	5 min		Primer annealing
72°C	20 min		Final elongation

Shown are the temperature (T) applied in each PCR step, as well as the time (t) the temperature is applied. The marked three steps are repeated for 35 cycles.

Table 28: **Finalized doped *in vivo* screening pool PCR amplification composition**

Reagent	Volume in µL
Pool DNA template, diluted in MQ	295
Pool fwd oligo	15
Pool rev oligo	75
dNTPs	10
Q5 reaction buffer (5x)	100
Q5 polymerase	5

Shown are the reagents applied in each pool PCR reaction, as well as the volumes used.

4.18 Motif-doped *in vivo* screening

To find azoCm dependent riboswitches with a higher regulatory factor (x-fold) than riboswitch candidate B2 (Table 26), four new plasmid pools containing randomized aptamers based on B2 were generated (4.17).

For *in vivo* screening, competent *S. cerevisiae* cells were transformed with the three pools B2-10, B2-N6 and B2-6N6, using the lithium acetate protocol (3.3.4). The transformed cells were plated on SCD-URA plates and grown for 3 d. Transformation efficiency (TE) was calculated as shown in Equation 8. As transformed plates with 1 ng plasmid diluted in 110 µL volume for the pools B2-10, B2-N6 and B2-6N6 yielded 56, 30 and 32 colonies, respectively, calculation efficiencies varied between 3330 to 6160 cfu/µg plasmid.

Single clones were inoculated in 96 well plates and *in vivo* screening was carried out according to chapter 3.3.8.

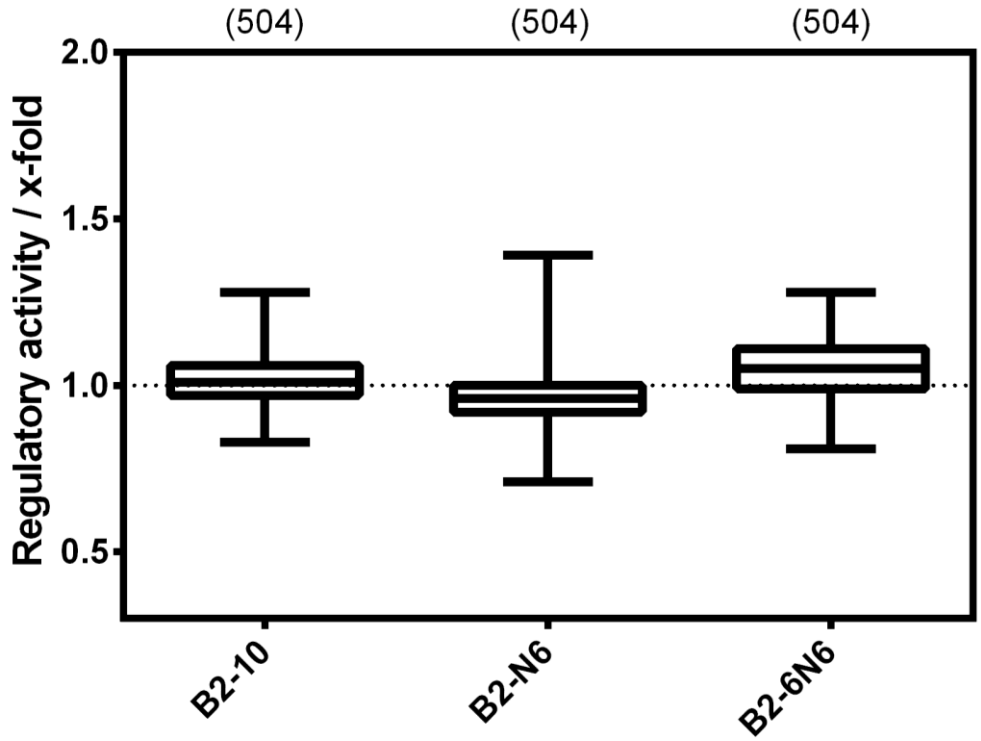

Figure 52: ***In vivo* screening of B2-derived pools B2-10, B2-N6 and B2-6N6** These boxplots show the summarized *in vivo* screening in *S. cerevisiae* cultures for the pools B2-10, B2-N6 and B2-6N6. For each investigated clone, the regulatory activity was calculated as the ratio of GFP fluorescence with and without 100 µM azoCm (x-fold). The numbers written above the boxplot indicate the number of clones analyzed. The median of all analyzed clones in B2-10 was 1.01, in B2-N6 0.96 and in B2-6N6 1.05.

In vivo screening of these pools showed no riboswitches with an improvement of the regulatory factor of B2, as shown in Figure 52. The median of all 3 pools lay between 1.05 and 0.96. Regarding pools B2-N6 and B2-6N6, this seemed to indicate that removal of the long upper left stem with its terminal loop destroyed any regulatory function. Regarding the pool B2-10, the *in vivo* screening results seemed to indicate that the degree of nucleotide permutation chosen was too high to yield any functional riboswitches, let alone some with a higher regulatory factor than B2.

For *in vivo* screening of the pool B2-5, *S. cerevisiae* cells were transformed with the protocol described in 3.3.5, in order to increase transformation efficiency. Transformed cells were plated on SCD-URA plates and grown for 3 d. Transformation efficiency (TE) was calculated according to Equation 8 and Equation 9, and yielded a TE of 2.29x 10^5 cfu/ng plasmid. This

showed that the transformation efficiency could be two orders of magnitude higher using yeast electroporation, making this transformation method useful, if large amounts of colonies should be screened.

Single clones were inoculated in 96 well plates and *in vivo* screening was carried out according to chapter 3.3.8.

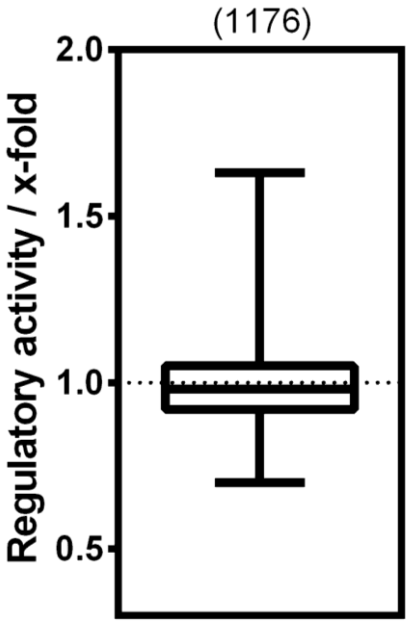

Figure 53: ***In vivo* screening of B2-derived pool B2-5** This boxplot shows the summarized *in vivo* screening in *S. cerevisiae* cultures for pool B2-5. For each investigated clone, the regulatory activity was calculated as the ratio of GFP fluorescence with and without 100 µM azoCm (x-fold). The number written above the boxplot indicates the number of clones analyzed. The median of all analyzed clones in B2-5 was 0.98.

In pool B2-5, seven functional aptamers with a regulatory factor of 1.25 to 1.3 were found. Sequence analysis of them showed, that more than 50% of them were actually the parent-switch B2. The other switches consisted of only two sequences, 8C8 and G3 (Figure 54 and Table 29). Their regulatory factors are shown in Figure 54 and were measured using a cytometer (Table 3, 3.3.7).

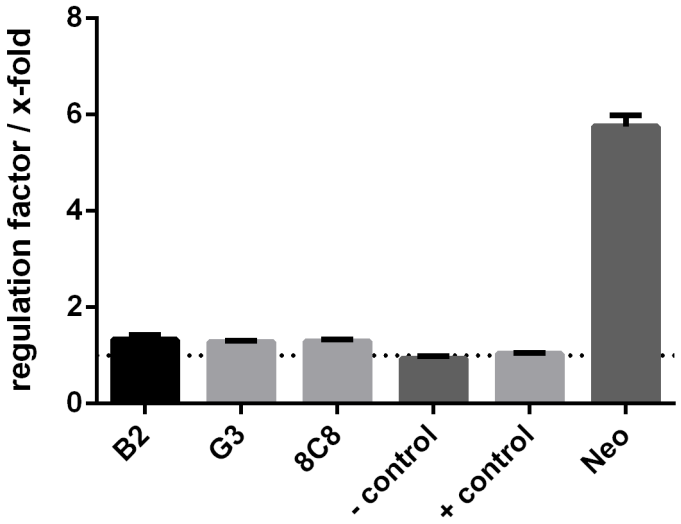

Figure 54: **Cytometric measurement of the aptamers B2, G3 and 8C8** Shown are the median regulatory factors of azoCm dependent regulatory aptamers B2, G3 and 8C8. As controls, cells with plasmids showing constant (+ control, pCBB005) or no GFP production (- control, pCBB006) were measured, as well as a sample containing the Neomycin-riboswitch (Neo, pCBB007). A dotted line marks a regulatory factor of 1.0. Four samples were measured for every construct and azoCm or Neomycin was added as a ligand. Measurements were performed on a cytometer (Table 3).

Figure 54 shows aptamers G3 and 8C8 to have comparable regulatory factors as B2 (1.28 for G3, 1.3 for 8C8, 1.33 for B2). Four samples of each aptamer were measured. Table 29 shows their sequences compared to sequence of B2, highlighting the base differences. As no other riboswitch was found, a composite sequence of the three aptamers was designed, shown in Table 29 (B2-1).

Table 29: **Development of potential riboswitch B2-1**

Riboswitch	Sequence
B2	GCTCCCTTTAGATGTTAGTCGAAGACATCTAACCTACGGGAAAGG AGACCAAAATG
G3	GCTCCCTTTAGA**G**GTTAGTCGAAGAC**C**TCTAACCTACGGGAAAGG AGACCAAAATG
8C8	GCTCCCTTTAGATGTT**T**GTCGAAGACATCTAACCTACGGGAAAGGA GACCAAAATG
B2-1	GCTCCCTTTAGA**G**GTT**T**GTCGAAGAC**C**TCTAACCTACGGGAAAGG AGACCAAAATG

Shown are the sequences of the three aptamers B2, G3 and 8C8. In G3 and 8C8, the nucleotides differing from the sequence of B2 are marked in red. Changing all three nucleotides in the sequence of B2 lead to the composite sequence B2-1, shown below with the changed nucleotides marked again in red.

This rationally designed riboswitch candidate B2-1 was synthesized via hybridization and amplification of two oligonucleotides (Table 6). Designing the oligonucleotides in a way that 5' and 3' single stranded DNA overhangs were generated, allowed the direct ligation of the gel-purified PCR product (Table 4) in a restriction enzyme linearized plasmid pCBB006 (Table 8). The generated plasmid containing the putative riboswitch B2-1 was sequenced. Yeast cells were transformed with it using the EZII protocol (3.3.3), and it was used in further *in vivo* analysis.

4.19 Validation of the riboswitch B2-1

In order to test whether the rationally designed riboswitch candidate B2-1 did show regulative activity, yeast cells containing the putative riboswitch B2-1, its parent switch B2, as well as the control plasmids pCBB005, pCBB006 and pCBB007 (Table 8) were inoculated in doublets in a 24 well plate. Measurements were performed as described in 3.3.7.

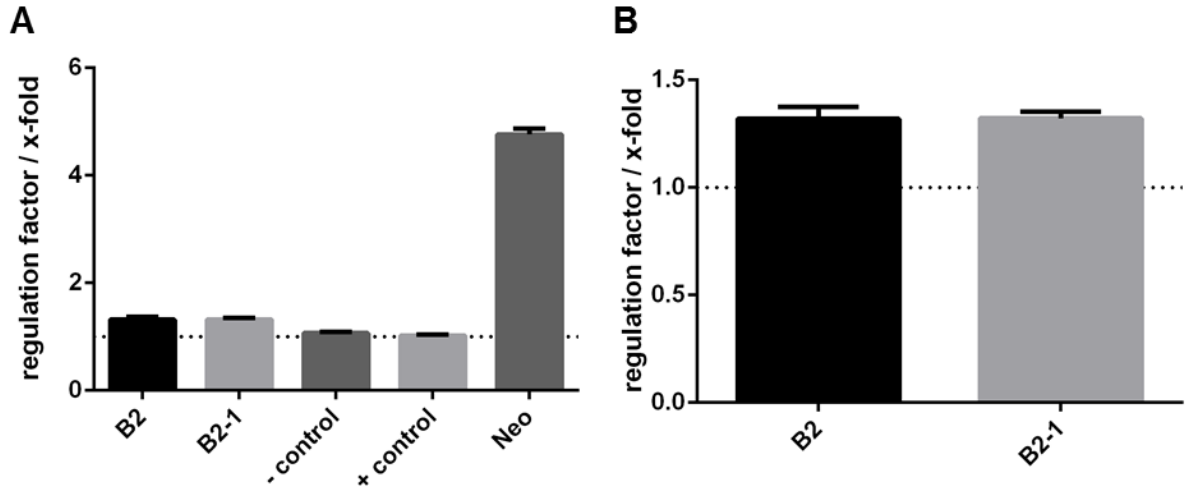

Figure 55: **Cytometric measurement of the riboswitch candidates B2 and B2-1 A** Shown are the median regulatory factors of azoCm dependent aptamers B2 and B2-1. As controls, cells with plasmids showing constant (+ control, pCBB005) or no GFP production (- control, pCBB006) were measured, as well as a sample containing the Neomycin-riboswitch (Neo, pCBB007). A dotted line marks a regulatory factor of 1.0. All samples were measured in duplicates and with azoCm or Neomycin as ligand using a cytometer (Table 3). **B** To better compare the riboswitch candidates B2 and B2-1, they are shown separately with another scale. The regulatory factor of B2 amounts to 1.319 (±0.055), while the regulatory factor of B2-1 is 1.322 (±0.031).

Figure 55 displays a comparable regulatory factor for the putative riboswitches B2-1 and B2 (B2-1 shows a regulatory factor of 1.32 (±0.03), and B2 1.32 (±0.05)), showing that the rationally designed riboswitch candidate did function in an azoCm dependent manner. As the

regulatory factor of B2-1 was considered very low, it was tested whether B2-1 could function in a dose-dependent manner, which would confirm that it could act as a riboswitch. To this end, yeast cells containing the riboswitch candidate B2-1 were inoculated in duplicates on a 24 well plate and incubated with different azoCm concentrations. Two independent measurements were carried out.

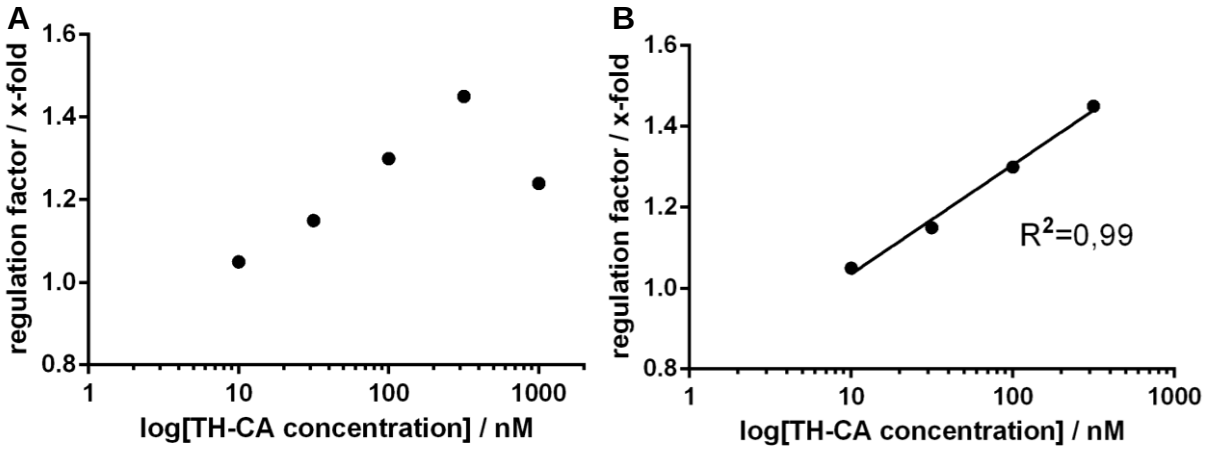

Figure 56: **Dose dependence of the regulatory factor of B2-1 riboswitch** Shown is the regulatory factor of the riboswitch B2-1 at increasing concentrations of its ligand azoCm. **A** Shown are ligand concentrations in the range of 10 nM to 1000 nM ligand. Shown is the mean value of two independent measurements. **B** Shown are ligand concentrations in the range of 10 nm to 316 nm. Shown is the mean value of two independent measurements. The coefficient of determination (R^2) of the linear regression is given.

Figure 56A shows a dose-dependent behavior for the riboswitch candidate B2-1 in the range of 10 nm to 360 nm ligand. The coefficient of determination (R^2) of the linear regression is 0.99, indicating a linear dose dependency (Figure 56B). Due to this dose-dependency, B2-1 is in the following referred to as "riboswitch B2-1". Application of 1000 nM ligand concentration to the yeast cell medium (SCD-URA, Table 11) lead to precipitation of the ligand into a visible residue at the incubation wells' bottom, therefore concentration of ligand in the solution was not reliable. Precipitation started upon addition of the ligand to the medium but seemed to increase at the end of the growth period, according to visual observation. It was concluded that the pH value of the yeast medium was conductive to this [239]. Due to this, Figure 56B depicts the dose dependence of the riboswitch B2-1 in the range from 10 nM to 316 nM, which shows exponential development. Starting at 10 nM, B2-1 shows a regulatory factor of 1.05 (±0.015), which climbs to 1.45 (±0.01) at a ligand concentration of 316 nM. This ligand dose-dependency of B2-1 seemed to indicate that B2-1 did in fact act as a riboswitch, albeit one with a low regulatory factor.

4.20 B2-1 based pools

To increase the regulatory factor of riboswitch B2-1, two new pools for *in vivo* screening based on the mfold-predicted structure of B2-1 were designed (Table 12). It was considered, that the plasmid region between the riboswitch and the promoter (5' UTR upstream of B2-1, Figure 57) might be involved in the formation of the riboswitches aptamer domain. Therefore, randomization of this region might yield a riboswitch displaying a better regulatory factor than B2-1.

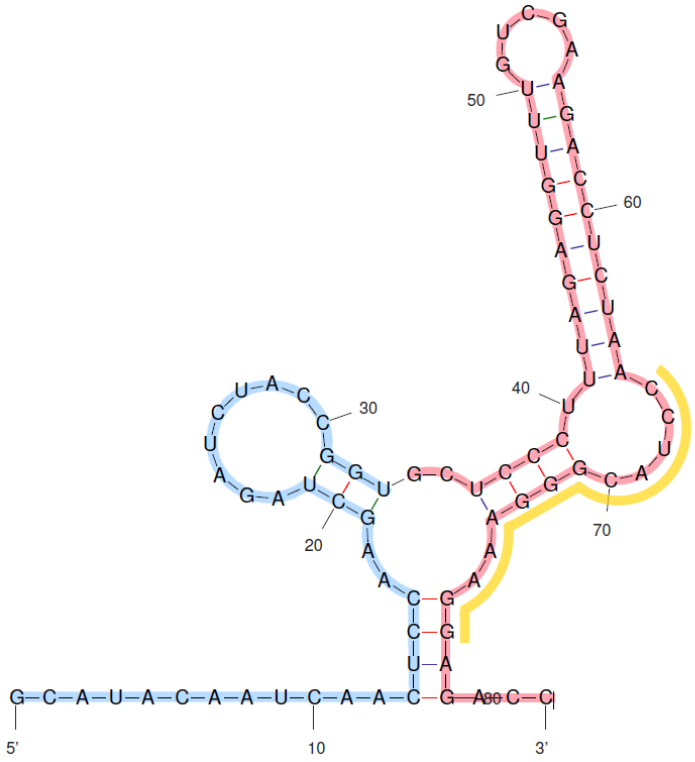

Figure 57: **Mfold predicted secondary structure of B2-1 with its 5' UTR region** Marked in red is the sequence of B2-1 stemming from the random region of the doped SELEX, marked in yellow is the light motif, and marked in blue are parts of the 5' UTR upstream of B2-1.

Based on this structure, pools 7 and 8 (Table 30) were designed, allowing either only the 5' UTR upstream of B2-1 to be randomized (pool 7), or the entire 5' UTR, including B2-1 itself (pool 8).

The pools were ordered from Seqlab, and were amplified using the PCR protocol and composition described in chapter 4.17.1 (Table 27, Table 28) using the primers "Library 7/8 fwd" and "Library 7/8 rev" (Table 6).

Table 30: **B2-1 based pools for *in vivo* screening**

Riboswitch	Sequence
B2-1 7	5’ AGCTATACCAAGCATACAATCAACTCCAAGCTAGATCTACCGGTGCTCCCTTTAGAGGTTTGTCGAAGACCTCTAACCTACGGGAAAGGAGACC 3’
B2-1 8	5’ AGCTATACCAAGCATACAATCAACTCCAAGCTAGATCTACCGGTGCTCCCTTTAGAGGTTTGTCGAAGACCTCTAACCTACGGGAAAGGAGACC 3’

Shown are the sequences of the two developed B2-1 derived pool for *in vivo* screening. Marked in red is the sequence of B2-1, marked in blue are the last nucleotides of the adh1 promoter on the plasmid pCBB. In the underlined region of the sequences, 2 nucleotides were randomized.

PCR protocol optimization was carried out regarding the amount of amplification cycles used. Figure 58 shows a distinct band at the expected size of 307 bp on a 3% agarose gel.

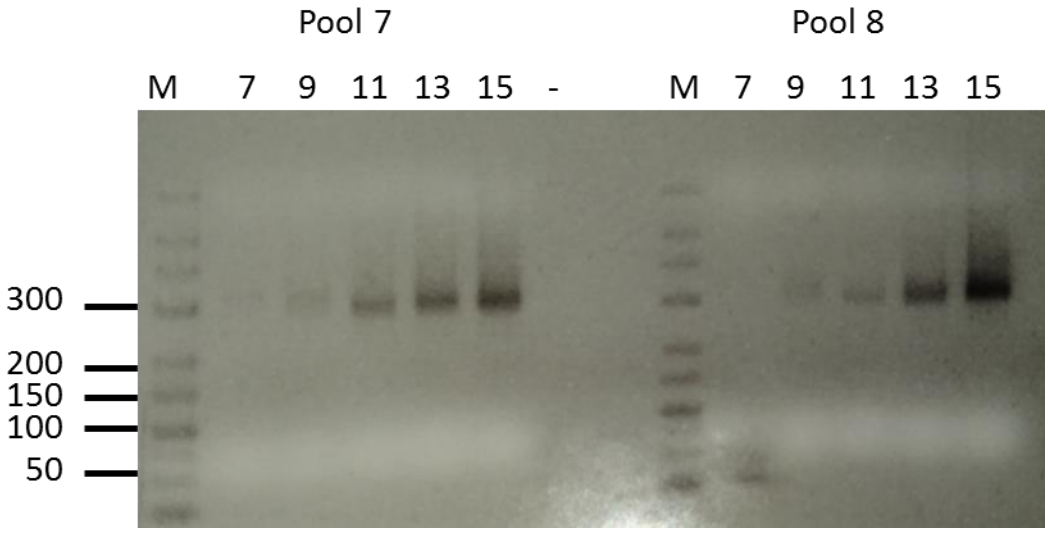

Figure 58: **Agarose gel of the PCR amplification-results of B2-1 derived pools for *in vivo* screening** Shown is a 3% agarose gel of the different amount of cycles tested to amplify the B2-1 riboswitch derived pools 7 and 8. The PCR program described in Table 27 was used. Shown from left to right in the lanes are: Marker (M), 7, 9, 11, 13, and 15 cycles and the negative control sample containing no template (-).

Figure 58 that 15 cycles of PCR amplification of pools 7 and 8 yielded strong bands on a 3% agarose gel without any overamplification. Therefore, the large-scale PCR amplification of the pool template DNA was carried out using the protocol described in chapter 4.17.1 but with only 15 cycles of amplification.

4.20.1 *In vivo* screening of B2-1 based pools

For *in vivo* screening of the pools B2-1 7 and 8, *S. cerevisiae* cells were transformed with the protocol described in chapter 3.3.5. 50 µL of transformed cells were plated on SCD-URA plates and grown for 3 d. Transformation efficiency (TE) was calculated according to Equation 8 and yielded a TE of 1.27x 10^5 cfu/ng plasmid for pool 7 and 1.4x 10^5 cfu/ng plasmid for pool 8. The remaining transformed cells were grown in a segregation approach, as described in chapter 4.15.1, to generate yeast cells containing only one plasmid each. After the final segregation step, cells were sorted on a cell sorter as described in chapter 4.15.1, the same two gates were used for sorting. 100000 cells per gate and pool were sorted, diluted to a density of 200 cells/µL, and plated on 20 SCD-URA plates for each pool and gate (7 high and low, 8 high and low). The remaining cells were grown in 8 mL of SCD-URA medium for 48 h at 30°C, then harvested and frozen in glycerol at -80°C for later use.

The plates were incubated for 3 d at 30°C. From them, single clones were inoculated in 96 well plates and *in vivo* screening was carried out according to 3.3.8 using a cytometer.

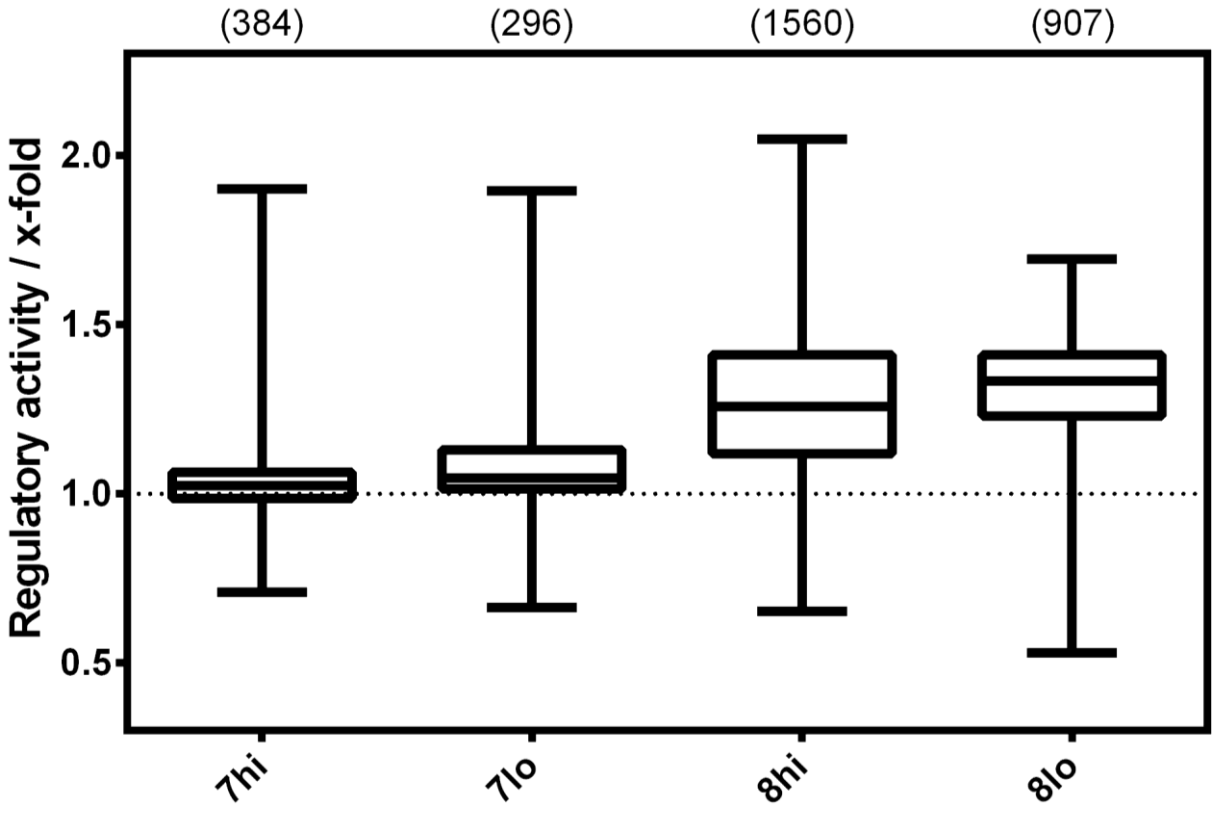

Figure 59: ***In vivo* screening of B2-1 derived pools** These boxplots show the summarized *in vivo* screening of *S. cerevisiae* cultures of the pool B2-1 derived pools 7 and 8. For each investigated clone, the regulatory activity was calculated as the ratio of GFP fluorescence with and without 100 µM azoCm (x-fold). The numbers written above the boxplot indicate the number of clones analyzed. The median of the analyzed clones from the pools was 1.02 (7hi), 1.05 (7lo), 1.26 (8hi) and 1.33 (8lo).

In vivo screening of the sorted cells from pools 7 and 8 showed no riboswitches with an improvement of the regulatory factor compared to B2-1, as shown in Figure 59. The median of pools 7high and 7low (7hi and 7lo, Figure 59) was 1.02 and 1.05. This seemed to indicate that allowing nucleotide randomization in the 5' UTR upstream of B2-1 destroyed all riboswitch function. Regarding the pools 8 high and low (8hi and 8lo, Figure 59), the *in vivo* screening results seemed to indicate that the degree of nucleotide permutation chosen was yielding functional riboswitches, but none with a higher regulatory factor than B2-1 was discovered. With medians of 1.26 and 1.33 (pools 8hi and 8lo, respectively), plenty of riboswitches with nucleotide permutations could be found. However, results from *in vivo* screening of pools 7hi and 7lo suggest that all those permutations take place in the B2-1 region of the randomized 5'UTR.

4.21 Determination of the binding constant of B2-1 aptamers using ITC

As the riboswitch B2-1 could not be improved regarding its regulatory factor using partially randomized *in vivo* screening approaches, more about the binding affinity of the RNA aptamer B2-1 should be found out. To this end, two RNA constructs were designed, based on the mfold predicted structure of B2-1 (Figure 57). The sequence of B2-1 was folded, and regions of the 5' UTR and the sequence of GFP were included, as they would be present in the mRNA transcript within yeast cells. To gather information by ITC which could reflect the behavior of the B2-1 riboswitch *in vivo*, these sequences were included. ITC construct B2-1 was a 102 nt long sequence (Figure 60, left). To see whether the 5' UTR and the GFP gene regions (marked in blue) were necessary for ligand binding, the truncated version B2-1 short was designed, consisting only of the sequence of B2-1 (marked in red, with the light motif marked in yellow), as well as 9 nt of the 5' UTR allowing the RNA to fold into the predicted stem formation shown in Figure 60 (right). B2-1 short was 59 nt long. The sequences for B2-1 and B2-1 short are shown in Table 31.

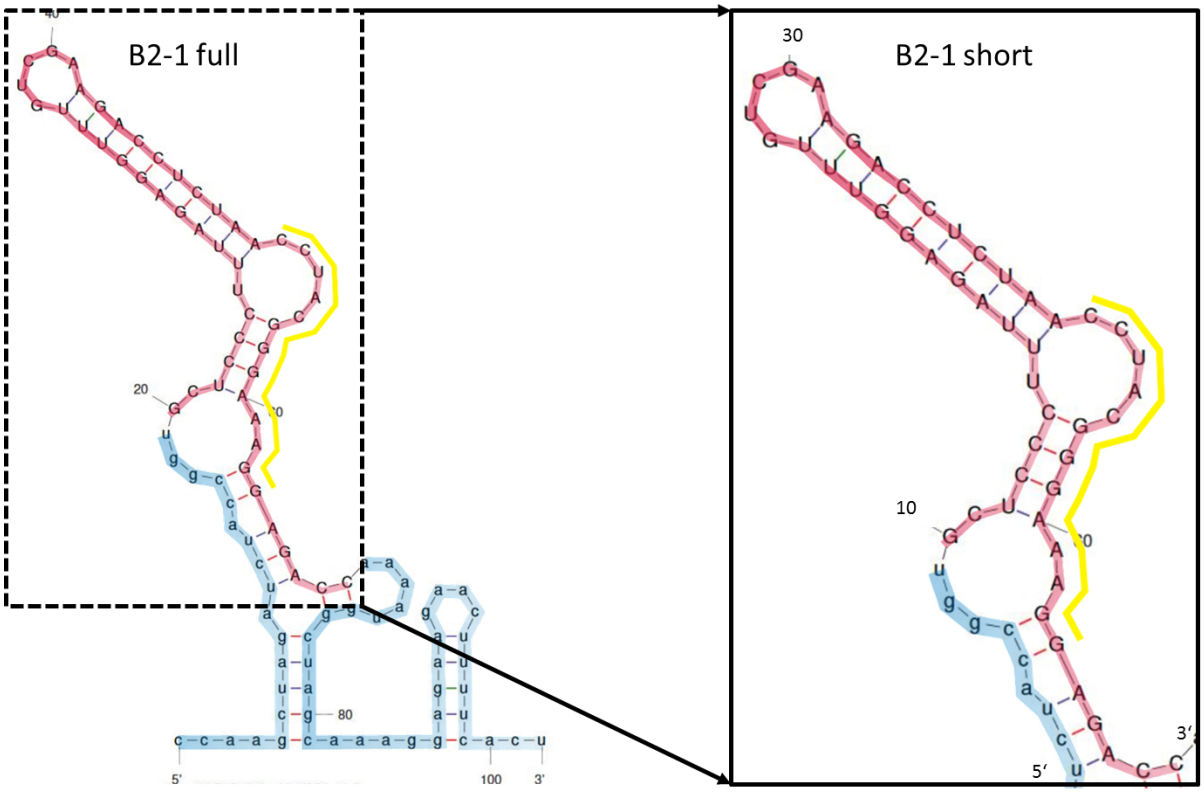

Figure 60: **Sequences and mfold predicted secondary structures of B2-1 and B2-1 short used in ITC** Shown are the mfold predicted structures of the sequences based on aptamers B2-1 which were designed for ITC. B2-1 is 102 nt, B2-1 short is 56 nt long. Marked in red is the sequence of B2-1, marked in yellow is the light motif, and marked in blue are parts of the 5‘ UTR upstream of B2-1, as well as parts of GFP gene, including Kozak sequence and ATG, downstream (3‘) of B2-1.

Table 31: **Sequences of B2-1 aptamers**

Aptamer	Length in nt	Sequence
B2-1	102	CCAAGCTAGATCTACCGGTGCTCCCTTTAGAGGTTTGTCGAAGA CCTCTAACCTACGGGAAAGGAGACCAAAATGGCTAGCAAAGGA GAAGAACTTTTCACT
B2-1 short	59	TCTACCGGTGCTCCCTTTAGAGGTTTGTCGAAGACCTCTAACCTA CGGGAAAGGAGACC

Shown are the aptamers B2-1 and short, and their respective length in nucleotides (nt), as well as their sequence. As shown in Figure 60, sequences from the 5’ and 3’ UTR of B2-1 are displayed in blue, the 50 nt core region from the doped SELEX pool (chapter 4.13, Figure 39) is shown in red, and the light motif is marked in yellow.

The shown sequences in Table 31 were generated by designing oligonucleotides compatible to each other and containing a T7 promoter (Table 6). RNA was generated by *in vitro* transcription as described in chapter 3.2.8 and purified using 8% PAA gels (3.2.11).

First, RNA B2-1full was measured according to the protocol described in chapter 3.2.13. For the measurement, the RNA aptamers were subjected to the folding program used in SELEX (3.4.3). The RNA was dissolved in 1x SELEX buffer, yeast tRNA was not added, as opposed to during SELEX. The DMSO concentrations in the RNA and ligand solution were adjusted to the same value to prevent unspecific dilution effects. B2-1 was measured with a 200 µM azoCm *trans* and azoCm *cis* solution, in the latter case the ligand was first irradiated with UV light (λ=365 nm), and the entire ITC measuring device (3.2.13) was covered with aluminum foil during the duration of the measurement. This should prevent the ligand from switching back to its *trans* state during the measurement. Results are shown in Figure 61 and Table 32. Using a two-site binding model (Figure 61), the kD for the first binding site yielded a mean kD of 23.5 ± 2.44 nM. The second binding site showed a mean kD of 3.375 ± 0.087 µM, two orders of magnitude lower binding than the first binding site. No binding to azoCm *cis* could be detected.

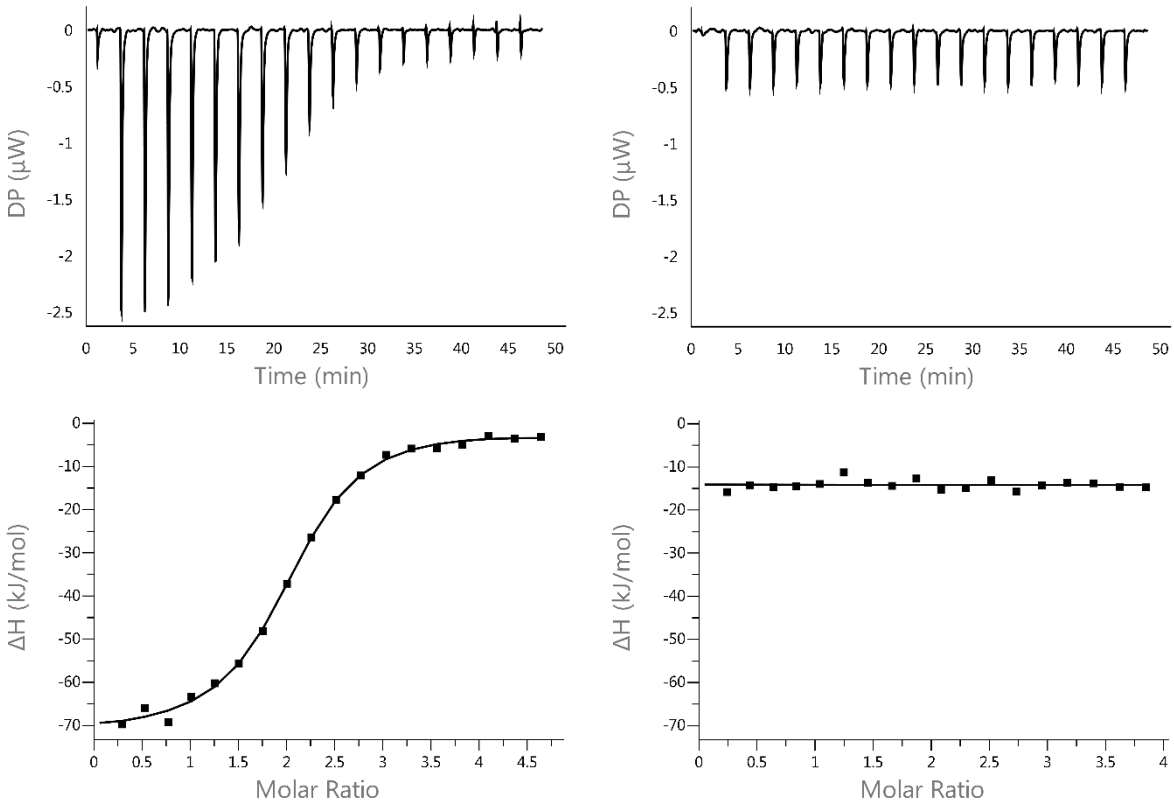

Figure 61: **Results of ITC of aptamer B2-1 with 200 µM azoCm *trans* (left) and 200 µM azoCm *cis* (right), two-site binding model**. The upper graphs show the raw data of the titration in µW. The lower graphs show the heat conversions in kJ/mol per injection obtained by integrating the peaks, plotted against the molar ratio of ligand/RNA. The solid line shows the curve adapted to the measurement points according to a two-site binding model (Table 12). Two measurements for every RNA-ligand combination were carried out. The mean kD can be found in Table 32.

B2-1 short was measured with a 100 µM azoCm *trans* and azoCm *cis* solution, the measurement of the *cis* compound was carried out under exclusion of light, again. Shown in Figure 62 are the ITC results for B2-1 short.

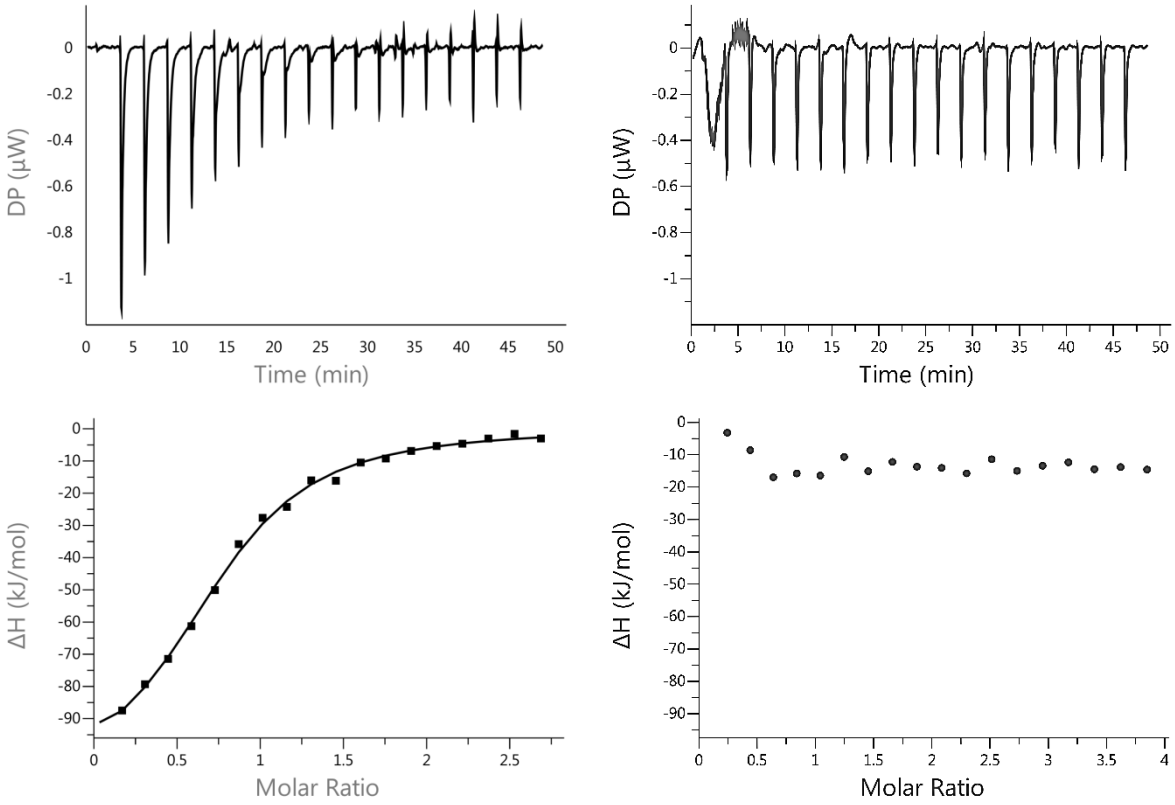

Figure 62: **Results of ITC of aptamer B2-1 short with 100 µM azoCm *trans* (left) and 200 µM azoCm *cis* (right), one-site binding model**. The upper graphs show the raw data of the titration in µW. The lower graphs show the heat conversions in kJ/mol per injection obtained by integrating the peaks and plotted against the molar ratio of ligand/RNA. The solid line shows the curve adapted to the measurement points according to a two-site binding model (Table 12). Two measurements for every RNA-ligand combination were carried out. The mean kD can be found in Table 32.

Measurements of B2-1 short with azoCm *trans* showed a value of n =0.667 ± 5.45x 10^{-2} binding sites. Fitting with a one-site binding model yielded a mean kD of 1.24 ± 222.5 µM of two measurements (Table 32). No binding to azoCm *cis* could be detected.

The summary of the mean kDs of all B2-1 derived RNA aptamer measurements are shown in Table 32.

Table 32: **Mean kD of ITC measured aptamers**.

Aptamer	Mean predicted ligand binding sites (n)	Mean kD azoCm *trans*	Mean kD azoCm *cis*
B2-1 (two-site model)	n1 = 1.8 ± $1.6x10^{-2}$ n2 = 9.46 ± 0,224	kD1: 23.5x 10^{-9} ± 2.44x 10^{-9} kD2: 3.375 x 10^{-6} ± 87.4x 10^{-9}	N/A
B2-1 short (one-site model)	n = 0.667 ± 5.45x 10^{-2}	1.24x 10^{-6} ± 222.5x 10^{-9}	N/A

Shown are the aptamers and the fitting model used to determine the mean kDs for binding azoCm *trans* and azoCm *cis*. Two measurements were carried out for each azoCm enantiomer. If no kD could be determined, N/A (not applicable) is given as a value.

The results from Table 32 make it clear, that B2-1 aptamer is able to bind azoCm in an isoform selective manner. While the *trans* isoform can be bound with a nanomolar to low micromolar dissociation constant (kD), the *cis* isoform does not show any binding affinity to B2-1, neither to its full or short version. This indicates a kD greater than 1 mM for azoCm *cis*, and therefore a discrimination between azoCm *trans* and *cis* for B2-1 of at least 5 orders of magnitude, and for B2-1 short of at least 3 orders of magnitude.

4.22 Summary of Results

In the course of this thesis, a successful SELEX against the ligand azoCm was carried out. A light SELEX protocol was developed and applied, as well. NGS analysis of the SELEX rounds yielded a 13 nt sequence motif which was enriched in the light SELEX rounds, but decreased in number in the affinity SELEX rounds. Using this light motif as a core sequence, a motif-doped SELEX was successfully performed, which showed a fast increase of RNA elution over the rounds. Using a FACS sorting based approach, aptamers from this motif-doped SELEX have been analyzed in an *in vivo* screening, which yielded a functional riboswitch called B2. Further *in vivo* screening approaches based on the sequence of riboswitch B2 could not increase its regulatory factor but lead to a more stable variant of B2 called B2-1. Riboswitch B2-1's regulatory factor could not be increased using randomized *in vivo* screening; however, a dose dependent regulation could be demonstrated. Using ITC measurements, the isoform selective binding of B2-1 could be verified and a kD in the nanomolar range could be determined.

5 Discussion

5.1 Aptamer libraries and SELEX

5.1.1 Aptamer libraries

The choice of an aptamer library lies at the beginning of every SELEX experiment. Different approaches to the choice of library exist, often depending on the application scenarios of the aptamers to be developed. Thus, pre-structured RNA libraries have been described, which convey a certain feature to the developed aptamers, e.g. inherent increased stability [112, 233]. Such a library, mixed 1:1 with an unstructured one, was formerly used in the research group to conduct a SELEX against azoCm [196]. As the results show, most aptamers from the final round of SELEX contained the pre-formed stem loop. The pre-structuring of the aptamers seemed to lead to a dominance of the enriched aptamers containing the stem-loop, potentially due to a greater inherent stability that the pre-formed stem loop conveys.

The aptamer library initially used in this work did not contain any pre-structuring elements. Aptamers resulting from the performed SELEX did not show an overbearing trend towards sequence or structural motifs, as the next generation sequencing (NGS) analysis of the SELEX demonstrated. However, round 6 and 9 of the SELEX have shown to contain dominant aptamer sequences, as 12 out of 20 tested sequences from rounds 6 and 9 were identical (aptamer "A", see chapter 4.5). As singling out individual aptamers, sequencing them and afterwards producing them *in vitro* to test individual binding properties is a time- and material consuming effort, but can provide limited information, high-throughput methods like NGS have come into the focus of aptamer researchers when studying SELEX [240]. Sequence motifs becoming enriched or losing prevalence in the pool can be tracked using NGS more easily and in a much greater sample size than using random samples. The NGS used in this work was particularly useful to compare influences of stringency enhancing methods, like introducing more wash steps, or starting a light elution protocol (see chapters 4.4, 4.9 and 4.12).

NGS analysis has shown itself to be an important tool to judge the success of a performed SELEX, because previous to the use of NGS methods, the SELEX process itself has been considered a black box [166]. As experiments using random samples from SELEX rounds in this work show (see chapters 4.5 and 4.11), selectively binding aptamers can be found using the described method. However, the tracking of the enrichment process of the light motif

through the rounds would not be possible using random samples, except for major single clone sequencing efforts for every round individually. NGS becomes a worthwhile tool here, because bias introduced by the researcher in such a hypothetical, alternative large-scale cloning and sequencing effort can be eradicated, and the information content gathered from NGS will always be higher than what can be achieved from manual single clone analysis.

A particular significant role in the selections carried out in this work seems to be played by the constant regions of the aptamer libraries. The ITC analysis of aptamer B2-1 indicate, that there is a dependence of the ligand binding on at least the 5' UTR of the aptamer, which was part of the constant regions of the doped SELEX library (see chapters 4.13, 4.21). While a majority of selected aptamers in literature bind their target independently of the constant regions [241], there are examples where the latter are part of the ligand binding regions [242-244]. In these cases, standard truncation experiments are not possible [245, 246]. While the truncated version of B2-1 (B2-1 short) shows isoform selective binding towards azoCm, the kD is two orders of magnitude lower and the amount of ligand binding sites (n) indicates that the stoichiometry towards azoCm has lessened (from n = 1.8 for B2-1 to n = 0.67 for B2-1 short). Further analysis of the aptamer B2-1 would be feasible to preclude attempts to truncate the aptamer, like structural analysis of the aptamer, or identification of the exact binding regions and stability conferring regions of the aptamer. As the binding regions might play a major role here, in future SELEX experiments it might be recommendable to choose a SELEX method that does not necessitate the inclusion of primer binding sites on the aptamer pool. Such primer-less SELEX methods exist, most of them relying on the enzymatic removal of the primer binding sites used for amplification prior to the RNA transcription step [109, 247, 248]. Application of primer-less SELEX methods could lead to shorter RNA aptamers from the beginning. This is particularly worth considering, as aptamer B2-1 was generated from a partly randomized pool containing a N50 sequences at its core, but B2-1 is 102 nt long, and its truncated version is 59 nt long, due to the constant regions of the aptamer.

5.1.2 Light-SELEX development

Some aptamers showing isoform selective binding against azoCm were generated during SELEX even without the introduction of a light SELEX method (see chapters 2.2.3, 2.2.4 and

4.5, as well as [196, 198]). To increase the dominance of the isoform selective aptamers, and to introduce a variation of a counter-SELEX step [65], a light SELEX was developed. In classical counter-SELEX, RNA is incubated with structurally similar targets in an additional SELEX step to remove those RNAs (unspecifically binding aptamers) able to bind the desired target and these decoy molecules. Light SELEX makes use of this method, by first letting the RNA bind to the real target azoCm *trans*, immobilized on the column, and then switching the conformation of azoCm to *cis*. RNAs which cannot bind to azoCm *cis* anymore are washed out of the column by the flow of buffer, making light SELEX similar to a "one-step" counter-SELEX. As counter-SELEX has been effective in yielding highly specific aptamers previously [249-251], it was thought to be a useful method, particularly when applied to the goal of generating isoform selective aptamers.

While literature shows examples of development of reversible light-selective aptamers, the protocols described stay very vague. Lee *et al*. [203], who developed a hammerhead ribozyme isoform selectively binding a dihydropyrene compound [252], described their light SELEX protocol as follows:

> …"were then irradiated with either visible (see above) or UV light (280–375 nm, from a Spectroline model EB-280C hand-held lamp, 46 W, with peak emission at 308 nm until the color of the bead-bound photo-switch either disappeared or appeared to its fullest extent."

Young & Deiters, having developed an aptamer selectively binding the closed spiropyran isoform and not the corresponding open merocyanin form of their compound [204], describe their light SELEX protocol as follows:

> "After binding had been detected, the gold slide was irradiated with UV light of 365 nm for approximately 10 min, dissociation and adsorption were monitored in real time, and the switching was repeated to demonstrate the reversibility of the aptamer binding […] using fiberoptics connected to a UV LED system (Prizmatix BLCC-02)."

While in Lee *et al*. the power and the wavelength of the UV light used are described, distance from the irradiated sample and irradiation time are not. Young & Deiters mention wavelength

of the used UV light and the producer of their light-source, but neither the distance from light-source to sample, nor the power of the light source are described [204].
According to the inverse square law, distance from a light-source affects energy uptake by the sample, as increased distance "dilutes" the amounts of photons reaching the irradiated object [253, 254]. To describe irradiation precisely, either the power of the light source and its distance from the object need to be given, or the photon density (power per surface area, typically W/m^2) needs to be determined and described. Therefore experiments cannot be reproduced accurately without this information.

The light SELEX protocol described in this work is much more detailed and can be followed easily by other researchers. The finalized light SELEX procedure will be published in Lotz *et al.* (see below) and tries to unite the maximum information possible to enable a reproduction of the experiment [198]:

> "RNA was eluted by irradiating the column with light (λ=365 nm, UVLED-365-1000-SMD, 0.15 A, 13.5 V, 16 x 1s) under exclusion of other light sources (distance from column to light source = 10 cm), while washing the column with 6 CV of 1x SELEX buffer"

Exact irradiation time, distance of the light-source to the sample and treatment of the sample during irradiation are described. The described procedure is considered complete, compared to the protocols described in literature previously, which were missing key information elements needed for reproduction of the experiments.
Further selections carried out against light-selective molecules might benefit from the here described process of protocol development. Also, it would be possible to adapt the finalized protocol to the needs of another SELEX procedure, as the materials used are low-tech and can be incorporated into existing processes quite easily.
An important pre-requisite for light-sensitive SELEX needs to be solved in every light SELEX process, however: exclusion of light of all undesired wavelengths is not a trivial matter when a researcher carries out the SELEX manually. Automated SELEX might be a solution to that, however, while several approaches have been described already, some as early as in 2005, they bring along their own limitations [255-257]. When carrying out a light-selective SELEX, all these considerations and technical necessities need to be weighed

carefully. Therefore, the detailed development of the light SELEX protocol described in this work was considered relevant to the SELEX community in general, and was included in the submitted publication Lotz *et al*. [198].

5.1.2.1 SELEX and NGS

NGS of SELEX has been first described in literature in 2011 [258]. While other nucleic acid libraries or genomes have been analyzed using this technique before [259-261], the first implications regarding the SELEX process itself have been described by the Glökler group [258]. Since then, with NGS methods becoming commercially available and easier to afford, various NGS based SELEX analysis have been published [133, 260, 262].

NGS has been used in this work, to compare light SELEX and affinity rounds, and to discover whether a motif is enriched using one method and not the other. It could be shown, that the discovered 13 nt sequence motif behaved differently in R7 to R9 as opposed to LS-7 to LS-9 (see chapter 4.12, Figure 37). Introduction of increased stringency steps in the affinity SELEX (chapter 4.4) did lead to a drastic decrease of the prevalence of the light-selective motif, while it was further enriched in the light SELEX rounds.

Using NGS to study the effect of stringency compared to the application of a light SELEX protocol on the SELEX was relevant in the course of this thesis to discover the light motif and track its enrichment. In future SELEX experiments time and resources could be saved by applying NGS early in the SELEX and planning the SELEX progress or the downstream experiments after SELEX according to the results from NGS. This would generate a better understanding of the SELEX progression, and could help identify factors that impact selection [263]. Also, being able to stop the SELEX early, due to earlier possible identification of enriched aptamer or motif families, could help avoid bias in the later SELEX rounds introduced e.g. during the PCR amplification steps between selection rounds [264].

More detailed analysis of the NGS data generated from this SELEX was published in Blank *et al*. [96]. They developed a secondary structure prediction algorithm based on the NGS data of the SELEX performed, allowing the discovery of secondary structure motifs by comparing aptamer sequences to each other.

5.2 Light-selective aptamers

5.2.1 Aptamer B2-1 and the light motif

The aptamer developed in this work, B2-1, shows a kD of 23 nM, and no binding to the *cis* isoform of its target molecule (determined using ITC, see Table 32).

ITC measurements could not detect any binding to the *cis* ligand, up to a final ligand concentration of 37.7 µM after titration of the ligand to the RNA. Hence, a kD of at least 1 mM is assumed.

Aptamer B2-1 contained a 13 nt sequence motif ("light motif", Figure 36), which was discovered by comparing aptamer sequences from different SELEX approaches (affinity SELEX Rudolph and light SELEX) to each other which showed the best discriminatory abilities between the *trans* and *cis* conformation of azoCm (Table 24). That this common motif was found in two different SELEX experiments using two different RNA pools strongly indicated that the light motif might be the optimal sequence for binding to azoCm. The analysis of the development of the partly randomized light motif during the doped SELEX (chapter 4.14) showed a strong re-orientation of several nucleotide positions, with seven positions of the light motif reaching a 100% nucleotide retention in all sequences in the last doped SELEX round.

As aptamer 42 contained the light motif as well, the structural analysis by in-line probing not only allowed improved secondary structure prediction for aptamer 42 by mfold, but also delivered indications towards the nucleotides involved in binding azoCm (see chapter 4.1) within the light motif. In-line probing results showed stabilization of two or three adenosine nucleotides at aptamer positions A33 to A35 (Figure 14), corresponding to positions 9 to 11 of the light motif (Figure 36). As these adenosines were part of the strongly retained nucleotides during the doped SELEX as well, the conclusion was drawn that these two to three nucleotides were mainly involved in azoCm binding in all aptamers containing the light motif. A comprehensive 3D structure of the aptamer B2-1 could be generated using NMR, or kinetic analysis of the aptamer could be carried out using smFRET (see chapter 2.1.14) to give more detailed information regarding the binding pocket of aptamer B2-1 and the role of the light motif in azoCm binding.

5.2.2 Light-switchable molecules and their potential applications

Next to aptamer B2-1developed in this work, another characteristic of the developed aptamer system needs to be discussed, namely the target molecule of the aptamer itself. Three published aptamers against light-switchable molecules have been published to date to the knowledge of the author. Lee *et al*. generated an aptamer binding to a dihydropyrene compound, called BDHP [203]. Young & Deiters carried out a SELEX against a spiropyran derivative (Spiropyran 1) [204], while Hayashi *et al*. carried out a SELEX against a small peptide containing an azobenzene group (KRAzR) [205, 206].

Table 33: **Listing of light-switchable molecules against which aptamers have been developed**

Ligand	Light-switchable ligand class	Specifications	Reference
BDHP-COOH	Dihydropyrene	Water soluble	Lee *et al*. [203]
Spiropyran 1	Spiropyran	Low water solubility, racemate	Young & Deiters [204]
KRAzR	Azobenzene	Water soluble	Hayashi *et al*. [205, 206]
azoCm	Azobenzene	Water soluble	Lotz *et al*. [198]

Apart from the spiropyran compound developed by Young & Deiters, all light-switchable compounds show good water solubility, a necessity when a biological application is considered. azoCm displays outstanding photochemical and biological stability even when tested in HeLa cell extract, as shown in Lotz *et al*. [198]. While all publications of aptamers binding to light-switchable molecules discuss potential applications in a biological setting, no data regarding toxicity of their compound *in vivo* have been published to the knowledge of the author.

Accordingly, for azoCm toxicity tests for bacteria (*E. coli, Bacillus subtilis*), yeast (*S. cerevisiae*) and human cell lines (HeLa) were performed. They showed that azoCm had no significant influence on cell growth [198]. Therefore, the aptamer-ligand-set B2-1 and azoCm would be well suited for biological applications.

Notably, the ligand concentrations used in the binding studies as well as the ITC experiments were in a range that would be applied in biological applications of the aptamer. These binding studies combined with the gathered toxicity data would allow a future application of the

developed aptamers and their switching system in genetic regulation systems like engineered riboswitches or biosensors.

5.2.3 Comparison of aptamer B2-1 to light-selective aptamers in literature

As previously described (see chapters 2.2.3 and 2.2.4), aptamers binding to one of two isoforms of a light-switchable molecule have been selected before [196, 203-206]. Lee *et al*. generated an aptamer with a 2 µM binding constant to its target (12 µM for the hammerhead ribozyme construct), while discriminating 35-fold against the undesired target isoform [203]. The most affine aptamer from Young & Deiters displayed a 14-fold discrimination between the two isoforms of their target molecule, with an approximate kD of 10 µM [204]. The aptamers developed by Hayashi *et al*. against an azobenzene peptide compound showed kDs in the range of 0.8 to 1.8 µM, with a 10-fold discrimination between the two isoforms [205, 206].

Table 34: **Listing of aptamers developed against light-switchable molecules**

Aptamer name	Ligand	Binding affinity of aptamer (kD)	Discrimination between isoforms	Reference
C8	BDHP-COOH	2 µM	35-fold	Lee *et al*. [203]
SP3	Spiropyran 1	10 µM	14-fold	Young & Deiters [204]
Aptamer 66	KRAzR	0.8 µM	10-fold	Hayashi *et al*. [205, 206]
42	azoCm	3.6 µM	$>10^3$-fold	Lotz *et al*. [198]
B2-1	azoCm	24 nM	$>10^5$-fold	Lotz *et al*. [198]
B2-1 short	azoCm	1.24 µM	$>10^3$-fold	see chapter 4.21

Lee *et al*. impressively demonstrated the coupling of their developed aptamer C8 to a communication module and successfully generated an *in vitro* functional ribozyme with a 900-fold regulation factor [203]. Such a system could well be an alternative strategy for the development of an *in vivo* functional RNA regulatory device instead of a riboswitch. However, no *in vivo* functional application by Lee *et al*. has been published to date.

The aptamer developed by Young & Deiters showed the weakest kD value of app. 10 µM when comparing all aptamers binding light-switchable molecules [204]. Because of the low solubility of the spiropyran in aqueous solutions, the comparatively weak affinity of its

aptamer, and its presence as a racemic mixture, a biological application of this system is not feasible.

The aptamer generated by Hayashi *et al*. is the most comparable to the aptamers described in this work, as the ligand was also an azobenzene compound [205, 206]. Selection was carried out in a similar manner, too, by immobilizing the peptide azobenzene on Affi-gel (Table 1) and generating ligand-derived columns. The most affine aptamer in the study of Hayashi *et al*. showed a 10-fold discrimination between the *trans* and *cis* compound with a kD of 0.8 µM. Hayashi *et al*. developed this aptamer without the application of a light SELEX protocol. Comparing the aptamer generated by Hayashi *et al*. to aptamer 42 which selectively binds azoCm, shows a comparable range of binding affinity. The kD of aptamer 42 against azoCm lay at 3.6 µM. The advantage of aptamer 42 over the aptamers developed by Hayashi *et al*. was its discrimination against azoCm *cis*. Comparing aptamer B2-1 to the light-selective aptamers described in literature shows B2-1 aptamer as the most affine aptamer to its intended target isoform to date, as its binds only to the *trans* isoform of its target molecule with a kD of 23 nM. Even the truncated version of B2-1, B2-1 short, displays a kD of 1.24 µM, which can compete with most described light-selective aptamers (see Table 34). Like aptamer 42, no binding to azoCm *cis* could be determined in the course of this work, leading to an assumed discrimination ability of B2-1 between azoCm *trans* and *cis* of more than 100000-fold.

As KRAzR, the molecule Hayashi *et al*. selected against, is also an azobenzene compound, it was considered whether the aptamers developed against azoCm (B2-1, Table 31 and 42, Table 24) showed any sequence homology to aptamer 66 (Table 34). A motif search using the software MEME was carried out (Table 12). A sequence homology region between the aptamers could be discovered, as shown in Table 35 (yellow marked nucleotides). Six conserved nucleotides could be found in an eight nt stretch which were identical in all three compared aptamers. As these nucleotides were located within the light motif (included in Table 35 for comparison), it was concluded that azobenzene-specific binding was taking place in this region, particularly because the three aptamers compared originate from three different SELEX experiments.

Table 35: **Sequence comparison of aptamers binding to azobenzene derivatives (including the light motif)**

Aptamer	Sequence
Light motif azoCm	5’ **CCUACGGGAAAGG** 3’
Aptamer B2-1	5’ CCAAGCUAGAUCUACCGGUGCUCCCUUUAGAGGUUUGUCGAA GACCUCUAA**CCUACGGGAAAGG**AGACCAAAAUGGCUAGCAAAG GAGAAGAACUUUUCACU 3’
Aptamer 42	5’ GGUUGACCCUACUGCUUCGGCAGG**CCUACGGGAAAGG**UAA CA 3’
Aptamer 66	5’ GGGAAUUCCGCGUGUGCACACCUCAACAACAAAAGGAUAAG**C UA**G**G**C**GA**GCCUUACCGAACGCGUCCGUUCGGAUCCUCAUGG 3’

Aptamers are shown in 5’ to 3’ orientation, sequence homologies between aptamers B2-1, 42 and 66 discovered by MEME (Table 12) are marked in yellow.

A notable characteristic for aptamers B2-1 and 42 is, that there are A and G rich sequences stretched in and after the light motif, which are largely missing in aptamer 66. As chloramphenicol (Cm) was used as a substituent for one side of the azoCm molecule, it was expected to find aptamers binding to azoCm readily. Cm has been shown to bind to a variety of aptamers, both RNA and DNA, without a defined sequence or structure motive contained in all of the examined sequences [265, 266]. While A-rich sequences in RNA and G-rich sequences in DNA have been reported as common in the analyzed aptamers, no fixed motif for the binding of Cm was described to date. As in nature, Cm work as an antibiotic in prokaryotes by binding to a rRNA segment in the large ribosomal unit of (50S), it has been inferred that Cm might show a tendency to bind to a variety of RNA sequences, and therefore can often interact unspecifically with RNA [265]. Therefore, aptamer 42 and B2-1 fit to the hypothesis, that chloramphenicol binds preferentially to purine-bases in RNA and DNA.

5.2.4 Comparison of light-selective aptamers recognizing azoCm

One aptamer developed in this thesis, B2-1, was analyzed regarding its binding affinity (kD) towards azoCm. Similar to aptamer 42, no binding to azoCm *cis* could be detected. Using a two-site binding model, a binding affinity of 23 nM on one binding site and 3.38 µM on the

second site was determined (Table 32). Therefore the full-length aptamer B2-1 is two orders of magnitude more affine to azoCm *trans* than aptamer 42 (kD = 3.6 µM). These results could be due to the application of a light SELEX step, as well as carrying out a motif doped SELEX afterwards. For aptamer 42, no light SELEX protocol was performed, similar to Hayashi *et al.* [206]. The double approach to first identify a light-selective motif, and then continuing with a motif doped SELEX, as carried out in this work, seems to have led to highly specific aptamers for the *trans* isoform of azoCm. As the binding to the target itself does not define the specificity in this work, but more importantly the discrimination of the aptamer between the *trans* and *cis* isoforms of azoCm, the aptamer B2-1 described here is the most specific aptamers for a light-switchable molecule to date to the knowledge of the author. A kD of 23 nM for the *trans* isoform, and no detectable binding to the *cis* isoform of azoCm indicate a kD of B2-1 to azoCm *cis* of at least 1 mM. The discrimination between the two isoforms would therefore be 10^5-fold.

Further evidence, that the aptamer B2-1 not only binds to *trans* azoCm specifically but also releases the ligand upon irradiation to its *cis* form, was generated by circular dichroism (CD) experiments carried out by Christoph Kaiser of the Wachtveitl group of the Goethe-University, Frankfurt [198, 267, 268]. He could show that no different behavior of aptamer 42 was observable, when azoCm was switched from its *trans* to its *cis* conformation in its presence. This indicated that, once bound by aptamer 42, azoCm was not released by the aptamer, whichever conformation the ligand presented. Aptamer B2-1, however, showed a reproducible difference in the CD measurement, depending on the conformation of the ligand. Reversible switching of the ligand from *cis* to *trans* and back led to correspondingly changing CD signals, indicating a change in aptamer structure as a response to the changed ligand conformation. These results, published in Lotz *et al*., strongly indicate a release of azoCm from the aptamer, once it switches to its *cis* form, as well as a new binding once it is present in its *trans* form again [198].

With a kD of 23 nM, aptamer B2-1 would be more affine to its ligand than most *in vitro* selected aptamers described in literature to date, including the flavin mononucleotide aptamer (kD = 500 nM [269]), the malachite green aptamer (kD = 117 nM [151]), and the extremely well studied theophylline aptamer (320 nM [65, 270]). The comparison to the theophylline aptamer is particularly interesting, because a synthetic riboswitch working *in vivo* in *B. subtilis* was developed from it [271]. While the kD of natural aptamers (stemming from natural riboswitches) is typically much lower (e.g. TPP riboswitch thiM: kD = 0.21 nM [272];

c-di-GMP class II: kD = 0.2 nM [273]), the construction of a synthetic riboswitch from an aptamer with a similar kD makes the successful construction of a riboswitch out of B2-1 feasible.

Summarily, the aptamers developed in the course of this work represent a novel set of an aptamer with its corresponding light-selective molecule. Advantages of the aptamer developed are its high binding affinity to its *trans* target molecule and no binding at all to the respective *cis* isoform. The target molecule azoCm itself has the advantages to show good switching capabilities and high water solubility, while showing no influence on cell growth.

The characteristics of the aptamer-ligand-set developed in this work make it a basis for further research in this field and classify it as a potential tool in future biological applications.

5.3 Light-selective riboswitches

5.3.1 *In vivo* screening methods and potential optimizations

As already emphasized in literature [129, 152, 229], *in vivo* screening methods of aptamers derived from SELEX should be employed if the aptamers are to be used as riboswitches in cells. An example for this is the neomycin riboswitch. Derived from a SELEX, none of the abundant riboswitches in the final SELEX rounds could show regulation of gene expression *in vivo*, even though highly affine aptamers for neomycin could be found [132]. Only the application of an *in vivo* screening step could yield functional riboswitches. Detailed NMR studies of the neomycin riboswitch made it clear, that the defining difference between neomycin binding aptamers and neomycin dependent riboswitches lay in the structural dynamics rather than an affine binding of an *in vitro* selected aptamer [274, 275].

As *in vivo* screening by hand is an extremely laborious and time-consuming endeavor, high-throughput methods are desirable [129, 152]. The primary method used for *in vivo* screening in this work was a manual one. Therefore, a limited number of clones can be screened per day, which could be significantly increased, if robotics platforms could be included in the methodology. Using a robotics platform e.g. to split cell cultures could also reduce experimental bias introduced by the researcher [276].

It should be mentioned however, that functional riboswitches have been discovered using manual *in vivo* screening with less clones screened than done in this thesis. An example for this is the ciprofloxacin riboswitch recently developed in our laboratory. Screening of the aptamers from two different SELEX rounds yielded two riboswitch candidates with 1.5- and 1.7-fold regulation factors in only app. 1100 tested *S. cerevisiae* colonies [133]. During this work, about 4300 *S. cerevisiae* colonies were tested from azoCm SELEX rounds (see chapters 4.2, 4.7, 4.10) without finding one aptamer showing regulatory function. Only the implementation of the FACS based screening allowed the discovery of aptamers with low regulatory function (1.25- to 1.35-fold) from 375 tested *S. cerevisiae* colonies (see chapter 4.16). While for the ciprofloxacin riboswitch, motif doped screening of app. 2400 *S. cerevisiae* colonies was sufficient for the generation of a riboswitch with 7.5-fold regulation factor, app. 5900 screened colonies in this work were not able to increase the regulation factor of B2-1 beyond 1.45-fold.

While some potentially functional riboswitches could be lost during a FACS sorting based *in vivo* screening, these pre-sorts could drastically improve the chances to find functional

riboswitches from SELEX. Further optimizations of the method could be carried out in the future, e.g. using a FACS sorter able to sort individual cells into medium well plates directly, without the need to plate and grow and inoculate cells manually [277-279]. Coupled to a robotics platform, this method could drastically improve the yield of synthetic riboswitches generated from aptamers, as the work of the researcher could be reduced to the scientifically relevant parts, like designing the pool used for SELEX, or designing the synthetic riboswitch platform by choosing strategies on where to insert the aptamer into the genomic context. While the machinery necessary for such an almost fully automated *in vivo* screening (potentially even coupled with automated SELEX) is to date still expensive and not easily integrated with each other, advances in these fields could provide a giant leap forwards in the field of synthetic riboswitch design as well.

Until robotics based screening methods are widely available, the two-pronged *in vivo* screening approach presented in this work, which combines FACS screening with classical *in vivo* screening, therefore seemed to yield results faster and in a more reliable manner than purely manual *in vivo* screening (see chapters 4.15 and 4.16) and could be applied in other riboswitch developments as well.

5.3.2 Riboswitch B2-1

The riboswitch B2-1 developed in this thesis is the first riboswitch known to date to bind a light-switchable target molecule to the knowledge of the author. Nevertheless, its regulatory factor was considered too low for testing a light-induced difference in gene expression (see chapter 4.19, Figure 55, Figure 56). As azobenzenes typically only show a 70-90% isomerization towards their *cis* isoform [280], testing the regulation of gene expression was considered too early in the development of the riboswitch itself during this thesis. Any effects measured could easily be considered “background noise”, therefore an increase of the initial regulation factor of the riboswitch was considered necessary. *In vitro* analysis of the aptamer derived from the riboswitch B2-1 did show affine binding to azoCm in the low nanomolar range and a high discrimination between azoCm *trans* and *cis*. However, the low regulation factor of riboswitch B2-1 was determined using the standard ligand concentration for *in vivo* screening in this work (100 µM). Dose dependency experiments have shown, that riboswitch B2-1 responds to azoCm in a dose dependent manner, confirming its functionality in

dependence of azoCm concentration (chapter 4.19, Figure 56). This indicated the possibility to improve this riboswitch to a switching factor allowing further experiments, particularly regarding the light-induced activation of gene expression.

Truncation experiments leading to B2-1 short showed a heavy reliance of the aptamers on their genetic context. Structural analysis of the aptamers could help to provide better knowledge regarding the binding of azoCm by B2-1, as well as regarding the design of a better regulating riboswitch B2-1. Several *in silico* design approaches for the development of riboswitches are described, which could be employed alternatively or additionally to any structural analysis gathered for B2-1 [140, 141, 281, 282]. For example, Wachsmuth *et al*. have used an *in silico* approach combined with additional optimization steps, to develop synthetic riboswitches that control transcription termination using the theophylline and tetracycline aptamers [142]. Borujeni *et al*. have developed a statistical thermodynamic model predicting the sequence-structure-function relationship for translation-regulating riboswitches that activate gene expression [281]. The secondary structure prediction software SICOR developed using the NGS data derived from the selections performed in this work could be another tool in the future development of synthetic riboswitches [96].

Summarily, riboswitch B2-1 can be viewed as fulfilling the first of two steps in constructing a light-responsive riboswitch: Ligand binding and the subsequent structural change of the riboswitch inhibiting gene expression has been proven for the *trans* form of azoCm (compare to chapter 2.1.11) using CD spectroscopy (see chapter 5.2.4) [198]. The reversibility of this binding has been verified *in vitro*, but still needs to be verified *in vivo*, once an optimized variant of B2-1 riboswitch exists. Then, the re-activation of gene expression upon irradiation of azoCm treated *S. cerevisiae* cells could be tested. A functional light-dependent riboswitch based on riboswitch B2-1 would be the first light-dependent riboswitch described in literature to date.

6 Outlook

In the course of this work, a new method for the selection of light-switchable aptamers has been developed. While several SELEX experiments were carried out, future variations of this SELEX method using automated techniques could improve results. Particularly the development of an experimental environment without light "noise" (light of other wavelengths) would make advanced methods possible, e.g. the selection of aptamers against the *cis* isoform of azobenzene ligands. For this, the entire SELEX would need to be carried out in an environment with only UV light present, which was technically impossible in the course of this thesis. The developed light SELEX protocol, however, is easily adaptable to other experimental set-ups and could benefit the scientific community in future experiments.

Aptamer B2-1 developed in this thesis shows light-selective binding to the *trans* isoform of azoCm, while selectively discriminating against its *cis* isoform, which has been shown in several individual experiments. Present knowledge shows, that B2-1 is more affine to its ligand as all published aptamers against light-switchable compounds to date, including aptamer 42 from a previous SELEX against azoCm. Experiments showed a dependence of the aptamer on its 5' and 3' UTR regions. While this has been reported for aptamers in literature previously, it makes application scenarios *in vivo* more difficult, as the aptamer could not be used as an exchangeable regulation element relying only on its core aptamer sequence. Optimization of the aptamer would need to begin with structural analysis, from which variants with changed or shortened sequence regions could be developed. These analysis results and engineering approaches could also translate to the *in vivo* functionality of the riboswitch B2-1 developed in this work. While regulation of gene expression in dependence of azoCm concentration in yeast medium has been demonstrated in this work, the regulation factor remained low. Further knowledge about the *in vitro* structure of B2-1 could improve its functionality *in vivo*, as rational design methods could be applied to improve the riboswitch. Useful for this would also be novel *in silico* design approaches for riboswitches, which are currently being developed in the Suess group [283].

A new SELEX strategy against azoCm could be considered as well, using a SELEX method under development in the Suess group at the moment (manuscript in preparation). This so-called "capture SELEX" includes a structural switching step in its selection process, which could be beneficial if aptamers with structural switching properties for the development of synthetic riboswitches are desired [284]. It would be possible, for example, to include the

light motif discovered in this work in the SELEX library, so SELEX with a motif doped pool could be carried out.

In summary, the first steps towards a light-regulated riboswitch have been successfully carried out in the course of this work. An aptamer-ligand set could be developed, which shows excellent properties for future applications, like high affinity between aptamer and ligand, as well as reversible ligand binding upon irradiation. The chosen ligand also shows low toxicity in several tested organisms and good switching properties in aqueous solution. The developed riboswitch is the first described riboswitch against a light-switchable compound to the knowledge of the author, even if its regulatory factor might be improved by further studies. In the course of this work, several methods to improve the *in vitro* and *in vivo* characteristics of the aptamer and the riboswitch B2-1 have been discussed, and strategies for future experiments have been developed.

The results generated from this work are expected to support the generation of a broad range of light-selective aptamers in the future. A basis for the development of a light-selective riboswitch has been established, and future experiments and strategies to achieve this goal have been laid out.

7 Appendix

7.1 Ehrenwörtliche Erklärung

Ehrenwörtliche Erklärung:

Ich erkläre hiermit ehrenwörtlich, dass ich die vorliegende Arbeit entsprechend den Regeln guter wissenschaftlicher Praxis selbstständig und ohne unzulässige Hilfe Dritter angefertigt habe.

Sämtliche aus fremden Quellen direkt oder indirekt übernommenen Gedanken sowie sämtliche von Anderen direkt oder indirekt übernommenen Daten, Techniken und Materialien sind als solche kenntlich gemacht. Die Arbeit wurde bisher bei keiner anderen Hochschule zu Prüfungszwecken eingereicht.

Darmstadt, den …26.09.2018

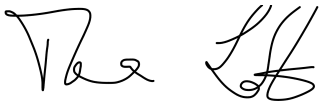

.....

7.2 Abbreviations and units

Table 36: **Abbreviations and units**

Abbreviation or unit	Meaning
%	percent
°C	degree Celsius
ΔATG-gfp	no start codon (ATG) in front of *gfp* gene
(e)GFP	(enhanced) green flurorescent protein
[α-^{32}P] UTP	Uridine triphosphate, labeled on the alpha phosphate group with [^{32}P]
[γ-^{32}P] ATP	Adenosine triphosphate, labeled on the gamma phosphate group with [^{32}P]
λ	wavelenght
µc s^{-1}	units of power used in ITC
µg	microgram
µL	microliter
µM	micromolar
µW	micro-watt
µΩ	micro-ohm
3’ UTR	three-prime untranslated region
^{32}P	Phosphorus-32, radioactive isotope of phosphorus
5’ UTR	five-prime untranslated region
A, C, G, U, T	Nukleotides in DNA and RNA sequences
A	Ampère
adh1 promoter	alcohol dehydrogenase 1 promoter
AP	Antarctic phosphatase
app.	approximately
asRNA	antisense RNA
ATG	start codon
ATP, CTP, GTP, UTP (NTPs)	Adenosine (-cytosin, guanin- thymidin) triphosphate (nucleoside triphosphates)
bp	base-pairs
B. subtilis	Bacillus subtilis
cDNA	complementary DNA
CE	capillary electrophoresis
cfu	Colony forming units
cm	centimeter
Cm	chloramphenicol
cpm	counts per minute
CRISPR/ Cas9	Clustered Regularly Interspaced Short Palindromic Repeats, CRISPR-associated

CV	Column volume(s)
d	day(s)
dATP, dCTP, dGTP, dTTP (summarized as dNTP)	desoxy-adenosin(-cytosin, guanin- thymidin) monophosphate
de novo	For the first time, from the beginning (latin: “of new”)
DMSO	Dimethyl sulfoxide
DNA	deoxyribonucleic acid
DS	Doped SELEX
DTT	Dithiothreitol
E. coli	Escherichia coli
e.g.	for example (latin: exempli gratia)
EDTA	Ethylenediaminetetraacetic acid
etc.	
F	Forward primer (oligo-nucleotide)
FACS	fluorescence activated cell sensing/sorting
g	gram
G	Guanidine nucleotide
gDNA	genomic DNA
g-force?	zuviele Gs
GFP	green fluorescent protein
gfp	green fluorescent protein gene
GOI	Gene of interest
h	hours
HR	homologous recombination
i.e.	for example (latin: in exemplia)
IgG	IgG Antibody
IR	Infrared
ITC	Isothermal titration calorimetry
k	kilo
kb	kilobasepairs
kCPM	kilo counts per minute (radioactivity)
kD	dissociation constant
kDa	kilodalton
kJ	kilojoule
kV	kilovolt
L	liter
LED	light-emitting diode
LiOAc	Lithiumacetat
lnc RNA	long non-coding RNA
LS	Light SELEX
m^2	square meter
mCherry	mCherry fluorescene protein

mCherry	mCherry fluorescene protein gene
MCS	multiple cloning site
min	minutes
miRNA	micro RNA
mL	milliliter
mM	millimolar
MQ	MilliQ (purified water)
mRNA	messenger RNA
ncRNA	Non-coding RNA
N/A	not applicable
N	Number of randomized nucleotides
N_{mean}	Arithmetic mean number of randomized nucleotides
N=N	Nitrogen double bond
n	number
NEB	New England Biolabs
Neo	Neomycin riboswitch gene
Neo	neomycin
ng	nanogram
NHS	N-Hydroxysuccinimid
nm	nanometer
nM	nanomolar
NMR	nuclear mangnetic resonance
nt	nucleotide(s)
mg	milligram
mL	milliliter
mM	millimolar
OD_{600}	Optical density at 600 nm
oligo	oligonucleotide
ORI	Origin of replication
P	Primer binding site
PAA	polyacrylamide
PCR	polymerase chain reaction
pers. comm.	personal communication
pH	acidity or basicity of an aqueous solution
pmol	picomole
PNK	polynucleotide kinase
pre-mRNA	primary transcript of RNA (unprocessed)
resp.	respective
R	Reverse primer (oligo-nucleotide)
R^2 (R square)	coefficient of determination
RNA	ribonucleic acid
RNAi	RNA interference
Rnase	Ribonuclease

rpm	rounds per minute (incubation or plate shakers)
rRNA	ribosomal RNA
RT	Room temperature, 25 °C
RT-PCR	Reverse transcription polymerase chain reaction
s	Second(s)
S. cerevisiae	Saccharomyces cerevisiae
SAM	*S*-Adenosyl methionine
SAXS	Small-angle X-ray scattering
SELEX	Systematic evolution of ligands by exponential enrichment
sRNA	small RNA
siRNA	small interfering RNA
smFRET	Single molecule fluorescence resonance energy transfer
SPR	surface plasmon resonance
SSC	saline-sodium citrate
ssDNA	single-stranded DNA
T	temperature
t	time
TAE	Tris base, acetic acid and EDTA buffer solution
TE	Transformation efficieny
TK	Transcription
TPP	thiamine pyrophosphate
tRNA	transfer RNA
TSS	transcription start site
UTP	Uridine-5'-triphosphate
UTR	untranslated region
UV	Ultra violet
V	Volt
v/v	Volume per volume
VIS	Visible light
W	Watt
w/v	weight per volume
x	x-fold
x G	times g-force (e.g. 17000 x G)

7.3 Curriculum vitae

Name	**Thea Sabrina Lotz**
Born	13.08.1989, Mainz, Germany
Nationality	German

03.2015 – present	**Doctoral candidate in the department of biology** Technische Universität Darmstadt **Thesis Title:** „Development of photo-responsive synthetic RNA devices”
01.2015 – present	**Supervision of the iGEM Team Technische Universität Darmstadt** Consulting, teaching and management of the team
10.2012 – 10.2014	**Master of Science - Biomolecular Engineering** Technische Universität Darmstadt **Thesis Title:** “Function and Regulation of ultralong 3’UTRs in the nervous system of *Drosophila melanogaster*“ **Grade:** 1,1 (with honours) | GPA 4,0 **Elective courses in:** Medicinal chemistry, Cell biology, Biochemistry
02.2012 – 10.2013	**Student member of the iGEM Team Technische Universität Darmstadt** Research and project work
10.2009 – 09.2012	**Bachelor of Science - Biomolecular Engineering** Technische Universität Darmstadt **Thesis Title:** “Über die Präsentation von Enzymen mit Relevanz in der weißen Biotechnologie auf der Oberfläche der Hefe *Saccharomyces cerevisiae*“ („Presentation of biotechnically relevant enzymes on the surface of the yeast *Saccharomyces cerevisiae*) **Grade**: 1,87 | GPA 3,0 **Elective courses in:** Radiation biology, biochemistry, development and stability of organisms
08.2001 – 06.2009	**German Abitur** Carl-Schurz-Gymnasium, Frankfurt/Main **Grade:** 1,0 | GPA 4,0 **Elective courses in:** Chemistry, Biology
08.1996 – 06.2001	**Elementary school** Wilhelm-Arnoul-Schule, Mörfelden-Walldorf

7.4 Acknowledgments

Ich möchte mich zum Abschluss dieser Arbeit bei all jenen bedanken, die mir – in welcher Form auch immer – zur Seite gestanden haben.
Meiner Prüferin und Chefin Beatrix Süß danke ich für die Chance, meine Doktorarbeit unter ihrer Anleitung durchführen zu dürfen – ich habe wirklich viel lernen können, und bei Weitem nicht nur Wissenschaftliches.
Meiner Zweitprüferin Felicitas Pfeifer möchte ich mich danken, dass sie sich die Zeit genommen hat, sich mit meinem Forschungsthema zu beschäftigen und mich freundlich zu unterstützen.
Meinem externen Prüfer Alexander Heckel gilt besonderer Dank für den energetischen, intensiven Austausch, und die vielen Denkanstöße die oft zu unserem Projekt beigetragen haben.
Meinem vierten Prüfer, Gerhard Thiel, danke ich für schnelle, unkomplizierte Kommunikation und die Bereitschaft sich mit meiner Arbeit auseinander zu setzen.

Aus der Arbeitsgruppe Süß gibt es viele denen besonderer Dank gebührt:
Zuallerst Dunja – ohne dich ist alles blöd! Ich würde dich sofort klonen, jeder sollte eine Dunja haben! Euch restlichen Pappenheimern bringe ich jederzeit wieder Tonnen an Eis mit oder backe euch Kuchen, es war sehr lustig mit euch zu arbeiten und zu leiden. Besonders möchte ich noch einmal das fabelhafte „kleine Labor“ herausheben, Adrien, Martin, Flo, Jeannine, Franzi, Cristina, Britta (die kleine), Adam, Michi, wir waren einfach immer die coolsten. Die ärmsten waren unbestreitbar die „Isolappen“, daher eine mitleidige Umarmung an Anetti und Stella, ihr werdet irgendwann dort fertig, oder wenigstens wird vielleicht die Klimaanlage repariert.

Die besten Mitarbeiten waren logischerweise meine Studenten. Georg, (ist gut diese), Max (Lachs) Zander, Thomas Dohmen (Team iGEM) und dem fleißigen, hilfsbereiten, fantastischen Leon Kraus. Es war mir immer eine Freude, Jungs!

Außerhalb der Arbeitsgruppe möchte ich speziell Sven (awesome cooperations), Schirin (Seelenklempnerei) und Doreen (Kaffee-Flucht an die Lichtwiese) danken.

Dr. Andreas Christmann sowie Doreen (Dr. Könning) halfen mir bei meinen FACS Experimenten, vielen vielen Dank für Eure Unterstützung!
Kris Kaiser und Sepp Wachtveitl von der Uni Frankfurt möchte ich für unsere gute Zusammenarbeit an unserem Licht-Paper danken, euer Input war immer zielführend, und Spaß hatten wir obendrein!
Ich möchte mich auch bei Heribert Warzecha bedanken, der jahrelang die größeren und kleineren Katastrophen der verschiedenen iGEM Teams managen „durfte“, und uns immer mit Rat und Tat zu Seite stand. Danke Heri, ohne Dich wäre iGEM so an der TUD nicht möglich!

Den iGEM Teams der letzten Jahre kann ich gar nicht genug danken! Ihr wart tolle Studierende, motiviert und clever, und habt fantastischen Einsatz gezeigt! Danke für euren tollen Teamgeist und dass ihr euch manchmal etwas von mir habt sagen lassen. Ohne euch wäre meine Doktorarbeit nur halb so schön gewesen, vermutlich habe ich mehr von euch lernen dürfen als ihr von mir!

Meinen Freunden möchte ich ebenfalls danken, besonders Larissa, Ines, Zoltan und Sebastian. Ich bin gespannt auf die nächsten 18-29 Jahre Freundschaft, was dann wohl so passiert?

Zuletzt möchte ich meiner Familie danken. Dass ich sie alle furchtbar lieb habe, wissen sie hoffentlich. Dass ich sie alle sehr bewundere, hoffentlich auch. Mein besonderer Dank gilt:

Kerstin – du bist für mich ein Vorbild der Erfolgreichen Frau und meine liebste Schwester!
Bene – vielen Dank für deine Untersützung, egal was ich mache! Ich hab dich so$^{\infty}$ lieb!
Papa – der effiziente, selbstbestimmte Alleskönner und Häuslebauer! Danke für alles!
Mama – die Wissenschaftlerin aus Leidenschaft, die Autodidaktin und die Macherin. Ohne dich läuft gar nichts!
Oma – von dir konnte ich Lernen, wie man glücklich und zufrieden lebt: Kuchen backen, ein Glas Wein trinken und sich freuen wie gut es einem doch geht!
Manu – du bist ein echtes Vorbild des selbstlosen Anpackens, und das stets gut gelaunt und freundlich!
Nina – du bist die beste Fast-Schwester die ich habe, bleib so hilfsbereit wie du bist und schick mir weiter verrückte Fotos!

8 References

[1] A. E. Isabella Ellinger, "Smallest Unit of Life: Cell Biology," *Comparative medicine: Anatomy and physiology*, pp. 19-33, 2014.

[2] P. Langerhans, "Beitrag zur mikroskopischen Anatomie der Bauchspeicheldrüse," Dissertation, Humboldt-Universität zu Berlin, Berlin, 1869.

[3] B. Alberts, B. r. Häcker, U. Schäfer, D. Morgan, A. Johnson, M. Raff, J. Lewis, K. Roberts, and P. Walter, *Molekularbiologie der Zelle*, 6. Auflage ed.: Wiley VCH, 2017.

[4] S. Leduc, *Études de biophysique*, Paris: A. Poinat, 1910.

[5] S. Leduc, "La Biologie Synthétique," *Ètudes de biophysique*, vol. A. Poinat, Paris, 1912.

[6] P. Jézéquel, E. Drouin, and F.-R. Bataille, *Stéphane Leduc: Précurseur controversé de la biologie synthétique?*, Paris: Éditions Glyphe, 2015.

[7] V. Noireaux, and A. Libchaber, "A vesicle bioreactor as a step toward an artificial cell assembly," *Proc Natl Acad Sci U S A*, vol. 101, no. 51, pp. 17669-74, Dec 21, 2004.

[8] C. E. Hodgman, and M. C. Jewett, "Cell-free synthetic biology: thinking outside the cell," *Metab Eng*, vol. 14, no. 3, pp. 261-9, May, 2012.

[9] Y. Elani, R. V. Law, and O. Ces, "Protein synthesis in artificial cells: using compartmentalisation for spatial organisation in vesicle bioreactors," *Phys Chem Chem Phys*, vol. 17, no. 24, pp. 15534-7, Jun 28, 2015.

[10] J. A. Brophy, and C. A. Voigt, "Principles of genetic circuit design," *Nat Methods*, vol. 11, no. 5, pp. 508-20, May, 2014.

[11] C. C. Liu, L. Qi, J. B. Lucks, T. H. Segall-Shapiro, D. Wang, V. K. Mutalik, and A. P. Arkin, "An adaptor from translational to transcriptional control enables predictable assembly of complex regulation," *Nat Methods*, vol. 9, no. 11, pp. 1088-94, Nov, 2012.

[12] V. K. Mutalik, L. Qi, J. C. Guimaraes, J. B. Lucks, and A. P. Arkin, "Rationally designed families of orthogonal RNA regulators of translation," *Nat Chem Biol*, vol. 8, no. 5, pp. 447-54, Mar 25, 2012.

[13] F. J. Isaacs, D. J. Dwyer, and J. J. Collins, "RNA synthetic biology," *Nat Biotechnol*, vol. 24, no. 5, pp. 545-54, May, 2006.

[14] M. Etzel, and M. Morl, "Synthetic Riboswitches: From Plug and Pray toward Plug and Play," *Biochemistry*, vol. 56, no. 9, pp. 1181-1198, Mar 7, 2017.

[15] A. J. F. Griffiths, *An introduction to genetic analysis*, 7. ed.: W. H. Freeman & Company, 2000.

[16] L. A. Urry, M. L. Cain, S. A. Wasserman, P. V. Minorsky, J. B. Reece, and N. A. Campbell, *Campbell biology*, Eleventh edition. ed., New York, NY: Pearson Education, Inc., 2017.

[17] J. D. Watson, *Recombinant DNA genes and genomes - a short course*, 3. ed.: W. H. Freeman & Company, 2007.

[18] T. A. Brown, *Gene cloning and DNA analysis: An introduction*, 5. ed.: Wiley-Blackwell, 2007.

[19] S. Kawai, W. Hashimoto, and K. Murata, "Transformation of Saccharomyces cerevisiae and other fungi: methods and possible underlying mechanism," *Bioeng Bugs*, vol. 1, no. 6, pp. 395-403, Nov-Dec, 2010.

[20] S. T. Smale, and J. T. Kadonaga, "The RNA polymerase II core promoter," *Annu Rev Biochem,* vol. 72, pp. 449-79, 2003.
[21] G. A. Maston, S. K. Evans, and M. R. Green, "Transcriptional regulatory elements in the human genome," *Annu Rev Genomics Hum Genet,* vol. 7, pp. 29-59, 2006.
[22] S. Ogbourne, and T. M. Antalis, "Transcriptional control and the role of silencers in transcriptional regulation in eukaryotes," *Biochem J,* vol. 331 (Pt 1), pp. 1-14, Apr 1, 1998.
[23] T. E. Dever, "Gene-specific regulation by general translation factors," *Cell,* vol. 108, no. 4, pp. 545-56, Feb 22, 2002.
[24] N. B. Leontis, J. Stombaugh, and E. Westhof, "The non-Watson-Crick base pairs and their associated isostericity matrices," *Nucleic Acids Res,* vol. 30, no. 16, pp. 3497-531, Aug 15, 2002.
[25] G. Varani, and W. H. McClain, "The G x U wobble base pair. A fundamental building block of RNA structure crucial to RNA function in diverse biological systems," *EMBO Rep,* vol. 1, no. 1, pp. 18-23, Jul, 2000.
[26] J. M. Berg, J. L. Tymoczko, and L. Stryer, *Biochemistry*, 8. ed.: Springer Spektrum, 2018.
[27] M. A. Matzke, and A. J. Matzke, "Planting the seeds of a new paradigm," *PLoS Biol,* vol. 2, no. 5, pp. E133, May, 2004.
[28] T. Watanabe, Y. Totoki, A. Toyoda, M. Kaneda, S. Kuramochi-Miyagawa, Y. Obata, H. Chiba, Y. Kohara, T. Kono, T. Nakano, M. A. Surani, Y. Sakaki, and H. Sasaki, "Endogenous siRNAs from naturally formed dsRNAs regulate transcripts in mouse oocytes," *Nature,* vol. 453, no. 7194, pp. 539-43, May 22, 2008.
[29] L. Wu, and J. G. Belasco, "Let me count the ways: mechanisms of gene regulation by miRNAs and siRNAs," *Mol Cell,* vol. 29, no. 1, pp. 1-7, Jan 18, 2008.
[30] L. He, and G. J. Hannon, "MicroRNAs: small RNAs with a big role in gene regulation," *Nat Rev Genet,* vol. 5, no. 7, pp. 522-31, Jul, 2004.
[31] D. D. Rao, J. S. Vorhies, N. Senzer, and J. Nemunaitis, "siRNA vs. shRNA: similarities and differences," *Adv Drug Deliv Rev,* vol. 61, no. 9, pp. 746-59, Jul 25, 2009.
[32] C. Wahlestedt, "Targeting long non-coding RNA to therapeutically upregulate gene expression," *Nat Rev Drug Discov,* vol. 12, no. 6, pp. 433-46, Jun, 2013.
[33] G. Storz, S. Altuvia, and K. M. Wassarman, "An abundance of RNA regulators," *Annu Rev Biochem,* vol. 74, pp. 199-217, 2005.
[34] F. Repoila, and F. Darfeuille, "Small regulatory non-coding RNAs in bacteria: physiology and mechanistic aspects," *Biol Cell,* vol. 101, no. 2, pp. 117-31, Feb, 2009.
[35] A. S. Mironov, I. Gusarov, R. Rafikov, L. E. Lopez, K. Shatalin, R. A. Kreneva, D. A. Perumov, and E. Nudler, "Sensing small molecules by nascent RNA: a mechanism to control transcription in bacteria," *Cell,* vol. 111, no. 5, pp. 747-56, Nov 27, 2002.
[36] A. Nahvi, N. Sudarsan, M. S. Ebert, X. Zou, K. L. Brown, and R. R. Breaker, "Genetic control by a metabolite binding mRNA," *Chem Biol,* vol. 9, no. 9, pp. 1043, Sep, 2002.
[37] W. C. Winkler, S. Cohen-Chalamish, and R. R. Breaker, "An mRNA structure that controls gene expression by binding FMN," *Proc Natl Acad Sci U S A,* vol. 99, no. 25, pp. 15908-13, Dec 10, 2002.
[38] R. T. Batey, "Riboswitches: still a lot of undiscovered country," *RNA,* vol. 21, no. 4, pp. 560-3, Apr, 2015.

[39] Z. F. Hallberg, Y. Su, R. Z. Kitto, and M. C. Hammond, "Engineering and In Vivo Applications of Riboswitches," *Annu Rev Biochem,* vol. 86, pp. 515-539, Jun 20, 2017.
[40] B. J. Tucker, and R. R. Breaker, "Riboswitches as versatile gene control elements," *Curr Opin Struct Biol,* vol. 15, no. 3, pp. 342-8, Jun, 2005.
[41] T. S. Lotz, and B. Suess, "Small-Molecule-Binding Riboswitches," *Microbiology Spectrum,* vol. 6, no. 4, 2018.
[42] W. Winkler, A. Nahvi, and R. R. Breaker, "Thiamine derivatives bind messenger RNAs directly to regulate bacterial gene expression," *Nature,* vol. 419, no. 6910, pp. 952-6, Oct 31, 2002.
[43] D. A. Rodionov, A. G. Vitreschak, A. A. Mironov, and M. S. Gelfand, "Comparative genomics of thiamin biosynthesis in procaryotes. New genes and regulatory mechanisms," *J Biol Chem,* vol. 277, no. 50, pp. 48949-59, Dec 13, 2002.
[44] N. Sudarsan, J. E. Barrick, and R. R. Breaker, "Metabolite-binding RNA domains are present in the genes of eukaryotes," *RNA,* vol. 9, no. 6, pp. 644-7, Jun, 2003.
[45] M. T. Cheah, A. Wachter, N. Sudarsan, and R. R. Breaker, "Control of alternative RNA splicing and gene expression by eukaryotic riboswitches," *Nature,* vol. 447, no. 7143, pp. 497-500, May 24, 2007.
[46] T. Kubodera, M. Watanabe, K. Yoshiuchi, N. Yamashita, A. Nishimura, S. Nakai, K. Gomi, and H. Hanamoto, "Thiamine-regulated gene expression of Aspergillus oryzae thiA requires splicing of the intron containing a riboswitch-like domain in the 5'-UTR," *FEBS Lett,* vol. 555, no. 3, pp. 516-20, Dec 18, 2003.
[47] N. Sudarsan, J. K. Wickiser, S. Nakamura, M. S. Ebert, and R. R. Breaker, "An mRNA structure in bacteria that controls gene expression by binding lysine," *Genes Dev,* vol. 17, no. 21, pp. 2688-97, Nov 1, 2003.
[48] A. Wachter, M. Tunc-Ozdemir, B. C. Grove, P. J. Green, D. K. Shintani, and R. R. Breaker, "Riboswitch control of gene expression in plants by splicing and alternative 3' end processing of mRNAs," *Plant Cell,* vol. 19, no. 11, pp. 3437-50, Nov, 2007.
[49] S. E. Bocobza, and A. Aharoni, "Small molecules that interact with RNA: riboswitch-based gene control and its involvement in metabolic regulation in plants and algae," *Plant J,* vol. 79, no. 4, pp. 693-703, Aug, 2014.
[50] M. T. Croft, M. Moulin, M. E. Webb, and A. G. Smith, "Thiamine biosynthesis in algae is regulated by riboswitches," *Proc Natl Acad Sci U S A,* vol. 104, no. 52, pp. 20770-5, Dec 26, 2007.
[51] M. Mandal, B. Boese, J. E. Barrick, W. C. Winkler, and R. R. Breaker, "Riboswitches control fundamental biochemical pathways in Bacillus subtilis and other bacteria," *Cell,* vol. 113, no. 5, pp. 577-86, May 30, 2003.
[52] M. Mandal, and R. R. Breaker, "Adenine riboswitches and gene activation by disruption of a transcription terminator," *Nat Struct Mol Biol,* vol. 11, no. 1, pp. 29-35, Jan, 2004.
[53] R. T. Fuchs, F. J. Grundy, and T. M. Henkin, "The S(MK) box is a new SAM-binding RNA for translational regulation of SAM synthetase," *Nat Struct Mol Biol,* vol. 13, no. 3, pp. 226-33, Mar, 2006.
[54] R. Rieder, K. Lang, D. Graber, and R. Micura, "Ligand-induced folding of the adenosine deaminase A-riboswitch and implications on riboswitch translational control," *Chembiochem,* vol. 8, no. 8, pp. 896-902, May 25, 2007.
[55] P. Y. Watson, and M. J. Fedor, "The glmS riboswitch integrates signals from activating and inhibitory metabolites in vivo," *Nat Struct Mol Biol,* vol. 18, no. 3, pp. 359-63, Mar, 2011.

[56] E. Loh, O. Dussurget, J. Gripenland, K. Vaitkevicius, T. Tiensuu, P. Mandin, F. Repoila, C. Buchrieser, P. Cossart, and J. Johansson, "A trans-acting riboswitch controls expression of the virulence regulator PrfA in Listeria monocytogenes," *Cell,* vol. 139, no. 4, pp. 770-9, Nov 13, 2009.
[57] N. Sudarsan, E. R. Lee, Z. Weinberg, R. H. Moy, J. N. Kim, K. H. Link, and R. R. Breaker, "Riboswitches in eubacteria sense the second messenger cyclic di-GMP," *Science,* vol. 321, no. 5887, pp. 411-3, Jul 18, 2008.
[58] W. C. Winkler, A. Nahvi, N. Sudarsan, J. E. Barrick, and R. R. Breaker, "An mRNA structure that controls gene expression by binding S-adenosylmethionine," *Nat Struct Biol,* vol. 10, no. 9, pp. 701-7, Sep, 2003.
[59] W. Gilbert, "Origin of life: the RNA world," *Nature,* vol. 319, pp. 618, 1986.
[60] R. R. Breaker, "Riboswitches and the RNA world," *Cold Spring Harb Perspect Biol,* vol. 4, no. 2, Feb 1, 2012.
[61] P. J. McCown, K. A. Corbino, S. Stav, M. E. Sherlock, and R. R. Breaker, "Riboswitch diversity and distribution," *RNA,* vol. 23, no. 7, pp. 995-1011, Jul, 2017.
[62] J. Rossmanith, and F. Narberhaus, "Exploring the modular nature of riboswitches and RNA thermometers," *Nucleic Acids Res,* vol. 44, no. 11, pp. 5410-23, Jun 20, 2016.
[63] G. Mayer, and T. Hover, "In vitro selection of ssDNA aptamers using biotinylated target proteins," *Methods Mol Biol,* vol. 535, pp. 19-32, 2009.
[64] P. Colas, B. Cohen, T. Jessen, I. Grishina, J. McCoy, and R. Brent, "Genetic selection of peptide aptamers that recognize and inhibit cyclin-dependent kinase 2," *Nature,* vol. 380, no. 6574, pp. 548-50, Apr 11, 1996.
[65] R. D. Jenison, S. C. Gill, A. Pardi, and B. Polisky, "High-resolution molecular discrimination by RNA," *Science,* vol. 263, no. 5152, pp. 1425-9, Mar 11, 1994.
[66] K. M. Song, S. Lee, and C. Ban, "Aptamers and their biological applications," *Sensors,* vol. 12, no. 1, pp. 612-31, 2012.
[67] J. Zhou, and J. Rossi, "Aptamers as targeted therapeutics: current potential and challenges," *Nat Rev Drug Discov,* vol. 16, no. 3, pp. 181-202, Mar, 2017.
[68] M. Famulok, and J. W. Szostak, "Stereospecific recognition of tryptophan agarose by in vitro selected RNA," *Journal of the American Chemical Society,* vol. 114, no. 10, pp. 3990-3991, 1992/05/01, 1992.
[69] A. Geiger, P. Burgstaller, H. von der Eltz, A. Roeder, and M. Famulok, "RNA aptamers that bind L-arginine with sub-micromolar dissociation constants and high enantioselectivity," *Nucleic Acids Res,* vol. 24, no. 6, pp. 1029-36, Mar 15, 1996.
[70] M. Rimmele, "Nucleic acid aptamers as tools and drugs: recent developments," *Chembiochem,* vol. 4, no. 10, pp. 963-71, Oct 6, 2003.
[71] P. Mallikaratchy, "Evolution of Complex Target SELEX to Identify Aptamers against Mammalian Cell-Surface Antigens," *Molecules,* vol. 22, no. 2, Jan 30, 2017.
[72] A. D. Ellington, and J. W. Szostak, "In vitro selection of RNA molecules that bind specific ligands," *Nature,* vol. 346, no. 6287, pp. 818-22, Aug 30, 1990.
[73] C. Tuerk, and L. Gold, "Systematic evolution of ligands by exponential enrichment: RNA ligands to bacteriophage T4 DNA polymerase," *Science,* vol. 249, no. 4968, pp. 505-10, Aug 3, 1990.
[74] C. Janeway, *Immunobiology: The Immune Sytem In Health & Disease*, 5. ed ed.: Garland Science, 2001.
[75] L. C. Bock, L. C. Griffin, J. A. Latham, E. H. Vermaas, and J. J. Toole, "Selection of single-stranded DNA molecules that bind and inhibit human thrombin," *Nature,* vol. 355, no. 6360, pp. 564-6, Feb 6, 1992.

[76] A. K. Dey, C. Griffiths, S. M. Lea, and W. James, "Structural characterization of an anti-gp120 RNA aptamer that neutralizes R5 strains of HIV-1," *RNA*, vol. 11, no. 6, pp. 873-84, Jun, 2005.
[77] M. H. Caruthers, A. D. Barone, S. L. Beaucage, D. R. Dodds, E. F. Fisher, L. J. McBride, M. Matteucci, Z. Stabinsky, and J. Y. Tang, "Chemical synthesis of deoxyoligonucleotides by the phosphoramidite method," *Methods Enzymol*, vol. 154, pp. 287-313, 1987.
[78] J. F. R. Ortigao, H. Rösch, M. Montenarh, A. Fröhlich, and H. Seliger, "Oligonucleotide Analogs with Terminal 3′,3′- and 5′,5′-Internucleotidic Linkages as Antisense Inhibitors of Viral Replication," *Antisense Research and Development*, vol. 1, no. 4, pp. 380-380, 1991.
[79] N. D. Abeydeera, M. Egli, N. Cox, K. Mercier, J. N. Conde, P. S. Pallan, D. M. Mizurini, M. Sierant, F. E. Hibti, T. Hassell, T. Wang, F. W. Liu, H. M. Liu, C. Martinez, A. K. Sood, T. P. Lybrand, C. Frydman, R. Q. Monteiro, R. H. Gomer, B. Nawrot, and X. Yang, "Evoking picomolar binding in RNA by a single phosphorodithioate linkage," *Nucleic Acids Res*, vol. 44, no. 17, pp. 8052-64, Sep 30, 2016.
[80] J. M. Healy, S. D. Lewis, M. Kurz, R. M. Boomer, K. M. Thompson, C. Wilson, and T. G. McCauley, "Pharmacokinetics and biodistribution of novel aptamer compositions," *Pharm Res*, vol. 21, no. 12, pp. 2234-46, Dec, 2004.
[81] S. Ni, H. Yao, L. Wang, J. Lu, F. Jiang, A. Lu, and G. Zhang, "Chemical Modifications of Nucleic Acid Aptamers for Therapeutic Purposes," *Int J Mol Sci*, vol. 18, no. 8, Aug 2, 2017.
[82] A. Wittmann, and B. Suess, "Engineered riboswitches: Expanding researchers' toolbox with synthetic RNA regulators," *FEBS Lett*, vol. 586, no. 15, pp. 2076-83, Jul 16, 2012.
[83] M. R. Dunn, R. M. Jimenez, and J. C. Chaput, "Analysis of aptamer discovery and technology," *Nature Reviews Chemistry*, vol. 1, pp. 0076, 10/04/online, 2017.
[84] E. S. Gragoudas, A. P. Adamis, E. T. Cunningham, Jr., M. Feinsod, D. R. Guyer, and V. I. S. i. O. N. C. T. Group, "Pegaptanib for neovascular age-related macular degeneration," *N Engl J Med*, vol. 351, no. 27, pp. 2805-16, Dec 30, 2004.
[85] E. W. Ng, D. T. Shima, P. Calias, E. T. Cunningham, Jr., D. R. Guyer, and A. P. Adamis, "Pegaptanib, a targeted anti-VEGF aptamer for ocular vascular disease," *Nat Rev Drug Discov*, vol. 5, no. 2, pp. 123-32, Feb, 2006.
[86] S. Yoon, and J. J. Rossi, "Emerging cancer-specific therapeutic aptamers," *Curr Opin Oncol*, vol. 29, no. 5, pp. 366-374, Sep, 2017.
[87] K. E. Maier, and M. Levy, "From selection hits to clinical leads: progress in aptamer discovery," *Mol Ther Methods Clin Dev*, vol. 5, pp. 16014, 2016.
[88] L. Cerchia, "Aptamers: Promising Tools for Cancer Diagnosis and Therapy," *Cancers (Basel)*, vol. 10, no. 5, May 3, 2018.
[89] K. Szeto, D. R. Latulippe, A. Ozer, J. M. Pagano, B. S. White, D. Shalloway, J. T. Lis, and H. G. Craighead, "RAPID-SELEX for RNA aptamers," *PLoS One*, vol. 8, no. 12, pp. e82667, 2013.
[90] L. Gold, "Oligonucleotides as research, diagnostic, and therapeutic agents," *J Biol Chem*, vol. 270, no. 23, pp. 13581-4, Jun 9, 1995.
[91] M. Djordjevic, "SELEX experiments: new prospects, applications and data analysis in inferring regulatory pathways," *Biomol Eng*, vol. 24, no. 2, pp. 179-89, Jun, 2007.
[92] J. Tao, and A. D. Frankel, "Arginine-binding RNAs resembling TAR identified by in vitro selection," *Biochemistry*, vol. 35, no. 7, pp. 2229-38, Feb 20, 1996.

[93] G. L. Lokesh, H. Wang, C. H. Lam, V. Thiviyanathan, N. Ward, D. G. Gorenstein, and D. E. Volk, "X-Aptamer Selection and Validation," *Methods Mol Biol,* vol. 1632, pp. 151-174, 2017.
[94] C. Smith, S. Heyne, A. S. Richter, S. Will, and R. Backofen, "Freiburg RNA Tools: a web server integrating INTARNA, EXPARNA and LOCARNA," *Nucleic Acids Res,* vol. 38, no. Web Server issue, pp. W373-7, Jul, 2010.
[95] S. Will, T. Joshi, I. L. Hofacker, P. F. Stadler, and R. Backofen, "LocARNA-P: accurate boundary prediction and improved detection of structural RNAs," *RNA,* vol. 18, no. 5, pp. 900-14, May, 2012.
[96] M. Schmidt, K. Hamacher, F. Reinhardt, T. S. Lotz, F. Groher, S. Jager, and B. Suess, "SICOR: Subgraph Isomorphism Comparison of RNA Secondary Structures," In revision.
[97] L. Yingfu, L. Yi, and S. Silverman, *Artificial Functional Nucleic Acids: Aptamers, Ribozymes, and Deoxyribozymes Identified by In Vitro Selection*, p.^pp. 47-108: Springer New York, 2009.
[98] W. H. Thiel, T. Bair, K. Wyatt Thiel, J. P. Dassie, W. M. Rockey, C. A. Howell, X. Y. Liu, A. J. Dupuy, L. Huang, R. Owczarzy, M. A. Behlke, J. O. McNamara, and P. H. Giangrande, "Nucleotide bias observed with a short SELEX RNA aptamer library," *Nucleic Acid Ther,* vol. 21, no. 4, pp. 253-63, Aug, 2011.
[99] F. Tolle, J. Wilke, J. Wengel, and G. Mayer, "By-product formation in repetitive PCR amplification of DNA libraries during SELEX," *PLoS One,* vol. 9, no. 12, pp. e114693, 2014.
[100] M. Takahashi, X. Wu, M. Ho, P. Chomchan, J. J. Rossi, J. C. Burnett, and J. Zhou, "High throughput sequencing analysis of RNA libraries reveals the influences of initial library and PCR methods on SELEX efficiency," *Sci Rep,* vol. 6, pp. 33697, Sep 22, 2016.
[101] M. Kwon, S. M. Chun, S. Jeong, and J. Yu, "In vitro selection of RNA against kanamycin B," *Mol Cells,* vol. 11, no. 3, pp. 303-11, Jun 30, 2001.
[102] C. Polonschii, S. David, S. Tombelli, M. Mascini, and M. Gheorghiu, "A novel low-cost and easy to develop functionalization platform. Case study: aptamer-based detection of thrombin by surface plasmon resonance," *Talanta,* vol. 80, no. 5, pp. 2157-64, Mar 15, 2010.
[103] E. Dausse, A. Barre, A. Aime, A. Groppi, A. Rico, C. Ainali, G. Salgado, W. Palau, E. Daguerre, M. Nikolski, J. J. Toulme, and C. Di Primo, "Aptamer selection by direct microfluidic recovery and surface plasmon resonance evaluation," *Biosens Bioelectron,* vol. 80, pp. 418-425, Jun 15, 2016.
[104] S. D. Mendonsa, and M. T. Bowser, "In vitro evolution of functional DNA using capillary electrophoresis," *J Am Chem Soc,* vol. 126, no. 1, pp. 20-1, Jan 14, 2004.
[105] D. A. Daniels, H. Chen, B. J. Hicke, K. M. Swiderek, and L. Gold, "A tenascin-C aptamer identified by tumor cell SELEX: systematic evolution of ligands by exponential enrichment," *Proc Natl Acad Sci U S A,* vol. 100, no. 26, pp. 15416-21, Dec 23, 2003.
[106] G. Aquino-Jarquin, and J. D. Toscano-Garibay, "RNA aptamer evolution: two decades of SELEction," *Int J Mol Sci,* vol. 12, no. 12, pp. 9155-71, 2011.
[107] S. C. Gopinath, "Methods developed for SELEX," *Anal Bioanal Chem,* vol. 387, no. 1, pp. 171-82, Jan, 2007.
[108] Z. Zhuo, Y. Yu, M. Wang, J. Li, Z. Zhang, J. Liu, X. Wu, A. Lu, G. Zhang, and B. Zhang, "Recent Advances in SELEX Technology and Aptamer Applications in Biomedicine," *Int J Mol Sci,* vol. 18, no. 10, Oct 14, 2017.

[109] F. Jarosch, K. Buchner, and S. Klussmann, "In vitro selection using a dual RNA library that allows primerless selection," *Nucleic Acids Res,* vol. 34, no. 12, pp. e86, Jul 19, 2006.
[110] M. Sassanfar, and J. W. Szostak, "An RNA motif that binds ATP," *Nature,* vol. 364, no. 6437, pp. 550-3, Aug 5, 1993.
[111] S. D. Seiwert, T. Stines Nahreini, S. Aigner, N. G. Ahn, and O. C. Uhlenbeck, "RNA aptamers as pathway-specific MAP kinase inhibitors," *Chem Biol,* vol. 7, no. 11, pp. 833-43, Nov, 2000.
[112] J. H. Davis, and J. W. Szostak, "Isolation of high-affinity GTP aptamers from partially structured RNA libraries," *Proc Natl Acad Sci U S A,* vol. 99, no. 18, pp. 11616-21, Sep 3, 2002.
[113] J. M. Carothers, S. C. Oestreich, J. H. Davis, and J. W. Szostak, "Informational complexity and functional activity of RNA structures," *J Am Chem Soc,* vol. 126, no. 16, pp. 5130-7, Apr 28, 2004.
[114] A. Ruscito, and M. C. DeRosa, "Small-Molecule Binding Aptamers: Selection Strategies, Characterization, and Applications," *Front Chem,* vol. 4, pp. 14, 2016.
[115] H. Hasegawa, N. Savory, K. Abe, and K. Ikebukuro, "Methods for Improving Aptamer Binding Affinity," *Molecules,* vol. 21, no. 4, pp. 421, Mar 28, 2016.
[116] A. L. Chang, M. McKeague, J. C. Liang, and C. D. Smolke, "Kinetic and equilibrium binding characterization of aptamers to small molecules using a label-free, sensitive, and scalable platform," *Anal Chem,* vol. 86, no. 7, pp. 3273-8, Apr 1, 2014.
[117] J. Ciesiolka, J. Gorski, and M. Yarus, "Selection of an RNA domain that binds Zn2+," *RNA,* vol. 1, no. 5, pp. 538-50, Jul, 1995.
[118] M. Famulok, "Molecular Recognition of Amino Acids by RNA-Aptamers: An L-Citrulline Binding RNA Motif and Its Evolution into an L-Arginine Binder " *J. Am. Chem. Soc.,* vol. 116, pp. 1698–1706, 1994.
[119] C. Meyer, U. Hahn, and A. Rentmeister, "Cell-specific aptamers as emerging therapeutics," *J Nucleic Acids,* vol. 2011, pp. 904750, 2011.
[120] M. Homann, and H. U. Goringer, "Combinatorial selection of high affinity RNA ligands to live African trypanosomes," *Nucleic Acids Res,* vol. 27, no. 9, pp. 2006-14, May 1, 1999.
[121] P. R. Andrews, D. J. Craik, and J. L. Martin, "Functional group contributions to drug-receptor interactions," *J Med Chem,* vol. 27, no. 12, pp. 1648-57, Dec, 1984.
[122] W. C. Winkler, A. Nahvi, A. Roth, J. A. Collins, and R. R. Breaker, "Control of gene expression by a natural metabolite-responsive ribozyme," *Nature,* vol. 428, no. 6980, pp. 281-6, Mar 18, 2004.
[123] J. J. Farmer, 3rd, "Vibrio ("Beneckea") vulnificus, the bacterium associated with sepsis, septicaemia, and the sea," *Lancet,* vol. 2, no. 8148, pp. 903, Oct 27, 1979.
[124] E. Loh, F. Righetti, H. Eichner, C. Twittenhoff, and F. Narberhaus, "RNA thermometers in bacterial pathogens," *Regulating with RNA in Bacteria and Archaea,* vol. 1, 2018.
[125] G. Nechooshtan, M. Elgrably-Weiss, A. Sheaffer, E. Westhof, and S. Altuvia, "A pH-responsive riboregulator," *Genes Dev,* vol. 23, no. 22, pp. 2650-62, Nov 15, 2009.
[126] P. Ceres, A. D. Garst, J. G. Marcano-Velazquez, and R. T. Batey, "Modularity of select riboswitch expression platforms enables facile engineering of novel genetic regulatory devices," *ACS Synth Biol,* vol. 2, no. 8, pp. 463-72, Aug 16, 2013.
[127] P. Ceres, J. J. Trausch, and R. T. Batey, "Engineering modular 'ON' RNA switches using biological components," *Nucleic Acids Res,* vol. 41, no. 22, pp. 10449-61, Dec, 2013.

[128] S. Topp, C. M. Reynoso, J. C. Seeliger, I. S. Goldlust, S. K. Desai, D. Murat, A. Shen, A. W. Puri, A. Komeili, C. R. Bertozzi, J. R. Scott, and J. P. Gallivan, "Synthetic riboswitches that induce gene expression in diverse bacterial species," *Appl Environ Microbiol,* vol. 76, no. 23, pp. 7881-4, Dec, 2010.
[129] C. Berens, and B. Suess, "Riboswitch engineering - making the all-important second and third steps," *Curr Opin Biotechnol,* vol. 31, pp. 10-5, Feb, 2015.
[130] S. E. Bocobza, and A. Aharoni, "Switching the light on plant riboswitches," *Trends Plant Sci,* vol. 13, no. 10, pp. 526-33, Oct, 2008.
[131] B. Suess, S. Hanson, C. Berens, B. Fink, R. Schroeder, and W. Hillen, "Conditional gene expression by controlling translation with tetracycline-binding aptamers," *Nucleic Acids Res,* vol. 31, no. 7, pp. 1853-8, Apr 1, 2003.
[132] J. E. Weigand, M. Sanchez, E. B. Gunnesch, S. Zeiher, R. Schroeder, and B. Suess, "Screening for engineered neomycin riboswitches that control translation initiation," *RNA,* vol. 14, no. 1, pp. 89-97, Jan, 2008.
[133] F. Groher, C. Bofill-Bosch, C. Schneider, J. Braun, S. Jager, K. Geißler, K. Hamacher, and B. Suess, "Riboswitching with ciprofloxacin—development and characterization of a novel RNA regulator," *Nucleic Acids Res.,* vol. 46, no. 4, pp. 2121--2132, 2018/01/13/, 2018.
[134] D. S. Kim, V. Gusti, S. G. Pillai, and R. K. Gaur, "An artificial riboswitch for controlling pre-mRNA splicing," *RNA,* vol. 11, no. 11, pp. 1667-77, Nov, 2005.
[135] W. J. Vogel M, Kluge B, Grez M, Suess B, "A small, portable RNA device for the control of exon skipping in mammalian cells," *Nucleic Acids Res,* pp. e64, 2018.
[136] P. Kotter, J. E. Weigand, B. Meyer, K. D. Entian, and B. Suess, "A fast and efficient translational control system for conditional expression of yeast genes," *Nucleic Acids Res,* vol. 37, no. 18, pp. e120, Oct, 2009.
[137] C. L. Beisel, Y. Y. Chen, S. J. Culler, K. G. Hoff, and C. D. Smolke, "Design of small molecule-responsive microRNAs based on structural requirements for Drosha processing," *Nucleic Acids Res,* vol. 39, no. 7, pp. 2981-94, Apr, 2011.
[138] C. I. An, V. B. Trinh, and Y. Yokobayashi, "Artificial control of gene expression in mammalian cells by modulating RNA interference through aptamer-small molecule interaction," *RNA,* vol. 12, no. 5, pp. 710-6, May, 2006.
[139] M. Felletti, J. Stifel, L. A. Wurmthaler, S. Geiger, and J. S. Hartig, "Twister ribozymes as highly versatile expression platforms for artificial riboswitches," *Nat Commun,* vol. 7, pp. 12834, Sep 27, 2016.
[140] G. Domin, S. Findeiss, M. Wachsmuth, S. Will, P. F. Stadler, and M. Morl, "Applicability of a computational design approach for synthetic riboswitches," *Nucleic Acids Res,* vol. 45, no. 7, pp. 4108-4119, Apr 20, 2017.
[141] P. Pradhan, N. Soni, L. Chaudhary, S. Mujwar, and K. Pardasani, *"In-silico Prediction of Riboswitches and Design of their Potent Inhibitors for H1N1, H2N2 and H3N2 Strains of Influenza Virus"*, 2015.
[142] M. Wachsmuth, S. Findeiss, N. Weissheimer, P. F. Stadler, and M. Morl, "De novo design of a synthetic riboswitch that regulates transcription termination," *Nucleic Acids Res,* vol. 41, no. 4, pp. 2541-51, Feb 1, 2013.
[143] D. Botstein, S. A. Chervitz, and J. M. Cherry, "Yeast as a model organism," *Science,* vol. 277, no. 5330, pp. 1259-60, Aug 29, 1997.
[144] F. Sherman, "Getting started with yeast," *Methods Enzymol,* vol. 194, pp. 3-21, 1991.
[145] F. Sherman, "Getting started with yeast," *Methods Enzymol,* vol. 350, pp. 3-41, 2002.

[146] P. Branduardi, and D. Porro, "*n*-butanol: challenges and solutions for shifting natural metabolic pathways into a viable microbial production," *FEMS Microbiol Lett,* vol. 363, no. 8, Apr, 2016.
[147] W. Tanner, and L. Lehle, "Protein glycosylation in yeast," *Biochim Biophys Acta,* vol. 906, no. 1, pp. 81-99, Apr 27, 1987.
[148] J. Nielsen, "Production of biopharmaceutical proteins by yeast: advances through metabolic engineering," *Bioengineered,* vol. 4, no. 4, pp. 207-11, Jul-Aug, 2013.
[149] S. Hanson, K. Berthelot, B. Fink, J. E. McCarthy, and B. Suess, "Tetracycline-aptamer-mediated translational regulation in yeast," *Mol Microbiol,* vol. 49, no. 6, pp. 1627-37, Sep, 2003.
[150] G. Werstuck, and M. R. Green, "Controlling gene expression in living cells through small molecule-RNA interactions," *Science,* vol. 282, no. 5387, pp. 296-8, Oct 9, 1998.
[151] D. Grate, and C. Wilson, "Inducible regulation of the S. cerevisiae cell cycle mediated by an RNA aptamer-ligand complex," *Bioorg Med Chem,* vol. 9, no. 10, pp. 2565-70, Oct, 2001.
[152] C. Berens, F. Groher, and B. Suess, "RNA aptamers as genetic control devices: the potential of riboswitches as synthetic elements for regulating gene expression," *Biotechnol J,* vol. 10, no. 2, pp. 246-57, Feb, 2015.
[153] A. Ettinger, and T. Wittmann, "Fluorescence live cell imaging," *Methods Cell Biol,* vol. 123, pp. 77-94, 2014.
[154] F. G. Prendergast, and K. G. Mann, "Chemical and physical properties of aequorin and the green fluorescent protein isolated from Aequorea forskalea," *Biochemistry,* vol. 17, no. 17, pp. 3448-3453, 1978/08/22, 1978.
[155] B. E. Jugder, J. Welch, N. Braidy, and C. P. Marquis, "Construction and use of a Cupriavidus necator H16 soluble hydrogenase promoter (PSH) fusion to gfp (green fluorescent protein)," *PeerJ,* vol. 4, pp. e2269, 2016.
[156] K. H. Arun, C. L. Kaul, and P. Ramarao, "Green fluorescent proteins in receptor research: an emerging tool for drug discovery," *J Pharmacol Toxicol Methods,* vol. 51, no. 1, pp. 1-23, Jan-Feb, 2005.
[157] J. Livet, T. A. Weissman, H. Kang, R. W. Draft, J. Lu, R. A. Bennis, J. R. Sanes, and J. W. Lichtman, "Transgenic strategies for combinatorial expression of fluorescent proteins in the nervous system," *Nature,* vol. 450, no. 7166, pp. 56-62, Nov 1, 2007.
[158] H. Adesnik, R. A. Nicoll, and P. M. England, "Photoinactivation of native AMPA receptors reveals their real-time trafficking," *Neuron,* vol. 48, no. 6, pp. 977-85, Dec 22, 2005.
[159] R. Y. Tsien, "The green fluorescent protein," *Annu Rev Biochem,* vol. 67, pp. 509-44, 1998.
[160] F. Sanger, and A. R. Coulson, "A rapid method for determining sequences in DNA by primed synthesis with DNA polymerase," *J Mol Biol,* vol. 94, no. 3, pp. 441-8, May 25, 1975.
[161] A. M. Maxam, and W. Gilbert, "A new method for sequencing DNA," *Proc Natl Acad Sci U S A,* vol. 74, no. 2, pp. 560-4, Feb, 1977.
[162] S. E. Levy, and R. M. Myers, "Advancements in Next-Generation Sequencing," *Annu Rev Genomics Hum Genet,* vol. 17, pp. 95-115, Aug 31, 2016.
[163] C. International Human Genome Sequencing, "Initial sequencing and analysis of the human genome," *Nature,* vol. 409, no. 6822, pp. 860-921, Feb 15, 2001.
[164] J. C. Venter, and o. authors, "The sequence of the human genome," *Science,* vol. 291, no. 5507, pp. 1304-51, Feb 16, 2001.

[165] C. International Human Genome Sequencing, "Finishing the euchromatic sequence of the human genome," *Nature,* vol. 431, no. 7011, pp. 931-45, Oct 21, 2004.
[166] M. Blank, "Next-Generation Analysis of Deep Sequencing Data: Bringing Light into the Black Box of SELEX Experiments," *Methods Mol Biol,* vol. 1380, pp. 85-95, 2016.
[167] N. B. Leontis, A. Lescoute, and E. Westhof, "The building blocks and motifs of RNA architecture," *Curr Opin Struct Biol,* vol. 16, no. 3, pp. 279-87, Jun, 2006.
[168] A. Serganov, L. Huang, and D. J. Patel, "Coenzyme recognition and gene regulation by a flavin mononucleotide riboswitch," *Nature,* vol. 458, no. 7235, pp. 233-7, Mar 12, 2009.
[169] R. Shiman, and D. E. Draper, "Stabilization of RNA tertiary structure by monovalent cations," *J Mol Biol,* vol. 302, no. 1, pp. 79-91, Sep 8, 2000.
[170] S. E. Butcher, and A. M. Pyle, "The molecular interactions that stabilize RNA tertiary structure: RNA motifs, patterns, and networks," *Acc Chem Res,* vol. 44, no. 12, pp. 1302-11, Dec 20, 2011.
[171] S. Halder, and D. Bhattacharyya, "RNA structure and dynamics: a base pairing perspective," *Prog Biophys Mol Biol,* vol. 113, no. 2, pp. 264-83, Nov, 2013.
[172] J. A. Liberman, and J. E. Wedekind, "Riboswitch structure in the ligand-free state," *Wiley Interdiscip Rev RNA,* vol. 3, no. 3, pp. 369-84, May-Jun, 2012.
[173] N. Kulshina, N. J. Baird, and A. R. Ferre-D'Amare, "Recognition of the bacterial second messenger cyclic diguanylate by its cognate riboswitch," *Nat Struct Mol Biol,* vol. 16, no. 12, pp. 1212-7, Dec, 2009.
[174] C. D. Stoddard, R. K. Montange, S. P. Hennelly, R. P. Rambo, K. Y. Sanbonmatsu, and R. T. Batey, "Free state conformational sampling of the SAM-I riboswitch aptamer domain," *Structure,* vol. 18, no. 7, pp. 787-97, Jul 14, 2010.
[175] W. G. Scott, J. T. Finch, R. Grenfell, J. Fogg, T. Smith, M. J. Gait, and A. Klug, "Rapid crystallization of chemically synthesized hammerhead RNAs using a double screening procedure," *J Mol Biol,* vol. 250, no. 3, pp. 327-32, Jul 14, 1995.
[176] S. D. Gilbert, R. K. Montange, C. D. Stoddard, and R. T. Batey, "Structural studies of the purine and SAM binding riboswitches," *Cold Spring Harb Symp Quant Biol,* vol. 71, pp. 259-68, 2006.
[177] A. L. Edwards, A. D. Garst, and R. T. Batey, "Determining structures of RNA aptamers and riboswitches by X-ray crystallography," *Methods Mol Biol,* vol. 535, pp. 135-63, 2009.
[178] J. Noeske, J. Buck, B. Furtig, H. R. Nasiri, H. Schwalbe, and J. Wohnert, "Interplay of 'induced fit' and preorganization in the ligand induced folding of the aptamer domain of the guanine binding riboswitch," *Nucleic Acids Res,* vol. 35, no. 2, pp. 572-83, 2007.
[179] O. M. Ottink, S. M. Rampersad, M. Tessari, G. J. Zaman, H. A. Heus, and S. S. Wijmenga, "Ligand-induced folding of the guanine-sensing riboswitch is controlled by a combined predetermined induced fit mechanism," *RNA,* vol. 13, no. 12, pp. 2202-12, Dec, 2007.
[180] B. Furtig, C. Richter, J. Wohnert, and H. Schwalbe, "NMR spectroscopy of RNA," *Chembiochem,* vol. 4, no. 10, pp. 936-62, Oct 6, 2003.
[181] J. Rinnenthal, J. Buck, J. Ferner, A. Wacker, B. Furtig, and H. Schwalbe, "Mapping the landscape of RNA dynamics with NMR spectroscopy," *Acc Chem Res,* vol. 44, no. 12, pp. 1292-301, Dec 20, 2011.

[182] A. Haller, M. F. Souliere, and R. Micura, "The dynamic nature of RNA as key to understanding riboswitch mechanisms," *Acc Chem Res,* vol. 44, no. 12, pp. 1339-48, Dec 20, 2011.
[183] K. C. Suddala, and N. G. Walter, "Riboswitch structure and dynamics by smFRET microscopy," *Methods Enzymol,* vol. 549, pp. 343-73, 2014.
[184] L. C. Hwang, J. Hohlbein, S. Holden, and A. Kapanidis, *Single-Molecule FRET: Methods and Biological Applications,* 2009.
[185] G. A. Soukup, and R. R. Breaker, "Relationship between internucleotide linkage geometry and the stability of RNA," *RNA,* vol. 5, no. 10, pp. 1308-25, Oct, 1999.
[186] E. E. Regulski, and R. R. Breaker, "In-line probing analysis of riboswitches," *Methods Mol Biol,* vol. 419, pp. 53-67, 2008.
[187] S. C. Gopinath, "Mapping of RNA-protein interactions," *Anal Chim Acta,* vol. 636, no. 2, pp. 117-28, Mar 23, 2009.
[188] J. Mulhbacher, and D. A. Lafontaine, "Ligand recognition determinants of guanine riboswitches," *Nucleic Acids Res,* vol. 35, no. 16, pp. 5568-80, 2007.
[189] C. Brieke, F. Rohrbach, A. Gottschalk, G. Mayer, and A. Heckel, "Light-controlled tools," *Angew Chem Int Ed Engl,* vol. 51, no. 34, pp. 8446-76, Aug 20, 2012.
[190] P. Klan, T. Solomek, C. G. Bochet, A. Blanc, R. Givens, M. Rubina, V. Popik, A. Kostikov, and J. Wirz, "Photoremovable protecting groups in chemistry and biology: reaction mechanisms and efficacy," *Chem Rev,* vol. 113, no. 1, pp. 119-91, Jan 9, 2013.
[191] N. Ankenbruck, T. Courtney, Y. Naro, and A. Deiters, "Optochemical Control of Biological Processes in Cells and Animals," *Angew Chem Int Ed Engl,* vol. 57, no. 11, pp. 2768-2798, Mar 5, 2018.
[192] S. J. Husson, A. Gottschalk, and A. M. Leifer, "Optogenetic manipulation of neural activity in C. elegans: from synapse to circuits and behaviour," *Biol Cell,* vol. 105, no. 6, pp. 235-50, Jun, 2013.
[193] J. C. Griepenburg, T. L. Rapp, P. J. Carroll, J. Eberwine, and I. J. Dmochowski, "Ruthenium-Caged Antisense Morpholinos for Regulating Gene Expression in Zebrafish Embryos," *Chem Sci,* vol. 6, no. 4, pp. 2342-2346, Apr 1, 2015.
[194] T. Lucas, F. Schafer, P. Muller, S. A. Eming, A. Heckel, and S. Dimmeler, "Light-inducible antimiR-92a as a therapeutic strategy to promote skin repair in healing-impaired diabetic mice," *Nat Commun,* vol. 8, pp. 15162, May 2, 2017.
[195] A. Jaschke, "Genetically encoded RNA photoswitches as tools for the control of gene expression," *FEBS Lett,* vol. 586, no. 15, pp. 2106-11, Jul 16, 2012.
[196] M. M. Rudolph, "Entwicklung und Anwendung synthetischer RNA-Schalter zur Regulation der Genexpression," Dissertation, Biology, Technische Universität Darmstadt, Darmstadt, 2015.
[197] K. Deisseroth, "Controlling the brain with light," *Sci Am,* vol. 303, no. 5, pp. 48-55, Nov, 2010.
[198] T. S. Lotz, T. Halbritter, C. Kaiser, M. M. Rudolph, L. Kraus, F. Groher, S. Wahl, J. Wachtveitl, A. Heckel, and B. Suess, "A light-responsive RNA aptamer for an azobenzene derivative," Submitted.
[199] T. Halbritter, "Development of a Light-Responsive Riboswitch and Investigation of Water-Soluble Spiropyran- and Azobenzene-Derivatives," Dissertation, Johann Wolfgang Goethe-Universität, Frankfurt am Main, 2017.
[200] A. A. Beharry, and G. A. Woolley, "Azobenzene photoswitches for biomolecules," *Chem Soc Rev,* vol. 40, no. 8, pp. 4422-37, Aug, 2011.

[201] M. Dong, A. Babalhavaeji, S. Samanta, A. A. Beharry, and G. A. Woolley, "Red-Shifting Azobenzene Photoswitches for in Vivo Use," *Acc Chem Res,* vol. 48, no. 10, pp. 2662-70, Oct 20, 2015.
[202] D. Bleger, and S. Hecht, "Visible-Light-Activated Molecular Switches," *Angew Chem Int Ed Engl,* vol. 54, no. 39, pp. 11338-49, Sep 21, 2015.
[203] H. W. Lee, S. G. Robinson, S. Bandyopadhyay, R. H. Mitchell, and D. Sen, "Reversible photo-regulation of a hammerhead ribozyme using a diffusible effector," *J Mol Biol,* vol. 371, no. 5, pp. 1163-73, Aug 31, 2007.
[204] D. D. Young, and A. Deiters, "Light-regulated RNA-small molecule interactions," *Chembiochem,* vol. 9, no. 8, pp. 1225-8, May 23, 2008.
[205] G. Hayashi, M. Hagihara, C. Dohno, and K. Nakatani, "Reversible regulation of binding between a photoresponsive peptide and its RNA aptamer," *Nucleic Acids Symp Ser (Oxf),* no. 51, pp. 93-4, 2007.
[206] G. Hayashi, M. Hagihara, and K. Nakatani, "RNA aptamers that reversibly bind photoresponsive azobenzene-containing peptides," *Chemistry,* vol. 15, no. 2, pp. 424-32, 2009.
[207] T. Halbritter, C. Kaiser, J. Wachtveitl, and A. Heckel, "Pyridine-Spiropyran Derivative as a Persistent, Reversible Photoacid in Water," *J Org Chem,* vol. 82, no. 15, pp. 8040-8047, Aug 4, 2017.
[208] C. Berens, A. Thain, and R. Schroeder, "A tetracycline-binding RNA aptamer," *Bioorg Med Chem,* vol. 9, no. 10, pp. 2549-56, Oct, 2001.
[209] F. Sievers, A. Wilm, D. Dineen, T. J. Gibson, K. Karplus, W. Li, R. Lopez, H. McWilliam, M. Remmert, J. Soding, J. D. Thompson, and D. G. Higgins, "Fast, scalable generation of high-quality protein multiple sequence alignments using Clustal Omega," *Mol Syst Biol,* vol. 7, pp. 539, Oct 11, 2011.
[210] H. McWilliam, W. Li, M. Uludag, S. Squizzato, Y. M. Park, N. Buso, A. P. Cowley, and R. Lopez, "Analysis Tool Web Services from the EMBL-EBI," *Nucleic Acids Res,* vol. 41, no. Web Server issue, pp. W597-600, Jul, 2013.
[211] W. Li, A. Cowley, M. Uludag, T. Gur, H. McWilliam, S. Squizzato, Y. M. Park, N. Buso, and R. Lopez, "The EMBL-EBI bioinformatics web and programmatic tools framework," *Nucleic Acids Res,* vol. 43, no. W1, pp. W580-4, Jul 1, 2015.
[212] M. Abramoff, P. Magalhães, and S. J. Ram, "Image Processing with ImageJ," *Biophotonics International,* vol. 11, no. 7, pp. 36-42, 2004.
[213] C. A. Schneider, W. S. Rasband, and K. W. Eliceiri, "NIH Image to ImageJ: 25 years of image analysis," *Nat Methods,* vol. 9, no. 7, pp. 671-5, Jul, 2012.
[214] M. Zuker, and A. B. Jacobson, "Using reliability information to annotate RNA secondary structures," *RNA,* vol. 4, no. 6, pp. 669-79, Jun, 1998.
[215] A. Waugh, P. Gendron, R. Altman, J. W. Brown, D. Case, D. Gautheret, S. C. Harvey, N. Leontis, J. Westbrook, E. Westhof, M. Zuker, and F. Major, "RNAML: a standard syntax for exchanging RNA information," *RNA,* vol. 8, no. 6, pp. 707-17, Jun, 2002.
[216] M. Zuker, "Mfold web server for nucleic acid folding and hybridization prediction," *Nucleic Acids Res,* vol. 31, no. 13, pp. 3406-15, Jul 1, 2003.
[217] J. Sambrook, E. F. Fritsch, T. P. Maniatis, D. W. Russell, and M. R. Green, *Molecular cloning: A Laboratory Manual,* 3rd ed.: Cold Spring Harbor Laboratory Press, 2001.
[218] O. Landt, H. P. Grunert, and U. Hahn, "A general method for rapid site-directed mutagenesis using the polymerase chain reaction," *Gene,* vol. 96, no. 1, pp. 125-8, Nov 30, 1990.
[219] D. Hanahan, J. Jessee, and F. R. Bloom, "Plasmid transformation of Escherichia coli and other bacteria," *Methods Enzymol,* vol. 204, pp. 63-113, 1991.

[220] P. Bouguer, *Essai d'optique sur la gradation de la lumière*, Paris: C. Jombert, 1729.
[221] J. H. Lambert, and E. Anding, *Lambert's Photometrie (1760)*.
[222] Beer, "Bestimmung der Absorption des rothen Lichts in farbigen Flüssigkeiten," *Annalen der Physik,* vol. 162, no. 5, pp. 78-88, 1852.
[223] N. Arnaud-Barbe, V. Cheynet-Sauvion, G. Oriol, B. Mandrand, and F. Mallet, "Transcription of RNA templates by T7 RNA polymerase," *Nucleic Acids Research,* vol. 26, no. 15, pp. 3550-3554, 1998.
[224] F. Sanger, S. Nicklen, and A. R. Coulson, "DNA sequencing with chain-terminating inhibitors," *Proc Natl Acad Sci U S A,* vol. 74, no. 12, pp. 5463-7, Dec, 1977.
[225] R. D. Gietz, and R. A. Woods, "Transformation of yeast by lithium acetate/single-stranded carrier DNA/polyethylene glycol method," *Methods Enzymol,* vol. 350, pp. 87-96, 2002.
[226] R. H. Schiestl, and R. D. Gietz, "High efficiency transformation of intact yeast cells using single stranded nucleic acids as a carrier," *Curr Genet,* vol. 16, no. 5-6, pp. 339-46, Dec, 1989.
[227] R. D. Gietz, and R. H. Schiestl, "High-efficiency yeast transformation using the LiAc/SS carrier DNA/PEG method," *Nat Protoc,* vol. 2, no. 1, pp. 31-4, 2007.
[228] L. Benatuil, J. M. Perez, J. Belk, and C. M. Hsieh, "An improved yeast transformation method for the generation of very large human antibody libraries," *Protein Eng Des Sel,* vol. 23, no. 4, pp. 155-9, Apr, 2010.
[229] B. Suess, and J. E. Weigand, "Aptamers as artificial gene regulation elements," *Methods Mol Biol,* vol. 535, pp. 201-8, 2009.
[230] A. Pena, J. Ramirez, G. Rosas, and M. Calahorra, "Proton pumping and the internal pH of yeast cells, measured with pyranine introduced by electroporation," *J Bacteriol,* vol. 177, no. 4, pp. 1017-22, Feb, 1995.
[231] C. Tuerk, P. Gauss, C. Thermes, D. R. Groebe, M. Gayle, N. Guild, G. Stormo, Y. d'Aubenton-Carafa, O. C. Uhlenbeck, I. Tinoco, Jr., and et al., "CUUCGG hairpins: extraordinarily stable RNA secondary structures associated with various biochemical processes," *Proc Natl Acad Sci U S A,* vol. 85, no. 5, pp. 1364-8, Mar, 1988.
[232] F. H. Allain, and G. Varani, "Structure of the P1 helix from group I self-splicing introns," *J Mol Biol,* vol. 250, no. 3, pp. 333-53, Jul 14, 1995.
[233] J. S. Paige, K. Y. Wu, and S. R. Jaffrey, "RNA mimics of green fluorescent protein," *Science,* vol. 333, no. 6042, pp. 642-6, Jul 29, 2011.
[234] B. Hall, J. M. Micheletti, P. Satya, K. Ogle, J. Pollard, and A. D. Ellington, "Design, synthesis, and amplification of DNA pools for in vitro selection," *Curr Protoc Mol Biol,* vol. 88, no. 1, pp. 24.2.1-24.2.27, Oct, 2009.
[235] B. Zimmermann, I. Bilusic, C. Lorenz, and R. Schroeder, "Genomic SELEX: a discovery tool for genomic aptamers," *Methods,* vol. 52, no. 2, pp. 125-32, Oct, 2010.
[236] K. A. Vander Meulen, S. Horowitz, R. C. Trievel, and S. E. Butcher, "Measuring the Kinetics of Molecular Association by Isothermal Titration Calorimetry," *Methods Enzymol,* vol. 567, pp. 181-213, 2016.
[237] L. Kraus, "*In vivo* und *in vitro* Charakterisierung von RNA-Aptameren," Bachelor-Thesis, Biology, Technische Universität Darmstadt, Darmstadt, 2016.
[238] V. Levenshtein, "Binary Codes Capable of Correcting Deletions, Insertions and Reversals," *Soviet Physics Doklady,* vol. 10, pp. 707, 1966.
[239] A. Pena, N. S. Sanchez, H. Alvarez, M. Calahorra, and J. Ramirez, "Effects of high medium pH on growth, metabolism and transport in Saccharomyces cerevisiae," *FEMS Yeast Res,* vol. 15, no. 2, Mar, 2015.

[240] M. Blind, and M. Blank, "Aptamer Selection Technology and Recent Advances," *Mol Ther Nucleic Acids,* vol. 4, pp. e223, 2015.
[241] M. C. Cowperthwaite, and A. D. Ellington, "Bioinformatic analysis of the contribution of primer sequences to aptamer structures," *J Mol Evol,* vol. 67, no. 1, pp. 95-102, Jul, 2008.
[242] T. W. Wiegand, P. B. Williams, S. C. Dreskin, M. H. Jouvin, J. P. Kinet, and D. Tasset, "High-affinity oligonucleotide ligands to human IgE inhibit binding to Fc epsilon receptor I," *J Immunol,* vol. 157, no. 1, pp. 221-30, Jul 1, 1996.
[243] T. Shtatland, S. C. Gill, B. E. Javornik, H. E. Johansson, B. S. Singer, O. C. Uhlenbeck, D. A. Zichi, and L. Gold, "Interactions of Escherichia coli RNA with bacteriophage MS2 coat protein: genomic SELEX," *Nucleic Acids Res,* vol. 28, no. 21, pp. E93, Nov 1, 2000.
[244] B. Shui, A. Ozer, W. Zipfel, N. Sahu, A. Singh, J. T. Lis, H. Shi, and M. I. Kotlikoff, "RNA aptamers that functionally interact with green fluorescent protein and its derivatives," *Nucleic Acids Res,* vol. 40, no. 5, pp. e39, Mar, 2012.
[245] E. Ouellet, J. H. Foley, E. M. Conway, and C. Haynes, "Hi-Fi SELEX: A High-Fidelity Digital-PCR Based Therapeutic Aptamer Discovery Platform," *Biotechnol Bioeng,* vol. 112, no. 8, pp. 1506-22, Aug, 2015.
[246] M. A. Vorobyeva, A. S. Davydova, P. E. Vorobjev, and A. G. Venyaminova, "Key Aspects of Nucleic Acid Library Design for in Vitro Selection," *Int J Mol Sci,* vol. 19, no. 2, Feb 5, 2018.
[247] W. Pan, P. Xin, and G. A. Clawson, "Minimal primer and primer-free SELEX protocols for selection of aptamers from random DNA libraries," *Biotechniques,* vol. 44, no. 3, pp. 351-60, Mar, 2008.
[248] A. Vater, F. Jarosch, K. Buchner, and S. Klussmann, "Short bioactive Spiegelmers to migraine-associated calcitonin gene-related peptide rapidly identified by a novel approach: tailored-SELEX," *Nucleic Acids Res,* vol. 31, no. 21, pp. e130, Nov 1, 2003.
[249] K. Setlem, B. Mondal, S. Ramlal, and J. Kingston, "Immuno Affinity SELEX for Simple, Rapid, and Cost-Effective Aptamer Enrichment and Identification against Aflatoxin B1," *Front Microbiol,* vol. 7, pp. 1909, 2016.
[250] F. Almasi, S. L. Mousavi Gargari, F. Bitaraf, and S. Rasoulinejad, "Development of a Single Stranded DNA Aptamer as a Molecular Probe for LNCap Cells Using Cell-SELEX," *Avicenna J Med Biotechnol,* vol. 8, no. 3, pp. 104-11, Jul-Sep, 2016.
[251] L. Wang, R. Wang, F. Chen, T. Jiang, H. Wang, M. Slavik, H. Wei, and Y. Li, "QCM-based aptamer selection and detection of Salmonella typhimurium," *Food Chem,* vol. 221, pp. 776-782, Apr 15, 2017.
[252] R. H. Mitchell, T. R. Ward, Y. Chen, Y. Wang, S. A. Weerawarna, P. W. Dibble, M. J. Marsella, A. Almutairi, and Z. Q. Wang, "Synthesis and photochromic properties of molecules containing [e]-annelated dihydropyrenes. Two and three way pi-switches based on the dimethyldihydropyrene-metacyclophanediene valence isomerization," *J Am Chem Soc,* vol. 125, no. 10, pp. 2974-88, Mar 12, 2003.
[253] M. H. Weik, *inverse square law,* p.^pp. 834-834, Boston, MA: Springer US, 2001.
[254] G. C. Goats, "Appropriate Use of the Inverse Square Law," *Physiotherapy,* vol. 74, no. 1, pp. 8, 1988/01/10/, 1988.
[255] D. Eulberg, K. Buchner, C. Maasch, and S. Klussmann, "Development of an automated in vitro selection protocol to obtain RNA-based aptamers: identification of a biostable substance P antagonist," *Nucleic Acids Res,* vol. 33, no. 4, pp. e45, Mar 3, 2005.

[256] J. Glokler, T. Schutze, and Z. Konthur, "Automation in the high-throughput selection of random combinatorial libraries--different approaches for select applications," *Molecules,* vol. 15, no. 4, pp. 2478-90, Apr 8, 2010.
[257] T. Hunniger, H. Wessels, C. Fischer, A. Paschke-Kratzin, and M. Fischer, "Just in time-selection: A rapid semiautomated SELEX of DNA aptamers using magnetic separation and BEAMing," *Anal Chem,* vol. 86, no. 21, pp. 10940-7, Nov 4, 2014.
[258] T. Schutze, B. Wilhelm, N. Greiner, H. Braun, F. Peter, M. Morl, V. A. Erdmann, H. Lehrach, Z. Konthur, M. Menger, P. F. Arndt, and J. Glokler, "Probing the SELEX process with next-generation sequencing," *PLoS One,* vol. 6, no. 12, pp. e29604, 2011.
[259] E. Dias-Neto, D. N. Nunes, R. J. Giordano, J. Sun, G. H. Botz, K. Yang, J. C. Setubal, R. Pasqualini, and W. Arap, "Next-generation phage display: integrating and comparing available molecular tools to enable cost-effective high-throughput analysis," *PLoS One,* vol. 4, no. 12, pp. e8338, Dec 17, 2009.
[260] A. Jolma, T. Kivioja, J. Toivonen, L. Cheng, G. Wei, M. Enge, M. Taipale, J. M. Vaquerizas, J. Yan, M. J. Sillanpaa, M. Bonke, K. Palin, S. Talukder, T. R. Hughes, N. M. Luscombe, E. Ukkonen, and J. Taipale, "Multiplexed massively parallel SELEX for characterization of human transcription factor binding specificities," *Genome Res,* vol. 20, no. 6, pp. 861-73, Jun, 2010.
[261] F. Buller, M. Steiner, K. Frey, D. Mircsof, J. Scheuermann, M. Kalisch, P. Buhlmann, C. T. Supuran, and D. Neri, "Selection of Carbonic Anhydrase IX Inhibitors from One Million DNA-Encoded Compounds," *ACS Chem Biol,* vol. 6, no. 4, pp. 336-44, Apr 15, 2011.
[262] M. Cho, S. Soo Oh, J. Nie, R. Stewart, M. Eisenstein, J. Chambers, J. D. Marth, F. Walker, J. A. Thomson, and H. T. Soh, "Quantitative selection and parallel characterization of aptamers," *Proc Natl Acad Sci U S A,* vol. 110, no. 46, pp. 18460-5, Nov 12, 2013.
[263] J. Hoinka, A. Berezhnoy, P. Dao, Z. E. Sauna, E. Gilboa, and T. M. Przytycka, "Large scale analysis of the mutational landscape in HT-SELEX improves aptamer discovery," *Nucleic Acids Res,* vol. 43, no. 12, pp. 5699-707, Jul 13, 2015.
[264] A. Levay, R. Brenneman, J. Hoinka, D. Sant, M. Cardone, G. Trinchieri, T. M. Przytycka, and A. Berezhnoy, "Identifying high-affinity aptamer ligands with defined cross-reactivity using high-throughput guided systematic evolution of ligands by exponential enrichment," *Nucleic Acids Res,* vol. 43, no. 12, pp. e82, Jul 13, 2015.
[265] D. H. Burke, D. C. Hoffman, A. Brown, M. Hansen, A. Pardi, and L. Gold, "RNA aptamers to the peptidyl transferase inhibitor chloramphenicol," *Chem Biol,* vol. 4, no. 11, pp. 833-43, Nov, 1997.
[266] J. Mehta, B. Van Dorst, E. Rouah-Martin, W. Herrebout, M. L. Scippo, R. Blust, and J. Robbens, "In vitro selection and characterization of DNA aptamers recognizing chloramphenicol," *J Biotechnol,* vol. 155, no. 4, pp. 361-9, Oct 10, 2011.
[267] J. Kypr, I. Kejnovska, K. Bednářová, and M. Vorlickova, *Circular Dichroism Spectroscopy of Nucleic Acids*: Wiley VCH, 2012.
[268] K. Nakanishi, *Circular dichroism: Principles and Applications,* 1. printing ed.: Vch Pub, 1994.
[269] P. Burgstaller, and M. Famulok, "Isolation of RNA Aptamers for Biological Cofactors by In Vitro Selection," *Angew Chem Int Ed Engl,* vol. 33, no. 10, pp. 1084-1087, 1994.

[270] F. M. Jucker, R. M. Phillips, S. A. McCallum, and A. Pardi, "Role of a heterogeneous free state in the formation of a specific RNA-theophylline complex," *Biochemistry,* vol. 42, no. 9, pp. 2560-7, Mar 11, 2003.
[271] B. Suess, B. Fink, C. Berens, R. Stentz, and W. Hillen, "A theophylline responsive riboswitch based on helix slipping controls gene expression in vivo," *Nucleic Acids Res,* vol. 32, no. 4, pp. 1610-4, 2004.
[272] R. Welz, and R. R. Breaker, "Ligand binding and gene control characteristics of tandem riboswitches in Bacillus anthracis," *RNA,* vol. 13, no. 4, pp. 573-82, Apr, 2007.
[273] E. R. Lee, J. L. Baker, Z. Weinberg, N. Sudarsan, and R. R. Breaker, "An allosteric self-splicing ribozyme triggered by a bacterial second messenger," *Science,* vol. 329, no. 5993, pp. 845-848, Aug 13, 2010.
[274] E. Duchardt-Ferner, S. R. Gottstein-Schmidtke, J. E. Weigand, O. Ohlenschlager, J. P. Wurm, C. Hammann, B. Suess, and J. Wohnert, "What a Difference an OH Makes: Conformational Dynamics as the Basis for the Ligand Specificity of the Neomycin-Sensing Riboswitch," *Angew Chem Int Ed Engl,* vol. 55, no. 4, pp. 1527-30, Jan 22, 2016.
[275] J. E. Weigand, S. R. Schmidtke, T. J. Will, E. Duchardt-Ferner, C. Hammann, J. Wohnert, and B. Suess, "Mechanistic insights into an engineered riboswitch: a switching element which confers riboswitch activity," *Nucleic Acids Res,* vol. 39, no. 8, pp. 3363-72, Apr, 2011.
[276] M. K. Conway, M. J. Gerger, E. E. Balay, R. O'Connell, S. Hanson, N. J. Daily, and T. Wakatsuki, "Scalable 96 well Plate Based iPSC Culture and Production Using a Robotic Liquid Handling System," *J Vis Exp,* no. 99, pp. e52755, May 14, 2015.
[277] G. W. Osborne, "Recent advances in flow cytometric cell sorting," *Methods Cell Biol,* vol. 102, pp. 533-56, 2011.
[278] G. W. Osborne, S. B. Andersen, and F. L. Battye, "Development of a novel cell sorting method that samples population diversity in flow cytometry," *Cytometry A,* vol. 87, no. 11, pp. 1047-51, Nov, 2015.
[279] O. R. Rodrigues, and S. Monard, "A rapid method to verify single-cell deposition setup for cell sorters," *Cytometry A,* vol. 89, no. 6, pp. 594-600, Jun, 2016.
[280] E. Fischer, M. Frankel, and R. Wolovsky, "Wavelength Dependence Of Photoisomerization Equilibria En Azocompounds," *Journal of Chemical Physics,* vol. 23, no. 7, pp. 1367-1367, 1955.
[281] A. Espah Borujeni, D. M. Mishler, J. Wang, W. Huso, and H. M. Salis, "Automated physics-based design of synthetic riboswitches from diverse RNA aptamers," *Nucleic Acids Res,* vol. 44, no. 1, pp. 1-13, Jan 8, 2016.
[282] M. Wachsmuth, G. Domin, R. Lorenz, R. Serfling, S. Findeiss, P. F. Stadler, and M. Morl, "Design criteria for synthetic riboswitches acting on transcription," *RNA Biol,* vol. 12, no. 2, pp. 221-31, 2015.
[283] A.-C. Groher, S. Jager, C. Schneider, F. Groher, K. Hamacher, and B. Suess, "Tuning the Performance of Synthetic Riboswitches using Machine Learning," Submitted.
[284] R. Stoltenburg, N. Nikolaus, and B. Strehlitz, "Capture-SELEX: Selection of DNA Aptamers for Aminoglycoside Antibiotics," *J Anal Methods Chem,* vol. 2012, pp. 415697, 2012.